POTENTIAL ROLES OF THE CHAPERONIN (HTPB), POLYAMINES, AND THE POLYAMINE BINDING PROTEIN (POTD) IN *LEGIONELLA PNEUMOPHILA* PATHOGENESIS

By

Gheyath K. Nasrallah

Submitted in partial fulfilment of the requirements
for the degree of Doctor of Philosophy

at

Dalhousie University
Halifax, Nova Scotia
May 2011

DALHOUSIE UNIVERSITY

DEPARTMENT OF MICROBIOLOGY AND IMMUNOLOGY

The undersigned herby certify that they have read and recommended to the Faculty of Graduate Studies for acceptance a thesis entitled "POTENTIAL ROLES OF THE CHAPERONIN (HTPB), POLYAMINES, AND THE POLYAMINE BINDING PROTEIN (POTD) IN *LEGIONELLA PNEUMOPHILA* PATHOGENESIS" by Gheyath K. Nasrallah in partial fulfilment of the requirement for the degree of Doctor of Philosophy.

Dated: May 17, 2011

External Examiner: _____

Co-Supervisor: _____

Co-Supervisor: _____

Examining Committee: _____

_____

_____

Departmental Representative: _____

DALHOUSIE UNIVERSITY

DATE: May 17, 2011

AUTHOR: Gheyath K. Nasrallah

TITLE: POTENTIAL ROLES OF THE CHAPERONIN (HTPB), POLYAMINES, AND THE POLYAMINE BINDING PROTEIN (POTD) IN *LEGIONELLA PNEUMOPHILA* PATHOGENESIS

DEPARTMENT OR SCHOOL: Department of Microbiology and Immunology

DEGREE: PhD CONVOCATION: October YEAR: 2011

_____

Signature of Author

DEDICATION

To my mother Afaf Al Hafi, my wife Sahar, and my sons Laith and Rayan, from whom I receive support and strength.

TABLE OF CONTENTS

LIST OF TABLES

LIST OF FIGURES

ABSTRACT

The intracellular pathogen *Legionella pneumophila* replicates in a membrane-bound compartment known as the *Legionella*-containing vacuole (LCV) where it abundantly releases its chaperonin HtpB, suggesting that HtpB may have virulence-related functions. To assess these functions, I attempted to construct an *L. pneumophila* Δ*htpB* mutant but was unable to do so, likely because *htpB* is essential. In the absence of genetic deletion, functional tests were used to study the released HtpB. A small portion of the HtpB in *L. pneumophila*-infected cells was found in the cytoplasm of the infected cells, as judged by the CyaA reporter assay. To identify potential functions of the HtpB present in the eukaryotic cytoplasm, *htpB* was ectopically expressed in *Saccharomyces cerevisiae*. HtpB induced pseudohyphal growth (PHG) in yeast, suggesting it interacts with eukaryotic targets. A yeast two-hybrid screen showed that HtpB interacted with SAMDC, an essential yeast enzyme encoded by *SPE2* that is required for polyamine biosynthesis. Overexpression of *SPE2* induced PHG in *S. cerevisiae*, suggesting that HtpB induces PHG by activating polyamine synthesis, and that *L. pneumophila* may require exogenous polyamines for growth. A pharmacological inhibitor of SAMDC reduced *L. pneumophila* replication in host cells, whereas exogenous polyamines enhanced intracellular growth. Bioinformatics revealed that most known enzymes required for polyamine biosynthesis in bacteria are absent in *L. pneumophila*, suggesting that *L. pneumophila* depends on exogenous polyamines transported from host cells. *L. pneumophila* possesses only one putative operon, *potABCD,* which encodes a polyamine transporter. Using GFP as a reporter of *potABCD* promoter (P_{potA}), we found that P_{potA} activity was turned on during exponential phase of growth *in vitro*. To test the potential function of this transporter in pathogenesis, *potD* was deleted. Although deletion of *potD* did not affect *L. pneumophila* growth *in vitro*, it reduced *L. pneumophila* attachment to phagocytic cells, intracellular growth, and the ability of the LCV to recruit vesicles. Collectively, these findings have contributed to a better understanding of the biology of *L. pneumophila* by suggesting that HtpB and PotD might collaborate to ensure a supply of polyamines required for the optimal intracellular growth of *L. pneumophila.*

LIST OF ABBREVIATIONS AND SYMBOLS USED

Ab	antibody
AD	activating domain
Amp^R	ampicillin resistant
ABC	ATP-binding cassette
BCYE	buffered charcoal yeast extract
BD	binding domain
BLAST	basic local alignment search tool
BSA	bovine serum albumin
BYE	buffered yeast extract
cAMP	cyclic adenosine monophosphate
Cat	chloramphenicol acetyl transferase
CBD	Calgary biofilm device
c-di-GMP	bis-(3', 5')-cyclic dimeric guanosine monophosphate
CFU	colony forming unit
CHO	Chinese hamster ovary
CyaA	calmodulin-dependent *Bordetella pertussis* adenylate cyclase
Cm^R	chloramphenicol resistant
Cpn	chaperonin
DFMO	difluoro methyl ornithine
DM	defined media
DMSO	dimethylsulfoxide
Dot	defective in organelle trafficking
EP	exponential phase
ERGIC	ER-Golgi intermediate compartment
FBS	fetal bovine serum
Gal	galactose
GAP	GTPase activating protein
GDA	gene duplication or amplification
GDP	guanosine diphosphate
GEF	guanine nucleotide exchange factor

GFP	green fluorescent protein
Gal	galactose
Gm^R	gentamicin resistant
Hsp60	60 kDa heat shock protein
Hsp10	10 kDa heat shock protein
HtpA	high temperature protein A
HtpB	high temperature protein B
Icm	intracellular multiplication
IFN	interferon
IgG	immunoglobulin G
IL	interleukin
IPTG	isopropyl β-D-1-thiogalactopyranoside
Km^R	kanamycin resistant
LAMP	lysosome-associated membrane protein
LB	Luria-Bertani
LCV	*Legionella*-containing vacuole
LD	Legionnaires' disease
LDH	lactate dehydrogenase
LLAPs	*Legionella*-like amoebal pathogens
LPS	lipopolysaccharide
MAb	monoclonal antibody
MEM	minimal essential media
MGBG	methylglyoxal-bis(guanyl hydrazone)
MIF	mature intracellular form
Mtz^R	mertonidazole resistant
NCBI	National Center for Biotechnology Information
ncRNA	non-coding RNA
NF-κB	nuclear factor κB
NEB	New England Biolab
OD	optical density
P	promoter

PAb	polyclonal antibody
PHB	poly β-hydroxybutyrate
PBS	phosphate buffered saline
PCR	polymerase chain reaction
PHG	pseudohyphal growth
PotD	spermidine/putrescine binding protein
ppGpp	guanosine 3',5'-bipyrophosphate
PPIase	peptidyl-prolyl-cis/trans isomerase
RF	replicative form
ROIs	reactive oxygen intermediates
RPMI	Roswell Park Memorial Institute
SAMDC	S-adenosyl methionine decarboxylase
SC	synthetic complete
SD	synthetic defined
SDS-PAGE	SDS-polyacrylamide gel electrophoresis
Sm^R	streptomycin resistant
SP	stationary phase
Std	standard deviation
Suc^R	sucrose resistant
TBS	tris buffered saline
TEM	transmission electron microscopy
Tet	tetracycline
TF	transmissive phase
TLR	toll-like receptor
TNF	tumor necrosis factor
T4SS	type IV secretion system
T4BSS	type IVB secretion system
TTBS	tween 20-tris buffered saline
VBNC	viable but non-culturable
Y2H	yeast two-hybrid

ACKNOWLEDGEMENTS

First and foremost, I want to thank Allah for giving me the strength to persevere through this endeavor. I would like to express my appreciation to my supervisor Dr. Rafael Garduno, for his patience, mentorship, and friendship. My co-supervisor Dr. Lois Murray, for her advice and support, and for hosting me in her lab for the first six months of my project. My supervisory committee members: Dr. Jessica Boyd, Dr. Ross Davidson, and Dr. Chris Richardson, and my graduate coordinator, Dr. Roy Duncan, for their invaluable help and guidance over the past few years. I would like to extend my gratitude to Dr. Carmen Buchrieser for agreeing to be my external examiner. I am deeply grateful to my lab members past and present: Hany Abdelhady, David Allan, Dr. Celia Lima, Elizabeth Garduno, Badii Al-Bana, Nichols Tompkins, Kaitlyn Carson, Andrew Caddell, Jen Chase, Mackenzie Howatt, Dr. Audrey Chong, and Dr. Angela Riveroll for their help and friendship throughout this process. My thanks to Ameer Jarrar, Dr. Jason LeBlanc, Dr. John David Vandike, Gary Sisson, Jermy Benjamin, Dr. Pak Poon, Julie Rye, Saima Sadiq, and Erin Brouwers, for their technical expertise and their wicked sense of humour. My most sincere gratitude to my family and friends for their support and confidence in me throughout the process. Last but not least, I want to acknowledge the Natural Science and Engineering Research Council (NSERC) of Canada for funding my project.

CHAPTER 1: INTRODUCTION

The following topics will be discussed in this Chapter: (i) the current literature regarding the ecology and molecular pathogenesis of *L. pneumophila*, (ii) polyamine biosynthesis, transport, and cellular functions with particular regard to the roles of polyamines in bacterial pathogenesis, (iii) the biology, classification, and the multiple functions of bacterial chaperonins, and (iv), the objectives and hypothesis of the work presented in this thesis.

1.1. An Overview of *L. pneumophila* Biology

1.1.1. Legionellosis

Legionellae are Gram-negative bacteria that inhabit freshwater environments or soil where they parasitize and replicate intracellularly in various protozoa (114). Legionnaires' disease (a severe atypical pneumonia) and Pontiac fever (a flu-like illness) are the two most typical presentations of legionellosis (120,279). The first documented outbreak of Legionnaires' disease (LD) occurred in 1976, in and around the Bellevue Stratford Hotel in Philadelphia, which was hosting a convention of the Pennsylvania Division of The American Legion (36,120). Several of the attending members contracted the disease and 34 people died (120). Several months after the Philadelphia outbreak, *L. pneumophila* was identified as the causative agent (120,279). While many hotel workers were sero-positive for *L. pneumophila* antibodies, they remained asymptomatic, indicating that the bacterium was cleared by the immune system after infection. In fact,

the most serious cases of LD occurred only among immunocompromised individuals, thus *L. pneumophila* was considered at the time an emerging opportunistic human pathogen.

It is now known that humans acquire LD by inhalation of *Legionella*-contaminated aerosols (fine airborne water droplets) with no person-to-person transmission being documented (114). The link between aerosols and LD was not established until a second large outbreak of LD occurred in Tennessee in 1978. This outbreak involved a contaminated evaporative condenser which resulted in a hospital-wide illness (114). The current understanding is that transmission of LD occurs primarily via contaminated water aerosols containing legionellae. Therefore, aerosol-generating devices, such as cooling towers, air conditioners, showers, and hospital ventilators are often implicated in the spread of LD (113,114,352).

Although fifty-four *Legionella* species containing 73 serogroups have been described (438), 90% of the LD cases in North America and Europe are caused by *L. pneumophila*, and the majority of strains isolated from patients belong to serogroup 1. The rest of the cases (10%) are caused by other *L. pneumophila* serogroups and other *Legionella* species (442) such as *L. longbeacheae*. Even though considered rare, *Legionella*-like amoebal pathogens (LLAPs), which are obligate intracellular bacteria closely related to *Legionella* spp., also account for a number of respiratory diseases (276). The mortality rate of LD varies from 5-30%, with a higher percentage occurring during nosocomial outbreaks among immunocompromised individuals (114). Studies have estimated that between 8,000 and 18,000 persons are hospitalized with legionellosis annually in the United States, a number that may be grossly underestimated since many

infections go unreported or misdiagnosed (114). The prevalence of LD in Canada is low, with approximately 75 cases reported annually (338). This is equivalent to 1.3-3.5 cases/1,000,000 people. *L pneumophila* serogroup 1 may be more common in Halifax than in other Canadian cities (275). Indeeed, *L. pneumophila* is currently considered as a chronic problem in the water system of some Halifax Hospitals. Therefore, our research can expand our knowledge of *L. pneumophila* ecology and the means by which it spreads, and aid our efforts in developing efficient methods for control of this bacterium.

For prevention of LD, there is no vaccine currently available against *L. pneumophila*. Keeping *Legionella* out of water systems is the key to preventing LD. Plumbing systems can be maintained to minimize the growth of legionellae. Water treatment using chemical biocides (monochloramine or chlorine dioxide), copper-silver ionization, and thermal control of the water in aerosol-generating systems are common measures used to minimize transmission of LD (114,405).

Erythromycin was the most effective treatment in the first documented LD outbreak of 1976. Recently, erythromycin has been replaced by newer macrolides, such as clarithromycin and azithromycin, or by respiratory quinolones such as levofloxacin, microfloxacin, and gemifloxacin (114,120). Although *L. pneumophila* is naturally resistant to beta-lactam antibiotics, there are no documented resistances against the clinically used antibiotics, making LD a treatable disease.

1.1.2. Culturing of Legionellae

L. pneumophila is able to grow *in vitro*, in buffered yeast extract (BYE) broth medium or on buffered charcoal yeast extract (BCYE) agar containing L-cysteine (311).

L-cysteine is added to the medium in excess because *L. pneumophila* is a cysteine-auxotroph and because L-cysteine is rapidly oxidized to L-cystine and thus becomes unavailable to the bacteria. To avoid oxidation of L-cysteine, iron salts, like ferric pyrophosphate, are added to BCYE agar to establish an equilibrium between cysteine and cystine, maintaining a steady-state level of cysteine that promotes growth (96). The other essential amino acids for *L. pneumophila* growth are provided in yeast extract (104), which also provides many nutrients (e.g. polyamines). Addition of activated charcoal to BCYE medium prevents photochemical oxidation of the medium, decomposes hydrogen peroxide and superoxide radicals, and prevents light-accelerated auto-oxidation of L-cysteine (179). *L. pneumophila* can be isolated dfrom respiratory fluids by growth on BCYE, and identified by appropriate colonial morphology (white, glistening, circular, smooth, and raised with entire edge.), and the requirement for L-cysteine (114).

1.1.3. Microbial Ecology of *L. pneumophila*

L. pneumophila wild-type strains are mainly inhabitants of aqueous environments where they replicate intracellularly in protozoa, or survive in biofilms (114,117,304). Since *L. pneumophila* is a cysteine auxotroph and unable to metabolize the oxidized form of cysteine (cystine), *L. pneumophila* growth is limited to an intracellular reducing environment where cysteine is accessible (96). It is not clear whether legionellae can multiply extracellularly in aquatic environments without protozoa, but many reports have suggested that they are able to survive for extended periods of time in aquatic biofilms (292,322,346,347). Biofilms provide nutrients and shelter and thus provide a suitable environment for bacterial persistence (114). It is widely known that *L. pneumophila*

forms long filaments, and filamentation has been linked to the ability of *L. pneumophila* to form biofilms and survive in freshwater (322). *L. pneumophila* microcolonies have been detected in biofilms without protozoa (348), and it has been experimentally shown that *L. pneumophila* was able to feed (by necrotrophy) on heat-killed microbial cells present in biofilms or water (401).

L. pneumophila multiplies intracellularly in different protozoa such as amoeba, some ciliates, and slime molds, yet amoebae are considered the primary natural host (352). Studying the interaction between amoeba and *L. pneumophila* has improved our understanding of *L. pneumophila* pathogenesis. It is strongly believed that protozoa protect *L. pneumophila* from eradication by treatment of water with biocides, which may explain why elimination of legionellae from water systems is often difficult. *L. pneumophila* can survive for extended periods in water as a viable but non-culturable (VBNC) form (6,386). It is thought that long-term survival of *L. pneumophila* in the VBNC state occurs after treatment of water with monochloramine and chlorine (6,386). The freshwater amoeba, *Acanthamoeba castellanii,* can resuscitate *L. pneumophila* from its environmental VBNC state (6,386), suggesting that the VBNC form is capable of initiating infections. Because amoebae are resisted to monochloramine, this might explain why the presence of amoebae in water is associated with resistance of *L. pneumophila* to monochloramine and quick re-colonization of water systems by legionellae (405).

Physiological changes in *L. pneumophila* that arise after growth within protozoa are believed to contribute to human infection. For instance, *L. pneumophila* harvested from amoeba cultures [thought to be the natural transmissive forms (TFs) of *L. pneumophila*] invade mammalian cells more robustly than agar-grown bacteria (67).

Furthermore, the ability of *L. pneumophila* to replicate in high titres inside protozoa allows for the delivery of a large infectious dose (352). In amoebae, or in freshwater ciliates such as *Tetrahymena* species, *L. pneumophila* are expelled in vesicles or pellets that could be easily inhaled to deliver a concentrated dose of legionellae in a single infectious particle (26,27). This observation was supported by Brieland et al. (37) who showed that, upon introducing a *L. pneumophila* co-culture with amoebae into mice, the bacteria caused a more severe lung pathology and higher mortality as well as higher bacterial counts in the mouse lung compared to infection with a pure *L. pneumophila in vitro* culture. The above findings suggest that the legionellae-protozoa interactions not only serve as a shelter against environmental stresses, but also induce virulence traits that prime the bacteria for infection of the human host (150).

1.1.4. Developmental Cycle and Differentiation of *L. pneumophila*

When exposed to environmental changes, bacteria alter their physiology to tolerate or to take advantage of the new conditions. For example, when soil bacteria such as like *Bacillus* or *Streptomyces* are exposed to harsh conditions, such as nutrient limitation, high temperature, or acidity, they differentiate from vegetative forms into resting cell forms called endospores (286). When the environment becomes favorable for replication, the endospores are reactivated and differentiate into vegetative forms. Similarly, nutrient limitation induces the intracellular pathogen *Chlamydia trachomatis* to differentiate from replicative reticulate bodies into environmentally resilient and non-replicative infectious elementary bodies (161).

Morphological differentiation of *L. pneumophila* in protozoa was reported in early studies (161,228,229,344). In 1986, Rowbotham (352) provided the first microscopic evidence for the existence of two morphologically different forms of *L. pneumophila*: (i) the non-replicative extracellular forms [recently named transmissive forms (TFs) or mature infectious forms (MIFs)], which are short, display high motility, and have numerous cytoplasmic inclusions of poly β-hydroxybutyrate (PHB), and (ii) the intracellular replicative forms (RFs), which lack these distinct morphologies (352). In 1994, Cirillo et al (67) described similar structural and morphological observations. These authors reported that amoebae-grown bacteria display a thicker cell wall, and denser cytoplasm than agar-grown bacteria.

Byrne and Swanson (45) suggested a model to describe the regulation of *L. pneumophila* biphasic developmental cycle *in vitro* (in laboratory cultures). They observed that *in vitro*-grown stationary phase (SP) bacteria, but not exponential phase (EP) bacteria, were salt sensitive (a phenotype of virulent *L. pneumophila* strains), motile, resistant to osmotic stress, cytotoxic, and competent in escaping intracellular digestion by macrophages. The authors suggested that SP bacteria correspond to the *in vitro* TFs of *L. pneumophila*. Consistent with the *in vitro*-grown model, a direct correlation of morphological changes to a developmental cycle was uncovered by ultrastructural analysis using HeLa cells or *Tetrahymena tropicalis* as hosts (26,102,138). During intracellular infection of HeLa cells, *L. pneumophila* alternates between replicative forms (RFs), which are equivalent to *in vitro* EP bacteria, and metabolically dormant, highly infectious cyst-like forms, or MIFs (which are the *in vivo* TFs) (138) (Fig. 1). For clarity, and because the term TFs is more widely used in the literature than MIFs, I will refer to

MIFs as the *in vivo* TFs and to SP bacteria as the *in vitro* TFs. Compared to the morphology of intracellular RFs, the *in vivo* TFs appear, by electron microscopy, as rods with an electron-dense cytoplasm largely occupied by PHB, a thickened cell-wall architecture, and a multi-laminated envelope of intracytoplasmic membranes formed via invagination of the cytoplasmic membrane. These distinct features of the *in vivo* TFs are thought to enhance their resistance to various stresses. Additionally, although the *in vivo* and the *in vitro* TFs display several similarities, they do show distinct morphological, physiological and biochemical characteristics (138). The *in vivo* TFs are more infectious (10-fold) and more resistant to rifampin (3- to 5-fold), gentamicin (10- to 1,000-fold), detergent lysis, and to high pH than the *in vitro* TFs (138). In addition, the *in vivo* TFs display a different protein expression profile compared to that of the *in vitro* TFs as determined by 2-dimentional gel electrophoresis as. These observations suggest that the *in vivo* TFs represent distinct differentiated forms of *L. pneumophila*.

The stage-specific transition (from EP to SP or from RF to TF) is emphasized by the intermediate morphological forms. Giménez staining can be used to distinguish between the *in vivo* TFs and RFs. The *in vivo* TFs retain the carbol-fuchsin red color (Giménez-positive) while RFs do not and are, therefore, stained green by the counterstain malachite green (Giménez-negative) (Fig. 1) (138). Although the *in vitro* TFs also display some phenotypic characteristics of differentiation (e.g. Giménez-positive staining), *in vitro,* they never fully differentiate into the *in vivo* TFs. It should be noted that *L. pneumophila* does not fully differentiate into *in vivo* TFs in macrophages, which could, to some extent, explain why LD is not a communicable disease (138). If *in vivo* TFs are the most infectious forms of *L. pneumophila*, and these forms are not efficiently produced

during the infection of macrophages (the primary target cells during human infection), it should be possible to explain the lack of person to person transmission based on this observation. In contrast, a study by Molofsky and Swanson (286) has shown that the *L. pneumophila* progeny arising after macrophage infection express several transmission traits such as motility, cytotoxicity, and resistance to environmental stresses, indicating that macrophages still can act as a differentiation niche for *L. pneumophila* . In summary, as drawn in Figure 1, it is clear that *L. pneumophila* has two transmissive forms. One is produced *in vitro*, when *L. pneumophila* reaches SP in broth cultures or agar plates, and one is produced *in vivo* after intracellular growth.

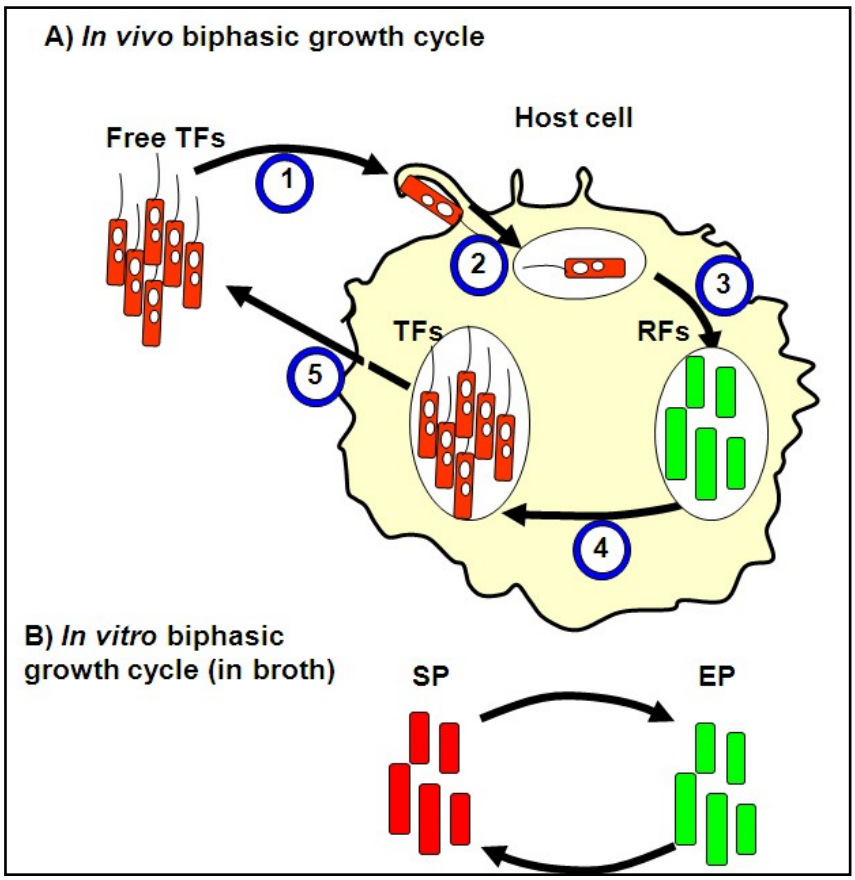

Figure 1. Simplified model illustrating the *L. pneumophila* biphasic growth cycles and the fact that it has two transmissive forms, one produced *in vivo* and one *in vitro*.

A. (1) A free-swimming transmissive form (TF) is engulfed by a host cell (amoebae, alveolar macrophage or HeLa cell) and **(2)** establishes a replicative vacuole that provides protection from host killing. **(3)** When nutrients and other conditions are favourable, intracellular bacteria repress transmissive traits and activate pathways that promote differentiation into replicative forms (RFs). **(4)** As conditions in the replicating compartment deteriorate, the RFs stop dividing and coordinately express traits that promote differentiation into *in vivo* TFs that are required for transmission to a new host cell after their release. **(5)** When TFs produced *in vivo* encounter a new host, a new cycle

begins **(1)**. **B.** Bacteria cultured in broth actively replicate in exponential phase (EP), and stop replicating when nutrients are scarce during stationary phase (SP). Legionellae in EP and SP display many attributes (especially morphological ones) of the *in vivo* replicative and transmissive forms, respectively**.** Adapted from Garduno et al. (138).

1.1.3.1. Regulation of *L. pneumophila* Differentiation

Similar to the stringent response in *E. coli*, when nutritional sources are limited, *L. pneumophila* enters SP *in vitro*. In SP, synthesis of new ribosomal RNA (rRNA), and assembly of new ribosomes are inhibited. Limitation in amino acids leads to inhibition of protein synthesis and accumulation of uncharged transfer RNAs (tRNAs) that are detected by the ribosome-associated RelA synthase (also known as ppGpp synthetase). RelA converts guanosine triphosphate (GTP) or guanosine diphosphate (GDP) to guanosine 3,5-bipyrophosphate (ppGpp), which is believed to be important for bacterial differentiation (159). In *L. pneumophila, relA* is dispensable, as a *relA* mutant grows and spreads efficiently in macrophages. This finding suggests the presence of another pathway that triggers synthesis of ppGpp and regulates differentiation. Indeed, it has been found that, in addition to amino acid starvation, fatty acid starvation also triggers synthesis of ppGpp through SpoT, which is a bifunctional enzyme that both synthesizes and hydrolyses ppGpp in response to the intracellular levels of fatty acids (79,80) (Fig. 2). Deletion of *spotT* can only be attained in the absence of *relA*, (i.e. only *relA* mutant, or *relA spoT* double mutant can be obtained, but not *spoT* mutant) (79), possibly due to the toxic effect resulting from accumulation of ppGpp that is synthesised by RelA but not hydrolyzed by SpoT. SpoT and RelA are important for *L. pneumophila* proliferation as a *relA/spoT* double mutant was unable to replicate in macrophages (79). Complementation of the *relA/spoT* double mutant with a plasmid carrying *relA,* under the control of an IPTG-inducible promoter, caused a 20-fold increase in CFU in relation to that of the double mutant 24 h post-macrophage infection. In contrast, complementation with *spoT* restored growth to parental strain levels (79). These results indicate that regulation of

ppGpp homeostasis either by synthesis or degradation is critical for *L. pneumophila* differentiation (79,80).

From atop its complex regulatory cascade, ppGpp exerts both direct and indirect control over downstream activators and repressors (Fig. 2). To respond to elevated ppGpp levels, *L. pneumophila* requires the LetA/LetS (*Legionella* transmission activator and sensor) two-component system (TCS) (79,80). TCSs contain a sensor histidine kinase (usually an integral cytoplasmic membrane protein) that senses signals which, upon activation, catalyzes its auto-phosphorylation. This sensor, in turn, activates (by phosphorylation) a response regulator which provides the signal output, usually activating or repressing the transcription of target genes. LetA/S is the most important and best characterized TCS in *L. pneumophila*, and is a homolog of the GacA/GacS TCS that is a global regulator of *Pseudomonas* gene expression. The mechanism by which ppGpp activates the LetA/LetS system remains unknown (79,80), but it could be speculated that the inner membrane sensor kinase LetS senses ppGpp either directly via its cytoplasmic domain or indirectly through an adaptor molecule. Once LetS is activated, it phosphorylates LetA, which is the downstream signal effector (Fig. 2).

L. pneumophila may also employ ppGpp to directly and (or) indirectly control the expression of the alternative SP sigma factor (known as RpoS, σ^S, or σ^{38}) by increasing its activity (79,80), and its expression is induced in the *in vitro* TF of *L. pneumophila* (158). RpoS is directly responsible for inducing only some transmission traits, e.g. flagellin expression, but works together with other factors to fully induce virulence in *L. pneumophila* TFs (15). As illustrated in Figure 2, LetA/S and RpoS coordinate their actions with other regulators [such as the flagellar sigma factor FliA (σ^{28}), the small RNA

binding protein, CsrA, the two non-coding RNAs (ncRNA) RsmY and RsmZ, and some GGDEF/EAL proteins] (356) for induction of multiple virulence traits.

When *L. pneumophila* TFs reach an environment with an adequate supply of intracellular nutrients, tRNAs get properly charged and the synthesis of fatty acids is resumed. This leads to a reduced activity of RelA/SpoT and a sharp decrease in ppGpp which, in turn, reverses the downstream signalling effects of LetA/S, resulting in down-regulation of transmissive traits (genes) and differentiation into RFs (286). In RFs, amino acid and carbohydrate metabolism are induced, synthesis of nucleic acids and cellular components is activated, and bacterial multiplication occurs. Upon exhaustion of nutrients, a new cycle begins where *L. pneumophila* then transitions from RF to TF (38), as described above. In TFs, the expression of virulence genes facilitating spread and transmission to a new host are upregulated. These genes include those encoding the flagellar apparatus, the type IV pilus machinery, and Dot/Icm-dependent and independent virulence factors.

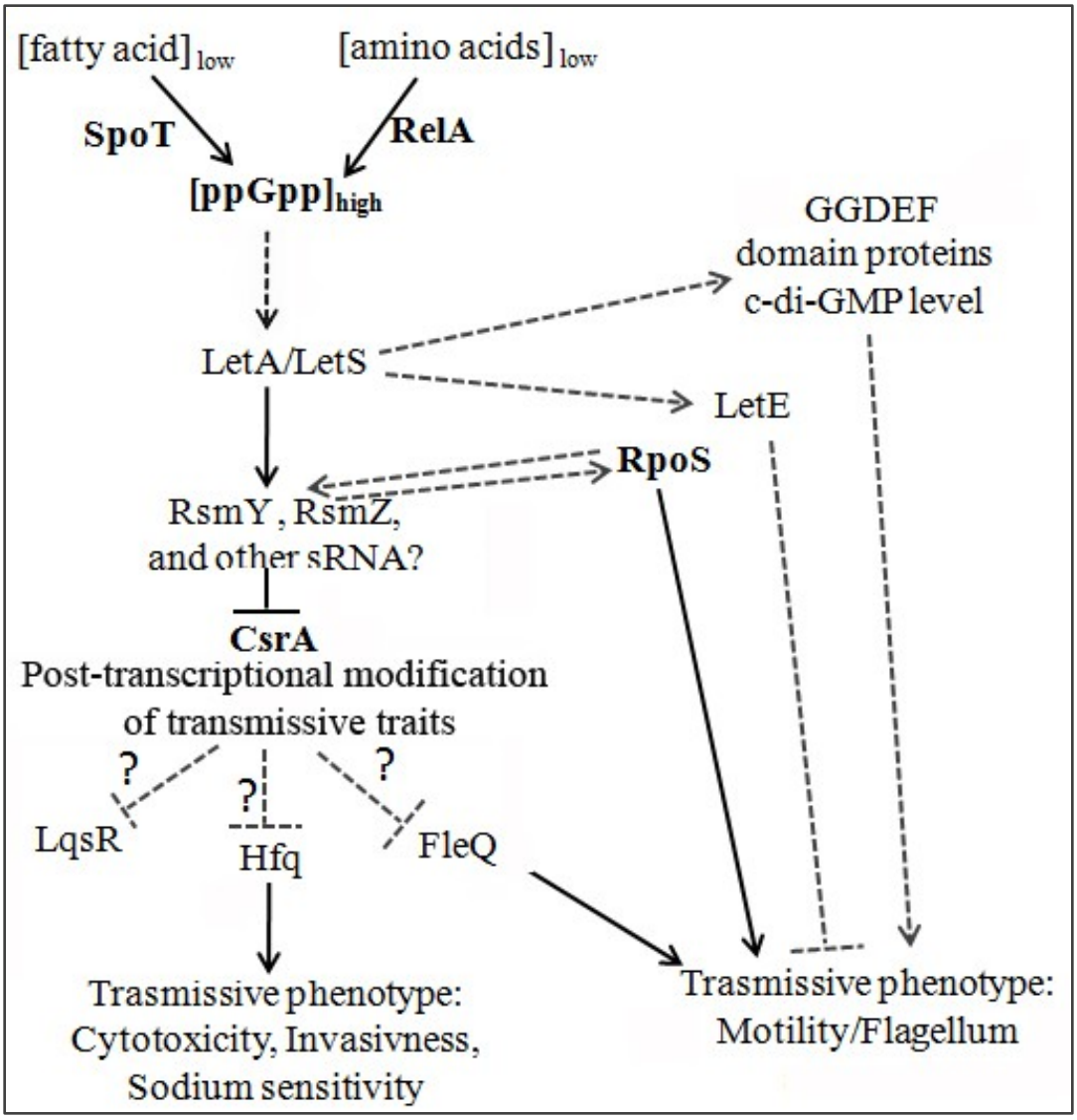

Figure 2. A model suggested by Sahr et al. (356), illustrating the regulatory network governing differentiation of *L. pneumophila* from non-virulent RF to virulent TF.

In TFs, amino acid and fatty acid starvation trigger, respectively, RelA and SpoT to produce (p)ppGpp that is sensed by the sensor kinase, LetS, which then phosphorylates LetA. "Phosphorylated LetA binds upstream of the small ncRNAs RsmY and RsmZ and activates their transcription". Recently other ncRNA have been identified, e.g. 6S RNA (101). "CsrA inhibits translation of *lqsR*, *hfq*, and *fleQ* (regulator of flagellum synthesis)

transcripts by binding near their ribosomal binding site. The presence of RsmY and RsmZ titrates CsrA away from its targets, which then enables translation of their mRNAs, leading to expression of transmissive phenotypes". Flagellum biosynthesis is not only controlled by the RsmYZ-CsrA pathway, but is also dependent on secondary regulatory pathways branching from the LetA/LetS two component regulatory system, probably via LetE. For instance, "LetA/LetS influences, directly or indirectly, cyclic-di-GMP levels, which may regulate motility". Finally, RpoS, known to positively induce flagella synthesis, also plays a role within the feedback loop between RsmY, RsmZ and RpoS."?" indicates hypothetical effects; dotted lines indicate effects that are unknown or mechanisms not yet confirmed. Adapted from Sahr et al. (356). (Used with permission from Carmen Buchrieser).

In addition to LetA/S, other TCSs are also involved in the regulation of *L. pneumophila* differentiation, but only few have been characterized. CpxA/CpxR is a TCS that regulates the expression of the *dot/icm* genes (128). PmrA/PmrS is implicated in intracellular growth and is a direct regulator of several Dot/Icm-translocated effector proteins (450). More recently, an orphan response regulator, LqsR, was characterized. LqsR is a pleiotropic regulator that promotes *L. pneumophila* interaction with host cells. The expression of LqsR is reported to be influenced by RpoS (385,406,407). The known position and interactions of these TCSs within the regulatory network shown in Fig. 2 have not been elucidated, except perhaps for LqsR, which seems to be placed downstream of CsrA (see below).

Small (non-coding) RNAs also play important roles in gene regulation and differentiation of *L. pneumophila*. As shown in Figure. 2, downstream from LetA/S are the small regulatory RNAs RsmY and RsmZ, which act by relieving carbon storage regulator (CsrA) repression of virulence genes by binding to the promoter region of *csrA* and inhbiting its transcription (118,285). The conserved small RNA-binding protein CsrA is a key regulator of the *L. pneumophila* biphasic life cycle, as CsrA acts as a global repressor of transmissive traits and is also an essential activator of intracellular replication (118,285) CsrA inhibits the expression of transmissive traits by binding to the ribosome binding site of transcripts encoding proteins required to confer transmissive traits, thus blocking their translation (118,285). The expression of CsrA is upregulated in RFs, and overexpression of CsrA in *L. pneumophila* inhibits the appearance of transmission traits (109,285). The RNA binding protein Hfq (RNA chaperone) has been shown to stabilize mRNAs by protecting them from RNase degradation. During the

replicative phase of *L. pneumophila*, Hfq increases the expression of CsrA by increasing the stability of the *csrA* mRNA (281). Although CsrA is required for induction of replicative genes and intracellular growth, deletion of *hfq* only slightly affects the intracellular growth of *L. pneumophila* (281). In the *in vitro* TF, RpoS positively regulates Hfq, whereas LetA represses the expression of Hfq. Therefore, in the *in vitro* TF, it seems that RpoS and LetA coordinately regulate the expression of Hfq (281).

In the last few years, it has become evident that small, non-coding regulatory RNAs (ncRNA) also play a general and important role in gene regulation (411). In *L. pneumophila,* the two ncRNA that are involved in the regulation of *L. pneumophila* differentiation are RsmY and RsmZ, which indirectly control several genes required for intracellular replication. Deletion of *rsmY* or *rsmZ*, individually, has little to no impact on induction of transmissive traits (virulence). However deletion of both *rsmY* and *rsmZ* (Δ*rsmYZ*) has drastic effects on *L. pneumophila* intracellular growth in amoebae and macrophages (356). LetA directly activates the expression of RsmY and RsmZ which then bind to and sequester CsrA, thereby abolishing its post-transcriptional repressive activity (356) (Fig. 2). Moreover, Faucher et al. (101) recently identified six additional ncRNAs in *L. pneumophila*. One of these, named *ssrS,* shows high structural similarity to the *E. coli* 6S. In *E. coli*, the 6S RNA inhibits transcription of genes controlled by σ^{70}, by binding and inactivating this RNA polymerase sigma factor (51). The *L. pneumophila ssrS* is highly expressed in the *in vitro* TF, and positively regulates genes encoding *dot/icm* system proteins, stress response genes, as well as genes involved in acquisition of nutrients. Deletion of *ssrS* significantly reduces *L. pneumophila* intracellular growth in

both protist and mammalian host cells, but the exact mechanism of action of *ssrS* in *L. pneumophila* is still to be determined (101).

The flagellar sigma factor, FliA, of *L. pneumophila* may activate promoters of virulence genes in addition to the promoters of the flagellar regulon because FliA was demonstrated to be required not only for the synthesis of the flagellum and for motility (109,170), but also for virulence (160,284). Another protein previously implicated in influencing flagellar expression is LetE (*Legionella* transmission enhancer protein) (16,160). The expression of *letE* was induced nearly 3-fold in a *letA* mutant strain suggesting that LetA directly or indirectly represses *letE* expression, and that the repression of flagellum synthesis in a *letA* mutant strain may be a result of *letE* repression (356). The mechanism by which LetE exerts its effect on fallageller expression is not fully unterstood. However, because the *letE* region does not appear to encode a protein (by analogy to homologous regulatory systems), Hammer et al. (160) suggested a model in which *letE* encodes a regulatory RNA.

Finally, a family of regulator proteins possessing a GGDEF or an EAL motif is up-regulated exclusively in the *in vivo* TF (38,213,349). Members of this GGDEF/EAL domain protein family are known to regulate the transition between motile and sessile bacteria found in biofilms when nutrients are scarce (349). This process is mediated by changes in the intracellular concentrations of bis-(3′-5′)-cyclic dimeric guanosine monophosphate (c-di-GMP) which is in turn regulated by the diguanylate cyclase and phosphodiesterase activities of the GGDEF/EAL proteins (349). In *Salmonella enterica* sv. Typhimurium, mutation in an EAL-domain protein has been linked to the ability of *Salmonella* to kill macrophages and to resist peroxide stress (176). In *E. coli,* CsrA has

recently been shown to indirectly control the levels of c-di-GMP by directly binding to the leader sequence of the mRNA of different GGDEF/EAL protein-encoding genes (213). The role of GGDEF/EAL proteins in regulation of the *L. pneumophila* transomissive traits expression (such as motility) is still hypothetical and needs further investigation (Fig 2)(356). In summary, as shown in Figure 2, the *L. pneumophila* differentiation cycle, which is linked to the induction of transmissive traits and virulence, is regulated by a complex network mainly controlled by LetA/S and RpoS.

1.1.5. *L. pneumophila* Intracellular Trafficking and Replication

The intracellular events that lead to *L. pneumophila* internalization, replication and exit from amoebae are similar to those in human alveolar macrophages, monocytes, and alveolar epithelial cells (Fig. 3), suggesting that the infection mechanisms used by *L. pneumophila* are conserved between hosts. After internalization of *in vivo* TFs by host cells, TFs reside within a membrane bound organelle known as the *Legionella*-containing vacuole (LCV), which does not traffic along the endosomal-lysosomal pathway and thus avoids acidification and fusion with lysosomes. Instead, the LCV recruits mitochondria, ribosomes and small vesicles derived from the endoplasmic reticulum (ER) and (or) Golgi apparatus (217,343), which remodel the LCV and make it similar to an ER-like vacuole. Bacterial replication begins in this ER-like compartment (196,296). The intracellular trafficking of the LCV is largely accomplished by the action of the *Legionella* type 4B secretion system (T4BSS), also known as the Dot/Icm system. Current views of the *L. pneumophila* growth cycle, from uptake to egress from the host cell, will be discussed below in a sequential manner after introducing the Dot/Icm

system, because it is the most studied virulence determinant and it is involved in almost every step of the intracellular growth cycle of *L. pneumophila*.

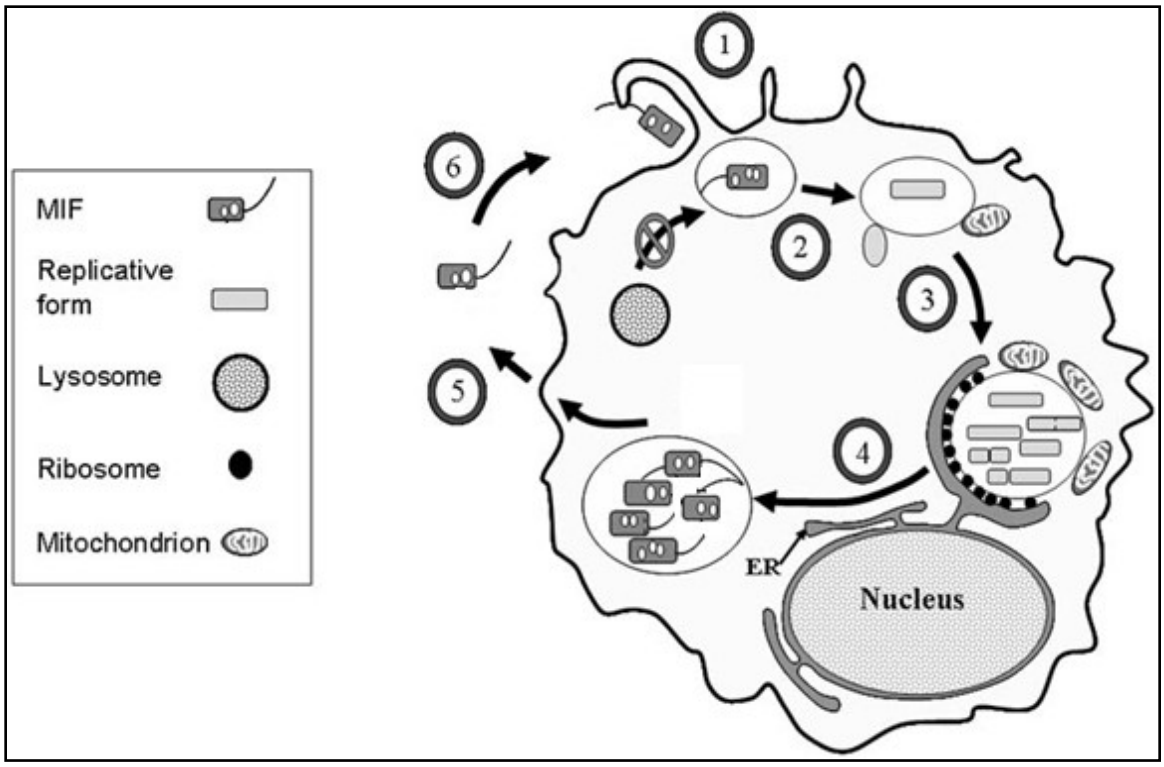

Figure 3. The intracellular events that lead to growth of *L. pneumophila* in host cell.

(1) The MIF (*in vivo* TF) enters a host cell and is contained within the LCV. (**2)** The LCV avoids fusion with lysosomes and associates with mitochondria and ER-derived vesicles. MIF differentiates into RF. (**3)** The LCV becomes associated with the ER, and the LCV membrane is lined with ribosomes. Bacterial replication begins. (**4)** Once replication stops, bacteria differentiate into mature MIFs. (5**)** Egress from the host cell to the extracellular milieu. (**6)** The released bacteria begin another round of infection. Adapted from Faulkner and Garduno (102).

1.1.5.1. Dot/Icm System

The *L. pneumophila* genome encodes for several type 4 secretion systems (T4SSs) (366), which are complex molecular machineries employed to deliver protein (or DNA) into other bacteria or into eukaryotic hosts. The number of T4SSs present in a particular strain of *L. pneumophila* might be different in relation to those found in other strains and isolates, and it is not clear why *L. pneumophila* requires multiple T4SSs. However, all virulent strains possess one common T4SS, the T4BSS (Dot/Icm system), which is essential for virulence.

The Dot/Icm system of *L. pneumophila* was discovered simultaneously by two independent laboratories (370,420), which explains why some genes are named *dot* (for defect in organelle trafficking), others *icm* (for intra-cellular multiplication), and others have two names (e.g. *icmE* = *dotG*). It is now known that the Dot/Icm system is encoded by 26 genes found on two loci in the *L. pneumophila* genome (372). The *dot/icm* genes show similarities to the *tra/trb* genes of conjugal plasmid transfer apparatuses of *E. coli*, and are able to transfer plasmid DNA from one bacterium to another (370,420). The gene products of these two genetic loci are thought to assemble into a molecular apparatus that spans the *L. pneumophila* cell envelope. The comprehensive structural design of the Dot/Icm system has not yet been established, but it is known that Dot/Icm functions as a molecular syringe to inject proteins (effectors) into host cells. The role of these effectors is to modulate a number of host cell functions, mainly related to organellar and vesicular trafficking (73,353,429). Indeed, phagosomes that contain *dot*/*icm* mutants fail to evade the endocytic pathway and quickly acquire endosomal markers such as the lysosomal-

associated membrane protein (LAMP-1), the small GTPase Rab5, and the vacuolar H^+-ATPase (V-ATPase) (70,73,261).

A total of 275 Dot/Icm translocated effectors have now been identified through multiple approaches involving bioinformatics and biochemical assays (42,448). Although the role of many of these effectors in the intracellular establishment of *L. pneumophila* is still unknown, recent investigations have provided insights into the functions of some of these effectors. It is believed that a number of effectors are served different functions in the intracellular events that lead to the growth of *L. pneumophila* in host cells. For example, some effectors are important for bacterial internalization, others are important for inhibition of lysosome fusion with the LCV, or remodelling of the LCV into ER-derived replicative organelle.

1.1.5.2. *L. pneumophila* Internalization

L. pneumophila has the ability to adhere, to invade, and to replicate in many cell types including phagocytic cells such as amoebae and macrophages as well as non-phagocytic cell lines such as HeLa and L929 mouse fibroblasts (107,139,392). Uptake of *L. pneumophila* into macrophages has been shown to occur through coiling phagocytosis (189), conventional phagocytosis (192,313,387) and macropinocytosis (423). The phagocytosis of *L. pneumophila* into macrophages is mediated by (i) host-derived factors: anti-*L. pneumophila* antibody acting in conjunction with complement promoted phagocytosis of the bacteria by alveolar macrophages (192,313), and (ii) bacterium-derived factors (presented below). The fact that *L. pneumophila* can infect a whole range of host cells, particularly non-phagocytic cells, provides strong evidence that, in addition

to host-derived factors, *L. pneumophila* uses several bacterial components (factors) to attach and to enter host cells. These include the type IV pilus, OmpS, Hsp60 (HtpB), Mip, RtxA, EnhC, LadC, and the Dot/Icm system. In this study (Chapter 5), we also identified the polyamine binding protein, PotD, as a *L. pneumophila* adhesion factor.

The initial interaction of *L. pneumophila* with host cells may involve type IV pili, also known as competence and adherence-associated pili (CAP) (388). Mutant strains defective in *pilE*, encoding the pilin of the type IV pilus, have reduced attachment to human macrophages, *Acanthamoeba polyphaga*, and HeLa cells (388). Additionally, mutations in *pilD* (which encodes the prepilin peptidase), impaired *L. pneumophila* growth in amoeba, human macrophages, and epithelial cells, suggesting that PilD has a role not only in attachment to host cell, but also in intracellular growth (257,259). This is expected because the *L. pneumophila* type 2 secretion system (T2SS), which is important for optimal intracellular growth of *L. pneumophila*, depends on the *pilBDC* locus, and PilD processes many proteins destined for the *L. pneumophila* T2SS (257,259,350,351).

The trimeric major outer membrane protein of *L. pneumophila* OmpS is composed of two 28 and one 31 kDa subunits cross-linked by interchain disulfide bonds. The trimeric oligomer is covalently anchored to the underlying peptidoglycan via the 31-kDa subunit (180,181). Treatment of *L. pneumophila* with anti-OmpS antibodies reduces the adherence of both virulent and isogenic avirulent strains of *L. pneumophila* to HeLa cell monolayers in a dose dependent manner (139), indicating that OmpS promotes binding of *L. pneumophila* to host cells.

The *L. pneumophila* chaperonin HtpB (Hsp60) is a surface localized protein that mediates attachment to and invasion of the non-phagocytic HeLa cells (139). HtpB-

coated beads compete with wild-type *L. pneumophila* for association with HeLa cells, suggesting that there are HtpB-specific receptors on HeLa cells. Pre-treatment of *L. pneumophila* with anti-HtpB antibodies or pre-treatment of HeLa cells with purified HtpB reduces the ability *L. pneumophila* to invade HeLa cells (139). HtpB-coated beads were also shown to activate macrophages to secrete IL-1β, a process that involves protein kinase C signalling. HtpB activates IL-1β secretion by macrophages even in the presence cytochalasin D (a compound that prevents bacterial uptake) (340), suggesting that HtpB is recognized at the macrophage cell surface, further supporting the existence of HtpB-specific host cell receptors that mediate *L. pneumophila* uptake and (or) activate signalling cascades.

The macrophage infectivity potentiator (Mip) is a member of the family of protein chaperones displaying peptidyl-prolyl-*cis*/*trans* isomerase (PPIase) activity. Some members of the family are known to play an important role in virulence (186). In *L. pneumophila*, Mip was shown to be a surface-expressed protein involved in entry into macrophages and protozoa, but not necessary for intracellular growth (66,435). Furthermore, inhibition of Mip PPIase activity abolishes early establishment of *L. pneumophila* in *A. castellanii* and human macrophages (164).

A locus designated *rtxA* (repeats in structural toxin) was found to enhance entry of *L. pneumophila* into monocyte and epithelial cells when overexpressed *in trans* (69). Deletion of *rtxA* led to a 50 % reduction in adherence of *L. pneumophila* to human monocytes and epithelial cells (68). The *rtxA* deletion mutant was also less cytotoxic than its parental strain and displayed a reduced ability to form pores in human monocytes (68,234). These findings suggest that the *rtxA* gene encodes a pore-forming cytotoxin

(234) that plays a role in adherence, entry and survival of *L. pneumophila* in both macrophages and protozoa. The mechanisms by which RtxA affects adherence and entry are not understood.

Cirillo et al. (69) identified additional factors required for efficient adherence and entry of *L. pneumophila* into human epithelial cells and macrophages. The products of the *enh* "enhanced entry" genes encode members of a superfamily of proteins with tetratricopeptide repeats [Sel-1 repeats, also known as small leucine-rich repeats (SLR)], which promote protein-protein interactions. Sel-1 repeats were shown to be required for efficient entry of *L. pneumophila* into macrophages and epithelial cells (21,297). *L. pneumophila* possesses five proteins with Sel1 repeats, three of which (LpnE, EnhC, and LidL) have been implicated in the ability of *L. pneumophila* to efficiently establish infection and/or manipulate host cell trafficking events. LpnE is important, not only for *L. pneumophila* entry into macrophages and epithelial cells, but also for efficient infection of *A. castellanii* and for replication of *L. pneumophila* in the lungs of A/J mice (297,299).

Another protein that is involved in the attachment of *L. pneumophila* to host cells is LadC, a putative adenylate cyclase localized to the bacterial inner membrane. *ladC* is one of a cohort of genes that are not active during *in vitro* growth but are induced during infection of macrophages. LadC is present only in *L. pneumophila* serogroup 1 and not in other, less pathogenic, species of *Legionella* such as *L. micdadei* (297). A *ladC* mutant exhibits a 10-fold reduction in adherence to THP-1 macrophages but no difference in uptake by THP-1 cells, compared to its parental strain. Furthermore, LadC contributes to the ability of *L. pneumophila* to replicate in macrophages, epithelial cells, *A. castellanii*, and the lungs of A/J mice (298).

Finally, the Dot/Icm system might participate in entry into host cells, as a mutant lacking *icmT* (encoding one of the inner membrane components of the Dot/Icm apparatus), shows decreased uptake compared to its parental strain (174). Efficient uptake of the Δ*icmT* mutant was restored by co-infection with wild-type *L. pneumophila* (73,174). In addition, overexpression of *dotA* (encoding one of inner membrane components of the Dot/Icm apparatus) in *L. pneumophila* was shown to enhance invasion of *L. pneumophila* and early establishment of LCVs. Immediately following uptake, a Dot/Icm-dependent event prevents the fusion of LCVs with the endosomal pathway (353). These findings suggest that upon host contact, the Dot/Icm system translocates effectors that participate in the entry process either by alteriring host cellular signals triggered during uptake, or directly by interacting with cell receptors (174,286,370,423).

1.1.5.3. Inhibition of Lysosome Fusion with the LCV

Shortly after the uptake of *L. pneumophila* by human macrophages, the newly formed LCV does not fuse with lysosomes, and remains non-acidic. The LCV does not acquire endocytic markers such as LAMP-1 (lysosome-associated membrane protein 1), Rab5 and Rab7 (small GTPases that regulate endocytic membrane-trafficking interactions), suggesting that the LCV stays isolated from the endocytic network (362,430). However, Sturgill-Koszyki and Swanson (390) showed that after 18 h of infection, the LCVs in A/J mouse bone marrow-derived macrophages did mature into acidic phagosomes. These findings suggest that the LCV behaves differently in different host cells.

Studies on *L. pneumophila dot/icm* mutants have provided insight into the mechanism by which *L. pneumophila* inhibits LCV fusion with lysosomes and avoids the host endocytic pathway. It was found that phagosomes containing *dot/icm* mutants (Δ*dotA*) acquire Rab5 and Rab7 in a temporal pattern, typical of phagosomes that progress into mature phagolysosomes (70,353). Furthermore, a *L. pneumophila* mutant that lacks the putative chaperone complex necessary for Dot/Icm-mediated translocation of a subset of effectors (Δ*icmS* or Δ*icmW*), recruits early endocytic vesicles and eventually fuses with lysosomes, but still can support limited replication (72). These findings indicate that some translocated effectors guided by IcmS/W are essential for blocking lysosomal fusion. Other Dot/Icm translocated effectors that seem to participate in blocking phagolysosome fusion are VipA, VipD, and VipF. These proteins were identified in a yeast screen looking for *L. pneumophila* proteins that cause vacuolar protein missorting in yeast (379). Although expression of VipD in yeast caused vacuolar missorting, a *vipD* mutant replicates normally inside amoeba (417). Therefore, it is uncertain whether these proteins prevent lysosomal fusion in infected cells, or their function is masked by other functionally redundant effectors.

A number of factors other than Dot/Icm and its effectors also play a role in inhibition of the LCV fusion with lysosomes. For example, this process can be mediated by pre-formed surface components because avoidance of fusion with lysosomes is not overcome by inhibition of bacterial protein synthesis with erythromycin (188) or treatment of *L. pneumophila* with formalin (214). Recently, latex beads coated with LPS-rich membrane vesicles shed by *in vitro* TFs of wild type *L. pneumophila* or a *dotA* mutant (but not by exponential phase bacteria) were found to inhibit phagosome-

lysosome fusion (108). Mutants lacking *lpnE*, *enhC*, or *lidL* (factors that promote *L. pneumophila* attachment) displayed impaired avoidance of LAMP-1 association (299). In addition, latex beads coated with surface-associated HtpB (but not beads coated with control proteins) also delayed fusion with lysosomes (65). These findings suggest that avoidance of LCV fusion with lysosomes is a regulated process where both Dot/Icm-dependent and independent factors are involved.

1.1.5.4. Mitochondria Recruitment to the LCV

As early as 15 to 30 minutes post-infection, the LCV membrane associates with mitochondria and many small secretory vesicles (188,217). Vacuoles containing a spontaneous avirulent mutant, later determined to be a *dot/icm* mutant, do not recruit mitochondria or smooth vesicles (190,274). In HeLa cells, the mitochondria remain attached to LCVs as late as 45 hours post-infection, suggesting that LCV-mitochondrial interaction continues throughout the intracellular cycle of *L. pneumophila* (137). In addition, the mitochondria remain attached to LCVs even after isolation by cell fractionation, suggesting that a tight fusion occurs between the mitochondria and the LCV membrane (65,409). The only *L. pneumophila* factor known to recruit mitochondria is HtpB. Beads coated with HtpB (but not uncoated beads or beads coated with control proteins) attract mitochondria in human macrophages and Chinese hamster ovary (CHO) cells (65). The significance of mitochondria recruitment and association with the LCV in the pathogenesis of *L. pneumophila* has not yet been determined (65).

1.1.5.5. Remodelling of the LCV into an ER-derived Replicative Organelle

Cellular eukaryotic proteins destined to locate in compartments other than the cytoplasm are synthesized by ribosomes and then translocated into the ER lumen where they are sorted and trafficked to their corresponding cellular compartments. Cargo proteins are transported from the ER through vesicles that bud off at ER exit sites, traffic through the ER-Golgi intermediate compartment (ERGIC), and reach the Golgi apparatus. At the Golgi, the cargo proteins either undergo additional post-translational modification or get prepared for further sorting to other cellular compartments, particularly the cell membrane. This is a multifaceted process controlled by many different molecular components including vesicle coat proteins (COP), small regulatory GTPases (GAPs and GEFs), and SNAREs [Soluble NSF (N-ethylmaleimide sensitive fusion) attachment receptor] (22,445). Some lipids and carbohydrates are also transported along the ER-Golgi route. Secretory vesicles targeted to the cell membrane are the ultimate supplier of lipids for intracellular pathogens that remodel their phagosome membrane, and their cargo provides nutrients to support bacterial growth (22,445).

The LCV intercepts early secretory vesicles (15 to 30 min after infection) prior to their transport through ERGIC and Golgi (187,217,409). The membranes of these vesicles make contact with and fuse along the surface of the LCV, where the exchange of membrane contents between the two compartments occurs (409). Analysis of host factors recruited to the LCV revealed that the ER is the source of these secretory vesicles (1,203,343,393,409). After four hours of infection, the LCV becomes studded with ribosomes and surrounded by the ER. The LCV is now ready for *L. pneumophila* replication (187,261,393).

Host regulators, such as Rab1 and Arf-1 (ADP ribosylation factor) that are important in vesicular trafficking from ER and Golgi to the phagosome, are found on wild-type but not on *dot/icm* mutant LCV. This indicates that Dot/Icm-injected effectors are responsible for recruitment of endocytic vesicles to the LCV (217,218). The role(s) of some of the Dot/Icm effecters such as RalF, DrrA, LepB, SidJ, SidA, SidC, and LidA that have functions related to remodelling of the LCV into an ER-derived replicative organelle will be discussed next.

The first characterized effector of the Dot/Icm system was RalF, which is required for localization of the host GTPase protein Arf-1(ADP ribosylation factor) to the LCV. RalF acts as a guanine-nucleotide exchange factor (GEF), exchanging GDP for GTP, thereby converting Arf1 from its inactive GDP bound form (Arf1-GDP) (46) into the active GTP bound form (Arf1-GTP) (294). Arf1 is an important regulator of endosomal vesicular trafficking and is thought to mediate the recruitment of ER and Golgi-derived vesicles to the LCV (87,88). Overexpression of RalF in yeast causes dramatic growth defects, and these defects are dependent on the ability of RalF to function as an Arf-GEF *in vivo* (46). Surprisingly, *ralF* mutants are still capable of evading the endocytic pathway to generate the LCV in protozoa and macrophages, despite absence of RalF-mediated recruitment of Arf1, suggesting functional redundancy of RalF (294).

Similar to the function of Arf-1, Rab-GTPases on membranes recruit cellular effectors that facilitate the transport, tethering and fusion of the vesicles. Biochemical analysis using Rab1 affinity columns, and a visual fluorescence microscopy screen to identify *L. pneumophila* mutants that no longer recruit Rab1 independently identified the Dot/Icm effector DrrA (also called SidM) as a protein partner of Rab1 (267,291). DrrA is

a highly specific Rab-GEF that catalyzes the GTP/GDP exchange on Rab1. (267,291). DrrA is a bifunctional enzyme, wherein one region is required for recruiting Rab1 to the LCV, while the second region stimulates Rab1 activation by guanine exchange (202,268). Although Rab1 is recognized to be important for LCV biogenesis, a *drrA* mutant did not show intracellular growth defects in macrophages (267), again suggesting the functional redundancy of Dot/Icm effectors. An additional Dot/Icm effector that also binds to Rab1 is LepB, which inactivates Rab1 by stimulating GTP hydrolysis, indicating that LepB is a GAP (GTPase –activating protein) that regulates removal of Rab1 from membranes (202). Overall, these studies show how *L. pneumophila* exploits at least three Dot/Icm effectors (RalF, DrrA and LepB) to regulate Rab1 functions.

In contrast to the *ralF* and the *drrA* mutants, which replicate normally in mammalian hosts despite their inability to recruit Arf1 or Rab1 to the LCV, a *dot/icm* mutant lacking the translocated effector SidJ is temporally delayed in the recruitment of ER proteins to the LCV and showed a significant intracellular growth defect. The mechanistic basis of these SidJ effects is unknown (260). This indicates that *L. pneumophila* simultaneously targets multiple functionally redundant pathways, explaining why in the absence of any single pathway, no obvious phenotype is observed.

Some Dot/Icm translocated effector proteins, such as SidC and SidA (329) and LidA (267), participate in remodelling of LCV without having GEF or GAP activity. These effectors localize to the LCV through interaction with phosphatidylinositol-4-phosphate [PI(4)-P]. The surface of the LCV is rich in PI(4)P, which is preferentially found on the *trans*-Golgi network and acts as a second messenger to mediate the export of early secretory vesicles from ER exit sites (329). The C-terminal end of SidC is

anchored into the membrane of the LCV by binding specifically to PI(4)P, while the N-terminal of SidC mediates interactions of SidC with the ER. A *sidC sidA* double mutant is still able to replicate normally in macrophages; however, the LCV acquires ER markers less efficiently than its parental strain (329). These examples suggest that some *L. pneumophila* effectors manipulate host cell PI(4)P to assist in the biogenesis of the LCV, possibly by acting as the anchoring sites for other Dot/Icm effectors (329).

In conclusion, *L. pneumophila* to possess many (275) Dot/Icm translocated effectors (448), which some of them play redundant roles related to organelle and vesicular trafficking (265,426). The functions of many of these effectors are still unknown and it is not easy to explain why *L. pneumophila* needs these many effectors. Perhaps, the accumulation of these effectors may be a result of the challenges faced by *L. pneumophila* in its replication in multiple and diverse host cells (448).

1.1.5.6. Nutrients Required for Intracellular Replication

L. pneumophila intracellular replication starts after association of the LCV with the ER. The differentiation of the transmissive form (TF) into the replicative form (RF) (Fig. 3) and the replication of *L. pneumophila* is belived to be governed by the nutrient availability in the LCV. Very little is known about the nutritional environment within the LCV. However, the nutrient requirements of *L. pneumophila in vitro* (in laboratory media) promoted examination of the requirements of intracellular LCV. *In vitro* studies indicated that *L. pneumophila* mainly depends on amino acids as a primary source of carbon, nitrogen, and energy. However, recent studies indicate that *L. pneumophila* is capable of utilizing sugars as carbon or energy sources during intracellular growth

(38,98,169). Although little is known about the nutrient requirements of *L. pneumophila* in the LCV, several recent observations suggest that amino acids and iron are integral to *L. pneumophila*'s fitness and survival. Furthermore, data from my research suggest that polyamines and polyamine transport are important for *L. pneumophila* intracellular growth (Discussed in Chapters 4 and 5). An overview about polyamine biosynthesis and transport, and the importance of these compounds in bacterial pathogenesis will be presented in Section 1.2.

Early work indicated that *L. pneumophila* relys on amino acids as the primary source of energy and some of them are essential for growth and differentialtion. For example, cysteine, methionine, serine, arginine, threonine, and valine are essential amino acids for *L. pneumophila* replication *in vitro*, and serine, glutamine, and glutamic acid are the preferred energy sources (141,402,403). During intracellular growth within LCVs, *L. pneumophila* has to acquire these essential amino acids from the host (402). Recently, it was established that the putative *L. pneumophila* valine transporter, PhtJ, is required for differentiation and optimal multiplication of *L. pneumophila* in macrophages (133,162). In addition, it was shown that the human macrophage amino acid transporter, SLC1A5, which is localized to the surface of LCV, is upregulated during macrophage infection with *L. pneumophila*, suggesting that SLC1A5 is important for intracellular establishment (431). Indeed, inhibiting the activity of SLC1A5 blocks *L. pneumophila* intracellular growth (431). Furthermore, it was established that the *L. pneumophila* threonine transporter, PhtA, is required for *L. pneumophila* intracellular growth and differentiation in macrophages. The growth defect displayed by a *phtA* mutant was rescued by the addition of exogenous threonine (361). Similarly, deletion of the gene encoding the

putative *L. pneumophila* valine transporter *milA* (later named *phtJ*), reduces *L. pneumophila* intracellular growth in macrophages by 100-fold (133,162). Ewan and Hoffman (96) suggested that the uptake mechanism of cysteine by *L. pneumophila* may represent a differentiation signal that would provide optimal growth of *L. pneumophila* within the LCV. Finally, bioinformatic analysis of PhtA and PhtJ indicates that these proteins are members of a moderately-sized family of transporters within the major facilitator superfamily (MFS) (58). These transporters may generally be utilized to scavenge sparse nutrients from the host cells, thus exploiting these cells as replicative niches (58). It can be concluded that the intracellular differentiation and replication of *L. pneumophila* in LCV strictly depend on the availability of amino acids in the LCV environment, and the uptake of these amino acids by the intracellular bacteria relies upon a number of efficient transport mechanisms.

In addition to the amino acids, many lines of evidence suggest that *L. pneumophila* growth within host cells is also dependent on iron. Human monocytes, treated with iron chelators, do not support *L. pneumophila* growth, a condition reversed by the addition of ferric iron. Treatment of infected cells with interferon restricts *L. pneumophila* growth within human macrophages (43,44). The mechanism involved in this restriction involves a reduction in the amount of intracellular iron, through an interferon-mediated down-regulation of transferrin receptor in macrophages (43,44). The iron requirement for optimal *L. pneumophila* growth in bacteriological minimal media is unusually high (>20 μM) compared to that needed by many other intracellular bacteria (~3 to 5 μM) (325). The fact that other phagosomal environments, such as those of *Salmonella*-containing phagosomes, contain as little as 0.1 μM iron (135), supports the

notion that the LCV can be an iron-limited environment. Thus, *L. pneumophila* may require an effective iron transport mechanism to exploit iron from host cells (325).

The body of literature that investigates how *L. pneumophila* acquires and assimilates iron is growing. *L. pneumophila* possesses Fur, a transcriptional regulator that is activated under iron-limited conditions. Several-Fur-regulated *L. pneumophila* genes were detected, and subsets of these genes were implicated in macrophage infection (171). For instance, a mutation in the Fur-regulated gene, *frgA*, encoding a homolog of the siderophore-producing synthetase of *E. coli*, significantly inhibits *L. pneumophila* growth in human macrophages (172). Putative iron transporters were also identified in *L. pneumophila* and mutations in the transporters *feoB* or *iraAB,* significantly inhibit *L. pneumophila* growth in macrophages and in an animal model (44,342). Recently, it was determined that when *L. pneumophila* is grown in a low-iron chemically defined medium, it secretes a low-molecular-weight compound, called legiobactin**,** that is similar to other bacterial siderophores (high affinity iron-chelating compounds) (258). Fe-siderophore complexes are actively transported across the outer membrane through specific receptors. In gram-negative bacteria, siderophores are transported into the periplasm via TonB-dependent receptors, and are transferred into the cytoplasm by ABC transporters. Deletion of genes required for synthesis of legiobactin, such as *lbtA* and *lbtB,* reduces *L. pneumophila* ability to infect A/J mice, indicating that legiobactin is required for optimal intrapulmonary infection by *L. pneumophila* (5). Overall, these findings idicates that amino acid and iron are essential elements required for of *L. pneumophila* growth *in vitro* and *in vivo*.

1.1.5.7. Egress from Host Cell

After exhausting the cellular nutrients, *L. pneumophila* must exit the infected host cell. It exits infected mammalian cells in two stages: first, by induction of apoptosis, which is independent of growth phase (132,157), and then by induction of necrosis, which is mediated by growth phase-dependent expression of proteins that have pore-forming activity (7,45). Following the completion of intracellular replication, *L. pneumophila* becomes highly cytotoxic and forms pores in the host cell membranes, ultimately leading to osmotic lysis and egress of the bacteria. Mutants defective in egress are also defective in pore formation which suggests that *L. pneumophila* produces a pore-forming cytolysin required for lysis of the wasted host cell (7,283). *L. pneumophila* mutants termed *rib* (release of intracellular bacteria) are able to evade the endocytic pathway and replicate intracellularly, but remain trapped in host protozoa and macrophages due to their lack of pore-forming ability (7,134,449) Furthermore two Dot/Icm effectors, LepA and LepB, were implicated in the active egress of *L. pneumophila* from protozoa, but not from mammalian cells (59). The mechanism by which LepA and LepB promote bacterial exit from protozoa is still unknown (59). A current model that summarizes the above findings suggests that after intracellular replication, *L. pneumophila* initiates a wave of pore formation that disrupts the LCV and promotes egress to the cytoplasm, followed by a second wave of pore formation that disrupts organelles and plasma membrane, resulting in host cell lysis and bacterial egress to the extracellular milieu (29,283), to begin another round of infection.

1.2. Overview of Polyamines

One of the novel findings of this study is that polyamines are required for optimal intracellular growth of *L. pneumophila.* Therefore, in the next few pages, I will introduce the polyamine biosynthetic pathways and transport mechanisms in eukaryotic and prokaryotic cells. Then I will present some of the multiple functions of polyamines, including their roles in: (i) stabilizing nucleic acid structures, (ii) cell cycle progression, (iii) regulation of gene expression and signalling, and (iv) membrane stabilization. A separate Section (1.2.5.4) will be designated for discussion of polyamines in bacterial pathogenesis. In Chapters 4 and 5, respectively, I will introduce the limited ability of *L. pneumophila* to synthesize polyamines (inferred by an *in silico* analysis of potential genes encoding polyamine biosynthetic enzymes), and the uptake of polyamines by the only putative polyamine transporter identified in *L. pneumophila*. Comprehensive reviews of additional aspects of polyamines can be found in references (74,316,394,395).

Polyamines are small aliphatic polycationic molecules with a hydrocarbon backbone and multiple amino groups. 'Biogenic polyamines' is a term specifically used to describe those polyamines found in living cells, which are essential for life. Putrescine, spermidine, and spermine are the most widely distributed cellular polyamines, while cadaverine is the least prevalent. Due to their positive charges at physiological pH, polyamines bind to various cellular macromolecules, including DNA, RNA, and proteins, which allows them to have effects in diverse cellular processes (74,246,316,394,395). A function of polyamines in which I became particularly interested, due to my results presented in Chapter 5, is the modulation of the activities of certain ion channels, including Na^+ channels, serving as gate keepers (82,206). Therefore, I will intoduce the

roles of polyamines as modulators of ion channels below. Due to the multifunctional nature of polyamines, homeostasis of polyamines is crucial and possibly maintained through the regulation of biosynthesis and transport of these compounds.

1.2.1. Polyamine Biosynthetic Pathways in Prokaryotes and Eukaryotes

In eukaryotes, the polyamine biosynthetic pathway is conserved and only shows minor variations (74,394). Two amino acids, arginine and ornithine, are the common precursors of eukaryotic polyamine biosynthesis (Fig. 4A). The diamine putrescine is synthesized via ornithine by the action of arginase and ornithine decarboxylase (ODC). Putrescine is converted to spermidine by the action of spermidine synthase, which uses aminopropylic groups derived from S-adenosylmethionine (SAM) by the action of S-adenosyl methionine decarboxylase (SAMDC). SAM, in turn, is synthesized from methionine in a reaction catalyzed by methionine adenosyltransferase. Spermine is synthesized by the addition of a second SAM-derived aminopropyl group to spermidine, catalyzed by the enzyme spermine synthase (Fig. 4A).

Bacteria utilize a polyamine biosynthetic pathway similar to that of eukaryotes, yet they exploit additional enzymes and precursors (Fig. 4B). For instance, in *E. coli*, putrescine can be synthesized either from ornithine, or directly from agmantine by the enzyme agmantinase (encoded by *speB*) (Fig. 4B). Spermine is not synthesized in *E. coli*, but uptake of exogenous spermine from the surrounding environment can fulfill *E. coli*'s cellular requirement for polyamines (89). Cadaverine is synthesized independently from putrescine, using lysine as the precursor for a one-step reaction catalyzed by lysine decarboxylase (Fig. 4B). *E. coli* synthesizes cadaverine during anaerobic growth at low

pH or, in general, in the absence of putrescine biosynthesis (425). In any other circumstance, cadaverine is not present in *E. coli* (425). Recent studies on *Vibrio cholerae*, revealed a new metabolic pathway for polyamine synthesis in this organism (252) (Fig. 4B). Bioinformatics revealed that this pathway could be also present in many other bacterial species, such as *Agrobacterium tumefaciens*, *Bartonella henselae*, *Brucella ovis*, *Bordetella bronchiseptica*, *Pasteurella multocida*, *and Pseudomonas fluorescens* (252).

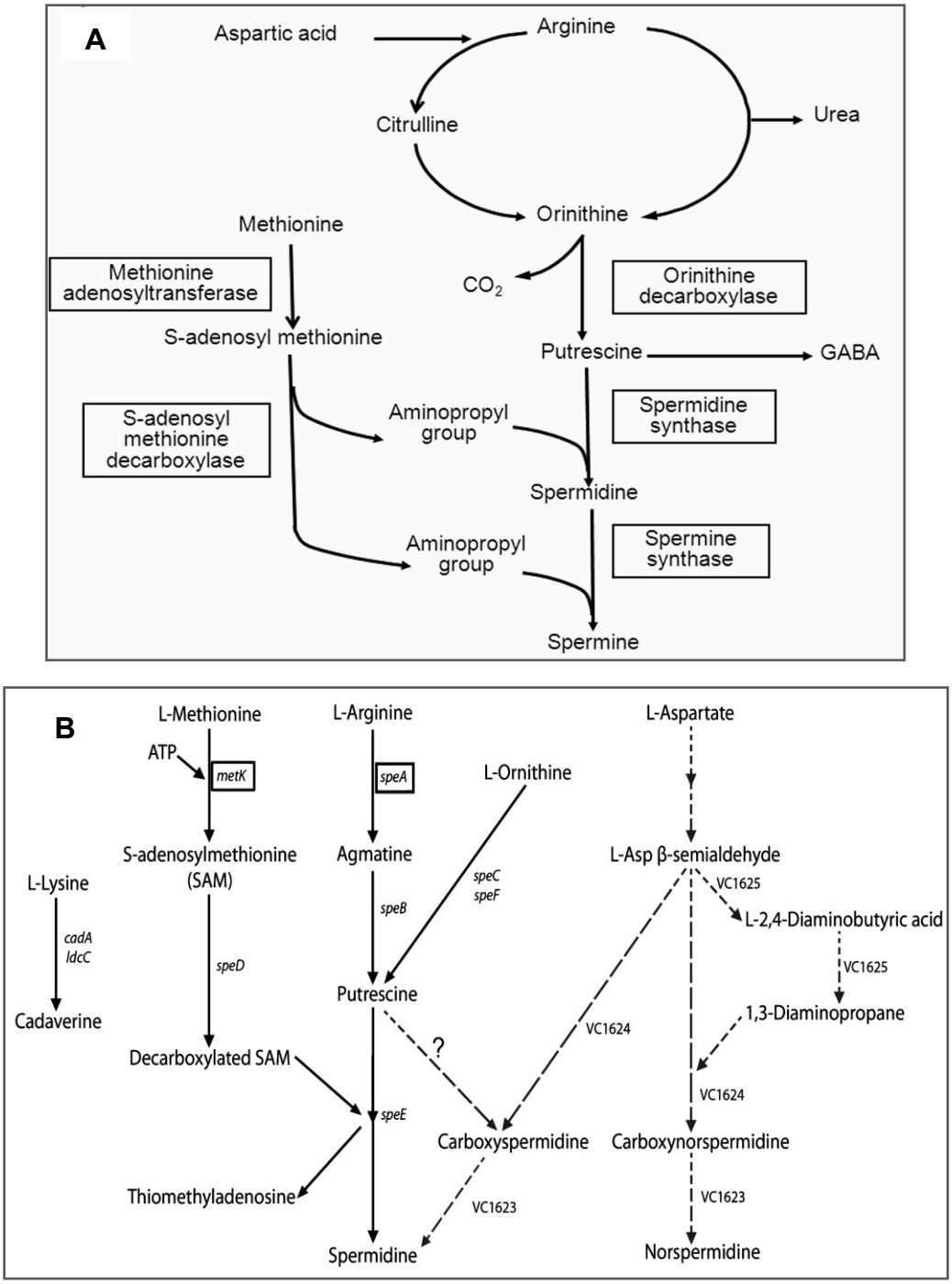

Figure 4. Polyamine biosynthetic pathways.

Polyamine synthetic pathway in eukaryotes **(A)** and in *E. coli* and *V. cholerae* **(B).** In **(A)** enzymatic nomenclature is given as full names in boxes. In **(B)** The *V. cholerae* pathway is marked by the broken-line arrows, and the enzymatic nomenclature is given by the

encoding gene names. For *V. cholerae*, genes encoding biosynthetic enzymes are indicated by a number beginning with VC. In alphabetical order: *cadA* (inducible lysine decarboxylase), *ldcC* (constitutive lysine decarboxylase), *metK* (methionine adenosyltransferase), *speA* (arginine decarboxylase), *speB* (agmatine ureohydrolase), *speC* (constitutive ornithine decarboxylase), *speD* (SAMDC), *speE* (spermidine synthase), *speF* (inducible ornithine decarboxylase), VC1623 (carboxynorspermidine decarboxylase), VC1624 (carboxynorspermidine dehydrogenase), and VC1625 (encoding a large fusion protein comprising the two enzymes di-aminobutyrate aminotransferase and di-aminobutyrate decarboxylase). The genes that have homologs in the *L. pneumophila* genome are indicated by boxes. **(A)** was adapted from www.pediatrie.be/POLINMIL.htm, and (**B)** adapted from reference (295) and used with permission from the Journal of Bacteriology.

1.2.2. Regulation of Polyamine Biosynthesis

Our understanding of regulation of polyamine biosynthesis and homeostasis is largely based on findings in *E. coli*, and model eukaryotic systems (e.g. yeast, and certain plant or animal cell lines). In *E. coli,* the polyamine biosynthetic pathway is regulated by the activity of two key enzymes: SAMDC (encoded by *speD*) and ODC (encoded by *speF*). SAMDC is the most important of the two in regulating intracellular levels of polyamines and homeostasis. In eukaryotes, polyamine biosynthesis is also regulated by ODC and SAMDC. Their activities are rapidly increased or decreased, through their fast turnover rate, in response to various stimuli. For example, the half-life enzymatic activity of ODC is 10 to 20 min (204,368) while that of SAMDC is 30 min (315,377). The activity of SAMDC can be regulated at the level of transcription, translation, or post-translational processing, including protein degradation. At the transcriptional level, increased levels of mammalian SAMDC mRNA have been seen in response to growth promoting factors, such as insulin, or in response to different polyamine inhibitors that result in a decline in intracellular spermidine levels (208,378,391). However, the increase in SAMDC mRNA levels in these reported cases was inadequate to explain the significant increase in cellular SAMDC contents (307,321,391), suggesting that SAMDC expression is regulated at the translational and (or) post-translational levels. Indeed, it has been shown that the processing rate of the pro-SAMDC into the mature α and β subunits is affected by different stimuli; for instance, the processing and activity of SAMDC are increased in response to the intracellular of levels of putrescine (226,319,320). The degradation of SAMDC is also regulated. However, the mechanisms involved in the degradation of SAMDC in response to polyamine levels, presence of polyamines

inhibitors, and other stimuli, are unknown (377,391). Similar to SAMDC, the activity of ODC is also regulated by multiple mechanisms. In nonproliferating eukaryotic cells, ODC activity is low and rapidly increases in response to growth factors, hormones, and nutrients. In addition, ODC is irreversibly inhibited by either putrescine or spermidine (74,316,394,395). The activity of ODC is also regulated by a group of proteins known as antienzymes (317). In response to increasing polyamine levels, particularly putrescine, the antienzymes bind ODC and target it for proteasomal degradation (317). Finally, it should be emphasized here that SAMDC and ODC activity can be specifically inhibited using different pharmacological inhibitors that are commercially available. I exploited pharmacological inhibition of these enzymes in my studies presented in Chapter 4.

1.2.3. Polyamine Transport

Polyamine transport systems in plants and mammals have been suggested, but are poorly characterized and understood. The proteins involved in polyamine transport systems in mammalian cells are unknown. Despite that, several polyamine-binding proteins have been detected in the plasma membranes of mammalian cells, using photoaffinity labelling methods. Their identification and participation in polyamine transport are still unconfirmed (105,106). On the other hand, polyamine transport systems in bacteria are well characterized (197,198).

Before presenting the mechanism of polyamine transport in bacteria it should be mentioned here that not all bacteria can synthesize polyamines to the same capacity (252,425). Depending on their biosynthetic capacity, bacteria rely, to various extents, on transport of exogenous polyamines to fulfill their cellular polyamine requirements. This

notion is supported by the fact that *E. coli* mutants unable to transport exogenous polyamines (224), or mutants unable to endogenously synthesize polyamines (396) grow at a lower rate in relation to their parental strains. Additionally, the genomes of several bacteria such as *Mycoplasma genitalium*, which does not encode any of the known bacterial enzymes required for polyamine synthesis, must rely solely on polyamine transport from the surrounding environment to maintain sufficient intracellular levels of polyamines (198). These observations demonstrate the importance of polyamine transport in bacterial growth and survival.

Bacteria have several transport systems that allow them to take up polyamines from the surrounding environment (197,198). These transport systems were first identified and studied in *E. coli* (197,198,225). *E. coli* have at least five polyamine transport systems. These systems can be classified into three groups: (i) ABC transporters, (ii) antiporters and (iii) uniporters. (i) ABC transporters have a cytoplasmic membrane channel that is energized by ATP that is, in turn, hydrolyzed by an integral membrane protein with an ABC domain. The putrescine specific transport system PotFGHI, which selectively transports putrescine, and the spermidine-preferential uptake system PotABCD, which transports spermidine with high capacity and putrescine with low capacity, are two examples of ABC polyamine transporters. (ii) Antiporters operate by exchanging compatible molecules, importing some polyamines and exporting amino acids or other polyamines. Examples of polyamine antiporters are: PotE that exchanges putrescine for ornithine, and CadB that exchanges lysine for cadaverine (197,198,375). (iii) Uniporters, which are a carrier proteins, work by binding to one molecule of solute at a time and transporting it with the solute gradient. The only known polyamine uniporter

is the newly described putrescine uniporter, PuuP (244,245). It is very important to mention here that not all the *E. coli* polyamine transport systems are present in other bacteria, and some bacteria have particular polyamine systems that are not present in *E. coli*. However, among the known polyamine transporters, the PotABCD transporter is the most widespread among bacteria (375). This transporter is the one that is present in *Legionella pneumophila* and the one that I characterized in Chapter 5. The wide distribution of the PotABCD transporter in bacteria suggests that this system provides a significant survival advantage over the other modes of polyamine transport.

1.2.4. Some of the Multiple Functions of Polyamines in Eukaryotes

1.2.4.1. Roles of Polyamines in Stabilization of DNA structure, DNA Replication, and Protein Synthesis

One of the main characteristics of polyamines is the ability to bind DNA and RNA. Polyamines can bind to the phosphate groups of DNA and neutralize their charges. They also have the ability to interact with nucleic acid bases and dock into the major or minor grooves of the DNA double helix (85,110,111). Polyamines can increase the melting temperature T_m of DNA in a dose dependent fashion (404), suggesting that they may have a significant role in stabilizing the DNA structure *in vivo*. Moreover, immunocytochemical studies have demonstrated that polyamines are coupled with highly compacted mitotic chromosomes (193,363), suggesting that polyamines have a stabilizing and regulating effect on the chromatin structure during cell cycle progression (248). Chromatin from cells exposed to prolonged depletion of polyamines is more sensitive to digestion by nucleases than chromatin from undepleted cells (23,248). Polyamines can promote the interactions of DNA with DNA-binding proteins by

inducing changes in the DNA structure and mediating DNA bending (20,76,163). In fact, the level of intracellular polyamines has been demonstrated to affect the binding of several transcription factors, such as the estrogen receptor, to DNA. In this case, polyamines directly affect the conformation of the estrogen responsive element in DNA (255). In addition to their roles in stabilizing and inducing conformational changes in the DNA structure, polyamines are also important in enhancing DNA replication and protein synthesis. For example, culturing of mammalian cells deficient in polyamine biosynthesis, without the addition of exogenous polyamines (248), or treatment of cells with polyamine synthesis inhibitors (121,122), readily slows down the rate of DNA replication and protein synthesis. Polyamine deprivation can also result in impairment of polysome (polyribosome) formation (398). Since polysomes read one strand of mRNA to simultaneously translate the same mRNA multiple times, impairment of polysome formation can leads to a decrease in the rate of protein synthesis (183). In addition, polyamines are thought to affect the rate of protein synthesis by their ability to bind to the secondary structures of mRNA, tRNA, and rRNA (439). However, this will be presented in detail in Section 1.2.5.1, in the context of the roles of polyamines in prokaryote biology, mainly because the role of polyamines in protein synthesis is better described in bacteria.

1.2.4.2. Roles of Polyamines in Cell Growth and Cell Cycle Progression

It is widely accepted that polyamines can act as intracellular growth-promoting factors. In eukaryotic cells, polyamines are considered essential for life since inhibition of polyamine synthesis blocks cell growth and division (74,316,394,395). Several molecular

mechanisms have been suggested to explain why polyamines can act as growth factors. The simplest explanation is based on their utilization as nutrients. However, the use of polyamines as carbon or nitrogen sources is poorly understood and documented. It has been demonstrated that, in eukaryotes, spermidine is a metabolic precursor of the unusual essential amino acid hypusine, which is involved in post-translational modification of the epsilon amino group of a particular lysine residue of the translational initiation factor elF5A that is essential for cell survival (310). Other proposed mechanisms to explain the role of polyamines as growth factors are more complicated. For instance, investigators have suggested that depletion of polyamines leads to cell cycle arrest possibly through alteration in expression of many growth-related genes (332,335-337). Despite the unclear mechanisms by which these gene expression patterns are regulated by polyamines, some hypotheses have been made. It is known that the cell cycle is regulated by a phylogenetically conserved family of protein kinases called cyclin-dependent kinases (Cdks), which include a catalytic subunit and a positive regulatory subunit that mediates progression of cell cycle. It has been found that polyamine depletion has an effect on the expression of several genes encoding Cdks. For example, changes in cyclin A, B1 and D1 expression have been reported after polyamine depletion (278). Indeed, polyamine depletion has been shown to enhance the activity of the cyclin inhibitors, p21 and p27, which in turn inhibit the expression of cyclin gene expression via a p53-dependent mechanism (335-337). Furthermore, rodent fibroblasts that overexpress SAMDC or ODC turn into highly replicating cells (for the reasons explained above) and are transformed into tumorigenic cells. The expression of cyclin inhibitor p27 in these transformed cells is greatly decreased, suggesting that p27 is a target of the polyamine-responsive cell cycle

control (332). Finally, it is thought that polyamines can also control cell cycle progression through regulation of cellular apoptotic mechanisms, yet the role of polyamines in apoptosis is controversial (365). As mentioned above, depletion of polyamines can lead to cell cycle arrest or apoptosis by affecting the p21/p27/p53/ cell cycle regulatory pathway. Additionally, polyamines can protect cells from apoptosis by stabilizing various cellular components, such as cell membranes and chromatin, or by regulating ion transport (presented below in Section 1.2.4.3) (365). Conversely, many reports have shown that accumulation of spermine and spermidine in the cell can lead to apoptosis and cell death. In this case, oxidation of these polyamines results in accumulation of hydrogen peroxide, which in turn triggers apoptosis (328,410,412,436). Thus, it can be concluded that polyamines can act as promoting, modulating or protective agents of apoptosis. Overall, these observations suggest that polyamines can regulate cell cycle progression in various ways.

Because polyamines are largely involved in regulating the cell cycle, one can easily predict that polyamines would be involved in carcinogenesis. Indeed, a search of publications in the PubMed database (publicly available online through the US National Center for Biotechnology Information website: http://www.ncbi.nlm.nih.gov/pubmed/) using the descriptors “cancer” and “polyamine”, yields ~10,560 hits, including 681 review articles, confirming the strong association between polyamines and carcinogenesis. Although a discussion of the role of polyamines in carcinogenesis would not be relevant in the context of my thesis, I think that the following findings should be mentioned because they provide evidence of how important polyamines are in cell biology. Many reports demonstrated that polyamine levels and polyamine biosynthesis

are highly elevated in many different cancer cells (317-319). Furthermore, many types of human cancerous cells show a significant increase in the levels of ODC and SAMDC activity. ODC, and to a lesser extent SAMDC, becomes activated after induction of cellular transformation via expression of various oncogenes (e.g. *neu,* v-*src*, and *ras*), or after treatment with chemicals known to induce carcinogenesis (13,184,185,319,381,382). Alternatively, overexpression of ODC or SAMDC activates various cellular signalling cascades, including some of the Ras-controlled pathways (12,14,306). Overalla, although it is clear that polyamaines have great effect on cell cycle progression, their exact functions in regulation of this process are yet to be elucidated.

1.2.4.3. Roles of Polyamines in Regulatortion of Ion Channels

In mammalian cells, intracellular polyamines are implicated in the regulation of Na^+, K^+, and Ca^{+2} ion channels (211,256,432,433). For instance, polyamines regulate the intrinsic gating and rectification of inward K^+ channels (112,302,303). Moreover, intracellular polyamines are responsible for inward rectification of AMPA (α-amino-3-hydroxy-5-methyl-4-isoxazolepropionic acid) and kainite receptors (which both respond to the neurotransmitter glutamate that mediates fast synaptic transmission in the central nervous system), through blocking the pore of the receptor channel, consequently preventing Na^+ or Ca^{+2} influx. Polyamines also interact with voltage-activated Ca^{+2} channels and cyclic nucleotide-gated channels (256). In addition to their direct effect on ion channels, polyamines, in particular spermine, promote the activity of V-ATPases, which acidify intracellular compartments by pumping protons across their membranes (140). These findings suggest that changes in intracellular levels of polyamines could largely alter the flow of several cations across membranes.

1.2.5. Some of the Multiple Functions of Polyamines in Prokaryotes

The roles of polyamines in the growth of bacteria are largely uncharacterized. However, studies using *E. coli* as a model have provided insights into the importance of polyamines in bacterial growth. An *E. coli* mutant lacking all the polyamine biosynthetic enzymes does not grow in the absence of air in a polyamine-free medium, and displays 50 % reduction in its growth rate when grown under aerobic conditions in the absence of exogenous polyamines. Thus, in *E. coli*, polyamines are essential for anaerobic growth, and crucial (yet not essential) for growth under aerobic conditions (56,252,375,395). That is, although the exact molecular mechanism by which polyamines enhance bacterial growth is unknown, many mechanisms have been suggested. These mechanisms are presented below.

1.2.5.1. Role of Polyamines in Proteins Synthesis

Similar to what I described for eukaryotes, in bacterial cells, polyamines mainly exist as complexes with nucleic acids, particularly RNA. Polyamines work in conjunction with Mg^{2+} to stabilize high-order RNA structures (200). Through binding to RNA, polyamines can induce unique changes in mRNA structure that can accelerate *in vitro* translation (200). Polyamines can also increase the rate of protein synthesis by other mechanisms, including binding to ribosomes or by increasing the accuracy of codon usage during protein synthesis (205), as well as by facilitating translational read-through of mRNAs with an UAA stop codon (173), or by enhancing synthesis of modified nucleosides important for tRNA synthesis (395). For instance, addition of exogenous

putrescine can restore the biosynthetic defect in a *Shigella flexneri* mutant unable to produce a modified nucleoside necessary for tRNA synthesis (90).

Igarashi and Kashiwagi suggested the "polyamine modulon" theory to explain how polyamines can act as cellular growth factors (199). They suggested that polyamines stimulate the synthesis of several key bacterial growth factors (such the oligopeptide uptake protein OppA) by causing conformational changes in the structure of mRNAs and tRNAs (199). Indeed, they showed that spermidine accelerates translation of OppA, by binding of spermidine to its GC-rich region near the Shine-Dalgarno (SD) sequence of *oppA* mRNA. This binding of spermidine causes structural changes in the SD sequence that leads to an efficient interaction of the AUG start codon with the 30S ribosomal subunit, thereby favoring the formation of an initiation complex (199,439). The translation of other bacterial growth factors is enhanced by a similar mechanism; these include: adenylate cyclase (CyaA), RNA polymerase σ^{38} subunit (RpoS), transcription factor of iron transport operon (FecI), and the transcription factor (Fis) that regulates a number of growth-related genes including rRNAs and some tRNAs (199). By DNA microarray, Igarashi and Kashiwagi found that 309 of 2,742 mRNA species in *E. coli* were up-regulated by polyamines (199). Among the 309 up-regulated genes, transcriptional enhancement of at least 58 genes might be attributable to increased levels of the transcription factors CyaA, RpoS, FecI, and Fis (199). In conclusion, it seems that polyamines enhance mRNA translation of a variety of bacterial genes in particular those that have direct effects on bacterial growth by either stabilizing its structure, or by inducing changes in secondary structure.

1.2.5.2. Roles of Polyamines in Bacterial Resistance to Stress

During infection, bacterial pathogens face oxidative stress from the host. This stress induces an adaptive response involving production of enzymes, such as superoxide dismutase (SOD) and catalase that protect these pathogens from the negative effects of reactive oxygen species (ROS). In addition to these antioxidant enzymes, the positively charged polyamines can function as direct scavengers of negatively charged ROS and can reduce ROS-mediated DNA damage (156). In an environment containing 95 % oxygen the growth of an *E. coli* mutant unable to synthesize polyamines is completely inhibited in spermidine free medium, but not in media supplemented with spermidine (56,252,375,395). Some reports indicate that exposure of bacteria to various stresses, including reactive oxygen and nitrogen species, induces expression of genes that are involved in polyamine biosynthesis and transport, supporting the idea of a protective role of polyamines against these stresses (32,374). Others indicate that addition of exogenous polyamines increase expression of genes that are key regulators of the response to oxidative stresses, such as *soxS* (216). Furthermore, polyamines also seem to play an important role in tolerance to acid stresses, particularly in intestinal pathogens. In *E. coli*, polyamines reduce the level of intracellular cAMP, which in turn induces the expression of glutamate decarboxylase (encoded by *gadA* or *gadB*) that contributes to acid resistance (215). Overall, induction of expression of genes that participate in bacterial resistance to stresses such as *soxS* and *gadA* by polyamines might facilitate survival of bacterial pathogen *in vivo*.

1.2.5.3. Interaction of Polyamines with Bacterial Surface Structures

Extracellular polyamines can be imported by bacteria or bind to negatively charged bacterial surface structures, where they can perform beneficial functions. These include stabilizing the bacterial cell envelope (395,397), controlling ion trafficking (82,83,206), and impairing binding of cationic antimicrobial peptides (147). With regards to the stabilization of the bacterial cell envelope, polyamines have been shown to stabilize halophilic bacteria, and other fragile microorganisms, by increasing the stability of the cell membrane or cell wall (395,397). Putrescine is a constituent of the outer membrane of *E. coli, Proteus mirabilis,* and *Salmonella enterica* (239,418). Cadaverine can be found covalently linked to the peptidoglycan of *Vellionella alcalescens* and *Selenomonas ruminantium* as an essential component during normal cell growth (219,235). In *E. coli*, polyamines play important roles in ion trafficking, primarily by modulating the functions of the trimeric outer membrane porins that are important in flow of hydrophilic molecules across the outer membrane. Spermidine and putrescine can alter the permeability of the outer membrane porins, OmpC and OmpF, by changing the charge and the size of the pores, leading to channel closure and a consequent decrease in outer membrane permeability (82,83,206). Overall, it seems that polyamines enhance bacterial cell survival not only by exerting their effect from within the cells but also through their association with the bacterial cell envelope.

1.2.5.4. Roles of Polyamines in Bacterial Pathogenesis

Polyamines enhance bacterial resistance to antibiotics though unknown mechanisms. It has been proposed that extracellular polyamines, which can be found in

abundance in human body fluids, modify the response of bacteria to antibiotics, possibly by altering the bacterial surface structure. In addition to their roles in controlling ion flow through the OmpF and OmpC porins (see Section 1.2.5.3), polyamines also have the ability to block the flow of certain β-lactam antibiotics through the same porins, increasing the resistance of *E. coli* to those antibiotics (83). Additionally, surface polyamines can increase resistance of *Neisseria gonorrhoeae* to cationic antimicrobial peptides and other mediators of the innate human host defence (147), possibly by masking the binding sites of these molecules on the bacterial surface. Finally, exogenous polyamines increase the resistance of *Pseudomonas aeruginosa* to cationic antibiotics, such as aminoglycosides and quinolones, perhaps by inducing the expression of the genes that are involved in modification of the LPS structure (247).

Polyamines have been implicated in biofilm formation, a process important for virulence of several bacterial pathogens, by enhancing bacterial adhesion, colonization and resistance to antibiotics. It has been suggested that polyamines serve as signaling molecules that mediate the bacterial attachment to biotic surfaces (221). Indeed, addition of exogenous norospermidine (a polyamine that contains one carbon less than spermidine) enhances *V. cholerae* biofilm formation. This effect is mediated by the periplasmic protein NspS (a homolog to the periplasmic spermidine/putrescine-binding protein PotD of *E. coli*) that is believed to act as a sensor for norspermidine (221). In this case, deletion of *nspS* decreases biofilm development and transcription of exopolysaccharide synthesis genes that are required for bacterial attachment to biotic surfaces (221). NspS is hypothesized to form a complex with the integral membrane protein MbaA, which has a periplasmic domain as well as cytoplasmic GGDEF and EAL

domains. MbaA has been previously identified as a repressor of *V. cholerae* biofilm formation. Proteins in the GGDEF and EAL protein families, have been shown to affect intracellular levels of the secondary messenger c-di-GMP (see Section 1.1.3.1 above) (210). Secondary messengers often have global effects on gene transcription. It is thus proposed that NspS interacts with the periplasmic domain of MbaA to regulate its enzymatic activity and that this interaction is modulated by binding of norspermidine to NspS (221). In other cases, intracellular polyamines also can regulate biofilm formation. For instance, reducing the levels of intracellular putrescine in *Yersinia pestis*, or norospermidine in *V. cholerae* (by deletion of genes involved in the synthesis of these two polyamines) inhibits biofilm formation (252,312). Addition of exogenous putrescine restores the biofilm formation ability of *Y. pestis* (252,312). Thus, polyamines can act as external signals, or as intracellular factors that trigger responses related to biofilm formation in a number of pathogenic bacteria.

Polyamines are also implicated in inducing the swarming phenotype that is important for motility of the pathogen *Proteus mirabilis* and colonization of the urinary tract (389). For example, inactivation of *speAB* (encodes for arginine decarboxylase and *speB* agmatine ureohydrolase, respectively) leads to a loss of the swarming phenotype, which can be restored by addition of exogenous putrescine that is transported into the bacterial cell through polyamine transporters such as PotFGHI, PotABCD, or PotE (389). It is thought that *P. mirabilis* uses polyamines as a cell-to-cell signaling molecule that induces differentiation from sessile into swarm cells (389). The mechanism by which putrescine enhances swarming of *P. mirabilis* is unknown, but it is possible that high levels of putrescine enhance expression of regulatory proteins controlling swarming

phenotypes (389). Alternatively, putrescine may have a direct effect on the bacterial cell surface of *P. mirabilis* resulting in cell-to-cell interactions that in turn trigger differentiation (389).

Some human pathogens can enhance their survival within the host by modulating polyamine biosynthesis in the host cell. It has been shown that in tissues inflamed as a result of microbial infection, polyamines are present in high concentrations (273), suggesting that the infectious agent activates host polyamine biosynthesis. In turn, increased levels of spermidine, spermine, and putrescine have been shown to induce polymorphonuclear leukocyte (PMN) apoptosis in a dose-dependent manner (273), suggesting that during inflammation (that results form infiltration of PMN to the site of infection), apoptosis of the inflamed tissue might occur. *H. pylori* also induces macrophage apoptosis by increasing the level of host polyamines at the site of infection (60,249). ODC activity is upregulated in *H. pylori*-infected macrophages and eradication of the infection leads to decreased activity of ODC (3). *H. pylori* also induces expression of the transcription factor c-Myc, which binds to the promoter region of ODC enhancing its expression (249). Interestingly, inhibition of either c-Myc or ODC activity reduces apoptosis of the *H. pylori*-infected macrophages. In host cells *H. pylori* also induces the expression of polyamine oxidase PAOh1 (a polyamine catabolic enzyme that catalyzes spermine oxidation to spermidine) (57). Oxidation of spermine by PAOh1 results in production of H_2O_2, which in turn induces depolarization of the mitochondrial membrane, and caspase activation, leading to macrophage apoptosis (57). Manipulating host polyamine metabolism during infection is thus be a common theme in bacterial pathogens. Further to these findings, I report in Chapter 4 of this thesis, that the *L.*

pneumophila chaperonin (HtpB) can interact with the host SAMDC, a key enzyme of the polyamine biosynthesis pathway in eukaryotes, and that reducing the activity of the host SAMDC significantly reduces *L. pneumophila* intracellular growth.

It is widely known that iron is crucial for the growth of bacterial pathogens, and that iron is not available in infected tissues because it is trapped by iron-binding proteins, like transferrin, which bind iron with high affinity. To strip iron from these host proteins and make it available for use some bacterial pathogens release siderophores, which are small compounds that have very high affinity for iron. Pathogens then obtain iron by efficiently binding and internalizing iron-loaded siderophores; therefore, siderophores are regarded as virulence factors. In *V. cholerae* (232), *E. coli* (308), and *Bacillus anthracis* (305), polyamines are important for siderophore production. Spermidine is used as a metabolic precursor in the synthesis of the siderophore petrobactine by *B. anthracis* (305). The siderophore of the intestinal pathogen *V. cholerae* contains norospermidine. Collectively, these reports suggest an important role for polyamines in iron-limited host environments (232).

Colicins are protein bacterial toxins encoded on plasmids of certain *E. coli* strains. They provide a competitive edge in tissues or host sites colonized with bacterial communities, mainly because colicins kill competing bacterial cells by forming pores in their cytoplasmic membrane. As mediators of colonization, colicins could be considered virulence factors. Polyamines appear to be important for both colicin production and resistance to colicins. The protective role of polyamines against colicins is clearly demonstrated by the fact that *E. coli* mutants deficient in putrescine and spermidine biosynthesis are more susceptible to colicins than are wild-type strains. The mechanism

of this protective role seems to be regulatory in nature, because in colicin-susceptible *E. coli* strains, exposure to polyamines reduces expression of TolA, BtuB, OmpF, and OmpC, which are outer membrane proteins involved in colicin uptake (308). Furthermore, exposure of *E. coli* to colicins results in overexpression of the spermidine/putrescine-binding periplasmic protein PotD (308), which is involved in the import of exogenous polyamines. Therefore, these finding suggests that an endogenous increase in polyamine biosynthesis, or an increase in the transport of exogenous polyamines, results in reduced uptake of, and increased resistance to, colicins. From the perspective of colicin-producing strains, spermidine and putrescine seem to be important for production of colicin (308). For instance, an *E. coli* mutant deficient in spermidine and putrescine synthesis shows a low level of colicin production, which is restored to wild-type levels by the addition of exogenous spermidine and putrescine (308). In conclusion, polyamines play a dual role as enhancers of colicin production, and as colicin-resistance factors, providing a survival benefit to both colicin-producing, and colicin-susceptible bacteria.

Although the transport of exogenous polyamines has been reported for several bacterial pathogens [reviewed in (375)], and the polyamine transport systems of *E. coli* have been well studied, the impact of bacterial import of exogenous polyamines in pathogenesis has only been studied in few bacterial pathogens. The genome of *S. pneumoniae* carries the polyamine transporter operon *potABCD* that shows a high degree of homology to the *E. coli* operon of the same name (421). Transcription of the the pneumococcal *potD* transporter increases in response to oxidative radicals or high temperature, and during host infection. The importance of a functional polyamine

transport in virulence is demonstrated by the fact that a *S. pneumoniae* Δ*potD* mutant displays a significant attenuation in the mouse model of systemic and pulmonary infection (421). Additionally, in Chapter 5 of this thesis, I provided several lines of evidence indicating that polyamine transport through the putative periplasmic spermidine/putrescine-binding protein PotD of *L. pneumophila* is important for pathogenesis.

In summary, research indicates that polyamines can act as bacterial growth factors through various mechanisms, including by acting as precursors of essential compounds such as siderophores, providing protection against various stresses, or by binding to RNA to enhance expression of key growth factors or protective enzymes

1.3. An Overview of Bacterial Chaperonin Biology

Chaperonins are a family of structurally and functionally conserved and essential proteins that are present in almost all prokaryotic and eukaryotic forms of life. The remarkable amino acid sequence and structural conservation across chaperonins highlights their functional importance. The fundamental functions of chaperonins are to assist other proteins to fold properly after translation, protect proteins from denaturation, and help denatured proteins to refold after stress, all in an ATP-dependent manner. Chaperonins have other cellular roles independent of protein folding. Some of these functions are presented in Section 1.3.4. Chaperonins have been classified into three groups based on their structure and evolutionary origin. Group I chaperonins (Cpn60, GroEL, Hsp60, or HtpB) are proteins found in bacteria and in eukaryotic organelles such as chloroplasts and mitochondria (154). Group II chaperonins are typically found in the

cytosol of archaea and eukaryotic cells (154). These chaperonins are also known as T-complex polypeptide 1 (TCP-1), TCP-1 ring complex (TriC), or chaperonin-containing TCP-1 (CCT). Recently, Techtmann & Robb (400) reported a third group of chaperonins found in several species of bacteria. These chaperonins are also known as TCP1-like chaperonins, because they are distantly related to both group I and II chaperonins. The best characterized group III chaperonin is the one present in the bacterium *Carboxydothermus hydrogenoformans* (400).

To facilitate the distinction between the group I chaperonins that are present in eukaryotic organelles versus those present in bacteria, the latter will be termed group I bacterial chaperonins. The following Sections will be devoted to a discussion of the group I bacterial chaperonins in terms of their function in protein folding, gene organization and regulation of their gene expression. Because this thesis is focused on studying the protein-independent functions of HtpB, a special Section will be designated to discuss the accessory function of group I bacterial chaperonins, including HtpB.

1.3.1. Structure and Protein folding Function of Bacterial Chaperonins

Group I bacterial chaperonins are termed GroEL, Hsp60, Cpn60 or HtpB. In the following Sections, the term GroEL will be used to refer to group I bacterial chaperonins in general, and the term HtpB (high temperature protein B) will be used to refer to the *L. pneumophila* chaperonin in particular.

Most of the characteristics of the group I bacterial chaperonins have been determined based on experiments done with the *E. coli* GroEL. These structural and functional studies of *E. coli* GroEL have established the role of group I bacterial

chaperonins as intracellular mediators of protein-folding (31,444), which currently constitutes their primary recognized function. GroEL is an essential protein in *E. coli* (103), whose intracellular level increases substantially in response to different environmental stresses (263,416). GroEL has been found to interact with approximately 300 polypeptides *in vivo* (194); however, only 85 of these are absolutely dependent on GroEL for folding (233). Thirteen of these 85 proteins are essential, which explains why the protein folding function of GroEL is also essential and why GroEL is required under all growth conditions (103,233).

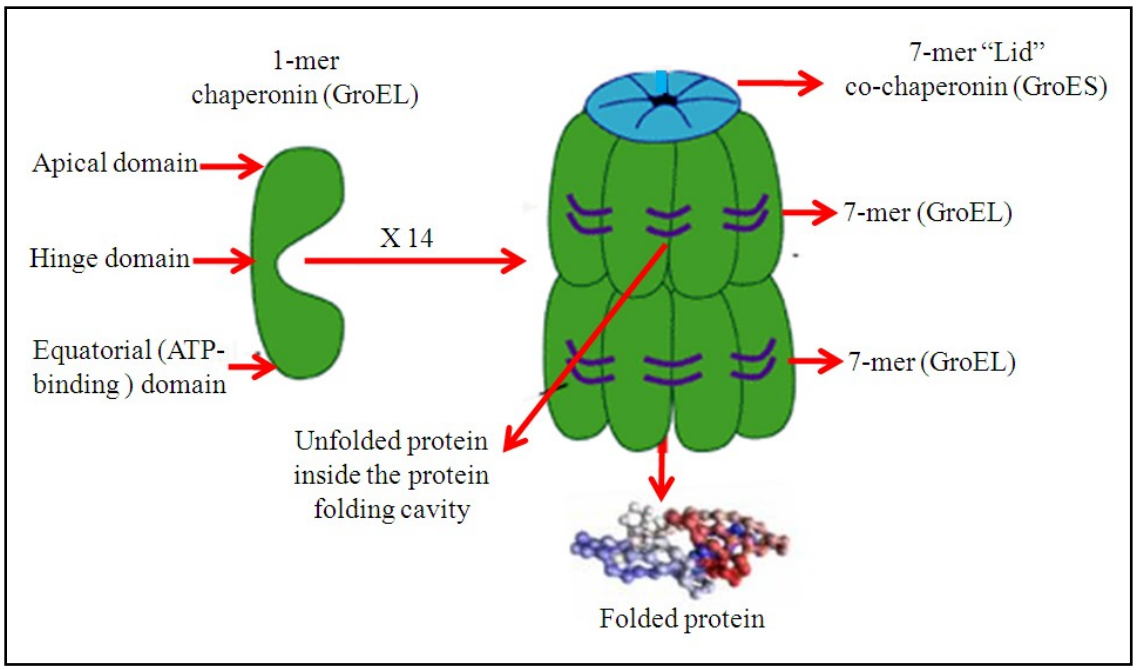

Figure 5. The simplified structure of GroEL and GroES, including some elements of the protein folding cycle.

To perform protein folding, GroEL forms homo-oligomeric 7-mer rings (33). Two of these 7-mer rings come together to form the 14-mer barrel complex. The cylindrical space formed inside the 14-mer GroEL barrel constitutes the protein folding cavity, which mediates protein folding in association with a third homo-oligomeric 7-mer ring of the co-chaperonin GroES (a protein of ~10-kDa also termed Cpn10, Hsp10, or HtpA). The GroES 7-mer ring serves as a lid that closes the end of the folding cavity that interacts with an unfolded substrate (upper 7-mer of the barrel) in an ATP-dependent manner. At any given point during the protein folding cycle, only one end of the barrel is capped. Once the protein substrate is folded, the co-chaperonin lid is disengaged and the folded protein is released (bottom 7-mer of the barrel). Adapted from http://www-ermm.cbcu.cam.ac.uk.

The protein folding mechanism of GroELis illustrated in Fig. 5. The double 7-mer -ring of GroEL forms a barrel structure with a large internal cavity where the unfolded protein substrate binds via hydrophobic interactions. Each GroEL monomer has three domains: (i) an apical domain, where the unfolded protein substrate and GroES bind; (ii) an equatorial domain, which it contains a binding site for ATP; and (iii) a hinge domain, which connects the two previous domains (34,93,233,263). The hinge domain undergoes conformational changes when ATP is bound to and hydrolyzed by the equatorial domain, allowing the substrate-binding surface to change from a hydrophobic to a hydrophilic state (34,93,233,263). The protein folding cycle starts when the internal surface of the cavity is in the hydrophobic state. The unfolded protein substrate binds to the hydrophobic surface of the cavity, and it is stretched to prevent its misfolding and aggregation. Once the unfolded protein is captured inside the hydrophobic cavity, the 7-mer GroES "lid" binds to the apical domains of the GroEL ring structure to enclose the unfolded protein. Subsequently, the binding and hydrolysis of ATP at the equatorial domains result in opening and rotation of the apical domains, enlargement of the cavity, and a change of the cavity's surface from a hydrophobic to a hydrophilic state. These conformational changes mark the end of one cycle and release of the protein substrate, which at this point might be either properly folded, or required to go through another cycle. ATP hydrolysis and release of ADP restores the hydrophobic conformation inside the cavity, leaving it ready to start another protein folding cycle. Detailed information about the folding mechanism of GroEL can be found in the following review articles (34,93,233,263).

1.3.2. Organization of the Chaperonin Genes in Bacteria

In *E. coli,* the *groES* and *groEL* genes are transcribed as a bicistronic mRNA from one operon called the *groE* operon (166). Studies of numerous bacterial genomes have pointed out that the *groE* operon organization is very well conserved in bacteria. They are all arranged in the same order, promoter-*groES*-*groEL* (369). An exception to this organization is found in *Mycobacterium bovis*, where *groES* and *groEL* are not present in an operon, but found in separate loci (369). Multiple copies of *groEL* have been detected among the genomes of several different Gram-negative α-proteobacteria. For example, *Bradyrhizobium japonicum* contains seven copies of the *groEL* gene (264). Duplication of chaperonin genes has also been reported in pathogenic bacteria such as *Chlamydia* (154,222,223), and *Mycobacterium tuberculosis* (238). In some bacteria with multiple copies of *groEL*, the *groEL* genes are present in separate loci (i.e. not coupled with *groES* in one operon), in addition to the *groE* operon (369). For instance, *Sinorhizobium meliloti* has four *groE* operons and one independent *groEL* gene expressed from its own promoter (48). The organization of the *groEL* gene in an operon (*groE*) is a common theme in most bacterial species with few exceptions such as those that have more than one copy of this gene.

1.3.3. Transcriptional Regulation of the *groE* Operon

One of the designations of GroEL chaperonins is "60-kDa heat-shock proteins (Hsp60)", mainly because chaperonins are induced during heat-shockwhen an *E. coli* culture is shifted from 30^{o}C to 42^{o}C, a 20-fold increase in the levels of GroEL can be observed (10). The molecular basis for this sharp induction resides in the presence of an

inducible promoter, found upstream of the constitutive σ^{70} promoter. The σ^{70} promoter ensures a low and constitutive level expression of the *groE* operon at all temperatures (444). The additional, inducible, promoter is recognized by the alternative sigma factor σ^{32} (or RpoH) (443). RpoH is a stress-responsive global transcriptional activator that recognizes the inducible promoters of several heat shock genes such as *dnaK, lon, clpP, htpG,* and *grpE*, whose gene products are all involved in relieving stress (443). The levels of RpoH, in turn, are regulated by two mechanisms. The first is a post-transcriptional mechanism in which the translation of *rpoH* mRNA is activated simply by a temperature-induced change in RNA secondary structure that facilitates translation initiation (289,443), The second is mediated by DnaK, a normally abundant chaperone that captures RpoH facilitating its degradation (443). Upon heat-shock, which results in extensive protein denaturation, unfolded proteins sequester DnaK, thereby releasing RpoH, which is then free to induce the heat shock genes (443). The *groE* operons of gamma proteobacteria (which includes *Legionella* spp.) are mainly regulated by similar RpoH-dependent mechanisms (369).

1.3.4. Accessory Function of Bacterial Chaperonins

Chaperonins were initially characterized as strictly cytoplasmic proteins because of their large molecular size, complex structural organization, and lack of known secretion signals. However, the protein-folding paradigm of bacterial chaperonins has changed with accumulating evidence that some bacterial chaperonins are found in extracytoplasmic locations. The extracytoplasmic chaperonins perform diverse cellular functions that are unrelated to their role in protein folding. Because part of my thesis is

focused on the protein folding-independent functions of the *L. pneumophila* chaperonin, I will provide here a short introduction on this subject and give example of some unique chaperonins functions found in several bacteria. In particular, I will focus on pathogenesis and will provide examples of chaperonins that play a role in attachment to host cells, stimulation of the host immune system, and maintenance of bacterial endosymbioses.

Several pathogenic bacteria display the chaperonin (GroEL) on the bacterial cell surface. The surface-associated chaperonins can perform several functions, including the enhancement of bacterial attachment to and invasion of host cells. For instance, the surface-exposed GroEL of *Mycobacterium avium* (331), *Helicobacter pylori* (47,437), *Chlamydia* sp (154,222,223), and *Clostridium difficile* (167), are involved in attachment to cells. The GroEL of *Salmonella enterica* serovar Typhimurium facilitates bacterial aggregation and binding to the intestinal mucosa (94). GroEL from *Haemophilus ducreyi* (309) and that of *Borrelia burgdoferi* (220) enhance attachment to host cells via binding to glycosphingolipids. The surface associated GroEL of *Brucella abortus* binds to cellular prion protein (PrP^c) and mediates entry of bacterium into host cells (424). Finally, GroEL found on the surface of the probiotic bacterium *Lactobacillus johnsonii* is involved in attachment to the intestinal mucus and epithelial cells.(25). These findings indicate that enhancing bacterial attachment to its host is one of the main functions of surface-associated chaperonins.

During the past few years, it has become clear that GroEL can be secreted from bacterial cells. As free soluble proteins secreted chaperonins can interact with a variety of cell types including epithelial endothelial, vascular and white blood cells, and activate

key cellular activities such as the synthesis of cytokines and adhesion proteins (236). These effects are mainly achieved through the interaction of free soluble chaperonins with eukaryotic cell surface receptors.

An important element of the surveillance and protection function of innate immune cells is the pattern recognition receptors (PRRs) that are present on the surface or in the cytoplasm of innate immune cells. Toll-like receptors (TLRs), present on the macrophage cell surface, recognize microbe-associated membrane patterns (MAMPs) such as LPS, peptidoglycan, microbial nucleic acids, lipoproteins and flagellin (2,243). Several studies demonstrate the ability of chaperonins to modulate host cell responses by acting as cellular signalling molecules via binding to TLRs (40,41,360,415). It has been shown that TLR2 and TLR4 can recognize the *Chlamydia* and human chaperonins (415). However, Bulut et al. (40) and Sasu et al. (360) demonstrated that chlamydial GroEL can interact only with TLR4, and not with TLR2. Mycobacterial and chlamydial chaperonins have been shown to activate signalling pathways via TLR4 to induce NF-kB activation (40,41). Additionally, Kol et al. (237) found that human Cpn60 and chlamydial GroEL activate human monocytes through CD14 signalling, a pathway shared by LPS. Purified bacterial chaperonins from *E. coli, Mycobacterium leprae*, and *Mycobacterium bovis,* can also act as signalling molecules. These chaperonins increase the levels of pro-inflammatory cytokine mRNA in macrophages (339,340), while purified GroEL from *M. tuberculosis* (123), and *C. trachomatis* (236) enhance the production of pro-inflammatory cytokines, such as IL-6, IL-8 and TNF-α, by monocytes. In addition to their function as immunostimulatory molecules of cytokines, chaperonins are also involved in activating cellular pathways that enhance cell adhesion and proliferation. For instance, GroEL from

E. coli (129) and *C. trachomatis* (236) can stimulate human vascular endothelial cells (HUVECs) to produce multiple adhesion molecules. Additionally, the GroEL *of Bartonella bacilliformis* induces the proliferation of HUVECs (282), and the GroEL from *C. pneumoniae* stimulates proliferation of human vascular smooth muscle cells via TLR4 and p44/42 mitogen-actvated protein kinase (MAPK) activation (360).

Several unique functions have been described for the chaperonins of endosymbiotic bacteria. These functions have been attributed to the effect of a few amino acid changes of the GroEL of these bacteria compared to the *E. coli* GroEL. Yoshida et al. (326) have shown that the GroEL from endosymbiotic *Enterobacter aerogenes* acts as an insect toxin. This toxic GroEL differs from the non-toxic GroEL from *E. coli* by eleven amino acids, four of which are critical for insect toxicity. In fact, the *E. coli* GroEL also becomes an insect toxin when these four residues are engineered to exactly match the amino acid sequence of the *E. aerogenes* GroEL (326). In *Buchnera aphidicola* (an aphid endosymbiont), GroEL is constitutively overexpressed and accounts for 10% of all protein produced, with only a small increase upon exposure of bacteria to high temperature (99). Amino acid sequence analysis of the *Buchnera* GroEL revealed specific amino acid substitutions in key positions within the peptide- and GroES-binding apical domains (99). It is thought that *Buchnera* GroEL has suffered an accelerated rate of amino acid substitutions after the symbiotic integration of *Buchnera* into the aphids. These amino acid changes are thought to enhance GroEL interaction with GroES, and with the *Buchnera* proteome , which is unstable due to increased mutation rates in its geneome (100). It is also thought that through these amino acid changes, the GroEL of *Buchnera* has acquired phosphotransferase activity as a novel histidine kinase (288).

Therefore, the constitutive overexpression of GroEL and the action of positive selection on the evolution of GroEL suggest that GroEL is responsible for the maintenance of the endosymbiotic lifestyle by buffering against the accumulation of slightly harmful mutations in the *Buchnera* genome (100). Finally, GroEL is speculated to perform functions related to root-nodulation and nitrogen-fixation in many endosymbiotic rhizobiae and nodulating bacteria such as *Sinorhizobium meliloti* and *Rhizobium leguminosarum* that have five and three copies of the *groEL* gene, respectively. (264). It is unclear why these endosymbionts require several chaperonins, but genetic studies have indicated that only one copy (thought to maintain the protein folding function) is essential (345), suggesting that rhizobiae could use the additional chaperonins to achieve different functions (142,146). Overall, the examples presented above strongly support the notion that few changes in amino acid in the bacterial chaperonins sequence can alter or add additional functions.

1.3.5. Historical Perspective of HtpB as an Unusual Chaperonin

A comprehensive review about HtpB can be found in reference (136). HtpB was first investigated because of its immunodominant properties (126), since HtpB was one of the most prominent antigens recognized by sera from patients with LD. Gabay and Horwitz (126) characterized HtpB as the major cytoplasmic membrane protein of *L. pneumophila*. A number of publications reported the existence of a 60 kDa antigen in many bacterial species that was referred to as the "common antigen" (383,384). Similarly, HtpB was also named a common antigen because the antibodies used to identify HtpB as a 58 kDa protein in immunoblots cross reacted with 60-kDa antigens

from several *Legionella* species and other bacteria (324). Because of its immunodominant properties, the role of HtpB was investigated in Guinea pigs. Immunization of Guinea pigs with HtpB induced a strong humoral immune response (30), however this response was not good enough to provide protection against a subsequent lethal challenge with *L. pneumophila* (427). Subsequently, *htpB* was cloned and its DNA sequence was determined by Hoffman et al. (177,178). They demonstrated by Southern blot that the genome of *L. pneumophila* bears only one copy of *htpB* (177). The *htpB* gene is part of an operon, where it is located downstream of the co-chaperonin gene *htpA* (177,178). Amino acid sequence analysis indicated that HtpB is a 548 amino acid chaperonin with a molecular weight of approximately 62 kDa. HtpB displays high degrees of identity and similarity (73.3%, 85%, respectively) to the *E. coli* GroEL (178). In agreement with the findings of Gabay and Horwitz (126), Hoffman et al. (178) also demonstrated that HtpB is one of the most abundant proteins detected in *L. pneumophila* under normal conditions with only a 2-fold increase upon heat shock. Conversely, the *E. coli*, GroEL is present in low levels under non-heat shock conditions and exhibits a more dramatic increase (~10-fold) after heat shock (178). Hoffman et al. (126) showed, by immunofluorescent microscopy, that HtpB is strongly detected on the surface of the virulent *L. pneumophila* strain SVir. In contrast, HtpB was weakly detected on the surface of the salt-tolerant avirulent derivative Avir strain. In a detailed ultrastructural study based on immunogold electron microscopy, using both polyclonal and monoclonal antibodies against HtpB, Garduno et al. (137) reported that ~58 % of the total *L. pneumophila* HtpB epitopes were extracytoplasmic (associated with the outer membrane and/or in the periplasm), ~26 % in

the cytoplasm, and an additional ~16 % localized to the cytoplasmic membrane In contrast, the *E. coli* GroEL was exclusively found in the cytoplasm.

The above unique characteristics of HtpB encouraged investigators from the Hoffman Laboratory to broadly investigate the role of HtpB in *L. pneumophila* virulence. Indeed, those investigators provided several lines of evidence that HtpB might have virulence-related roles. These include (i) the surface-associated HtpB-mediated attachment to and invasion of HeLa cells (139), (ii) the upregulated expression of HtpB upon contact with L929 murine cells or human monocytes (107). and the high levels of HtpB expression are maintained during the course of intracellular infection (107), leading to its accumulation in the lumen of the LCV (137), (iii) the increased production of HtpB by *L. pneumophila* within L929 cells and monocytes correlates with virulence because spontaneous salt-tolerant, avirulent mutants of *L. pneumophila* are unable to upregulate the expression of HtpB upon contact with these cells (107), and (iv) the mature infectious forms (MIFs), thought to be the natural transmissible forms of *L. pneumophila,* display increased amounts of envelope and surface-associated HtpB, compared to agar-grown bacteria (138). Together, these observations indicate suggest that HtpB is an unusual chaperonin, present in unusual cellular locations, that may play an important role in intracellular establishment of *L. pneumophila.*

1.4. Rationale, Hypothesis and Objectives

The fundamental functions of chaperonins are to assist other proteins to fold properly after translation, protect proteins from denaturation, and help denatured proteins to refold after stress. Many reports have suggested that bacterial chaperonins, including

HtpB, may have virulence-related functions. The best approach to establish a definitive role of HtpB in virulence would be genetic studies performed with *L. pneumophila* deletion mutants lacking *htpB*. However, because chaperonins are widely accepted to be essential for bacterial survival (103,444), no one has previously attempted to generate an *htpB* deletion mutant. Instead, our lab developed different functional models to characterize the possible role of HtpB in *L. pneumophila* pathogenesis.

A former graduate student in our lab (Dr. Angella Riveroll) expressed HtpB in the cytoplasm of *Saccharomyces cerevisiae*. She showed that HtpB induces pseudohyphal growth (PHG) in *S. cerevisiae* via a Ras2-activated signalling pathway, a phenotype that cannot be induced by HtpB homologs from *E. coli* (GroEL), or *S. cerevisiae* (Hsp60p) (63,341). Dr. Riveroll suggested that this induction of PHG by HtpB occurs via interaction with a *S. cerevisiae* protein(s). Another former graduate student in our lab (Dr. Audrey Chong) showed that HtpB, but not GroEL, is involved in reorganization of actin filaments when expressed in the non-phagocytic cell line CHO. She also showed that HtpB-coated beads mimic the ability of virulent *L. pneumophila* to attract mitochondria when added to CHO cells and U937 human-derived macrophages (63,65). Furthermore, Dr. Chong showed, using immunogold electron microscopy, that abundantly released HtpB in the LCV of infected macrophages can reach the cytoplasmic face of the LCV. She also showed that HtpB can reach the cytoplasm of infected CHO cells and proposed that in this compartment, HtpB might interact with mammalian host protein(s). The interaction of HtpB with host cell proteins might lead to mitochondrial attraction to the LCV and reorganization of actin filaments. The multiple functions observed for HtpB and the fact that some of these functions are related to virulence, proved an involvement of

HtpB in *L. pneumophila* pathogenesis *in vivo*, and opened an experimental need to identify host protein targets for HtpB. Therefore, my thesis work was focused on these aspects of HtpB research.

I proposed that the intracellularly released-HtpB recruits or interacts with an eukaryotic partner protein(s) that would be identifiable by the yeast two hybrid method. Furthermore, I hypothesized that the interaction of HtpB with this partner protein would trigger a specific intracellular eukaryotic signaling cascade (as opposed to an extracellular cascade mediated by surface receptors) responsible for the aforementioned intracellular changes directed by HtpB.

According to the aforementioned findings and rationale, the specific objectives of my research project are as follows:

I- To specifically assess the role of HtpB in *L. pneumophila* pathogenesis *in vivo* by constructing an *htpAB* deletion mutant in the presence of the *groE* operon (Chapter 3).

II- To determine whether HtpB can reach the cytoplasm of infected macrophages using the CyaA reporter assay (Chapter 4).

III- To identify the putative eukaryotic targets for HtpB using the yeast two-hybrid system (Chapter 4).

IV- To characterize the identified HtpB eukaryotic target protein and its functional effects on *L. pneumophila* intracellular growth (Chapters 4 and 5).

CHAPTER 2: MATERIALS AND METHODS

Materials and methods used in more than one Chapter will be described under the common Materials and Methods section (Section 2.1). Specific sections are designated to describe the materials and methods used only in Chapter 3 (Section 2.2), Chapter 4 (Section 2.3), and Chapter 5 (Section 2.4).

2.1. Common Materials and Methods

2.1.1. Strains and Growth Conditions

Bacterial and yeast strains used in this study are described in Table 1. *L. pneumophila* strains were grown at 37°C on buffered charcoal yeast extract agar (BCYE) (311), or at 37°C with agitation (200 rpm in a New Brunswick C25KC shaker incubator) in buffered yeast extract broth (BYE). BCYE and BYE were supplemented with streptomycin (100 µg/mL) and, for growth of Lp02, with thymidine (100 µg/mL). The defined medium (DM) of Pine et al. (323) was also used, but without choline. Media ingredients and antibiotics were obtained from Sigma-Aldrich (St Louis, MO), MP Biomedicals (Santa Ana, CA–previously ICN Biomedicals), Fisher Scientific (Fair Lawn, NJ), or BDH (Toronto, ON). *Escherichia coli* strains were grown at 37°C on Luria-Bertani (LB) agar (357), or at 37°C with agitation (as above) in LB broth. Bacterial transformants harbouring the plasmids listed in Tables 2 and 3 were grown in culture media containing the appropriate antibiotics. For selection of *L. pneumophila* transformants, the following antibiotic concentrations were used: 100 µg/mL

streptomycin, 10 µg/mL gentamicin (Gm), 40 µg/ml kanamycin (Km), 20 µg/mL metronidazole (Mtz), and 4 µg/mL chloramphenicol (Cm). For DH5α, 100 µg/mL ampicillin, 40 µg/mL Km, 10 µg/mL Gm, or 20 µg/mL Cm were used. Long term storage of bacteria was done at −70°C in nutrient broth containing 10% dimethylsulfoxide (357).

2.1.2. Molecular Techniques

2.1.2.1. Isolation of *L. pneumophila* Genomic DNA

Genomic DNA was isolated from 3 mL of *L. pneumophila* grown overnight in BYE. Bacterial cells were collected by centrifugation (15,000 x *g*, 2 min) and resuspended in 440 µl of Tris-EDTA buffer (TE) (10 mM Tris-HCl pH 8.0 and 1 mM EDTA pH 8.0). Fifty microliters of proteinease K (10 mg/mL in 50 mM Tris-HCl pH 8.0 and 1 mM $CaCl_2$) and 10 µl of 10% sodium dodecyl sulfate (SDS) were added. After 1-2 h incubation at 37°C with gentle rocking, the mixture was sequentially extracted with equal volumes (500 µl) of: i) buffer-saturated phenol; ii) phenol/chloroform 1:1 (v/v); and iii) chloroform/isoamyl alcohol 24:1 (v/v). Between each extraction step, samples were subjected to centrifugation (15,000 x *g,* 10 min, 4°C) and supernatants were transferred to clean microcentrifuge tubes. The genomic DNA was then precipitated overnight at -20°C with 0.1 volumes of 0.3 M sodium acetate pH 5.0 and 2 volumes of absolute ethanol. Precipitated DNA was washed with ice-cold 70% ethanol, and air dried (for ~10 min). Genomic DNA was resuspended in 100 µL TE buffer, quantitated by spectrophotometry at 280 nm, and stored at 4°C until use.

2.1.2.2. Plasmid and DNA Purification

Bacterial plasmids and yeast shuttle vectors used in this study are described in Tables 2 and 3, respectively. Plasmid purification from *E. coli* DH5α was performed with the Spin Miniprep or Midiprep kit (QIAGEN, Mississauga, Ontario, Canada). Isolation of DNA fragments from agarose gels was carried out with a QIAquick gel purification kit (QIAGEN). Constructed plasmids were verified by DNA sequence analysis carried out by DalGen (Dalhousie University, NS, Canada), or Genome Quebec (McGill University, Quebec, Canada).

2.1.2.3. Polymerase Chain Reaction (PCR)

PCR amplifications were performed on a T-personal thermal cycler (Biometra, Germany) using *Taq* DNA polymerase (MBI Fermentas) or Platinum *Pfx* DNA polymerase (Invitrogen) using the buffers and conditions provided by the supplier. The following standard PCR conditions were used unless indicated otherwise: 94°C (5 min), followed by 30 cycles of 94°C (30 s), 55°C (30 s), and 72°C (1 min per kb of PCR amplification product), and a final extension at 72°C for 7 min. PCR primers (Table 4) were synthesized by Integrated DNA Technologies, Inc. (Coralville, IA).

2.1.2.4. T/A Cloning and DNA Ligation

T/A cloning was used to clone PCR amplicons (amplified by the*Pfx* DNA polymerase) into a bacterial plasmid (pBluescript) (357). The PCR amplification products were incubated with *Taq* polymerase (2.5 U enzyme/100 μL volume) (MBI Fermentas) in 1X buffer (MBI Fermentas) containing 2 mM dATP (Invitrogen) for 2 h at 72°C,

followed by gel extraction purification. pBluescript was digested with *Eco*RV (New England Biolabs), and then dTTPs (Invitrogen) were added to the plasmid as described above.

DNA ligations were performed using T4 DNA ligase (NEB) at 14°C overnight. An insert/vector ratio of 5:1 was used. Ligation reactions consisted of the appropriate volume of insert and vector DNA, 1 μL of T4 DNA ligase, 2 μL of 10X T4 DNA ligase buffer (New England Biolabs) with the final volume adjusted to 10 μL with sterile ddH_2O.

2.1.2.5. Preparation of Electrocompetent *E. coli* DH5α Cells

Ten mL of *E. coli* DH5α cultures were grown overnight at 37°C with agitation (200 rpm). These bacteria were diluted 1:20 into pre-warmed LB broth and grown to an OD_{620} of ~0.6. Bacterial cells were harvested by centrifugation (3,000 x *g*, 15 min, 4°C). The cells were washed twice with ice cold ddH_2O, and resuspended in 50 mL of cold 10 % glycerol, washed in 50 mL 10 % glycerol, and finally resuspended in 2 mL cold 10 % glycerol. The cells were stored at -70°C in 40 μL aliquots.

2.1.2.6. Preparation of Electrocompetent *L. pneumophila* Cells

Overnight lawns of *L. pneumophila* inoculated from a 3 day old BCYE plate culture with appropriate selection were harvested into 20 mL sterile ddH_2O and centrifuged at 3000 x *g* for 10 min at 4°C. The cells were resuspended in 20 mL of cold

10% glycerol, washed twice in 10 mL 10 % glycerol, and finally resuspended in 200 μL cold 10 % glycerol. The cells were stored at -70°C in 40 μL aliquots.

2.1.2.7. Bacterial Transformation by Electroporation

Glycerol-treated electrocompetent *E. coli* DH5α cells (stored at -70°C) were thawed on ice. One μL of plasmid DNA (~1 μg/μL) was added to the thawed cells and incubated on ice for 20 min. The DNA/cell mixture was transferred to a pre-chilled 2 mm gap electroporation cuvette, and transformed by electroporation at 2.5 kilovolt (kV) using a MicroPulser® (BIO-RAD laboratories Inc.). The cells were then transferred to 300 μL of pre-warmed LB broth and incubated at 37°C for 1 h with gentle agitation, then plated on LB agar with appropriate antibiotic selection (357).

L. pneumophila strains Lp02 and JR32 were transformed by electroporation as detailed by Viswanathan and Cianciotto (419). Five μL of plasmid DNA (~1 μg/μL) was added to the thawed glycerol-treated electrocompetent *L. pneumophila* cells (strains Lp02 and JR32) and incubated on ice for 20 min. The DNA/cell mixture was transferred to a pre-chilled 1 mm gap electroporation cuvette, and electroporated at 2.1 kV using a MicroPulser® (BIO-RAD laboratories Inc.). The cells were then transferred to 2 mL of pre-warmed BYE and incubated at 37°C for 3 h with gentle agitation. The cells were pelleted by centrifugation at 4500 x *g* for 5 min. The supernatant was removed, the cells gently resuspended with 125 μL of fresh pre-warmed BYE and plated onto BCYE agar at 5 μL, 10 μL, and 100 μL per plate with the appropriate selection. The plates were incubated at 37°C for 5-7 days. Colonies were replica plated and screened either by PCR or immunoblot analysis.

2.1.2.8. Protein Electrophoresis, Immunoblotting, and Densitometry

Bacterial cell pellets from 1-mL suspensions with an OD_{620} of 1.0 unit, were solubilized in 100 µL of Laemmli sample buffer, and 10 µL per lane were subjected to sodium dodecyl sulfate-polyacrylamide gel electrophoresis (SDS-PAGE) in a 12 % (w/v) acrylamide vertical slab mini-gel. For yeast samples, 10^8 pelleted cells (800 x *g* for 5 min) were resuspended in 200 µL of sample buffer containing the α-yeast protease inhibitor cocktail (Sigma), and mechanically broken by adding ~100 µL of acid-washed and baked glass beads (BT-5 high impact beads, 40-50 µm diameter, Supply America Company Inc., Norfolk, Virginia) and vortex mixing at 4°C for 15 min. Samples were then boiled for 5 min, unbroken cells and cell wall debris pelleted at 15,000 x *g*, and 10 µL of the supernatant per lane subjected to SDS-PAGE.

For immunoblotting (414), proteins resolved by SDS-PAGE were transferred onto nitrocellulose membranes using a BIO-RAD electrotransfer apparatus (Model Mini-Protean®II), and then immunostained with the appropriate primary monoclonal antibody (MAb) [GW2X4B8B2H6 (165) for HtpB, mtHsp60 MAb (Stressgen, Victoria, BC) for yeast mitochondrial Hsp60p, or GroEL MAb (Stressgen) for the *E. coli* chaperonin], or polyclonal in-house HtpB-specific rabbit serum (PAb) (65). All MAbs were diluted 1:1,000, and PAb 1:5,000, in Tris buffer solution (TBS) containing 0.1% (w/v) bovine serum albumin (BSA). Secondary antibodies were alkaline phosphatase conjugates of either anti-mouse or anti-rabbit IgG (Cedarlane Laboratories Ltd.) diluted 1:5,000 in TBS containing 0.1% (w/v) BSA. Densitometry of immunostained proteins was done as follows: To first visualize transferred proteins, nitrocellulose membranes were stained

with a 0.2% (w/v) solution of Ponceau-S (Allied Chemical Co., New York, NY) prepared in 3% (w/v) trichloroacetic acid, 3% (w/v) sulfosalicylic acid, and a reference digital image was acquired. Membranes were then immunostained and analyzed using the "single-band analysis" function of GelPro 2.0 software (Media Cybernetics Inc.). Values of optical density were corrected for differences in loading and electro-transfer efficiency, using the optical density data of three well-defined protein bands from the Ponceau-S-stained reference image.

2.1.3. Culture of Mammalian Cell Lines

Human U937 cells (a gift from Dr. Andrew Issekutz, Dalhousie University) or THP-1 derived macrophages (a gift from Dr. Robert Anderson, Dalhousie University)were routinely cultured as undifferentiated cells in suspension in RPMI-1640 (Gibco-Invitrogen Grand Island, NY) supplemented with 10% fetal bovine serum (FBS) (HyClone, Logan, UT), 2 mM L-glutamine (Gibco), 100 U/mL penicillin, and 100 μg/mL streptomycin and incubated at 37^{o}C in 5% CO_2. Before infection, U937 or THP-1 cells were induced to differentiate into adherent, macrophage-like cells with fresh medium containing 60 ng/mL phorbol 12-myristate 13-acetate (PMA, Sigma). PMA-activated U937 cells or THP-1 were washed three times with RPMI-1640 and transferred to 24 or 48-well plates (Falcon-BD Biosciences Canada, Mississauga, Ontario, Canada) at approximately 5 x 10^5 and 8 x 10^4cells/well, respectively. Mouse L929 cells (a gift from Dr. Spencer Lee, Dalhousie University) were routinely grown at 37^{o}C, 5% CO_2 in minimal essential medium (MEM) (Gibco), supplemented with 5 % FBS, 100 U/mL

penicillin, 100 μg/mL streptomycin, and 250 ng/mL amphotericin B (Gibco). Before infection, L929 cells were allowed to attach on 24-well plates at ~5 x 10^5 cells/well.

2.1.4. Intracellular Growth and Attachment Assay

Monolayers of L929 cells, THP- and U937-derived macrophages, or *A. Castellanii* (prepared as in Section 2.4.1) were seeded in 24 or 48-well plates as described above (in Section 2.1.3). *L. pneumophila* inocula were suspended in medium specific for each cell type (inocula preparation is described in detail in sections involving cell infection) and added to the wells of 24-well plates in duplicate or triplicate. The 24-well plates were centrifuged at 500 x *g* for 10 min to promote cell contact with bacteria, and then incubated for 90 min at 37°C in 5% CO_2 to allow internalization of legionellae by the cells. After infection, the inocula were removed and the monolayers were washed 2 to 4 times with warm PBS to remove free bacteria. Cells were then either lysed in 0.05% triton (vol/vol) to determine CFU/well (set as time 0 value, or to determine the number of attached bacteria), or replenished with MEM (for L929 cells), RPMI-1640 (for macrophages), or modified Neff's (for amoeba monolayers). Five μg/mL chloramphenicol and 1 mM IPTG were added to the above media if needed. To determine CFU/well at 24 and (or) 48 h post infection, the supernatant of the infected monolayers was removed, the cells were lysed with 0.05% Triton X-100 (vol/vol), and the supernatants and the lysates were combined. Bacterial cell counts were performed using ddH_2O as diluent, and plating onto BCYE agar with incubation for at least 3 days at 37ºC. The number of colony forming units (CFU) per well was then calculated.

2.1.5. Bioinformatic Analysis

DNA sequences of genes encoding known polyamine biosynthetic enzymes in *E. coli* and *Vibrio cholerae* (56,252,375,395) were obtained from GenBank®, at the National Center for Biotechnology Information (NCBI) website (http://www.ncbi.nlm.nih.gov). To identify *L. pneumophila* gene sequences similar to the obtained sequences of the *E. coli* and *Vibrio cholerae* genes encoding known polyamine biosynthetic enzymes, the nucleotide BLAST tool (NCBI website) was used to (ii) compare the obtained sequences from *E. coli* and *V. cholerae* against the four *L. pneumophila* genome sequences available from NCBI (Philadelphia-1, Lens, Paris and Corby), (ii) compare sequence similarity of the *potABCD* operon genes of the *L. pneumophila* Philadelphia-1 and *E. coli* K-12 strain. The BLAST search was optimized for the "somewhat similar sequences (blastn)" option. Additionally, the BLAST tool was used to identify yeast proteins encoded by the positive yeast two-hybrid (Y2H) library plasmids. The Genius Pro™ 5.3 (Biomatters Ltd, New Zealand) bioinformatics software was used for PotD amino acid sequence alignment.

2.1.6. Statistical Analysis

Statistical significance of differences between experimental values was assessed using the Student *t*-test, or the one or two-way ANOVA test, using Minitab software version 15.1.30.0 (Minitab Inc., State College, PA). *P* values less than 0.05 were considered to represent significant differences between groups.

2.2. Materials and Methods Used in Chapter 3

2.2.1. Construction of *L. pneumophila* LpgroE+ Strain

A schematic representation of the approach followed to create LpgroE+ strain is shown in Chapter 3 in Figure 7A. The non-functional *thyA* gene (encoding thymidine synthase) of Lp02 was targeted to be replaced with the *E. coli groE* operon. Allelic replacement of *thyA* with *groE* was performed using the counter selectable plasmid pBRDX (65,251,287) which consists of the pBOC20 backbone (carrying *cat* and *sacB*) with an added *rdxA* gene of *Helicobacter pylori*, encoding a nitroreductase capable of activating metronidazole to its bactericidal form (35). The regions flanking the *thyA* gene of *L. pneumophila* strain Lp02 were amplified by PCR. For the upstream region, primer pair thyAP1/thyAP2 was used to produce an amplicon of 611 bp (F1). For the downstream region, primer pair thyAP3/thyAP4 was used to produce an amplicon of 561 bp (F2). The F1 amplicon, cleaved at terminal *Not*I and *Spe*I restriction sites, and the F2 amplicon, cleaved at terminal *Spe*I and *Xho*I restriction sites, were ligated, sequentially, into appropriately cleaved pBlueScript KS to generate pBSF1/F2*thyA*. A DNA fragment of 5.2 kb containing the $lacI^q$ repressor and P_{trc} promoter (P_{tac} IPTG inducible promoter) upstream of the *groE* operon and the kanamycin resistance (Km^R) cassette (*km3*) [$lacI^q$-P_{tac}:*groE-km3*] was amplified by PCR from plasmid pTrcKm (4) using primer pairs (Ptrc99F and Ptrc99R). In pTrcKm, the *groE* operon expression is driven by the P_{tac} promoter, while the Km^R cassette expression is driven by its own promoter. The $lacI^q$-P_{tac}:*groE-km3* (named *groE-km*) amplicon was cleaved at flanking *Spe*I sites was ligated into the *Spe*I site of pBSF1/F2*thyA* to create pBSΔ*thyA*:*groE-km3.* Subsequently, the 6.3 kb Δ*thyA*:*groE-km3* fragment, which is flanked upstream by the *Not*I restriction site of F1

and downstream by the *Xho*I restriction site of F2,was subcloned into the *Not*I and *Xho*I sites of pBRDX (Fig. 7A). The resulting plasmid, pBRDXΔ*thyA*:*groE-km3* (Fig. 7A), was introduced into Lp02 by electroporation as detailed in Section 2.1.2.7. The allelic recombinants (potential Δ*thyA* mutants) were selected from a population of Km^R resistant colonies by replica plating onto a medium containing 5% (wt/vol) sucrose (Suc) or 20 μg/mL metronidazole (Mtz). Plasmid loss was confirmed by testing for the loss of chloramphenicol resistance (Cm^R). The Km^R, Suc^R, Mtz^R, and Cm^S Lp02 colonies were screened by PCR for the absence of the *thyA* gene using thyAF and thyAR internal primers. The expression of GroEL from the potential Δ*thyA* mutants was confirmed by immunoblot using monoclonal antibody MAb specific to GroEL as described in Section 2.1.2.8. The newly constructed Lp02 strain (Δ*thyA, groE*$^+$) used for further work was named LpgroE+.

2.2.2. Attempt to Delete *htpAB* from *L. pneumophila* Strain LpgroE+

A schematic representation of the approach followed to attempt the construction of a Δ*htpAB* mutant in LpgroE+ is shown in Chapter 3, in Figure 8A. Allelic replacement of *htpAB* with a Gm^R cassette was attempted using the counter-selectable plasmid pBRDX as described in Section 2.2.1. Briefly, 700 bp of upstream and 620 bp downstream flanking DNA sequences of the *htpAB* of *L. pneumophila* Lp02 were amplified by PCR using the primer pairs P1/ P2 (for the upstream or F1 region) and P3/P4 (for the downstream or F2 region). The F1 amplicon cleaved at the terminal *Not*I and *Bam*HI restriction sites and the F2 amplicon cleaved at the terminal *Bam*HI and *Xho*I restriction sites were ligated sequentially into the appropriately cleaved pBluescriptKS to

generate pBS:F1F2*htpB*. A 650 bp DNA fragment containing a gentamicin resistant (Gm^R) cassette was cleaved at flanking *Bam*HI sites from plasmid pPH1J1 (175) and ligated into the *Bam*HI site between the F1 and F2 of pBS:F1F2*htpB* to generate pBS:F1-*gm*-F2*htpB*. Subsequently, the F1-*gm*-F2*htpB* fragment (1920 bp), flanked upstream by the *Not*I restriction site of F1 and downstream by the *Xho*I restriction site of F2,wassubcloned into the *Not*I and *Xho*I sites of pBRDX to generate pBRDXΔ*htpAB*:*gm* (Fig. 8A), which was then electroporated into *L. pneumophila* strain LpgroE+ as described in Section 2.1.2.7.. The allelic recombinants (potential LpgroE+Δ*htpAB* mutants) were selected as described in Section 2.2.1.

2.2.3. Attempt to Delete *htpAB* from *L. pneumophila* Strains JR32 and Lp02

A schematic representation of the approach followed to attempt theconstruction of a Δ*htpAB* mutant in *L. pneumophila* strain Lp02 or JR32 using a Km^R cassette is shown in Figure 9A (Chapter 3). An attempt to delete *htpAB* from the parent strains JR32 or Lp02 was made using the same primers, cloning method, and selection strategies described above (Section 2.2.3) to construct pBRDXΔ*htpAB*:*gm,* except the Km^R cassette from plasmid p34S-*km3* (86) (restricted by *Bam*HI) was used instead of the Gm^R cassette (shown in Fig. 9A).The new plasmid pBRDXΔ*htpAB*:*km3* was electroporated into strains Lp02 and JR32 as described in Section 2.1.2.7. The allelic recombinant colonies (potential JR32Δ*htpAB* or Lp02Δ*htpAB* mutants) were selected and screened as described in Section 2.2.1

2.2.4. Southern Blot

Chromosomal DNA from *L. pneumophila* strain Lp02 or LpgroE+ was isolated by phenol/chloroform extraction as described in Section 2.1.2.1. The isolated DNA was digested with various restriction enzymes and subjected to electrophoresis on a 0.8% agarose gel. The DNA was transferred onto a nylon membrane (Hybond^{Tm}-N+ membrane, Amersham Pharmacia Biotech) by placing the nylon membrane on the top of a stack of paper towels, then placing the gel on top of the nylon membrane. Pressure was evenly applied to the gel by placing 3 sheets of filter paper and a 0.5 kg weight on top of the gel. Suction solution (0.4 M NaOH) drawn through a filter paper wick was passed through the gel into the stack of paper towels to enhance DNA transfer from the gel onto the nylon membrane. After DNA transfer for a minimum of 2 h, the nylon membrane was separated from the gel and soaked in 2 x SSC buffer for 5 min. The nylon membrane was then placed between 2 pieces of filter paper and the DNA was immobilized by microwaving for 30 s. Three different DNA fragments were amplified by PCR from template genomic DNA of strain Lp02 to be used as probes: (i) F1htpAB (700 bp), using primers P1 and P2, (ii) the Gm^R cassette (250 bp), using primers gmF and gmR, and (iii) *htpB* (750 bp), using primers htpBF and htpBR. The amplified probes were subjected to 0.8 % agarose gel electrophoresis, purified from the gel using the QIAquick gel purification kit (QIAGEN), and labelled using the DIG-High Prime DNA Labelling and Detection Starter Kit–I (Roche Applied Science). DNA hybridization with the probes and probe detection were done as described in the kit manual.

2.3. Materials and Methods Used in Chapter 4

2.3.1. Strains and Growth Conditions

Bacterial and yeast strains used in Chapter 4 are described in Table 1, while bacterial plasmids and yeast shuttle vectors are described in Tables 2 and 3, respectively.

S. cerevisiae strains were cultured at 30°C on YEP-Dextrose (YEPD) agar [per litre: 10 g yeast extract, 20 g peptone, 20 g agar, and 100 mL of 20 % (wt/vol) dextrose], YEP-Galactose agar, which has the same formula as YEPD, but galactose is substituted for dextrose, or Synthetic Complete (SC) medium [per litre: 1.7 g YNB without amino acid, 10 g succinic acid, 6 g NaOH, 2 g $(NH_4)_2SO_4$, 100 mL of 20 % (wt/vol) dextrose, 20 g agar, and 10 ml of 0.2 (wt/vol) of the following supplements: arginine, histidine, leucine, isoleucine, lysine, methionine, phenylalanine, tryptophan, tyrosine, threonine, valine, adenine, and uracil,] or synthetic defined (SD) medium (which has the same formula as SC, but lacks amino acids or purine and pyrimidine bases) was used to select and grow plasmid-carrying prototrophs (155,341). To induce expression of genes cloned into pEMBLyex4 or pPP389 (under the control of a galactose-inducible promoter, dextrose was substituted by galactose in SD medium. Yeast strains were stored at –70 °C in SD liquid medium with 10% glycerol.

2.3.2. Construction of Plasmids

Translocation assay constructs: N- and C-terminal *htpB* fusions to *cyaA* (encoding the calmodulin-dependent *Bordetella pertussis* adenylate cyclase subunit) were constructed in pJC158 (59) by Audrey Chong (62). I used plasmids pAC17, pAC2, pJC158, and pJC203 (all derivatives of pMMB207C) described in Table 2.

Constructs for protein expression in yeast: The plasmids used for expression of chaperonins in yeast under the control of a galactose-inducible promoter were constructed by Angela Riveroll (341). These constructs, pEMBLyex4::*htpB,* pEMBLyex4::*groEL,* pEMBLyex4::*HSP60,* pEMBLyex4::*hsp60*Δ1-72, pPP389::*htpB*, pPP389::*HSP60* and pPP389::*hsp60*Δ1-72 (all derivatives of pEMBLyex4), are listed in Table 3 only as a reference. The open reading frame of *SPE2* (1191 bp), encoding yeast SAMDC, was amplified by PCR using primers SPE2-F and SPE2-R on template genomic DNA of *S. cerevisiae* strain 21R, and ligated into the *Pst*I and *Bam*HI sites of pPP389 to create pPP389::*SPE2*.

Yeast two-hybrid bait: Plasmid pGBD-C1::*htpB* encoding the GAL4 DNA binding domain fused at the N-terminus of HtpB (GAL4DBD-HtpB) was constructed by Angela Riveroll (341).

2.3.3. Yeast Transformation

Lithium acetate transformation was used to introduce yeast shuttle vectors into yeast cells according to a standard protocol (144). A culture of *S. cerevisiae* cells was grown overnight to a density of 2 x 10^7 cells/mL (enumerated in a Coulter particle counter, ZM, Coulter Electronics, Mississauga, Ontario) in YEP-Dextrose. Approximately 2 x 10^8 cells were harvested by centrifugation and resuspended to 2 x 10^6 cells/mL in 100 mL pre-warmed YEP-Dextrose medium and grown to a final density of 2 x 10^7 cells/mL. The freshly grown cells (~10^9) were washed with 10 mL ddH_2O, resuspended in 1 mL ddH_2O and transferred to 1.5 mL microcentrifuge tube. The cells were then washed with 1 mL of freshly diluted 1X TE/lithium acetate solution [100 mM

lithium acetate in 1 X TE (0.01 M Tris-HCl, 0.01 M EDTA), pH 7.5] and resuspended to a cell density of ~2 x 10^9 cells/mL in 1X TE/lithium acetate. Fifty µL of the yeast cell suspension was mixed with 1 µg transforming DNA, 50 µg single stranded salmon sperm DNA and 300 µL polyethylene glycol (PEG 3350) solution (50 % PEG (w/v) in 10X TE/lithium acetate solution). The cells were then washed and incubated at 30°C with agitation for 30 min. The cells were heat shocked at 42 °C for 15 min and were then pelleted by centrifugation at 4000 x *g* for 5 min. The cells were then resuspended in 1X TE and plated onto appropriate selective media.

2.3.4. Rapid Plasmid Isolation from Yeast

Two mL of overnight broth-grown yeast cells were pelleted and resuspended in 200 µL of solution I (100 mM NaCl, 10 mM Tris-HCIpH 8.0, 1 mM EDTA, 0.1% SDS, w/v). Acid-washed glass beads (0.4 mm diameter, sterilized at 160°C overnight) were added until just below the level of the liquid and vortexed at maximum speed for 2 min. 200 µLice cold solution II (0.2 M NaOH, 1% Triton X-100, w/v) was then added. Following a 5 min incubation on ice the sample was then treated with an equal volume of phenol-chloroform-isoamyl alcohol (25:24:1, v/v). This mixture was briefly vortexed and centrifuged for 2 min. The aqueous upper phase was transferred to a clean tube and used to electroporate electrocompetent DH5α.

2.3.5. Pseudohyphae Formation and Invasive Growth

Yeast cells grown at 30°C with agitation (150 rpm) in YEP-Dextrose or SD medium with 2% dextrose, including appropriate selection, were harvested in exponential

phase. Cells (~10^7) were washed in water, diluted to 10^{-3}, 10^{-4}, 10^{-5} and 10^{-6} in inducing medium, spotted in duplicate 100 µL drops on solid inducing medium plates, and incubated at 30°C in a humid chamber. Cell elongation and unipolar budding were scored 15 to 20 h after inoculation (while the inoculum drops were still wet) by light microscopy using the 40X objective of a Nikon DIAPHOT-TMD inverted microscope. To test for invasive growth, plates were incubated for five days, surface-washed with a stream of ddH_2O, and observed as above. Photographs were captured with a Nikon 2000 camera using 35-mm Fuji film, or digitally with a Pro-series monochrome camera and Image-Pro 4.0 software (Media Cybernetics Inc., Silver Springs MD).

2.3.6. Yeast Two-Hybrid Screen of Yeast Genomic Library

Plasmid pGBD-C1::*htpB* was transformed into strain Y153 and expression of the *GAL4DBD::htpB* gene fusion was confirmed by immunoblot (Fig. 14, Chapter 4) using monoclonal antibody GW2X4B8B2H6 (165), directed against HtpB. Y153 harboring pGBDC-1::*htpB* was grown overnight in SD medium lacking tryptophan at 30°C with shaking and harvested by centrifugation. Cells (~5 x 10^9) were resuspended in 1 L of prewarmed YPE-Dextrose and incubated at 30°C for 4 h with shaking until the cell concentration was 2 x 10^7 per mL. Cells were harvested by centrifugation, and the pellet was washed twice with cold dH_2O, and 100 mM lithium acetate. Then, 100 µl (~1 µg/µL w/v) of the yeast genomic DNA plasmid library (a combination of pGAD-C1:DNAx, pGAD-C2:DNAx, and pGAD-C3::DNAx constructs) was transformed into strain Y153 harboring pGBDC-1*::htpB*. Transformants were plated on triple-dropout SD medium (TDO) lacking leucine and tryptophan (to select for transformants), and histidine (to

screen for potential interactions via activation of the *HIS3* reporter gene). 3-aminotriazole (30 mM) (Sigma) was added to the TDO medium to suppress potential false expression of *HIS3* reporter gene (207). Plates were incubated for 4-5 days at 30^{o}C before a β-galactosidase filter assay (71) was performed to screen for potential interactions leading to the activation of *lacZ*. For the filter assay, transformants (producing colonies of at least 2 mm) were streaked into new TDO plates containing 3-aminotriazole and incubated for 3 days at 30^{o}C. Nitrocellulose filters were then used to lift the cells from plates and were plunged into liquid nitrogen for 15 seconds, followed by 5-min thawing at room temperature. This freeze-thaw cycle was repeated 3 times. The filters were placed on a circle of filter paper soaked with Z-buffer containing 1 mg/ml X-gal (Sigma) and incubated at 30^{o}C for 1 hour. Streaks with blue color were considered positives for interaction. The corresponding library plasmids from these positive clones were isolated and transformed into *E.* coli strain DH5α for plasmid amplification. The amplified plasmids were isolated and sent for DNA sequence determination (Dal-Gen) of the yeast library DNA fragment. The BLAST-P algorithm (8) was used to identify proteins encoded by the positive Y2H library fragments.

2.3.7. Yeast Two-Hybrid Screen of a HeLa cDNA Library

The haploid yeast strain Y187 was the host strain for the MATCHMAKER GAL4 HeLa cDNA library (BD Bioscience, Palto Alto, CA). The HeLa cDNA library was cloned into plasmid pGADT7-Rec to create plasmids that encode Gal4-AD-HeLa cell fusion proteins. (For simplicity, the HeLa library plasmid was named pGADT7::cDNAx). For the Y2H assay, the yeast strains Y187, bearing the cDNA library and strain AH109,

bearing plasmid pGBD-C1::*htpB* and were mated and diploids selected by plating on SD medium with appropriate supplements as described in the MATCHMAKER two-hybrid system user manual (71). Blue colonies that grew on media lacking leucine and tryptophan (to select for the mated AH109-Y187 diploid strains), and lacking histidine and adenine (to select for positive interaction via activation of *HIS3* and *ADE2* reporter genes), and supplemented with X-α-gal (to select for positive interaction via activation of *MEL1* reporter gene) were considered to express HeLa cell proteins that interacted with HtpB. The pGADT7::cDNAx library plasmids were isolated from the positive clones, and the putative proteins encoded by the HeLa cDNA(s) carried on the positive Y2H plasmids were identified as described in 2.3.6.

2.3.8. Translocation Assays

L. pneumophila strains Lp02 and JR32 carrying plasmid pAC17, pAC2, pJC203, pJC158, or pMMB207C, were grown to mid-exponential phase (EP) (OD_{620} ~1.5 to 2.0) at 37^{o}C in BYE containing 5 μg/mL chloramphenicol, and treated with 1 mM IPTG, for at least 2 h, to induce expression of the plasmid-encoded proteins. Bacteria were then pelleted and resuspended in αMEM with 5% FBS, 5 μg/mL chloramphenicol, and 1 mM IPTG before infecting CHO-*htpB* cells at a bacteria:cell ratio of ~600:1. Doxycycline (10 ng/mL) was maintained throughout the assays with CHO-*htpB* cells to repress expression of HtpB (65). For infection of U937-derived macrophages, bacteria were resuspended in RPMI-1640 with 10% FBS, 1% glutamine, 5 μg/mL chloramphenicol and 1 mM IPTG, and inoculated at a bacteria:cell ratio of ~100:1. Centrifugation at 500 x *g* for 15 min was used to promote contact between host cells and bacteria. Cells were then incubated for 90

min (CHO-*htpB* cells) or 30 min (U937 macrophages) at 37°C in 5% CO_2 to allow internalization and intracellular establishment of legionellae. cAMP was extracted and measured using the enzyme immunoassay Biotrak kit, following the protocol suggested by the manufacturer (Amersham, Pharmacia). Femtomoles of cAMP/internalized bacterium were then calculated, for which a gentamicin protection assay was performed in triplicate to quantify the number of internalized bacteria. Briefly, after the 30 or 90 min infection period, and 3 washes with warm PBS, monolayers of infected CHO-*htpB* cells or U937 cells were treated for 1 h with αMEM or RPMI-1640 containing 5% FBS and 100 μg/mL gentamicin. The monolayers were then washed 3 times with warm PBS and lysed in ddH_2O to determine, by dilution plating, the number of intracellular bacteria (reported as colony forming units [CFU] per well) that survived the gentamicin treatment. Dilution plating was performed as described in Section 2.1.4.

The functionality and expression of the CyaA-HtpB fusion, as well as the lack of effect of any ectopic HtpB on cAMP levels, were confirmed in CHO-*htpB* cell lysates by quantifying cAMP levels after mixing with whole cell lysates of strain JR32 carrying pAC2 or pAC17. Lysates were produced by sonication as follows: After IPTG induction for 2 h, JR32 legionellae in late exponential phase were harvested and suspended to ~10^9/mL in αMEM with 5 % FBS, 1 mM IPTG, and 86 μg/mL protease inhibitor cocktail (Sigma). CHO-*htpB* cells grown to confluency were trypsinized from one 25 cm^2 flask (~4 x 10^5 cells) and suspended in 7 mL of αMEM with 5% FBS, 1 mM IPTG and 74 μg/mL protease inhibitor cocktail. Bacteria were sonicated (Vibra Cell, Sonic & Materials Inc, USA) in 10 cycles of 1-min pulse followed by 3-min incubation on ice, whereas CHO cells were sonicated for 3 cycles. Bacterial lysates (1 mL) were incubated

with 0.8 mL of CHO cell lysate for 20 min at 37°C, in a 24-well plate. Proteins were precipitated from the mixture with 1 M HCl added to a final concentration of 50 mM, followed by neutralization with 0.5 M NaOH. cAMP was extracted and quantified as above. All experiments with CHO-*htpB* cells were done by Dr. Audrey Chong.

2.3.9. Effect of Pharmacological Inhibitors of Polyamine Synthesis on the Intracellular Growth of *L. pneumophila*

Methylglyoxal-bis(guanyl hydrazone) (MGBG) and α-difluoro methyl ornithine (DFMO) (MP Biomedicals) at concentrations up to 100 μM in MEM (for L929 cells), or RPMI-1640 (for U937 macrophages), were prepared immediately before use. *L. pneumophila* strains grown for 2-3 days on BCYE was harvested and suspended in MEM or RPMI-1640 (containing the different concentrations of MGBG or DFMO) to ~10^7 bacteria/mL, and added in triplicate to L929 or U937 cells in 24-well plates to a bacteria:cell ratio of 100:1. Plates were centrifuged at 500 x *g* for 10 min to promote bacterial-eukaryotic cell contact, and incubated at 37°C in 5% CO_2 for 90 min. Monolayers were then washed 3X with PBS to remove free bacteria. Cells were then either lysed in ddH_2O to determine CFU/well (set as time 0 value), or replenished with FBS-free MEM or RPMI-1640 containing the corresponding concentrations of MGBG or DFMO, and then lysed in ddH_2O to determine CFU/well at 24 and (or) 48 h post infection, as described above in Section 2.1.4.

2.3.10. Effect of MGBG or DFMO on Cell Viability

The vital stain Trypan blue was used to determine the effect of MGBG and DFMO on host cell viability.L929 or U937 cells were plated in a 24-well plate (Becton Dickinson, Franklin Lake) in 1 mL MEM or RPMI, respectively, at 10^5 cells/well. After cells attached and spread, the medium was removed and 1 mL of fresh medium containing 100 μM MGBG or DFMO was added to 12 wells (test), whereas 1 mL of fresh medium without drugs was added to the remaining 12 wells (control). Cells were then incubated at 37°C, 5% CO_2 for up to 48 h. At 0, 24 and 48 h, the supernatants (1 mL) from 3 control and test wells (containing floating cells) were collected in separate 1.5 mL microcentrifuge tubes. Adherent cells were then detached using 500 μL of 0.25% trypsin-EDTA in PBS (Invitrogen) per well for 10 min, and added to the previously collected supernatant. Equal volumes of sample and 0.4% Trypan blue (Invitrogen), were mixed and cells were counted using a hemocytometer (Improved Neubauer chamber, Hausser Scientific, Horsham, PA). The percentage of non-viable (blue) cells were calculated over a total count of 1,000 cells per sample.

2.3.11. Effect of Exogenous Polyamines on *L. pneumophila* Growth

To test the effect of exogenous polyamines in *L pneumophila* growth in static culture, BYE broth or DM containing different concentrations of individual polyamine (MP Biomedicals) was inoculated to an initial OD_{620} of 0.2 units with *L. pneumophila* strain JR32 grown in BYE to an OD_{620} of 2-3 units. Fresh DM with or without polyamines was inoculated to an initial OD_{620} of 0.09 units with strain JR32 grown in polyamine-free DM to an OD_{620} of 0.18 units. The inoculated media were dispensed into

a flat-bottom 96-well plate (Falcon Plastics-BD), at 16 wells/condition and 250 µl/well. Cultures were incubated at 37°C in a humid box. Static growth was monitored by measuring OD_{620} in a Benchmark Plus multi-well plate reader (BIO-RAD Canada, Mississauga ON).

To test the effect of exogenous polyamines in *L pneumophila* growth in rolling culture, starting inocula were prepared from a culture of *L. pneumophila* strain JR32 grown in BYE to an OD_{620} of 2.5, and used to start new cultures with an initial OD_{620} of 0.05. For growth in SD medium, bacterial cells harvested by centrifugation from BYE cultures grown to an OD_{620} of 2.5 were washed once with PBS and used to inoculate new cultures to an initial OD_{620} of 0.15. Cultures were grown with or without putrescine and spermidine (both from MP Biomedicals) to a final concentration of 0.2 mM. All cultures were then incubated at 37°C with agitation (200 rpm). Growth was monitored for up to 48 h by measuring OD_{620} using an UNICO® UV-2100 spectrophotometer (EDVOTEK, MD).

To test the effect of exogenous polyamines on the intracellular growth of *L. pneumophila*, L929 cells were prepared for infection and processed to obtain CFU/well counts as described above in Section 2.3.8 with the following changes: The FBS-free MEM used to add the bacterial inoculum, and maintain the polyamine-treated cells during the infection period, was supplemented with spermine and spermidine (at a final concentration of 100 µM). For wells infected with *L. pneumophila* pre-treated with polyamines, the bacterial inoculum was prepared from strain JR32 grown to stationary phase in BYE broth supplemented with spermine and spermidine (both at a final

concentration of 100 μM). Harvested bacteria were washed to ensure that no additional spermidine or spermine was present in the inocula.

2.4. Materials and Methods Used in Chapter 5

Bacterial strains and plasmids used in Chapter 5 are described in Tables 1 and 2, respectively.

2.4.1. Culture of *Acanthamoeba castellanii*

The *A. castellanii* Neff's isolate (a gift from David Spencer, Dalhousie University) was maintained at 25°C in Neff's vitamin enriched medium (77) and grown at 37°C for the purpose of infection with *L. pneumophila*. Amoebae were cultured in Neff's media in 75-cm^2 tissue culture flask at 37^oC, as adherent cells until confluence was reached. The medium containing non-adherent amoebae was removed and replaced by fresh Neff's medium. The adherent amoebae were taken off the flask by vigorous tapping. The resulting suspension was transferred to 24-well plates at ~2.5 x 10^5 amoeba/well. Plates were incubated at room temperature for 2 h to let the amoeba adhere. At the time of infection, the Neff's medium was removed from the wells and replaced with modified Neff's medium (consisting of Neffs medium lacking glucose, yeast extract, and multi-vitamin mix).

2.4.2. Construction of Plasmids

Plasmids for construction of Δ*potD* mutant**:** allelic replacement of *potD* with a Km^R cassette was done using the counter selectable plasmid pBRDX (65,251). Briefly,

700 bp of upstream, and downstream, flanking DNA sequences of the *potD* gene of *L. pneumophila* JR32 were amplified by PCR using the primer pairs potDP1/potDP2 (for the upstream or F1 region) and potDP3/potDP4 (for the downstream or F2 region). The F1 amplicon cleaved at *Not*I and *Bam*HI restriction sites, and the F2 amplicon cleaved at *Bam*HI and *Xho*I restriction sites were ligated sequentially into pBluescript KS to create pBS: F1F2Δ*potD*. The Km^R cassette from plasmid p34S-Km3 (86) was isolated by restriction with *Bam*HI, and ligated into the corresponding *Bam*HI site of pBS: F1F2Δ*potD* (between F1 and F2) to generatepBS:F1-Km-F2Δ*potD.*Subsequently, the F1-Km-F2Δ*potD* fragment was cleaved by *Not*I and *Xho*I and subcloned into the *Not*I and *Xho*I sites of pBRDX to generate pBRDXΔ*potD:km* (Fig. 6A).

Complementation plasmids: pMMB*:potD* or pMMB-P_{potA}*:potD* were constructed inthe pMMB207C backbone. To construct pMMB-*potD,* the putative coding region of *potD* was amplified by PCR from chromosomal DNA of JR32 using primers FpotDcomp and RpotDcomp. FpotDcomp 5'-end contains a *Sac*I restriction site, while RpotD-comp 5'-end contains an*Xba*I restriction site. After digestion with *Sac*I and *Xba*I, the promoterless *potD* amplicon was ligated into the same (*Sac*I-*Xba*I) restriction sites downstream of the P_{tac} promoter of pMMB207C to generate pMMB*:potD*. To construct pMMB-P_{potA}*:potD,* the putative coding region of the *potA* promoter, 200 bp upstream of the potA start codon*,* was amplified by PCR from chromosomal DNA of JR32 using primers FpotA and RpotA. The FpotDcomp 5'-end encodes an *Eco*RI, while the RpotD-comp 5'-end encodes a *Sac*I restriction site After digestion with *Eco*RI and *Sac*I, the P_{potA} amplicon was ligated into the same restriction sites of pMMB:*potD* to generate pMMB-P_{potA}*:potD.*

Plasmids carrying reporter constructs: A 1028 bp DNA fragment encoding *potD* was cleaved from pMMB-P_{potA}*:potD* with *Sac*I and *Sph*I, to generate pMMB-P_{potA}. Subsequently, the promoterless *gfp* DNA fragment from plasmid pBH6119 (159) was cleaved with *Sac*I and *Sph*I and ligated into the corresponding restriction sites of pMMB-P_{potA} to generate pMMB-P_{potA}*:gfp*. To ensure that GFP expression was exclusively driven byP_{potA}, the DNA region of pMMB-P_{potA}*:gfp* encoding the P_{tac} promoter was removed by restriction with *Apa*I and *Eco*RI, followed by end filling with Klenow polymerase (NEB) and blunt ligation. Plasmid pMMB-P_{potA}*:gfp* was cut with *Apa*I and *Sac*I to remove the P_{potA} and P_{tac} promoter regions, and blunt ligated to create the promoterless GFP plasmid pMMB:*gfp* (negative control for expression of GFP).

2.4.3. Construction of *L. pneumophila* JR32 Δ*potD* Mutant Strain

The counter selectable delivery plasmid pBRDXΔ*potD*:*km* (Fig. 6A) was transformed into *L. pneumophila* JR32. Km^R transformants were selected on BCYE agar supplemented with 40 μg/ml Km. The allelic recombinants (potential *potD* deletion mutants) were then selected from a population of Km^R colonies by replica plating onto a medium containing 5% (w/v) sucrose (Suc) or 20 μg/ml of Mtz. Plasmid loss was confirmed by testing for the loss of Cm^R.

2.4.4. Δ*potD* Mutant Confirmation

To confirm deletion of *potD* in JR32, potential *potD* mutants showing the phenotypes Cm^S, Km^R, Suc^R, and Mtz^R were further screened by PCR for the absence of the *potD* gene using the *potD* internal primers, potDprobeF and potDprobeR (Fig. 6B).

Then, to confirm that PotD was replaced by Km^R cassette and that the cassette was inserted in the correct locus, the potential Δ*potD* mutant colonies screened by PCR for the absence of *potD* were further tested using primers potDP5 and potDP6 (Fig. 6A), in combination with primers designed for amplification of the kanamycin cassette (kmF and kmR). When the primer pairs potDP5/kmR or potDP6/kmF were used, a DNA fragment of approximately 1.7 Kb was amplified suggesting that the Km^R cassette was inserted in the correct location (Fig. 6C). To verify that only *potD* was replaced by the Km^R cassette, and that *lpg1137* (downstream gene of *potD*) and *potC* (upstream gene of *potD*) remained unaffected, another PCR test was performed. PCR reactions using primer pairs potDP5 and potDP2, or potDP3 and potDP6 were used to check the integrity of *lpg1137* or *potC*, respectively. Two DNA fragments of ~0.8 Kb representing *lpg1137* and *potC*, were amplified (Fig. 6D), suggesting that these two genes were intact.

2.4.5. Bacterial Morphology

Bacterial smears were prepared from 4-day old colonies of *L. pneumophila* strains grown on BCYE agar plates. Smears were air dried, heat fixed, stained with 0.2% (wt/vol) crystal violet solution, and examined on an Olympus microscope (model BX61).

2.4.6. NaCl and KCl Sensitivity Assay

To measure NaCl or KCl sensitivity of broth-grown *L. pneumophila* strain JR32 (45), BYE cultures grown to exponential phase (EP) (OD_{620} between 1.0 to 1.5) and SP (OD_{620} ~3.0) were diluted in ddH_2O and then plated on BCYE with or without 100 mM

NaCl or KCl. The percentage of bacteria that were sodium resistant was calculated with the following formula: (CFU on BCYE with 100 mM NaCl / CFU on BCYE) X 100.

2.4.7. *ΔpotD Mutant* Growth Curves *in vitro*

To monitor the growth of *L. pneumophila* in BYE, starting inocula were prepared from a culture of *L. pneumophila* grown in BYE to an OD_{620} of 2.5, and used to start new cultures with an initial OD_{620} of 0.05. For growth in SD medium, bacterial cells harvested by centrifugation from BYE cultures grown to an OD_{620} of 2.5 were washed once with PBS and used to inoculate new cultures to an initial OD_{620} of 0.15. Cultures were grown with or without putrescine and spermidine (both from MP Biomedicals) to a final concentration of 0.2 mM. All cultures were then incubated at 37^{o}C with agitation (200 rpm). Growth was monitored for up to 48 h by measuring OD_{620} using an UNICO® UV-2100 spectrophotometer (EDVOTEK, MD).

2.4.8. Evaluation of Biofilm Formation

Biofilm formation under static conditions was quantified by the crystal violet incorporation assay, using the Calgary biofilm device (CBD, *MBEC*^{TM} Biofilms Technology Ltd., Calgary, Alberta, Canada) (54). The CBD is a 96-well plate format device, which allows the formation of biofilms on pegs attached to the plate lid. Biofilm formation by *L. pneumophila* was quantified as described by Mampel et al. (272)with a slight modification. Briefly, overnight cultures (OD_{620} 2.0 to 3.0) of *L. pneumophila* strains (carrying pMMB207C or pMMB-P_{potA}-*potD*) were diluted 1:10 in fresh BYE containing 5 μg/mL chloramphenicol. Two hundred μL of the diluted *L. pneumophila*

cultures was used to inoculate 21 wells per strain. Each well was filled with. The plate was incubated for 5 days at 30°C in a wet box to prevent desiccation of the wells. To quantify the bacteria adhere to the pegs, the lid was placed in a 96-well plate filled with 200 µL of 0.2% (w/v) crystal violet solution. The pegs were washed twice with PBS to eliminate any unbound crystal violet. The bound crystal violet was then solubilized in 200 µL of 95% ethanol, and 150 µl aliquots were assayed to determine absorbance at 570 nm using a plate reader (Benchmark Plus, BIO-RAD).

2.4.9. Evaluation of the *ΔpotD* Mutant Attachment

THP-1 derived macrophages were seeded in 24-well plates as described in Section 2.1.3. *L. pneumophila* strains JR32(pMMB207C), Δ*potD*(pMMB207C) and Δ*potD*(pMMB:*potD*) were grown to mid-EP at 37^{o}C in BYE containing 5 µg/mL chloramphenicol, and treated with 1 mM IPTG, for at least 3 h, before use. IPTG was used to induce expression of the plasmid-encoded PotD in Δ*potD*(pMMB:*potD*). The bacteria were pelleted and resuspended in RPMI-1640 with 10% FBS, 5 µg/mL chloramphenicol, and 1 mM IPTG and then added in triplicate to the THP-1 macrophages cultured in the wells of 24-well plates to a bacteria:cell ratio of ~10:1 or 100:1. The rest of the infection procedure was as described in Section 2.1.4 except that after infection for 90 min, the inocula were removed and the monolayers were washed 4 times with warm PBS to remove free bacteria, then the bacteria were lysed and counted as described in Section 2.14.

2.4.10. Intracellular Growth Assay of the Δ*potD* Mutant

Monolayers of L929 cells, U937-derived macrophages, and *A. castellanii* were seeded in 24-well plates as described in Section 2.1.3. *L. pneumophila* inocula preparation and infection procedure were done as described in Section 2.4.9., except for L929 monolayers, where the bacterial pellets were resuspended in MEM containing 5% FBS and 5 μg/mL chloramphenicol, and 1 mM IPTG and then added to the wells in triplicates to a bacteria:cell ratio of 20:1. The rest of the infection procedure and determination of CFU count/well after 0, 24, and 48 h, were performed as described in Section 2.1.4.

2.4.11. Study of P_{potA} promoter Activity

To study P_{potA} activity, the GFP reporter assay (251) and immunoblotting were used to determine the levels of GFP expression from strains JR32(pMMB-P_{potA}:*gfp*)or JR32(pMMB:*gfp*)**.** Briefly, bacterial stains were grown in BYE as described in Section2.4.7.Samples were then obtained every four hours. Following determination of OD_{620}, bacteria were harvested by centrifugation, resuspended in PBS, and adjusted to an OD_{620} of 3.0 units. For fluorometric determination of GFP expression level, the adjusted bacterial suspensions were dispensed in triplicate in a black 96-well plate with clear bottoms (Costar 3603, Corning Inc, NY) at 250 μl/well. Fluorescence intensity was measured on a VICTOR™ X5 multi plate reader (Perkin Elmer, Ontario, Canada) using 485 nm excitation and a 510 nm emission filter. Values were expressed as arbitrary fluorescence units normalized to 1.0 OD_{620} unit (relative fluorescence unit).

GFP expression from bacterial cell pellets was assessed by SDS- PAGE followed by immunoblotting as described in Section 2.1.2.8. For determination of GFP expression

levels from the intracellularly grown-*L. pneumophila,* U937 cells seeded in 12-well plates were infected with strain JR32(pMMB-P_{potA}:*gfp*) at a bacteria to cell ratio of 100:1 as described in Section 2.1.4. After, 24, 48 and 96 h post-infection, the U937 infected cells were lysed with ddH_2O, bacteria and U937 cells debris were harvested by centrifugation and then treated with sample buffer, followed by SDS-PAGE, and transferred to nitrocellulose membranes, as described in Section 2.1.2.8. After electrotransfer, the nitrocellulose membrane was immunostained with the appropriate polyclonal PAb [GFP PAb alkaline phosphatase conjugate (GFP11-AP) [Cedarlane Laboratories Ltd), chloramphenicol acetyl transferase (Cat) PAb (Sigma)]. The two primary PAbs were diluted 1:2,000 in Tris buffer solution (TBS) containing 0.1% (w/v) bovine serum albumin (BSA). Secondary antibodies for Cat PAb were alkaline phosphatase conjugates of anti-rabbit IgG (Cedarlane Laboratories Ltd.) diluted 1:5,000 in TBS containing 0.1% (w/v) BSA. Densitometry of immunostained protein bands was as described in Section 2.1.2.8. Values of optical density of GFP bands were corrected for differences in loading and electro-transfer efficiency, using the corresponding values of the optical density of the CAT bands.

2.4.12. Cytotoxicity Assay

Contact dependent cytotoxicity was quantified as a percentage of lactate dehydrogenase (LDH) release from U937 macrophages after a 3 h incubation with *L. pneumophila* (234). Briefly, U937 cells were seeded in a 48-well plate at ~ 8x 10^4cells per well. *L. pneumophila* strains grown to late EP (OD_{620} ~2.5) were harvested and suspended in serum free RPMI-1640 with 5µg/ml chloramphenicol to ~10^7 bacteria/mL

and then added to the U937 macrophages in the 48-well plate to a bacteria:cell ratio of 100:1. The plate was then centrifuged at 500 x *g* for 10 min to promote contact of bacteria with macrophages. After an incubation period of 3 h at 37^{o}C, portions of the supernatant were assayed for the activity of LDH using the Toxo-7 kit according to the manufacturer's instructions (Sigma). Supernatants from uninfected wells were used as negative controls to define the background levels of LDH, and the 100 percent positive LDH release control was achieved by lysing the cells with the lysis solution provided with the kit.

2.4.13. Competition Assay

Competition assays were done according to the published method of Beuzon and Holden adapted to cell culture by Faucher et al. (28,101). To differentiate between the competing strains, the parental strain JR32 was labelled with GFP (by expression from plasmid pMMB207-Km14-GFPc) and the Δ*potD* mutant strain was labelled with Ds-Red (by expression from plasmid pSW001). For simplicity, the parental strain was named JR32-GFP and the Δ*potD* mutant strain Δ*potD*-RED. U937 macrophages were seeded in 12-well plates at ~1 x 10^6 cells per well. JR32-GFP and Δ*potD*-Red strains were harvested from 3 day old BCYE plates and resuspended in RPMI containing 10% FBS and 5 µg/ml chloramphenicol, to a density of ~10^8 bacteria/mL. JR32-GFP and Δ*potD*-Red were mixed at a 1:1 ratio and the bacterial mixture was added to the wells at a bacteria: cell ratio of 40:1. The rest of the infection protocol was as described in Section2.1.4, except that, prior to lysing the cells at 24 and 48 h post-infection, two images were captured from two random fields of each well (with each field containing

400 to 500 cells) using the 20X objective lens of an Olympus inverted fluorescent microscope (model THY-100) and a video camera (Evolution QEI, Media Cybernetics Inc.). The number of cells infected by JR32-GFP (green cells) or Δ*pot*D-Red (red cells) and non-infected cells (gray) were scored using the Image Pro Plus software (Media Cybernetics Inc). The percentage of green or red cells was calculated using the flowing formula: [number of green or red cells per field/ total number of the cells (green + red + gray) per field] X 100.

To calculate the competitive index (CI) (28,101), the number of bacteria in the inoculum mix and the number of intracellular bacteria at 24 and 48 h post infection was determined by serial dilution in ddH_2O and plating on BCYE as described in Section 2.1.4. To count and distinguish between the JR32-GFP green colonies and the Δ*potD*-Red red colonies, an ultraviolet lamp (UMV-57, UVP_{INC}, San Gabriel, CA) was used in a dark room to illuminate the plates. The CI at 24 or 48 h was calculated using the following formula: output [(number of green CFU/ number of red CFU) at 24, or 48 h] divided by the input [(number of green CFU / number of red CFU) in the inoculum mix at time 0]. To control for any possible biological effect of the proteins expressed from the plasmids (pMMB207-Km14-GFPc and pSW001), carried by the competing strains, this experiment was repeated with strains JR32-Red (JR32 strains carries pSW001) and Δ*potD*-GFP (Δ*potD* strain carries plasmid pMMB207-Km14-GFPc) (see Table 1).

2.4.14. Assessment of the LCV Ultrastructural Features by Electron Microscopy

U937 macrophages were seeded in a 6-well plate at ~2 x 10^6 cells per well. *L. pneumophila* strains grown for 2-3 days on BCYE was harvested and suspended in

RPMI-1640 containing 10% FBS and 5µg/ml Cm to a density of ~10^9 bacteria/mL, and then added to wells to a bacteria:cell ratio of 100:1. After an infection period of 8 h, the inocula were removed and cells were washed once with warm PBS. Adherent cells were then detached for 10 min by using 500 µL per well of 0.25% trypsin-EDTA (Invitrogen) in PBS. Supernatants containing the detached macrophages were removed. Macrophages were then pelleted by centrifugation at 500 x *g* and fixed by resuspending in cacodylate buffer (0.1 M sodium cacodylate, pH 7) containing 2.5 % glutaraldehyde. The cells were fixed, and allowed to settle by gravity, overnight, at 4^{o}C. The cell pellet was then washed three times in cacodylate buffer before post-fixation in 1 % osmium tetroxide for 1 h at 4 ^{o}C. Then, cells were *in-bloc* stained with aqueous uranyl acetate, dehydrated in acetone, embedded in epoxy resin, ultrathin sectioned, and post-stained with uranyl acetate and lead salts (137). Sectioned specimens were observed on a JEOL JEM 1230 transmission electron microscope, and high-resolution images were captured with a Hamamatsu ORCA-HR digital camera. About 50 macrophages from each experiment were examined to score the number of LCV per macrophage, the number of associated vesicles per LCV, number of mitochondria per LCV, and whether or not LCVs showed the presence of ER.

2.4.15. Lysosome Association Assay by Immunofluorescence

U937 macrophages were seeded onto 22 x 22 mm (Size 0) glass coverslips (Fisher Scientific) placed inside 12-well plates, at ~5 x 10^5 cells per coverslip. JR32-RED or Δ*potD*-RED strains grown for 2-3 days on BCYE were harvested and suspended in RPMI-1640 containing 10% FBS and 5µg/ml chloramphenicol to ~10^8 bacteria/mL and then added to the wells to a bacteria:cell ratio of 100:1. Plates were centrifuged at 500 x

g for 10 min to promote contact of bacteria with macrophages, and incubated at 37°C in 5% CO_2 for 8 h. Monolayers were then treated for 45 min with RPMI-1640 containing 100 μg/mL gentamicin to kill extracellular bacteria. The macrophages were then gently washed 3 times with warm PBS to remove the unattached and killed bacteria. The cells were then fixed with 3% paraformaldehyde in PBS (vol/vol), permeabilized with methanol for 10 sec, and blocked with 2% BSA in PBS for 30 min. To assess colocalization of the LCVs with lysosomes, the lysosomal marker LAMP-1 was stained by monoclonal antibody H4A3-s (obtained as hybridoma cell culture supernatant from the Developmental Studies Hybridoma bank, Iowa) at a 1:2 dilution, followed by Alexa fluor 488-conjugated goat anti-mouse antibody (Invitrogen) diluted at 1:200. Unattached antibodies were removed by gentle washing with PBS and the stained coverslips were mounted on glass slides with ProLong Gold Antifade (Invitrogen). Intracellular bacteria were identified as red fluorescent particles and labelled lysosomes were identified as green vesicles or rings. The co-localization of bacteria with LAMP-1 labelled lysosomes (yellow bacteria, or red bacteria surrounded by a green ring) was quantitated by fluorescence microscopy.

2.5. Tables, Figures, and Legends to Figures

Table 1. Bacteria and yeast strains used.

	Selection marker(s)	Characteristics	Reference /source
Bacterial Strains			
L. pneumophila			
JR32	Sm^R	Salt sensitive isolate of AM511 (AM511: Philadelphia 1, serogroup 1, restriction deficient, modification positive)	(355)
JR32(pMMB207C)	Sm^R, Cm^R	JR32 carrying pMMB207C	This study
JR32(pMMB-P_{potA}:*gfp)*	Sm^R, Cm^R	JR32 carrying pMMB-P_{potA}:*gfp*	This study
JR32(pMMB:*gfp*)	Sm^R, Cm^R	JR32 carrying the promoterless pMMB:*gfp*	This study
JR32-GFP	Sm^R ,Cm^R, Kan^R	JR32 constitutively expressing GFP from plasmid pMMB207-Km14-GFP	This study
JR32-RED	Sm^R ,Cm^R,	JR32 constitutively expressing DsRed from plasmid pSW001	This study
Δ*potD*	Sm^R , Kan^R	JR32 derivative carrying Km^R cassette in place of *potD*	This study
Δ*potD*(pMMB:*potD*)	Sm^R, Kan^R, Cm^R	Δ*potD* carrying pMMB:*potD*	This study
Δ*potD*(pMMB-P_{potA}:*potD*)	Sm^R, Kan^R, Cm^R	Δ*potD* complemented strain carrying pMMB-P_{potA}:*potD*	This study
Δ*potD*-GFP	Sm^R, Kan^R, Cm^R	Δ*potD* constitutively expressing GFP from plasmid pMMB207-Km14-GFPc	This study
Δ*potD*-RED	Sm^R, Kan^R, Cm^R	Δ*potD* constitutively expressing DsRed from plasmid pSW001	This study
Lp02	Sm^R	Philadelphia-1, serogroup 1, salt sensitive, restriction deficient, thymidine auxotroph	(24)
LpgroE+	Sm^R, Km^R	Lp02Δ*thyA, lacI*$^{q+}$ *Ptrc:groE*$^{+}$-*km3*	This study
MB379	Sm^R, Kan^R	Lp02 Δ*rpoS* mutant	(15)
E. coli			
DH5α		F^{-}Φ80 Δ*lacZ*ΔM15 Δ(*lacZYA-argF*)*U*169 *supE*44 *hsdR*17 *recA*1 *endA*1 *gyrA*96 *thi*-1 *relA*1	Clontech
Yeast strains			

	Selection marker(s)	**Characteristics**	**Reference /source**
W303		*MATα leu2-3112 ura3-1 his3-11 15 trp1-1 ade2-1*	G. Jonston
Y187		*MAT*α *ura3-52his3-200 ade2-101trp1-901leu2-3*, *112gal4Δmet– gal80ΔURA3::GAL1*$_{UAS}$*-GAL1*$_{TATA}$*-lacZ*	Clontech
21R		*MAT***a** *ade1 leu2-3112 ura3-52*	(212)

Table 2. Bacterial plasmids used.

	Selection marker(s)	**Characteristics**	**Reference /source**
Bacterial plasmids			
pAC2	Amp^R, Cm^R	pMMB207C with *cyaA:htpAB* chimera	(66)
pAC17	Amp^R, Cm^R	pMMB207C with the *htpB:cyaA* chimera	(66)
pBluescript II KS	Amp^R	High-copy plasmid used as a general cloning vector in *E. coli*	Stratagene
pBRDX	Cm^R	Suicide delivery vector, *rdxA sacB*	(35)
pBRDXΔ*htpB:gm*	Cm^R, Gm^R	Suicide delivery vector for potential LpgroE+/Δ*htpAB*	This study
pBRDXΔ*htpB*:*km3*	Cm^R, Km^R	Suicide delivery vector for potential JR32Δ*htpAB*	This study
pBRDXΔ*potD*:*km*	Cm^R, Kan^R	Suicide delivery vector for allelic replacement of *potD*	This study
pBRDXΔ*thyA::groE -km3*	Cm^R, Km^R	suicide delivery vector for LpgroE+ carries $lacI^{q+}P_{tac}$:$groE^+$-*km3*	This study
pJC158	Amp^R, Cm^R	pMMB207C derivative carrying the *lepA:cyaA* fusion	(59)
pJC203	Amp^R, Cm^R	pMMB207C derivative carrying the *cyaA* gene	(59)
pMMB207C	Amp^R ,Cm^R	RSF1010 (IncQ, *lac*Iq, P*tac, oriT*) derivative with Δ*mobA* and the P*tac* IPTG-inducible promoter.	(59)
pMMB:*gfp*	Amp^R ,Cm^R	pMMB207C derivative without P_{tac}, promoterless *gfp*	This study
pMMB*:potD*	Amp^R ,Cm^R	pMMB207C derivative carrying *potD* under the control of the P_{tac} promoter	This study
pMMB-P_{potA}*:gfp*	Amp^R ,Cm^R	pMMB207C derivative without P_{tac}, GFP expression is controlled by P_{potA}	This study
pMMB-P_{potA}*:potD*	Amp^R ,Cm^R	pMMB207C derivative, PotD expression is controlled by the *potABCD* operon promoter region (P_{potA})	This study
pMMB207-Km14-GFPc	Amp^R, Cm^R, Kan^R	pMMB207C derivative, constitutively expressing GFP	(272)
pSW001	Amp^R, Cm^R	pMMB207C derivative, constitutively expressing Ds-Red	(272)

	Selection marker(s)	**Characteristics**	**Reference /source**
pTrcKm	Amp^R, Km^R	pTrc99A derivative carries the *lacI*^{q} repressor and P_{trc} promoter *(*IPTG inducible promoter) upstream of the *groE* operon and Km^R resistance cassette	(4)

Table 3. Yeast shuttle vectors used.

	Selection marker	**Characteristics**	**Reference or source**
pEMBLyex4	Amp^R, Ura^+, Leu^+	High-copy plasmid used as a yeast expression vector controlled by the galactose-inducible hybrid promoter *GAL1-CYC1*	(95)
pEMBLyex4:: *groEL*	Amp^R, Ura^+, Leu^+	pEMBLyex4 carrying the *E. coli groEL* gene	(341)
pEMBLyex4:: *htpB*	Amp^R, Ura^+, Leu^+	pEMBLyex4 carrying the *L. pneumophila htpB* gene optimized for expression in *S. cerevisiae*	(341)
pEMBLyex4:: *HSP60*	Amp^R, Ura^+, Leu^+	pEMBLyex4 carrying the *S. cerevisiae* wild type *HSP60* gene	(341)
pEMBLyex4:: *hsp60* Δ1-72	Amp^R, Ura^+, Leu^+	pEMBLyex4 carrying the *S. cerevisiae hsp60* gene lacking the N-terminal region encoding the mitochondria-targeting sequence	(341)
pGAD-C1	Amp^R, Leu^+	Yeast two-hybrid plasmid encoding the *GAL4* trans-activating domain, controlled by a modified *S. cerevisiae* P_{ADH1} promoter.	(207)
pGAD-C1::DNAx, pGAD-C2::DNAx, pGAD-C3::DNAx	Amp^R, Leu^+	pGAD-C1, -C2, and –C3 carrying highly representative genomic libraries from *S. cerevisiae* strain YM706 in reading frames 1, 2, and 3, respectively.	(207)
pGBD-C1	Amp^R, Trp^+	Yeast two-hybrid plasmid encoding the *GAL4* DNA-binding domain (DBD) controlled by a modified P_{ADH1} promoter.	(207)
pGBD-C1::*htpB*	Amp^R, Trp^+	pGBD-C1 carrying the *GAL4DBD::htpB* gene fusion	(341)
pGADT7	Amp^R, Leu^+	Yeast two-hybrid plasmid encoding the *GAL4* trans-activating domain, controlled by a modified *S. cerevisiae* P_{ADH1} promoter	Clontech
pPP389	Amp^R, Ura^+, Leu^+	pEMBLyex4 in which the defective *leu2-d* gene was replaced by a wild-type *LEU2* allele	* P. Poon

	Selection marker	Characteristics	Reference or source
pPP389::*HSP60*	Amp^R, Ura^+, Leu^+	pPP389 carrying the *S. cerevisiae* wild type *HSP60* gene	(341)
pPP389::*hsp60* Δ1-72	Amp^R, Ura^+, Leu^+	pPP389 carrying the *S. cerevisiae hsp60* gene lacking the N-terminal region encoding the mitochondria-targeting sequence	(341)
pPP389::*htpB*	Amp^R, Ura^+, Leu^+	pPP389 carrying the *htpB* gene	(341)
pPP389::*SPE2*	Amp^R, Ura^+, Leu^+	pPP389 carrying the *S. cerevisiae SPE2* gene	
pSE1111	Amp^R, Trp^+	pGAD-C1 encoding the yeast Snfl protein fused to the GAL4 DNA binding domain	(91)
pSE1112	Amp^R, Leu^+	pGAD-C1 encoding the yeast Snf2 protein fused to the GAL4 DNA binding domain	(91)

* Means no reference is available

Table 4. PCR primers used.

Primer name	Sequence from (5' to 3' end)	Restriction site[a]
F1potDseq	AGC AAC CTT GCT TTC TGA ATT TT	None
FpotA	C CC **GAATTC**AGAAATGGAACAGGCAATGA	*Eco*RI
FpotDcomp	CCCCC **GAGCTC** ATGAAAATTTTTTCATTGCTGCT	*Sac*I
gmF	GCT TAC GTT CTG CCC AAG TT	None
gmR	GGC GGT ACT TGG GTC GAT	None
htpBF	AA GACAGCAAAGCTATTG	None
htpBR	GCACGTGTTGAAGATGCT	None
kmF	GAC**GGATCC**ACGTTGTGTCTCAAAATCTCTGA	*Bam*HI
kmR	GAC**GGATCC**CGGCTACCGAGCTCTTAGAA	*Bam*HI
P1	CCCC**GCGGCCGC**TCAAGAGGTGTTGCTTCAGG	*Not*I
P2	CCCC **GGATCC**CCATACGACGAACAACAACG	*Bam*HI
P3	CCCC**GGATCC** TGGGCGGAATGATGTAATTT	*Bam*HI
P4	CCCC **CTCGAG** GGCACTGATTCCATATCAACTG	*Xho*I
P6	TGA ATG AAT CGC TCA TTT TAC G	None
P7	CCC **ACTAGT** GGA CAG GAA CCA TGG GAA GT	*Spe*I
potDP1	CCCC**GCGGCCGC**TTTTGCAGTCTTGCCTTTCC	*Not*I
potDP2	CCCC **GGATCC**GGGAACAGTTAAAACTTGCTTTTT	*Bam*HI
potDP3	CCCC**GGATCC**ATGTAAGAAGAGCGAGCAGCA	*Bam*HI
potDP4	CCCC **CTCGAG** TTCATTACAATGGCATGGGTTT	*Xho*I
potDP5	CCCC**GCGGCCGC**AGAACGAGAACCCCAGTTGA	*Not*I
potDP6	CCCC **CTCGAG** TTCATTACAATGGCATGGGTTT	*Xho*I
potDprobeF	TAT GTG CTT TGA AGG CAT CG	None
potDprobeR	TGC CAA GCT AAG AGC CAG TC	None
PtrcF	GGCGC **ACTAGT**ATGGCATGATAGCGCCC	*Spe*I
PtrcR	GGCGC **ACTAGT**CCTACTCAGGAGAGCG	*Spe*I
RpotA	CCCCC **GAGCTC**CAATCACAAACTTTGTTCCC	*Sac*I
RpotDcomp	CCCCC **TCTAGA**CTAAAAAGCAAGTTTTAACTGTT	*Xba*I
SPE2-F	CCC**GGATCC**ATGACTGTCACCATAAAAGAAT	*Bam*HI
SPE2-R	AATT**CTGCAG** TATTTTCTTCTGCAATTTC	*PstI*I
thyAP1	GGCGC **GCGGCCGC**CGTGGGGTATGATATATCC	*Not*I
thyAP2	GGCGC **ACTAGT**TGGCCAACTTCTCCATT	*Spe*I
thyAP3	GGCGC **ACTAGT**TCCTTTCAATATCGCTTC	*Spe*I
thyAP4	GGCGC **CTCGAG**AATTCGTAATCACGGCAAC	*Xho*I
thyAF	GCTGATGGACGCACCATTG	None
thyAR	ATACATCGGCTGAGCGTTG	None

[a] Restriction sites are shown in the primer sequence as underline-boldface text.

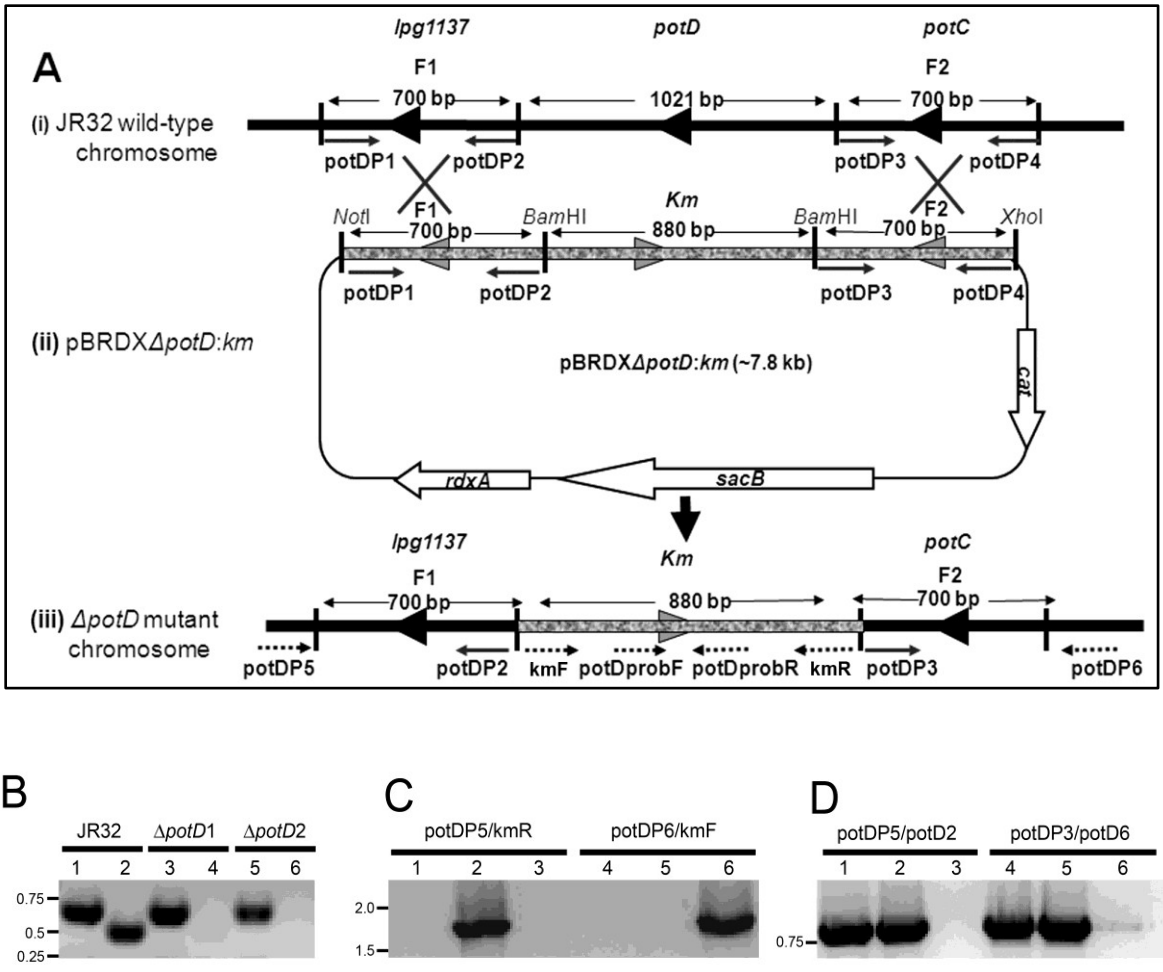

Figure 6. A schematic representation (not to scale) of the approach followed to delete *potD* from the genome of *L. pneumophila* strain JR32 by allelic replacement.

(A) (i) Area of the JR32 chromosome (not to scale) showing the potD locus and its flanking genes (the hypothetical gene *lpg1137* and *potC*). Direction of transcription of each gene is indicated by a big arrowhead. **(ii)** Map of plasmid pBRDXΔ*potD:km*. The *potD* flanking regions F1 and F2 were generated by PCRusing primer pairs potDP1/potDP2 and potDP3/potDP4, respectively. The restriction sites flanking F1 and F2 are indicated. The large Xs indicate the areas of recombination between the JR32 chromosome and pBRDXΔ*potD:km*. **(iii)** Expected result after allelic replacement.

Primers used for confirmation of loss of *potD* and insertion of Km^R cassette are indicated by small broken arrows underneath the Δ*potD* mutant strain chromosome. Panels **B-D** are sections of ethidium bromide-stained agarose gels showing DNA bands of interest. (**B)** Identification of Δ*potD* mutant colonies by PCR analysis.PCR products amplified from genomic DNA of the *L. pneumophila* strains indicated on top of the agarose gel, using primers potDprobeF/potDprobeR (lanes 2, 4, and 6).The internal primers for amplification of *htpB* (encoding the *L. pneumophila* chaperonin), htpBF/htpBR, were used as a positive control for the PCR reaction (lanes 1, 3, and 5). (**C)** Insertion of the Km^R cassette in the *potD* locus. A PCR product of ~1.7 kb was amplified by PCR from the Δ*potD* mutant chromosome when potDP5/kmR primers (lane 2) or potDP6/kmF (lane 6) were used. The JR32 strain (lanes 1 and 4) or pPRDXΔ*potD::km* (lanes 3 and 5) were used as negative control for the PCR. (**D)** *potC* and *lpg1137* were not affected by allelic replacement. A *potC* or a *lpg1137* amplicon (~800 bp) was amplified from Δ*potD* mutant chromosome (lanes 1 and 4) as well as the positive control JR32 strain (lanes 2 and 5). pPRDXΔ*potD::km* (lanes 3 and 6) was used as negative control for the PCR. Primers used in these PCR reactions are indicated on top of the agarose gel. Molecular size standards (Kb) are marked at the left side of the agarose gels. The Δ*potD* mutant was consructed by Kaitlyn Carson and Gheyath Nasrallah.

CHAPTER 3: THE *HTPAB* OPERON OF *LEGIONELLA PNEUMOPHILA* IS ESSENTIAL AND CANNOT BE COMPLEMENTED BY THE *ESCHERICHIA COLI GROE* OPERON

Gheyath K. Nasrallah[1],Dennis Orton[1], Elizabeth Gagnon[1], and Rafael A. Garduno[1,2],*

[1] Department of Microbiology and Immunology, Dalhousie University, Halifax, Nova Scotia, Canada.

[2] Department of Medicine – Division of Infectious Diseases, Dalhousie University, Halifax, Nova Scotia, Canada.

*Corresponding author

A manuscript submitted to the Canadian Journal of Microbiology was adapted from this Chapter.

Nasrallah *et al*. manuscript (2011-0133).

3.1. Abstract

The chaperonin of the intracellular bacterium *L. pneumophila*, HtpB, is abundantly released inside host cells during the course of infection, suggesting that HtpB may have virulence-related functions. To assess such potential functions *in vivo*, it would be desirable to construct an *htpB* deletion mutant. Previously, we showed that direct deletion of *htpB* in *L. pneumophila* strain Lp02 was not possible, likely because its gene product, HtpB, is essential for protein folding (65). In an attempt to overcome the essentiality barrier, the *htpAB* operon homolog from *E. coli* (the *groE* operon), was first inserted into the chromosome of *L. pneumophila* strain Lp02. Subsequently, we attempted to delete the *htpAB* operon by allelic replacement with a gentamicin-resistance (Gm^R) cassette, in the strain carrying *groE*. Although ~500 Gm^R clones showed an antibiotic selection phenotype compatible with a successful allelic replacement, *htpAB* was still present in 200 of these clones as demonstrated by PCR. Southern blot and PCR analysis suggested that the Gm^R cassette had, apparently, been inserted in a duplicated *htpAB* locus. However, multiple copies of *htpAB* in Lp02 could not be identified by Southern blot using Lp02 chromosomal DNA digested with eight different restriction enzymes. These results suggest that: (i) *htpAB* is essential in *L. pneumophila*, (ii) *htpAB* cannot be genetically complemented by *groE*, and (iii) attempts to delete *htpAB* under strong phenotypic selection result in unexplained genetic rearrangements that appear to involve duplication of the *htpAB* locus.

3.2. Introduction

Reports on the importance of heat shock proteins (HSPs) in bacterial pathogenesis are accumulating (50,107,231,250,266,441)**.** The two dominant bacterial HSP families, represented by Hsp60 (known as chaperonin) and Hsp70, have been regarded for many years as immunodominant antigens (230,441). The basic functions of HSPs (particularly chaperonins) are to assist proteins to fold into their native state, protect proteins from denaturation, help proteins to refold after stress, and assist in the translocation of proteins across membranes (380). Upregulation of HSPs might result from stress encountered during the course of infection indicating that HSPs could act as pathogenic determinants (39,178,250). For instance, bacterial chaperonins can mediate adherence to mammalian cells (124,139), and activate eukaryotic signaling cascades (269,446), all to the advantage of bacterial pathogens.

L. pneumophila is a Gram-negative environmental bacterial pathogen that naturally replicates within freshwater amoebae inside a specialized vacuole called the *Legionella*-containing vacuole (LCV). Upon inhalation of contaminated water aerosols by susceptible individuals*, L. pneumophila* reaches the alveoli and replicates within human alveolar macrophages (also inside LCVs) resulting in a severe atypical pneumonia known as Legionnaires' disease (113,114).

The *L. pneumophila* chaperonin, known as HtpB*,* is functionally diverse and plays protein folding-independent roles. The expression of HtpB is upregulated upon contact with L929 murine cells or human monocytes (107). High levels of HtpB expression are maintained during the course of intracellular infection (107), leading to its accumulation in the lumen of the LCV, as has been shown in infected HeLa cells (137). The increased

production of HtpB by *L. pneumophila* within L929 cells and monocytes correlates with virulence because spontaneous salt-tolerant, avirulent mutants of *L. pneumophila* are unable to upregulate the expression of HtpB upon contact with these cells (107). In addition, HtpB has been found in association with the *L. pneumophila* cytoplasmic membrane (30,127), as well as on the bacterial cell surface (137), where it can mediate attachment to and invasion of HeLa cells (139). The mature infectious forms (MIFs), thought to be the natural transmissible forms of *L. pneumophila,* display increased amounts of envelope and surface-associated HtpB, compared to agar-grown bacteria (138). Recently, we reported that microbeads coated with purified HtpB [but not uncoated beads or beads coated with control proteins (*E. coli* GroEL or BSA)] were sufficient to attract mitochondria to LCV and transiently modify the organization of actin microfilaments in mammalian cells. These two post-internalization events of HtpB coated beads mimic the early trafficking events of virulent *L. pneumophila* (65). As an *L. pneumophila* factor that mediates cell entry (139), alters trafficking of the LCV, continues to be abundantly produced inside the LCV (137) and is released into the host cell cytoplasm (Fig 11, Chapter 4 of this thesis), HtpB clearly plays a significant role in the intracellular establishment of *L. pneumophila.*

A comparison of the aligned amino acid sequences of *E. coli* GroEL and *L. pneumophila* HtpB revealed that these proteins have high degrees of amino acid identity and similarity (73.3%, 85%, respectively) (177,178). The *E. coli groEL* gene is transcribed with the co-chaperonin *groES* as an operon from one promoter (154). Similarly, *htpB* is co-transcribed with *htpA* (co-chaperonin gene) also from one single promoter(178). To function properly in protein folding, GroEL must work in conjunction

with GroES (154). The amino acid sequences of GroES and HtpA revealed that these proteins also have high degree of identity and similarity (66%, and 87%, respectively). Therefore, based on the high degree of amino acid sequence similarity between GroEL and HtpB, and GroES and HtpA, it could be predicted that HtpB and GroEL have a similar structure and that HtpB works together with HtpA in protein folding (177,178).

We hypothesized that construction of a Δ*htpB L. pneumophila* mutant would be a direct way to assess the role of *htpB* in virulence. However, in a previous report, we showed that deletion of *htpAB* could not be attained, and proposed that *htpAB* is an essential operon (65). To overcome the experimental barrier imposed by the essential nature of *htpAB*, we attempted to delete *htpAB* in *L. pneumophila* strain Lp02 carrying the *E. coli groE* operon in its chromosome (strain LpgroE+). The rationale behind this approach is that, because of the high degree of homology between *groE* and *htpAB, groE* should genetically complement the loss of *htpAB*. Despite the expression of *groE* in strain LpgroE+, we were unable to delete *htpAB*, suggesting that the *htpAB* operon is essential and cannot be genetically complemented by *groE.*

3.3. Results

3.3.1. Strain LpgroE+ Expresses the *E. coli groE* operon

L. pneumophila strain Lp02 is a thymidine auxotroph that harbors a loss of function mutation in the *thyA* gene encoding thymidine synthase (24). Since *thyA* is already non-functional in strain Lp02,itwas targeted to be replaced with a DNA fragment containing the $lacI^q$ repressor, the *groE* operon under the control of the P_{tac} promoter, and a Km^R cassette (*$lacI^q$-P_{tac}:groE-km3)*. Allelic replacement of *thyA* with the *$lacI^q$-*

P_{tac}*:groE- km3* DNA fragment was achieved using pBRDX as described in Figure 7. Of ~50 Cm^S, Km^R, Suc^R, and Mtz^R colonies, 20 colonies were selected to be tested, by PCR, for *thyA* deletion using the internal primers thyAF and thyAR. Of those 20 colonies, 11 tested negative for the presence of *thyA*, indicating that *thyA* was deleted from the genome (Fig. 7B, 2 clones are shown). The level of GroEL produced by Δ*thyA* mutants grown in BYE in the presence or absence of IPTG (to induce expression from the P_{tac} promoter), was assayed by immunoblot using a MAb specific for GroEL (Fig. 7C). There was no significant difference in the levels of GroEL between the IPTG-induced and non-induced Δ*thyA* mutants (Fig. 7C), indicating that $LacI^q$ does not effectively repress the P_{tac} promoter in *L. pneumophila* Δ*thyA* strains. This is, in fact, a useful feature of the Δ*thyA* strain because the natural expression of *L. pneumophila* HtpB is constitutively high. The Δ*thyA* strain with the highest basal GroEL expression was selected for deletion of the *htpAB* operon. This strain was named LpgroE+.

3.3.2. The *htpAB* Operon Is Essential in LpgroE+ and Cannot be Deleted.

Once the expression of GroEL was confirmed in LpgroE+, we attempted to replace the *htpAB* operon of this strain with a Gm^R cassette using plasmid pBRDXΔ*htpB:gm* as diagrammed in Figure 8A(ii). More than 500Gm^R LpgroE+ colonies were replica plated onto appropriate media to select for potential LpgroE+Δ*htpAB* mutants. Approximately 200 Gm^R, Mtz^R, Suc^R, and Cm^S potential LpgroE+*ΔhtpAB* colonies were tested by PCR for the presence of *htpB* using htpBF and htpBR primers. Surprisingly, all of the clones with the correct selection phenotype tested positive for the

presence of *htpB* (Fig. 8B) and still expressed HtpB as judged by immunoblot (Fig. 8C). These results indicate that the clones screened still contained a functional *htpAB* operon.

Because these tested clones still harbor *htpAB*, we then addressed the question of whether the Gm^R cassette was integrated in the LpgroE+ chromosome at a locus other than *htpAB*. A second PCR analysis was performed on ten potential LpgroE+*ΔhtpAB* random clones using primers that bound outside of the cloned upstream and downstream regions of the *htpAB* operon (P6 and P7) in combination with primers designed for detection of the Gm^R cassette (gmF and gmR) (Fig. 8A). When P7 and gmF primers were paired, an amplification product of ~1070 bp was produced from those potential LpgroE+*ΔhtpAB* clones (Fig. 8D) corresponding to the expected size of the downstream *htpAB* region of the planned insertion [Fig. 8A(iii)]. The identity of the 1,070 bp amplification product was confirmed by taking advantage of the *Hin*dIII site situated ~150 bp proximal to the hybridization site of the P7 primer (Fig. 8A). Upon digestion of this 1,070 amplicon with *Hin*dIII, Upon digestion of the 1,070 bp amplicon with *Hin*dIII, a 921 bp DNA fragment was produced due to the cleavage of the of the 150 bp (Fig. 8D). These results indicated that the flanking region downstream of the Gm^R cassette corresponded to the DNA sequence of the region created by the planned insertion.

A similar analysis of the flanking region upstream of the Gm^R cassette produced unexpected results. When P6 and gmR primers were paired, no PCR amplification product was produced from those potential LpgroE+Δ*htpAB* clones, suggesting that the upstream region of the inserted Gm^R cassette does not correspond to the region created by the planned insertion. The lack of amplification product on this PCR reaction was not due to failure of the P6 primer. In that, positive PCR reactions using primer pair P6 and P7

(Lanes a, Fig. 8F) produced an amplicon of the expected size (3.5 kb) when the *L. pneumophila* strains Lp02 and LpgroE+ were used as template [refer to Fig 7A(i) and Fig. 8A(i)]. Collectively, these results may explain why the potential LpgroE+Δ*htpAB* mutant strains showing the correct selection phenotype still expressed HtpB. It appears that either the Gm^R cassette was inserted in a duplicated copy of the *htpAB* operon, thereby generating an upstream flanking region different from the one upstream of the *htpAB* operon, or a chromosomal rearrangement occurred during the homologous recombination between the chromosome of strain LpgroE+ and plasmid pBRDXΔ*htpAB:gm*, which maintained both a functional Gm^R cassette and the intact *htpAB* operon.

3.3.3. LpgroE+ and Its Parent Strain Lp02 Have Only One Copy of the *htpAB* Operon

We wanted to investigate whether a second copy of the *htpAB* locus, or part of it, was present in strain *LpgroE+*, or whether it was created in a potential LpgroE+Δ*htpAB* mutant strain during homologous recombination between the chromosomal *htpAB* locus of LpgroE+ and plasmid pPRDXΔ*htpAB:gm*. Southern blot analysis was used to examine chromosomal DNA from LpgroE+ and a potential *LpgroE+*Δ*htpAB* mutant, which had been digested with *Eco*RI or *Hin*dIII. These two enzymes were chosen because they have restriction sites located adjacent to and within the *htpAB* locus (Fig. 8A), enabling us to accurately predict the size of expected hybridization fragments.DNA probes derived from the F1htpAB up stream flanking region of the *htpAB* operon, as well as from the Gm^R cassette (Materials and Methods, Section 2.2.5), were used. When the blot was hybridized with the F1htpAB probe, bands of ~3.2 and ~2.3 kb were detected in the

DNA from LpgroE+ [Fig. 8E(i)],exactly corresponding to the expected size of *Eco*RI and *Hin*dIII fragments, respectively, of the LpgroE+ parent strain [compare with Fig. 8A(i)]. However, an extra band was detected in each of the *Eco*RI and the *Hin*dIII DNA digests from the potential LpgroE+Δ*htpAB* mutant strain [Fig. 8E(ii)], confirming a duplication of the F1htpAB region. We confirmed that these two extra bands contained the Gm^R cassette in a sister Southern blot hybridized with a probe specific for the Gm^R cassette [Fig. 8E(ii)].The size of the new *Eco*RI band of the potential LpgroE+Δ*htpAB* mutant strain (~1500 bp), was exactly of the size expected after the planned deletion [compare with Fig. 8A(iii)]. However, the size of the new *Hin*dIII band (~3.2 kb) [Fig. 8E(i)] did not correspond to the size expected after the planned replacement of *htpAB* with the Gm^R cassette, which should have been ~ 2.6 kb [compare with Fig. 8A(iii)].

Collectively, these results indicate that the Gm^R cassette was inserted in a duplicated *htpAB* locus with the correct downstream region but an altered upstream region. The existence of more than one *htpAB* locus in LpgroE+ strain was clearly ruled out by the results shown in Figure 8E(i), where a single band was detected for both the *Eco*RI and *Hin*dIII digests of LpgroE+ DNA. Therefore, the duplication of *htpAB,* or part of it, must have happened by an unusual recombination event that occurred between plasmid pBRDXΔ*htpB*:*gm* and the *htpAB* locus.

To confirm that the *L. pneumophila* parent strain, Lp02, does not contain a duplicated region of *htpB*, Lp02 genomic DNA was digested with eight different restriction enzymes, separated by agarose gel electrophoresis, and subjected to Southern blotting (Fig. 9). The blot was hybridized with a 750 bp DNA probe derived from *htpB* (Materials and Methods Section 2.2.4). As can be seen in Figure 9, the probe detected

only one distinct band in every lane indicating that, in the absence of any genetic manipulation, the genome of strain Lp02 contains only one copy of *htpB*. Therefore, based on the Southern blot results obtained with Lp02, LpgroE+, and putativeLp02groE+Δ*htpB* strains, we suggest that the duplication of the *htpAB* region occurred during our attempt to delete *htpAB*.

3.3.4. The *htpAB* Operon Could not Be Replaced by a Kanamycin-resistance Cassette in *L. pneumophila* Strains JR32 and Lp02.

To rule out the unlikely, yet possible, option that the essential nature of *htpAB* is strain-dependent, we attempted to replace *htpAB* in strain JR32. Additionally, to determine if the Gm^R cassette, itself, triggers genetic rearrangements, we attempted to replace *htpAB* in strains JR32 and Lp02 with a Km^R cassette (Fig. 10A). Strains JR32 and Lp02 were transformed with pBRDXΔ*htpAB:km3* and transformants were selected on BCYE plates supplemented with kanamycin. Out of 300 JR32and 270 Lp02 Km^R clones that were replica plated on appropriate media for identification of potential JR32Δ*htpAB* or Lp02Δ*htpAB* mutant strains, ~125 clones of each strain were Cm^S, Km^R, Suc^R, Mtz^R. Of the total pool of potential JR32Δ*htpAB* and Lp02Δ*htpAB*mutants, 120 clones were randomly selected to test, using PCR, the presence or absence of *htpB* using primers htpBF and htpBR (Figure 10B). We also tested by immunoblot 30 randomly selected clones of the total JR32/Lp02 pool for HtpB expression. The presence of *htpB* or HtpB was detected in all of the clones screened by PCR or immunoblot (Fig. 10B&C), suggesting that all screened colonies of potential JR32Δ*htpAB*orLp02Δ*htpAB*mutants still contained a functional *htpAB* operon.

To determine whether the Km^R cassette had followed the same fate of the Gm^R cassette described above (Section 3.3.3), a total of 25 potential JR32Δ*htpAB*and25 Lp02Δ*htpAB* clones were subjected to another PCR analysis using primers P6 and P7 (which bound outside of the cloned upstream and downstream regions of the *htpAB* locus) in combination with primers kmF and kmR (designed for detection of the kanamycin cassette) (Fig. 10A). When primers P7 and kmR were paired, a predicted ~1600 bp amplification product was produced from the potential JR32/Lp02Δ*htpAB* clones, confirming that the Km^R cassette had integrated into the correct region of the *htpAB* locus (Fig. 10D). However, no PCR amplification products were detected when P6 and kmF primers were paired (Fig. 10D). These results suggest that the Km^R cassette was also integrated in a duplicated *htpAB* locus with a unique upstream region following a mechanism similar to that described above for the Gm^R cassette (Section 3.3.3).

3.4. Discussion

We attempted to construct a Δ*htpAB* mutant in *L. pneumophila* strains Lp02 and JR32, to generate a valuable tool that we could use to investigate the direct impact of *htpAB* on the intracellular establishment of *L. pneumophila.* However, we could not delete *htpAB* by allelic replacement, even in the presence of the *E. coli groE* operon, whose gene products were expected to complement the essential functions of HtpA/HtpB. The explanations that we could provide for these results are that: (i) the *htpAB* operon is essential for *L. pneumophila*, (ii) *groE* could not genetically complement the *htpAB* operon, and (iii) that any attempt to delete the *htpAB* is met with cryptic genetic rearrangements. To survive under strong antibiotic and sucrose counter-selection, the

genetic material of *L. pneumophila* was rearranged to keep both the *htpAB* operon and the gm^R cassette. Therefore, a duplication of the *htpAB* locus appeared to happen due to unusual recombination events.

The failure to delete the *htpAB* operon from the chromosomes of LpgroE+, JR32 or Lp02 using plasmid pBRDX was not due to failure in the methodology that we used. In fact, we were able to delete the non-functional *thyA* from Lp02 using the same methodology. In addition, we used the plasmid pBRDX to replace the *potD* gene with a Km^R cassette (Chapter 5 of this thesis) and others have successfully used pBRDX to delete several *L. pneumophila* genes (251,287). Therefore, it is clear that it is the essential nature of *htpAB* and not the experimental tools used that hindered the *htpAB* deletion.

In *E. coli*, it has been shown that temperature-sensitive mutants in *groE* can be created (143). Therefore a temperature-sensitive *htpB* mutant could, in principle, be created as an alternative to Δ*htpAB* mutant. However this mutant would likely show secondary defects arising from defective folding of many proteins, and phenotypic changes in this mutant could not be unambiguously assigned to the defective HtpB. Another alternative to deletion of *htpAB* would be to down-regulate the expression of HtpB. However, other investigators (97) could not delete the stress regulator gene *rpoH* (a sigma factor required for the expression of *htpAB*) from the genome of *L. pneumophila* or replace the *rpoH* promoter by a controllable IPTG-inducible promoter. In addition, although they observed a reduced amount of *htpB* transcripts in clones carrying antisense sequences for *rpoH* or *htpB*, the levels of HtpB were not reduced (97). These results suggest that *L. pneumophila* requires high levels of HtpB and is capable of increasing the efficiency of translation of the *htpB* mRNA.

To date, multiple copies of chaperonin genes have been detected among several different Gram negative α-proteobacterial genomes, either alone or in conjunction with co-chaperonin genes. For example, *Sinorhizobium meliloti* and *Bradyrhizobium japonicum* contain five copies of the *groEL* homolog. Duplication of chaperonin genes has also been reported in pathogenic bacteria such as *Chlamydia,* and *Mycobacterium tuberculosis* (154,222,223). Using Southern blot analysis, Lema and Brown (253) previously suggested, that *L. pneumophila* has a duplication of the *htpAB* operon, whereas Hoffman et al. (177) suggested that *Legionella* has only one *htpAB* locus. Due to these conflicting results, we considered the possibility of an *htpAB* operon duplication in strain Lp02, but the Southern blot results shown in Figure 10 clearly confirm that strain Lp02 genomic DNA has only one copy of the *htpAB* operon [Fig. 8E(i) and 10]. Moreover, our results are compatible with the DNA sequencing results of the five available *L. pneumophila* genomes from strains Philadelphia-1 (61), Paris, Lens (52), Corby (145), and Alcoy (78), since none of these strains contains multiple copies of the *htpAB* operon. Therefore, it seems that the Southern blot findings by Lema and brown were experimentally incorrect.

We showed in this report that *groE* could not genetically complement *hptAB*. Conversely, Hoffman et al. (177) could not complement a temperature sensitive *groEL* mutation in *E. coli* strain CG218 [groEL100(Ts)] with *htpB* in *trans*. This is pertinent because it indicates that GroEL and HtpB are either not functionally equivalent or their functions are species specific.

Gene duplication or amplification (GDA) may occur as a result of retro-transposition or an error in homologous recombination (unequal crossing-over between

two DNA fragments) (447). The product of this error in recombination is a duplication at the site of the exchange and a reciprocal deletion (399). GDA of essential genes results in additional copies of the gene that are free from selective pressure and thus allow mutations without deleterious consequences to the organism, as long as one copy maintains the essential functions. This freedom from consequences allows for mutation of novel genes that could potentially increase the fitness of the organism or code for new functions. Recent data suggest that, in response to the presence of antibiotics, GDA constitutes an important adaptive mechanism in bacteria. For example, bacterial resistance to β-lactams, trimethoprim and sulphonamides can be conferred by increasing the copy number of the genes encoding antibiotic hydrolytic enzymes, target enzymes, or efflux pumps, making GDA more similar to a regulatory response (359). It is possible that, in our hands, the htpAB locus was duplicated under gentamicin or kanamycin antibiotic selection, and then one of the duplicated copies was replaced by the Gm^R or Km^R cassette.

In conclusion, our studies represent an example of how bacteria such as *L. pneumophila* manage to avoid deletion of an essential gene, and provide evidence that although high degrees of sequence similarity do exist between bacterial chaperonins, the genes encoding these chaperonins are not necessarily interchangeable. In the absence of genetic deletion, the use of functional protein models becomes more relevant, as will be shown in Chapter 4, where *Saccharomyces cerevisiae* was used as a model to understand the virulence-related functions of HtpB.

3.5. Acknowledgments

David Allan and Mackenzie Howatt, are gratefully acknowledged for their technical help in cloning. We thank Dr. Lois Murray, Dr. Jessica Boyd, and Dr. Nikhil Thomas for their helpful suggestions. We also thank Dr. Paul Hoffman for generously providing antibodies against HtpB. This work was supported by a Discovery grant from NSERC to RAG.

3.6. Figures and Legends to Figures

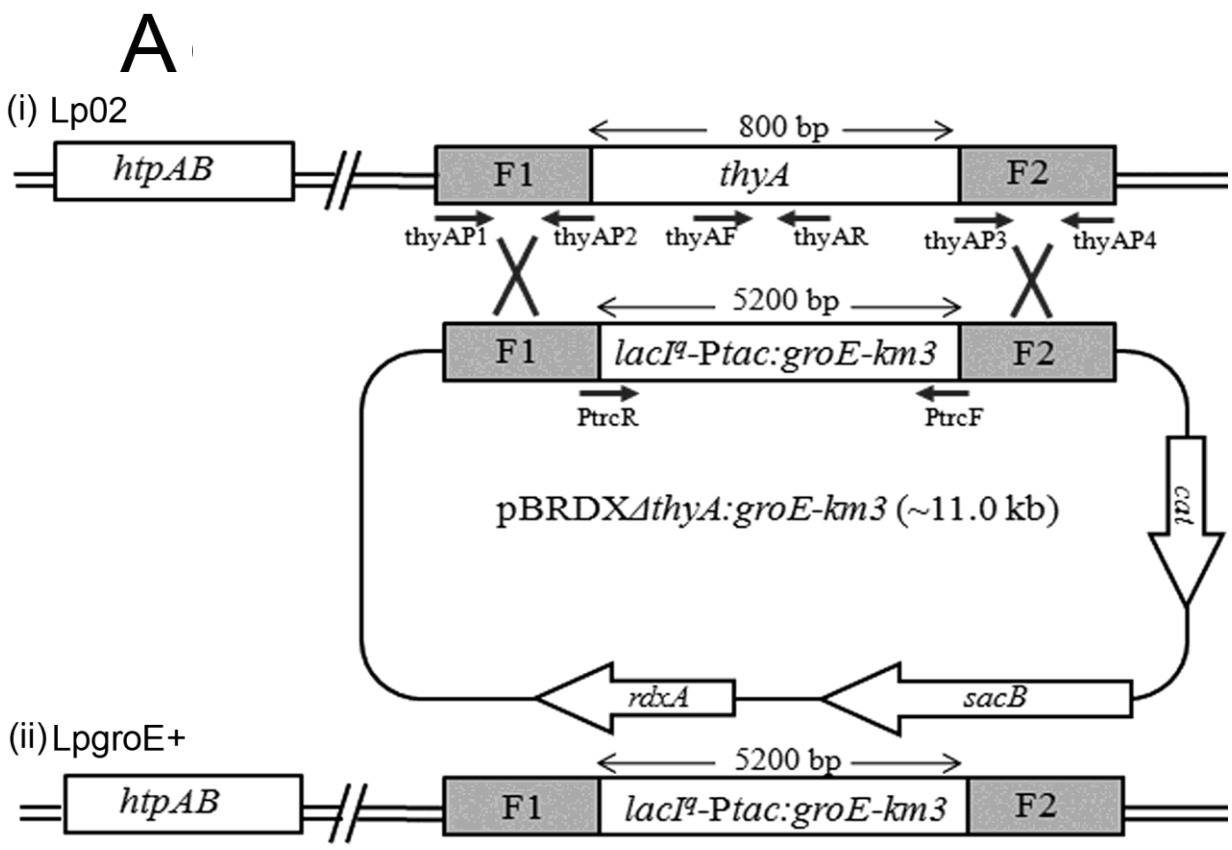
A
(i) Lp02
800 bp
htpAB
F1
thyA
F2
thyAP1
thyAP2
thyAF
thyAR
thyAP3
thyAP4
5200 bp
F1
lacIq-Ptac:groE-km3
F2
PtrcR
PtrcF
pBRDXΔthyA:groE-km3 (~11.0 kb)
cat
rdxA
sacB
(ii) LpgroE+
5200 bp
htpAB
F1
lacIq-Ptac:groE-km3
F2

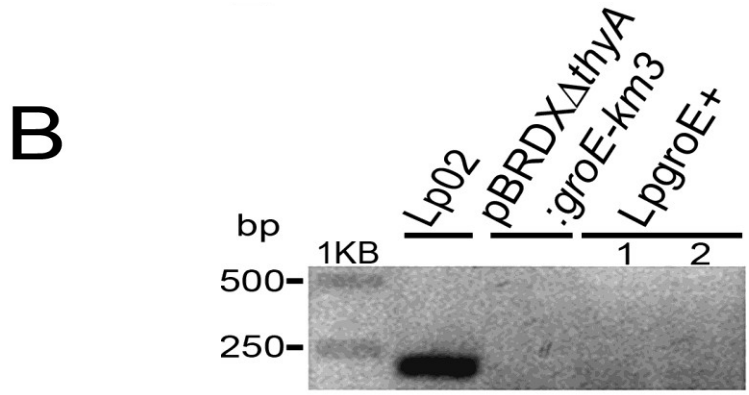
B
Lp02
pBRDXΔthyA
:groE-km3
LpgroE+
bp
1KB
1
2
500
250

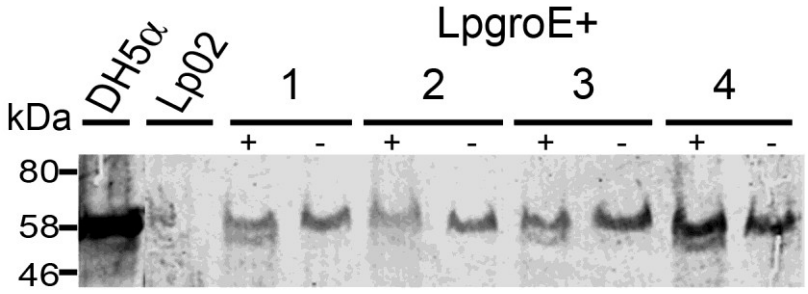
C
LpgroE+
DH5α
Lp02
1
2
3
4
kDa
+
-
+
-
+
-
+
-
80
58
46

Figure 7. Construction of the LpgroE+ strain and confirmation of the replacement of *thyA* with the *groE* operon.

(**A)** Schematic representation (not to scale) of the approach followed to replace *thyA* from the genome of strain Lp02. **(i)** Area of the Lp02 genome showing the *htpAB* operon at a distant location in relation to the *thyA* gene, and the *lacI*^{q}-P$_{tac}$-*groE-km3*DNA fragment carried in the counter selectable vector pPRDXΔ*thyA*:*groE-km3* between the flanking regions of the *thyA* gene. **(ii)** Diagram representing LpgroE+ chromosome after replacement of *thyA* with*lacI*^{q}-P$_{tac}$-*groE-km3*. The *thyA* flanking regions (F1) and (F2) were amplified from the genome of strain Lp02 by PCR using primer pairs thyAP1/thyAP2 and thyAP3/thyAP4, respectively. The *lacI*^{q}-P$_{tac}$-*groE-km3*DNA fragment (~5200 bp) was amplified by PCR from plasmid pTrcKm using primers PtrcF and PtrcR and cloned between the F1 and F2thyA fragments. The resulting fragment, F1-*lacI*^{q}-P$_{tac}$-*groE-km3*-F2, was subcloned into plasmid pBRDX to generate pBRDXΔ*thyA*:*groE-km3,* and used to construct a LpgroE+ strain by allelic replacement. (**B**) Ethidium bromide-stained agarose gel showing PCR amplicons obtained usingprimers thyAF and thyAR, which amplify a ~240 bp DNA fragment from*thyA,* confirmed that potential Lp02Δ*thyA* (LpgroE+) clones do not yield an amplification product for *thyA* (2 LpgroE+ clones are shown). DNA from strain Lp02 and pBRDXΔ*thyA:groE-km3* was used as a positive and negative control, respectively, for the presence and absence of *thyA*. The sizes of DNA standards (bp) are indicated at the left side of the gel. (**C**) LpgroE+ clones were grown in BYE medium to exponential phase in the presence **(+)** or absence **(-)** of IPTG**.** Whole cell lysates from four LpgroE+ clones (including the 2 LpgroE+ clones used in panel **B**) were separated by SDS-PAGE,

transferred to a nitrocellulose membrane, and immune stained with MAb specific for GroEL Whole cell lysates from strains *E. coli strain* DH5α and *L. pneumophila* strain Lp02 were used as positive and negative controls, respectively, for presence of GroEL. The position and size (kDa) of protein standards are indicated at the left side of the blot. This figure was generated by Gheyath Nasrallah.

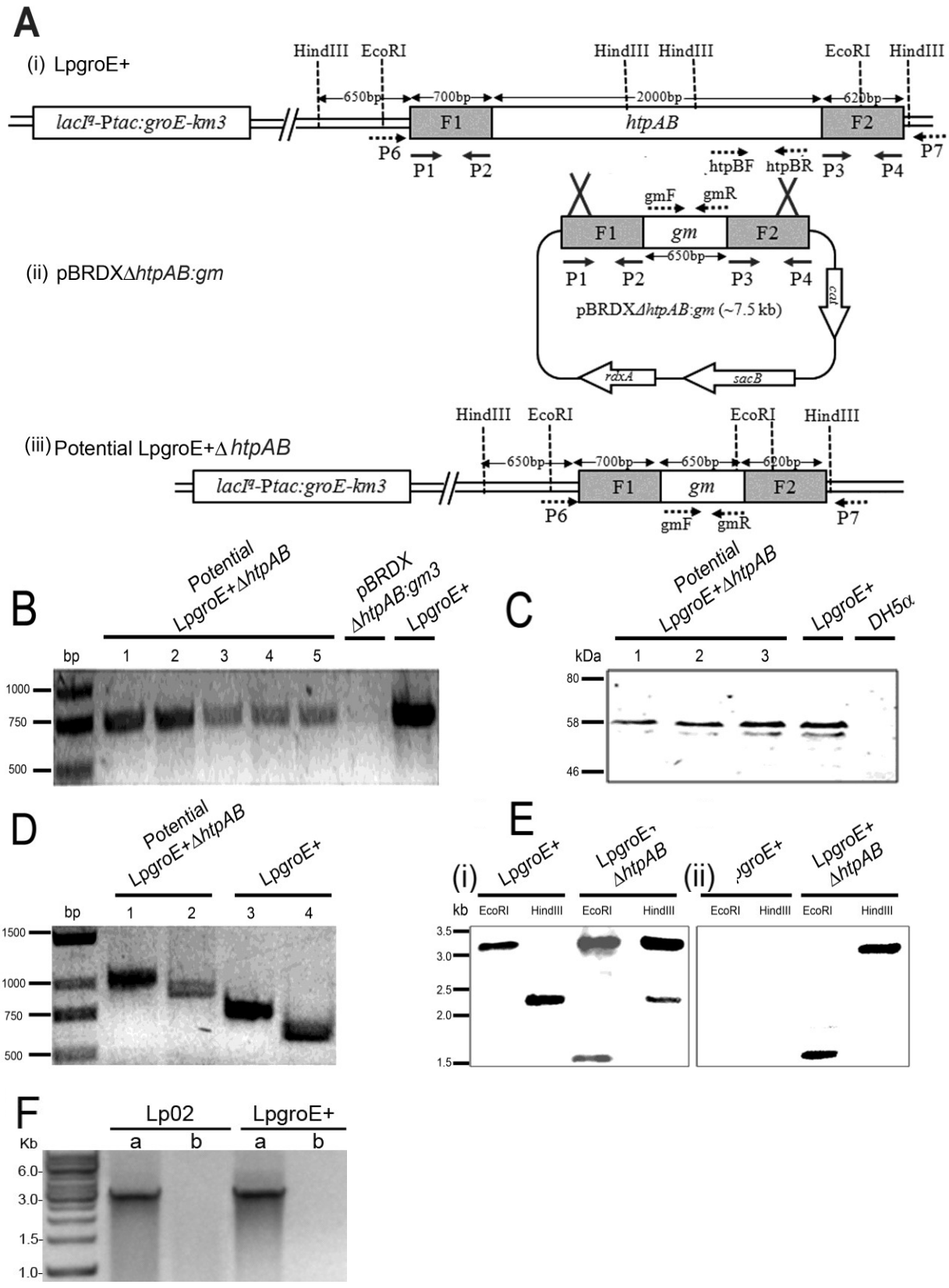
A
(i) LpgroE+
HindIII EcoRI
HindIII HindIII
EcoRI HindIII
650bp
700bp
2000bp
620bp
lacIq-Ptac:groE-km3
F1
htpAB
F2
P6
P1
P2
htpBF
htpBR
P3
P4
P7
(ii) pBRDXΔhtpAB:gm
gmF
gmR
F1
gm
F2
650bp
P1
P2
P3
P4
cat
pBRDXΔhtpAB:gm (~7.5 kb)
radA
sacB
(iii) Potential LpgroE+Δ htpAB
HindIII EcoRI
EcoRI HindIII
650bp
700bp
650bp
620bp
lacIq-Ptac:groE-km3
F1
gm
F2
P6
gmF
gmR
P7
B
Potential LpgroE+ΔhtpAB
pBRDX ΔhtpAB:gm3
LpgroE+
bp
1
2
3
4
5
1000
750
500
C
Potential LpgroE+ΔhtpAB
LpgroE+
DH5α
kDa
1
2
3
80
58
46
D
Potential LpgroE+ΔhtpAB
LpgroE+
bp
1
2
3
4
1500
1000
750
500
E
(i)
LpgroE+
LpgroE+ ΔhtpAB
(ii)
LpgroE+
LpgroE+ ΔhtpAB
kb
EcoRI
HindIII
EcoRI
HindIII
EcoRI
HindIII
EcoRI
HindIII
3.5
3.0
2.5
2.0
1.5
F
Lp02
LpgroE+
a
b
a
b
Kb
6.0
3.0
1.5
1.0

Figure 8. Attempt to construct an LpgroE+Δ*htpAB* mutant strain and confirmation of the duplication of the *htpAB* flanking regions.

(A) Schematic representation (not to scale) of the allelic replacement approach followed to attempt deletion of *htpAB* from the genome of strain LpgroE+. **(i)** Area of the LpgroE+ genome showing the *htpAB* operon at a distant location in relation to the *lacI*^{q}-P$_{tac}$-*groE-km3* DNA fragment. **(ii)** Counter selectable plasmid pPRDXΔ*htpAB:gm*with a Gm^{R} cassette between the flanking regions of the *htpAB* operon, used to construct potential LpgroE+Δ*htpAB*mutants by allelic replacement. **(iii)** Potential configuration of the LpgroE+Δ*htpAB:gm* chromosome after the predicted replacement of *htpAB* with the Gm^{R} cassette.The *Eco*RI and *Hin*dIII restriction sites of *htpAB* and flanking regions are indicated in **(i)** and **(iii)** as a reference to interpret the PCR results shown in panel **D** and the Southern blot results shown in panel **E**. **(B)** Ethidium bromide-stained agarose gel showing the colony PCR products amplified from the bacterial clones shown on top of the gel using primers htpBF and htpBR. All potential LpgroE+Δ*htpAB* mutant clones (clones 1-5 are shown) display a 750 bp amplification product. Strain LpgroE+ and plasmid pBRDXΔ*htpAB:gm* were used as a positive and negative amplification control templates, respectively, for the presence and absence of *htpB*. The position and size of DNA standards (bp) are indicated.**(C)** Whole cell lysates from 3 potential LpgroE+Δ*htpAB* clones were separated by SDS-PAGE, transferred to a nitrocellulose membrane, and immunostained with MAb specific for HtpB. Whole cell lysates from strains LpgroE+ and *E. coli* DH5α were used as positive and negative controls, respectively, for the presence of HtpB. The position and size (in kDa) of protein

standards are indicated. **(D)** Ethidium bromide-stained agarose gel showing PCR amplicons confirming that the inserted Gm^R cassette is flanked by the correct region downstream from the *htpAB* locus. Primers P7 and gmF directed amplification of an expected 1070 bp DNA fragment from the potential LpgroE+Δ*htpAB* mutant strains (lane 1: only one clone is shown). The PCR amplification product of lane 1 was digested with *Hin*dIII to produce DNA fragments of 921 bp (lane 2).and 150 bp (not shown in the gel). Primers P7 and P3 were used in a control PCR reaction to amplify an expected 800 bp DNA fragment (lane 3) from strain LpgroE+ that was digested with *Hin*dIII to produce DNA fragments of 650 bp (lane 4) and 150 bp (not shown in the gel). The position and size of DNA standards (bp) are indicated. **(E)** Southern blot confirms that chromosomal DNA from potential LpgroE+Δ*htpAB* mutants have both an intact *htpAB* locus, and a second locus with the inserted Gm^R cassette. Chromosomal DNA from the parent strain Lpgro*E*+ and the potential LpgroE+Δ*htpAB* mutant were digested with *Eco*RI or *Hin*dIII, separated through a 0.8 % agarose gel electrophoresis, and transferred to a nylon membrane. Labelled DNA fragments derived from F1htpAB (700 bp) or the Gm^R cassette (250bp), were used as a hybridization probes in **(i)** and **(ii)**, respectively. The relative positions of DNA standards (Kbp), shown at the left of the blot, were determined from the ethidium bromide-stained agarose gel prior to DNA transfer. **(F)** Ethidium bromide-stained agarose gel showing the 3.5 Kb PCR product amplified from the bacterial strains shown on top of the gel using primers P6 and P7 (lanes **a).** Negative control reactions were performed using primers P6 and gmR (lanes **b**). The position and size of DNA standards (Kb) are indicated. This figure was generated by Gheyath Nasrallah.

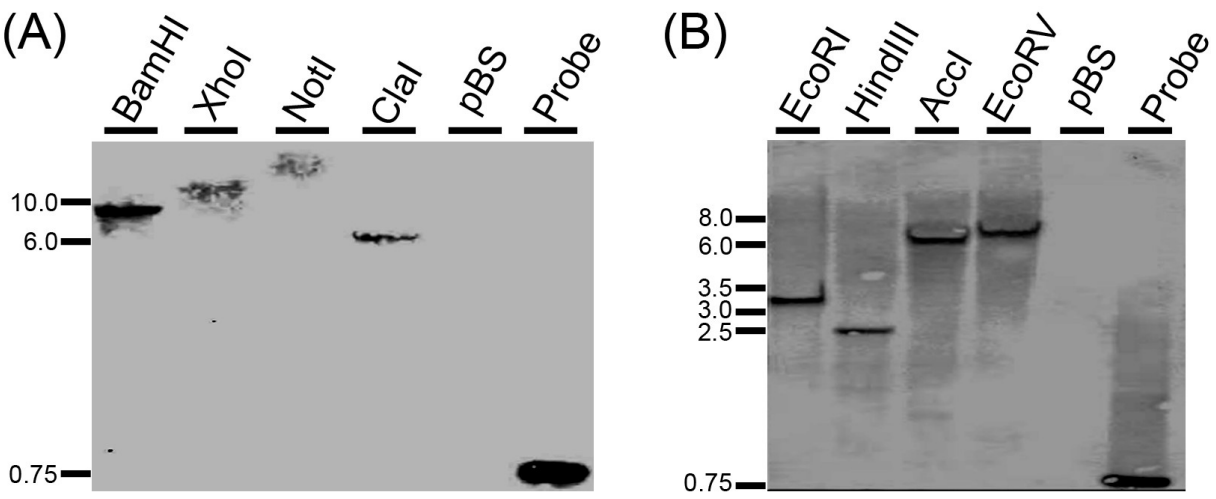

Figure 9. Southern blot analysis confirming that *L. pneumophila* strain Lp02 has only one copy of the *htpAB* locus.

Lp02 chromosomal DNA was digested with the indicated restriction enzymes (**A** and **B**), separated through a 0.8 % agarose gel electrophoresis, and transferred onto nylon membranes. An *htpB* internal fragment of 750bp (amplified by PCR using primers htpBF and htpBR), was used as hybridization probe in **(A)** and **(B)**. Plasmid pBluescript (pBS), and the *htpB* internal fragment (probe) were used as negative and positive hybridization controls, respectively. The relative positions of the indicated molecular size standards (Kb) were determined from the ethidium bromide-stained agarose gel prior to transfer of DNA. This Figure was generated by Elizabeth Gagnon and Gheyath Nasrallah.

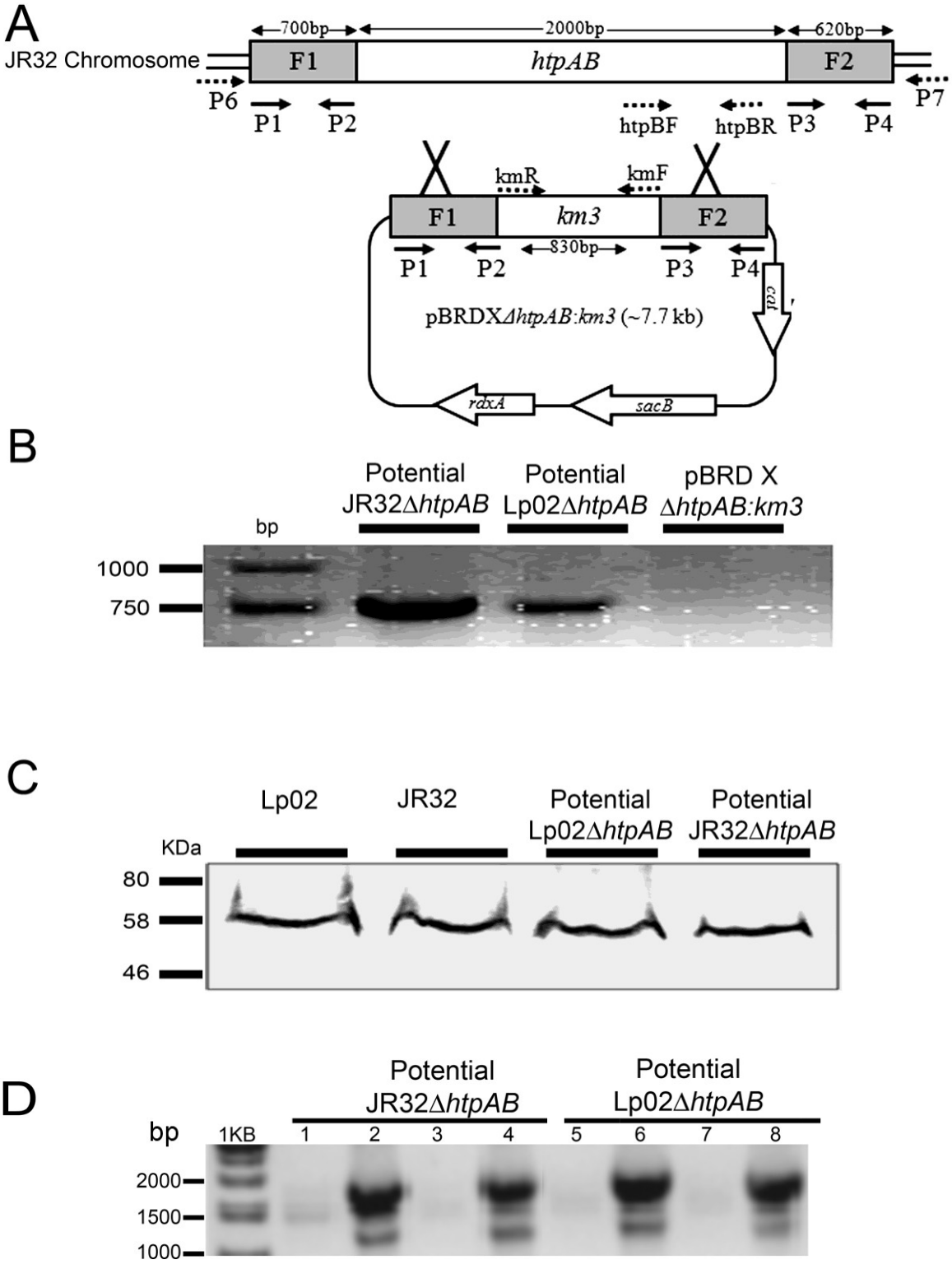
A
JR32 Chromosome
700bp
2000bp
620bp
F1
htpAB
F2
P6
P1
P2
htpBF
htpBR
P3
P4
P7
kmR
kmF
F1
km3
F2
830bp
P1
P2
P3
P4
cat
pBRDXΔhtpAB:km3 (~7.7 kb)
radA
sacB
B
Potential JR32ΔhtpAB
Potential Lp02ΔhtpAB
pBRD X ΔhtpAB:km3
bp
1000
750
C
Lp02
JR32
Potential Lp02ΔhtpAB
Potential JR32ΔhtpAB
KDa
80
58
46
D
Potential JR32ΔhtpAB
Potential Lp02ΔhtpAB
bp
1KB
1
2
3
4
5
6
7
8
2000
1500
1000

Figure 10. The *htpAB* operon could not be replaced by a Km^R cassette in *L. pneumophila* strains JR32 and Lp02.

(A) Schematic representation (not to scale) of the allelic replacement approach followed to attempt replacement of *htpAB* from the genome of strain. JR32 or Lp02 with a Km^R cassette carried in the counter selectable plasmid pBRDX*ΔhtpAB:km3* (**B)** Ethidium bromide-stained agarose gel showing the PCR amplicons generated using primers htpBF and htpBR, confirming that potential JR32*htpAB* or Lp02Δ*htpAB* mutant clones (only one representative clone from each strain is shown) display a 750 bp *htpB* amplification product. Plasmid pBRDXΔ*htpAB:gm* was used as a negative control for *htpB*. The positions and sizes of DNA standards (bp) are indicated. **(C)** Whole cell lysates from potential JR32Δ*htpAB* and Lp02Δ*htpAB* mutant clones were separated by SDS-PAGE, transferred to a nitrocellulose membrane, and immunostained with MAb specific for HtpB. Whole cell lysates from strains JR32 and Lp02 were used as positive controls for the presence of HtpB. The positions and sizes (in kDa) of protein standards are indicated. **(D)** Ethidium bromide-stained agarose gel showing PCR amplicons confirming that the inserted Km^R cassette is flanked by the correct region downstream of the *htpAB* locus, but not the correct *htpAB* upstream region. A PCR reaction using primers P7 and kmR amplified an expected 1600 bp from two potential JR32Δ*htpAB* (lanes 2, 4), or twopotential Lp02Δ*htpAB* (lanes 6 and 8) clones. DNA from the same clones was used as template in a second PCR reaction using primers P6 and kmF, where no amplification product was produced, in the two potential JR32Δ*htpAB* clones (lanes 1 and 3) or the two potential Lp02Δ*htpAB* (lanes 5 and 7).The positions and sizes of DNA standards (bp) are indicated This Figure was generated by Dennis Orton and Gheyath Nasrallah.

CHAPTER 4: *LEGIONELLA PNEUMOPHILA* REQUIRES POLYAMINES FOR OPTIMAL INTRACELLULAR GROWTH– POTENTIAL ROLE OF THE HTPB IN MODULATING HOST CELL POLYAMINES

Gheyath K. Nasrallah[1], Angela L. Riveroll[1], Audrey Chong [1], Lois E. Murray [1], P. Jeffrey Lewis [2], and Rafael A. Garduño[1,3],*

[1] Department of Microbiology and Immunology, Dalhousie University, Halifax, Nova Scotia, Canada.

[2]Atlantic Veterinary College, University of Prince Edward Island, Charlottetown, Prince Edward Island, Canada,

[3]Department of Medicine – Division of Infectious Diseases, Dalhousie University, Halifax, Nova Scotia, Canada.

*Corresponding author

Adapted from an accepted manuscript (*Journal of Bacteriology)* with modifications.

Nasrallah *et al*. manuscript (JB01506-10 Version 2)

4.1. Abstract

The Gram-negative intracellular pathogen *Legionella pneumophila* replicates in a membrane-bound compartment known as the *Legionella*-containing vacuole (LCV) into which it abundantly releases its chaperonin, HtpB. To determine whether HtpB remains within the LCV, or reaches the host cell cytoplasm, we infected U937 macrophages and CHO cells with *L. pneumophila* expressing a translocation reporter consisting of the *Bordetella pertussis* adenylate cyclase enzyme: HtpB fusion. These infections led to increased cAMP levels, suggesting that HtpB reaches the host cell cytoplasm. To identify potential functions for cytoplasmic HtpB, we expressed it in the yeast *Saccharomyces cerevisiae*, where HtpB induced pseudohyphal growth (PHG). A yeast-two-hybrid screen showed that HtpB specifically interacted with S-adenosyl methionine decarboxylase (SAMDC), an essential yeast enzyme (encoded by *SPE2*) that is required for polyamine biosynthesis. Increasing the copy number of *SPE2* also induced PHG in *S. cerevisiae*, thus we speculated that (i) HtpB induces PHG by activating polyamine synthesis, and (ii) *L. pneumophila* may require exogenous polyamines for growth. A pharmacological inhibitor of SAMDC significantly reduced *L. pneumophila* replication in L929 mouse cells and U937 human macrophages, whereas exogenously added polyamines favoured intracellular growth, confirming that polyamines and host SAMDC activity promote *L. pneumophila* proliferation. Bioinformatic analysis revealed that most known enzymes required for polyamine biosynthesis in bacteria (including SAMDC) are absent in *L. pneumophila*, suggesting that this bacterium must scavenge exogenous polyamines. We hypothesize that HtpB may function to ensure a supply of polyamines in host cells, which are required for the optimal intracellular growth of *L. pneumophila*.

4.2. Introduction

Chaperonins constitute a family of highly conserved proteins found in all prokaryotic and eukaryotic organisms (154). Their primary role is to facilitate the folding of nascent and stress-denatured proteins into their functional native states, in an ATP-dependent manner (221). Group I chaperonins, referred to as Hsp60, Cpn60 or GroEL, are prokaryotic proteins found in bacteria and in eukaryotic organelles such as mitochondria and chloroplasts (154). Group II chaperonins, also known as CCT or TCP-1, are found in the eukaryotic cytosol and in the Archaea (154). Structural and functional studies of *E. coli* GroEL have established the role of group I chaperonins as intracellular mediators of protein-folding (31,444). GroEL is an essential protein in *E. coli* (103), whose intracellular level increases substantially in response to different stressful stimuli (263,416). The protein-folding paradigm of group I chaperonins has changed with accumulating reports of surface- and membrane-associated chaperonins that perform other diverse functions. For instance, the extracytoplasmically localized chaperonins of *Haemophilus ducreyi*(124), *Helicobacter pylori*(47,437), *Borrelia burgdorferi*(367), and *Clostridium difficile*(167) have been implicated in adhesion and (or) cell invasion. It has also been shown that some surface-exposed bacterial chaperonins have the capacity to interact with mammalian cell surface receptors to initiate signaling events that result in cytokine production(330). Moreover, the functional flexibility of group I chaperonins is demonstrated by the role of the *Mycobacterium leprae* chaperonin as a protease (326), the *Enterobacter aerogenes* GroEL as an insect toxin (440), and the *E. coli* GroEL as a lipochaperonin (413).

Legionella pneumophila, a Gram-negative intracellular amoebal pathogen, is also an opportunistic human pathogen that replicates in mononuclear leukocytes (191) and causes Legionnaires' disease in susceptible individuals (296). The *L. pneumophila* 60-kDa chaperonin, encoded by the *htpB* gene (61,177), is expressed at high levels under steady state conditions, with only a 2-fold increase in expression following heat shock (254). This is in sharp contrast to the normally low levels of expression of GroEL in *E. coli*, and the ~20-fold increase in expression upon heat shock (177,254). We have been unable to delete *htpB* from the *L. pneumophila* genome (65), suggesting that it is an essential gene. Therefore, our HtpB studies are based on the use of functional protein tests.

HtpB expression is upregulated in the presence of L929 cells and monocytes, even prior to *Legionella* internalization, and a high level of expression is maintained throughout intracellular infections (107), leading to accumulation of HtpB in the lumen of the *Legionella*-containing vacuole (LCV), as observed in L929 cells, monocytes and HeLa cells (107,137,178). More than 40% of the cell-associated HtpB epitopes detectable by immunogold labelling are membrane-associated, periplasmic or cell-surface localized in *L. pneumophila*(137), and we have previously established that the surface-localized HtpB acts as an adhesion and invasion factor in HeLa cells (139). Furthermore, microbeads coated with purified HtpB (but not uncoated beads or beads coated with control proteins) were sufficient to attract mitochondria and transiently modify the organization of actin microfilaments in human macrophage and Chinese hamster ovary (CHO) cell lines (65). Although HtpB could function by signalling across the cell and

LCV membranes after binding to host cell surface receptors, it is also possible that HtpB reaches the cytoplasm of infected cells and interacts with cytoplasmic targets.

In this study, we determined that HtpB is not confined to the lumen of the LCV, but reaches the host cell cytosol. To identify potential functions for cytoplasmic HtpB, we expressed it in the genetically tractable eukaryote *Saccharomyces cerevisiae* and found that it induces pseudohyphal growth (PHG) and specifically interacts with SAMDC, an enzyme required for biosynthesis of the polyamines spermidine and spermine in eukaryotic cells. Pharmacological inhibition of SAMDC activity significantly reduced the intracellular multiplication of *L. pneumophila* in mammalian cell lines. Moreover, the addition of exogenous polyamines enhanced the intracellular growth of *L. pneumophila*, collectively suggesting that host polyamine biosynthesis and elevated levels of polyamines are important for the optimal intracellular growth of *L. pneumophila*.

4.3. Results

4.3.1. HtpB Reaches the Cytosol of *L. pneumophila* Infected Cells

Immunoelectron microscopy data previously suggested that HtpB is exposed on the cytoplasmic face of LCVs (62,107). To determine whether HtpB indeed reaches the cytoplasm of infected cells, we used the CyaA reporter system, which has been used before to establish the translocation of *L. pneumophila* type IV secretion effectors (46,59,81,293). Initially, we used CHO-*htpB* cells as part of a series of functional studies aimed at assessing the responses of mammalian cells to HtpB (65). The ectopic expression of HtpB in CHO-*htpB* is controlled by a tetracycline-responsive promoter, in

which *htpB* expression is turned off in the presence of doxycycline (Tet-off). CHO-*htpB* cells not expressing ectopic HtpB and infected with strains Lp02 or JR32 expressing the HtpB-CyaA fusion showed a significant increase in cAMP levels ($P<0.05$, Fig. 11a) compared to host cells infected with *L. pneumophila* harboring the empty vector control, or the CyaA only construct. Cells infected with *L. pneumophila* expressing the CyaA-HtpB fusion showed lower cAMP levels in comparison to those infected with *L. pneumophila* expressing HtpB-CyaA (Fig. 11b), suggesting that the N-terminus of HtpB either is important for translocation, or interferes with CyaA activity. To rule out the latter we showed that a large increase in cAMP was detected after mixing a host cell lysate with a lysate from strain JR32 expressing the CyaA-HtpB fusion (Fig. 11b). This increase was comparable to that induced by the lysate of JR32 expressing the LepA-CyaA fusion (LepA is a Dot/Icm effector used as a positive translocation control), suggesting that the lower level of cAMP produced by CHO-*htpB* cells infected with *L. pneumophila* expressing CyaA-HtpB was not due to a defect in CyaA activity, or to low expression of the fusion protein. HtpB reaches the cytoplasm of infected cells was then confirmed in U937-derived macrophages (Fig. 11c). Overall, the levels of cAMP in macrophages were higher than in CHO-*htpB* cells.

4.3.2. Inducible Expression of HtpB in *S. cerevisiae*

Knowing that HtpB reaches the cytoplasm of infected cells, we set out to investigate potential functions for cytoplasmic HtpB in the genetically tractable eukaryote *S. cerevisiae*. Expression of ectopic HtpB in yeast cells grown in inducing medium containing galactose was confirmed by immunoblot (Fig. 12a). No growth differences

were detected between two HtpB-expressing clones and a clone carrying the empty vector control in YEP-Galactose (inducing) liquid medium (compare Fig. 12b & c). However, the expression of HtpB caused an approximately 2-fold reduction in colony numbers in relation to yeast cells grown on glucose (Fig. 12b, inset) or yeast cells carrying the empty plasmid pEMBLyex4 (Fig. 12c, inset), suggesting that solid medium imposed a slight growth restriction on yeast cells expressing HtpB. Expression of HtpB in liquid cultures coincided with the initiation of growth, 10 h after placing yeast cells in YEP-Galactose (Fig. 12c).

4.3.3. HtpB Stimulates *S. cerevisiae* to Form Pseudohyphae

In nature, *S. cerevisiae* cells form pseudohyphae when nitrogen becomes limiting (131). Haploid yeast strains may also differentiate and become invasive under glucose limitation (241,242). On nitrogen-replete solid medium containing galactose, cells of the haploid yeast strain W303-1b expressing HtpB from plasmid pEMBLyex4::*htpB*, elongated and budded in a unipolar direction (Fig. 13a), and after 5 days at 30ºC, they produced some agar-invasive filamentous colonies (Fig. 13b). W303-1b cells carrying the empty vector, pEMBLyex4, remained ovoid when grown on the same medium (Fig. 13c) and were not agar-invasive (Fig. 13d). The same pseudohyphal phenotype (as shown in Fig. 13a & c) was observed in cells of strain W303-1b harboring the construct pPP389::*htpB*. To be able to check the HtpB-mediated phenotype in a glucose-replete medium, HtpB was expressed from pGBD-C1::*htpB*, a construct that drives expression of the GAL4DBD-HtpB chimera using a modified alcohol dehydrogenase promoter (P_{ADH1}) (Fig. 14). Yeast strain W303-1b carrying pGBD-C1::*htpB* also formed pseudohyphae 15-

20 h after inoculation on SD solid medium with glucose (Fig. 15).Therefore, induction of PHG by HtpB occurs in nitrogen- and glucose-replete media.

4.3.4. Other Type I Chaperonins Do Not Stimulate *S. cerevisiae* to Form Pseudohyphae

The *S. cerevisiae* mitochondrial chaperonin (Hsp60p) (systematic name: YLR259C, SGD™), shares 54.5 % protein sequence identity with HtpB (Accession: AAA25299, NCBI Entrez Protein) according to the Lalign program (314). Unlike HtpB, Hsp60p has a positively charged motif at its N-terminus that is necessary for import into yeast mitochondria. A complete *HSP60* construct and a construct lacking the mitochondrial import motif (*hsp60*Δ1-72) were expressed in strain W303-1b to produce either full-length Hsp60p or the truncated Hsp60Δ1-24p, as confirmed by immuno-blot (Fig. 16a). In contrast to HtpB-expressing cells, W303-1b cells expressing either Hsp60p or Hsp60Δ1-24p did not form pseudohyphae (Fig. 16b). Results were the same when either vector, pPP389 or pEMBLyex4, was used for chaperonin expression.

GroEL, the *E. coli* Hsp60 (Accession: AAC77103, NCBI Entrez Protein), shares 75.5% protein sequence identity with HtpB according to the Lalign program (314). We set out to determine if the few amino acid differences between GroEL and HtpB would result in functional differences in relation to pseudohyphae formation in yeast. Yeast strain W303-1b expressing *E. coli* GroEL from pEMBLyex4::*groEL* (Fig. 16a) did not form pseudohyphae (Fig. 17b to d). Collectively, these data indicate that the ability to alter yeast cell morphology does not represent a general characteristic of group I chaperonins.

4.3.5. S-Adenosyl Methionine Decarboxylase (SAMDC) Interacts with HtpB in *S. cerevisiae*

We hypothesized that there is a specific interaction between HtpB and a yeast protein involved in PHG. To test this hypothesis, we conducted a yeast two-hybrid (Y2H) screen using as bait the Gal4DBD-HtpB chimera, which is functional for PHG induction (Fig. 15). Circa 8 x 10^8 yeast clones carrying yeast genomic library plasmids were screened and two strongly positive clones were identified (pGAD-C1::*20A* and pGAD-C1::*20B*) (Fig 18A). To rule out interaction artefacts and confirm the specificity of these Y2H protein-protein interactions, these two library plasmids were co-transformed into fresh Y153 cells with the empty plasmid pGBD-C1 or plasmid pSE1111 (encoding an irrelevant protein, Table. 3), which served as negative interaction controls (Fig 18B). Only Y153 co-transformants bearing pGBD-C1::*htpB* and pGAD-C1::*20A* or pGBD-C1::*htpB* and pGAD-C1::*20B* showed positive interactions (Fig. 18B). DNA sequence determination revealed that the 20A DNA library fragment encodes the last 233 amino acids of SAMDC (residues 166-396), whereas the 20B DNA fragment encodes only the last 206 amino acids (residues 189-396), suggesting the C-terminus of SAMDC is sufficient to interact with HtpB. *SPE2*, the *S. cerevisiae* gene that encodes SAMDC. In yeast, SAMDC is a conserved and essential enzyme required for aerobic growth (17-19) and for synthesis of the polyamines spermidine and spermine (74,394).

4.3.6. The Mammalian Small Heat Shock Protein (Hsp10) Interacts with HtpB in HeLa Cells

We have previously shown that HtpB is involved in reorganization of actin filaments when expressed in the non-phagocytic CHO cells and that it mimics the ability

of virulent *L. pneumophila* to attract mitochondria when added to CHO and U937 human-derived macrophages in the form of HtpB coated beads (65). We hypothesized that there is a specific interaction between HtpB and a mammalian protein (s) involved in these two phenotypes. To test this hypothesis, we conducted a second Y2H screen using, as bait, the Gal4DBD-HtpB chimera to test for HeLa cell proteins (Gal4AD-HeLa proteins) that interacts with HtpB. Approximately 5 x 10^6 yeast clones carrying HeLa cDNA library plasmid (pGADT7::cDNAx) were screened, and 21 positive clones were identified. DNA sequence determination revealed that all of the 21 positive clones encoded the mammalian small heat shock protein Hsp10**.** One of these positive clones was chosen and the encoding plasmid named pGADT7::*HSP10***.** Hsp10 is the co-chaperonin that, together with the mitochondrial chaperonin (Hsp60p), mediates protein folding in the mitochondrial matrix (154). The eukaryotic Hsp10 and Hsp60 proteins are synthesized in the cytoplasm and imported through the mitochondrial membranes into the mitochondrial lumen. Additionally, Hsp10 has been detected on the surface of mitochondria (354) to mitochondria. Therefore, the HtpB-Hsp10 interaction could be relevant to the recruitment of mitochondria to the LCV.

4.3.7. Overexpression of SAMDC Induces PHG in Yeast

Knowing that a transient increase in both the level of polyamines and the activity of polyamine synthetic enzymes characterizes the yeast-to-hyphae transition in many fungal species (152,168,201,277,358), we hypothesized that overexpression of SAMDC could result in PHG in *S. cerevisiae*. To test this hypothesis we increased the *SPE2* copy number in strain W303-1b as a means to enhance SAMDC activity. It has been noted

elsewhere that when *SPE2* is carried on a yeast high copy plasmid, the activity of SAMDC in *S. cerevisiae* increases ~50-fold in relation to that of *S. cerevisiae* that does not bear the plasmid (226)**.** In our hands the presence of the high-copy number plasmid pPP389::*SPE2* in W303-1b also induced PHG (Fig. 19). Thus, over-expression of either HtpB or its interacting protein, SAMDC, induces the same phenotype in *S. cerevisiae*.

4.3.8. SAMDC Activity Promotes *L. pneumophila* Replication in Host Cells

To determine whether *L. pneumophila* requires the activity of host SAMDC during intracellular growth in mammalian cells, we infected cells treated with two inhibitors of polyamine biosynthesis. MGBG acts as a specific, competitive and irreversible inhibitor of SAMDC (75,422,434), and DFMO is an irreversible inhibitor of ornithine decarboxylase (271,327), an enzyme required for the synthesis of putrescine, a precursor to spermidine. We initially found that treatment of mouse L929 cells with MGBG significantly inhibited *L. pneumophila* intracellular replication at 24 and 48 h post infection, whereas DFMO inhibition was only significant 48 h post infection (Fig. 20a). The pharmacological inhibition of SAMDC by MGBG was clearly dose-dependent in both L929 cells (Fig. 20b) and in U937 macrophages (Fig. 20c), suggesting that host SAMDC, but not necessarily host ornithine decarboxylase, needs to remain fully active to support the optimal early replication of *L. pneumophila* in mammalian cells.

At concentrations of 100 μM neither MGBG nor DFMO was significantly toxic to L929 cells or U937 macrophages , as determined by Trypan blue staining. In addition, neither MGBG nor DFMO at a final concentration of 100 μM showed a direct inhibitory effect on *L. pneumophila* replication in BYE. These toxicity results suggest that the

inhibition of *L. pneumophila* growth in L929 and U937 cells was not due to a drug-mediated killing of infected cells, or to a direct effect of MGBG or DFMO on *L. pneumophila*.

4.3.9. Addition of Exogenous Polyamines Enhances the Growth of *L. pneumophila in vitro*

Exogenous polyamines enhance *L. pneumophila* growth *in vivo*, therefore, we set out to test whether we could see a similar effect *in vitro*. Supplementing BYE medium with polyamines enhanced the growth of strain JR32 *in vitro* (Fig. 21a & 21d) and for spermidine, this effect was dose-dependent (Fig. 21b). The beneficial effect of exogenous polyamines was clearly seen in define medium (DM) (Fig. 2c &e) where spermidine was confirmed to be the most beneficial polyamine for *L. pneumophila* growth *in vitro*. The treatment of L929 cells with exogenous spermidine and spermine (added at the time of infection) caused a significant increase in the intracellular growth of *L. pneumophila* 24 h post infection, relative to the untreated cells (Fig. 22a). A synergistic effect was observed when the bacterial inoculum was pre-grown in polyamines, and the host cells were treated with polyamines (Fig. 22), indicating that, although not beneficial on its own, pre-growth of *L. pneumophila* in BYE with polyamines either contributed to a higher net concentration of these polyamines in intracellular legionellae, or predisposed these legionellae to better use the excess polyamines added to host cells. Additionally, treatment of U937 macrophages and *L. pneumophila* with exogenous spermidine and spermine also enhances intracellular growth (Fig. 22b), confirming the importance of polyamines in the intracellular growth of *L. pneumophila*.

4.3.10. The *L. pneumophila* Genome Does Not Encode Most of the Known Prokaryotic Polyamine Biosynthetic Enzymes

To understand why *L. pneumophila* benefits from host SAMDC activity and (or) exogenous polyamines, we assessed *in silico* the metabolic capacity of *L. pneumophila* to synthesize polyamines. In a comparative analysis against known conserved prokaryotic pathways of polyamine biosynthesis (56,252,375,395), we found that most of the enzymes required for polyamine biosynthesis in *E. coli* and *Vibrio cholerae* (Fig. 23), are not encoded by the *L. pneumophila* genome. The only genes encoding polyamine biosynthetic enzymes in *L. pneumophila* were *metK* (methionine adenosyltransferase), and *speA* (arginine decarboxylase) (Fig. 23), suggesting that *L. pneumophila* cannot synthesize all polyamines. Although our results cannot rule out the possibility that the genome of *L. pneumophila* encodes polyamine biosynthetic enzymes bearing no sequence similarity to other known bacterial enzymes, a dependence on exogenous polyamines was strongly suggested by our growth results in liquid cultures (Fig. 21) and within U937 macrophages and L929 cells (Fig. 22).

4.4. Discussion

HtpB reaches the cytoplasm of *L. pneumophila* infected cells, as indicated here by the CyaA reporter assay. This result implies that, in addition to its external role as an invasion factor in non-phagocytic cells (139), HtpB could play internal roles as a cytoplasmic effector, as previously suggested by the HtpB-mediated alteration of actin filaments in CHO-*htpB* cells (65). Using *S. cerevisiae* as a model eukaryote, we have now shown that HtpB induces PHG and interacts with the cytoplasmic enzyme SAMDC. This interaction, together with the observation that increased SAMDC activity also

induces PHG, suggested a potential link between HtpB function and polyamines, and allowed us to speculate that *L. pneumophila* might use HtpB to manipulate polyamine levels in host cells to achieve optimal intracellular growth.

Based on our current knowledge, we propose the following physiological model to explain how the known HtpB functions are linked to *L. pneumophila* pathogenesis: (i) Surface-exposed HtpB, which increases in the presence of L929 cells and monocytes (107), as well as during differentiation of *L. pneumophila* into mature infectious forms (138), serves as a ligand for cell surface receptors and mediates attachment to and invasion of human non-phagocytic cells (139). (ii) Intracellular *L. pneumophila* abundantly releases HtpB into the lumen of the LCV (137,178). (iii) In experiments with phagocytosed HtpB-coated beads in CHO cells and macrophages, HtpB signals across the phagosomal membrane to attract mitochondria and transiently alters the actin cytoskeleton of host cells (65). (iv) HtpB from the LCV lumen reaches the host cell cytoplasm (this study) where it could interact with SAMDC and increase the intracellular pool of polyamines.

The mechanism by which HtpB reaches the host cell cytoplasm is as yet undefined. Considering that HtpB is abundantly released into the LCV by *L. pneumophila*(137,178) the low level of cAMP detected in cells infected with *L. pneumophila* carrying the C-terminal HtpB-CyaA fusion (in relation to the cAMP levels attained during infections with *L. pneumophila* carrying the LepA-CyaA fusion), suggests that only small amounts of HtpB reach the host cell cytoplasm, or that fusion to CyaA artificially reduces the efficiency of HtpB passage into the host cell cytoplasm. As proposed for *L. pneumophila*'s flagellin (428), free HtpB in the lumen of the LCV could

passively cross the LCV membrane. Alternatively, HtpB contained in outer membrane vesicles (130) could reach the host cell cytoplasm upon fusion of these vesicles with the LCV membrane. Since neither process directly translocates HtpB, they would differ fundamentally from the active Dot/Icm-dependent translocation of effectors such as LepA (130). The accidental delivery of HtpB into the host cell cytoplasm in our experiments (due to bacterial cell lysis and LCV rupture) is unlikely, mainly because it was controlled for by the very low levels of cAMP observed after infection with *L. pneumophila* carrying only the CyaA construct, and by the inability of *L. pneumophila* carrying the N-terminal CyaA-HtpB fusion to efficiently induce increased amounts of cAMP (Fig. 11).

In spite of the high amino acid sequence similarity that exists between bacterial chaperonins, we have shown recently that HtpB is capable of performing unique roles that are not shared by the *E. coli* protein GroEL (65). Microbeads coated with purified HtpB, but not GroEL, attracted mitochondria and transiently modified the organization of actin microfilaments in mammalian cells (65). We also demonstrated here that the ability of HtpB to activate PHG in *S. cerevisiae* is not shared by GroEL, or by the *S. cerevisiae* mitochondrial chaperonin (Hsp60p) expressed in the yeast cytosol. Unique functions of bacterial chaperonins have been previously reported, which can be attributed to the effect of a few residues. The insect toxin GroEL from endosymbiotic *Enterobacter aerogenes* (comprising 545 residues) differs from the non-toxic *E. coli* GroEL by eleven amino acids, of which only four are critical for toxicity. When the non-toxic *E. coli* GroEL was engineered at the four critical residues to resemble the *E. aerogenes* GroEL it, too, became a potent insect toxin (440). In the case of the Hsp65 chaperonin of

Mycobacterium leprae, which acts as a protease, only three amino acids (Thr-375, Lys-409 and Ser-502) comprise the threonine catalytic group responsible for protease activity (326). Differences in the signaling abilities of bacterial chaperonins, accompanied by a variety of downstream consequences (330), have also been previously reported. For instance, the 60-kDa chaperonins of *Actinobacillus actinomycetemcomitans* and *E. coli* were extremely active stimulators of bone resorption in a mouse model, whereas the chaperonins of *Mycobacterium tuberculosis* and *Mycobacterium leprae* showed no such activity (330). Because HtpB and *E. coli* GroEL differ in 137 amino acids scattered throughout the entire protein, it is not easily discernable which of these residues would confer on HtpB its unique property to interact with SAMDC and trigger PHG in yeast.

The term 'polyamines' describes a group of polycationic compounds present in all cells. Polyamines are similarly important in prokaryotes and eukaryotes, being crucial for normal cell growth, DNA and protein synthesis, and eukaryotic cell differentiation, proliferation, and signaling (74,318,320). By definition, these compounds have more than one amino group, and are commonly synthesized using amino acids as precursors (74,318,320). Based on the fact that a strong correlation exists between elevated polyamine levels and fungal filamentation (152,168,201,277,358) , it seems reasonable to surmise that the activation of PHG by HtpB, via its interaction with SAMDC, is mediated by increased concentrations of intracellular polyamines in *S. cerevisiae*. In this view, it is predicted that yeast cells expressing HtpB would have elevated levels of spermidine and spermine. SAMDC is a rate-limiting enzyme key in the biosynthesis of polyamines, which is tightly regulated in eukaryotic cells (320). Like other rate-limiting enzymes, SAMDC has a short half-life, its basal activity is low, and it is rapidly induced by

different stimuli (316,318,320). Furthermore, SAMDC is synthesized as an inactive proenzyme that in response to different stimuli undergoes an intramolecular cleavage reaction to form the active enzyme (226,319,320). Thus, it is possible that one or more of the processes that affect the activity of SAMDC could be modulated upon interaction with HtpB. For instance, the chaperonin activity of HtpB could extend the half-life of SAMDC, protecting it from early degradation, or the presence of HtpB could increase the rate of proenzyme cleavage.

It was surprising that in spite of screening ~5 x 10^6 yeast clones of the HeLa cDNA library by Y2H, SAMDC was not identified. In theory, this HeLa Y2H screen should be sufficient to cover 250X the estimated 2 x 10^4 protein-encoding mRNAs present in the human genome. The interaction of HtpB with the mitochondrial co-chaperonin (Hsp10) could have potential implications for the already identified effects of HtpB on mammalian cells. The HtpB-Hsp10 interaction could be relevant to mitochondrial recruitment because Hsp10 has been detected on the surface of mitochondria, as well as in other extra-mitochondrial locations where Hsp10 moonlights as the early pregnancy factor (354). Finding Hsp10 in extra-mitochondrial locations is not entirely surprising because Hsp10 is a mitochondrial protein whose encoding gene resides in the cell nucleus, and it is synthesized in the eukaryotic cytosol, from where Hsp10 needs to be imported into the mitochondria. While the import of proteins into mitochondria is mostly co-translational, it is possible that some Hsp10 molecules could stay on the mitochondrial surface (bound to the import apparatus) after translation.

The physiological model advanced at the beginning of the discussion of this chapter (Section 4.4) predicts that HtpB modulates the intracellular pool of polyamines in

host cells. These polyamines could then be transported into the LCV and directly used by *L. pneumophila* to grow optimally (nutritional role), and (or) change the physiology of the host cell to favour *L. pneumophila* proliferation (intracellular signaling role). The nutritional role of host polyamines is supported by the *in vitro* enhancement of *L. pneumophila* growth in liquid media supplemented with polyamines (Fig. 21), and by the limited ability of *L. pneumophila* to synthesize polyamines, predicted from our bioinformatic analysis (Fig. 23). However, an alteration of host cell physiology in favour of intracellular *L. pneumophila* (independent from a merely nutritional effect) cannot be ruled out by our results. For instance, the lack of inhibition by DFMO of *L. pneumophila* replication at 24 h post-infection (Fig. 20a), could mean that SAMDC activity, rather than increased concentrations of spermidine and spermine, was necessary for the optimal growth of *L. pneumophila*. This is all the more plausible knowing that inhibition of ornithine decarboxylase by DFMO is known to increase SAMDC activity (320). However, DFMO might simply have a late effect on the polyamine pool of host cells due to its slow uptake (371), its inability to effectively reduce spermine levels in treated cells (151), or the expected long period required to exhaust the levels of putrescine, and consequently spermidine, in host cells.

It should be noted here that the overall biological effect of polyamines on *L. pneumophila in vitro* and in cultured cells, was simply to enhance the growth of this organism. In all instances tested here, *L. pneumophila* was able to grow in the absence of added polyamines, and (or) the presence of pharmacological inhibitors of polyamine biosynthesis. Nonetheless, optimal growth of *L. pneumophila* was only achieved when polyamines were plentiful and host cell SAMDC activity was uninhibited. Thus, while

not essential in principle, polyamines still could play an important role in enhancing the growth of *L. pneumophila* during its intricate interactions with host cells, and ultimately tilt the outcome of the infection in favour of this pathogen.

The role of polyamines in the growth and virulence of human pathogens has recently attracted increased attention (375). For instance, *H. pylori* decreases macrophage survival by modulating the activity of host ornithine decarboxylase (60). Similarly, *Pneumocystis jiroveci* upregulates polyamine biosynthesis, in turn thought to induce apoptosis of alveolar macrophages (249). Other reports have implicated polyamines in biofilm formation by several bacterial human pathogens. The inactivation of genes involved in polyamine synthesis, such as *speA* or *speC* [encoding arginine decarboxylase and ornithine decarboxylase, respectively (refer to Fig 23)] reduced attachment of *Yersinia pestis* to a solid surface (312) and deletion of *speAB* operon [encoding arginine decarboxylase and agmatine ureohydrolase, respectively (refer to Fig. 23)] in *Proteus mirabilis* eliminates swarming (389). In *V. cholerae*, deletion of genes involved in polyamine metabolism (252) or transport (221,373), severely reduced its ability to form biofilms. It has been demonstrated that in eukaryotic and prokaryotic cells, polyamines can be used as precursors for the synthesis of some biological molecules that are critical for cell growth (232,310)(264) For example, in *V. cholerae* (232), *E. coli*(308), *Bacillus anthracis* (305), polyamines serve as precursors for synthesis of siderophores. Siderophores are small secreted compounds required for iron acquisition, which is crucial for bacterial growth (see Section 1.2.5.4, Chapter 1). Finally, a *Streptococcus pneumoniae potD* mutant (unable to effectively transport exogenous polyamines) showed a significant attenuation in murine virulence models (421),

suggesting that during infection, bacteria, such as *S. pneumoniae*, need to acquire polyamines from their host in order to achieve full virulence. In fact, in chapter 5 of this thesis, we demonstrated that *L. pneumophila* mutant with defects in the polyamine transporter PotABCD show a significantly lower level of intracellular growth in relation to its parent strain. Additionally, we have shown in this chapter that increased levels of exogenous polyamines, as well as increased host SAMDC activity, have an enhancing effect on the intracellular growth of *L. pneumophila*. We proposed a potential role for the HtpB chaperonin in this process. Because polyamines have multiple functions in bacterial human pathogens, further studies on utilization of polyamines and their physiological effects are warranted to uncover new mechanisms used by *L. pneumophila* to survive and proliferate within host cells.

4.5. Acknowledgements

Kaitlyn Carson, Andrew Caddell, and Hany Abdelhady, Nicholas Tompkins are gratefully acknowledged for their help with statistical analyses, dilution-plating for CFU counts, and U937 cell activation, respectively. We thank Dr. Howard Shuman for generously providing plasmids, antibodies against LepA, and *L. pneumophila* strains, as well as Dr. Paul Hoffman for antibodies. We acknowledge the following individuals for providing plasmids and (or) strains needed for our work: David Allan, David Balasundaram, Gerald Johnston, H.-U. Mösch, Jim Hopper, Joseph Vogel, Pak Poon, Paul Sigler, Philip James, Ralph Isberg, and Stephen Elledge. We thank the reviewers of our manuscript for the many valuable comments that helped to improve it. This work was

funded by independent grants from the Natural Sciences and Engineering Research Council of Canada (NSERC) to RAG and LEM.

4.6. Figures, and Legends to Figures

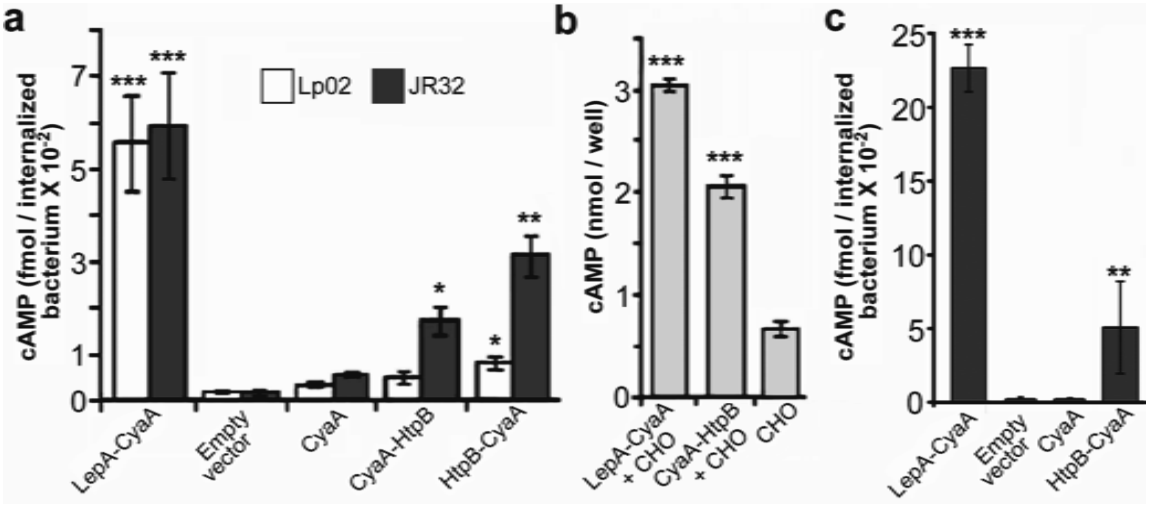

Figure 11. An adenylate cyclase reporter assay showing that HtpB reaches the cytosol of *L. pneumophila*-infected CHO-*htpB* cells.

(a) CHO-*htpB* cells were infected for 90 min with *L. pneumophila* strain Lp02 or JR32, expressing theCyaA-HtpB or HtpB-CyaA fusion protein. *L. pneumophila* strains carrying the empty vector (pMMB207C) and strains expressing only CyaA or the LepA-CyaA fusion served as negative or positive translocation controls, respectively.cAMP levels in CHO-*htpB* cells infected with the strins expressing the CyaA-HtpB or the HtpB-CyaAfusion protein is significantly higher than the cells infected with the negative control strains **(b)** cAMP levels measured after mixing CHO-*htpB* whole cell lysates with lysates from JR32 expressing the LepA-CyaA fusion (positive control), or the CyaA-HtpB fusion. The lysate of CHO-*htpB* cells alone served as a negative control and indicated that even if some ectopic HtpB was produced in these cells, it did not result in increased cAMP levels. (**c**) cAMP levels in U937-derived macrophages infected for 30 min with *L. pneumophila* strain JR32 expressing the HtpB-CyaA or the LepA-CyaA fusion protein. JR32 cells carrying the CyaA only construct or the empty vector served as negative translocation controls. Means and standard deviations were obtained from

triplicate samples (n=3). Results shown are from one of two independent experiments. **a&b of this figure** were generated by Dr. Audrey Chong, while **C** was generated by Gheyath Nasrallah. Adapted from reference (295) and used with permission from the Journal of Bacteriology.

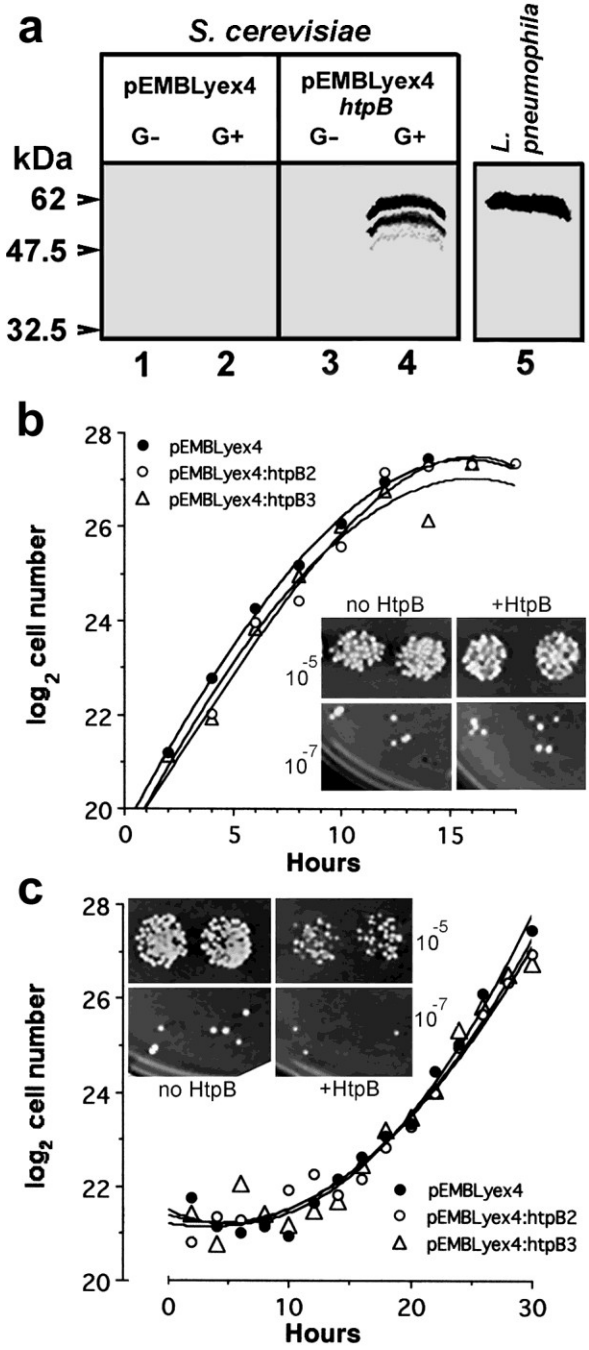

Figure 12. Expression of the *L. pneumophila* chaperonin, HtpB, in *S. cerevisiae*.

(**a**) Immuno-blot of whole cell lysates from the yeast strain W303-1b bearing the vector pEMBLyex4 (lanes 1 and 2), or the galactose-inducible construct pEMBLyex4::*htpB*

(lanes 3 and 4), and grown in non-inducing medium with dextrose (G–) or inducing medium with galactose (G+) as carbon source. The blot was probed with an HtpB-specific monoclonal antibody. The full-length ectopic HtpB expressed in yeast (lane 4) and the HtpB from *L. pneumophila* (lane 5) migrated to a similar position, but the ectopic HtpB showed degradation products. The position and mass (kDa) of pre-stained protein markers are indicated. (**b and c**) Growth curves at 30°C of yeast strain W303-1b carrying pEMBLyex4 (one clone) or pEMBLyex4::*htpB* (two clones designated pEMBLyex4::htpB2 and pEMBLyex4::htpB3) in YEP-Dextrose **(b)** or YEP-Galactose **(c)**. Insets: growth at 30°C of serially diluted suspensions spotted in duplicate (10^{-5} and 10^{-7} dilutions shown) on solid medium containing dextrose (**b**) or galactose (**c**). The inocula for the spots contained equivalent numbers of yeast cells carrying either pEMBLyex4 (no HtpB) or pEMBLyex4::*htpB* (+HtpB). This Figure was generated by Dr. Angela Riveroll. Adapted from reference (295) and used with permission from the Journal of Bacteriology.

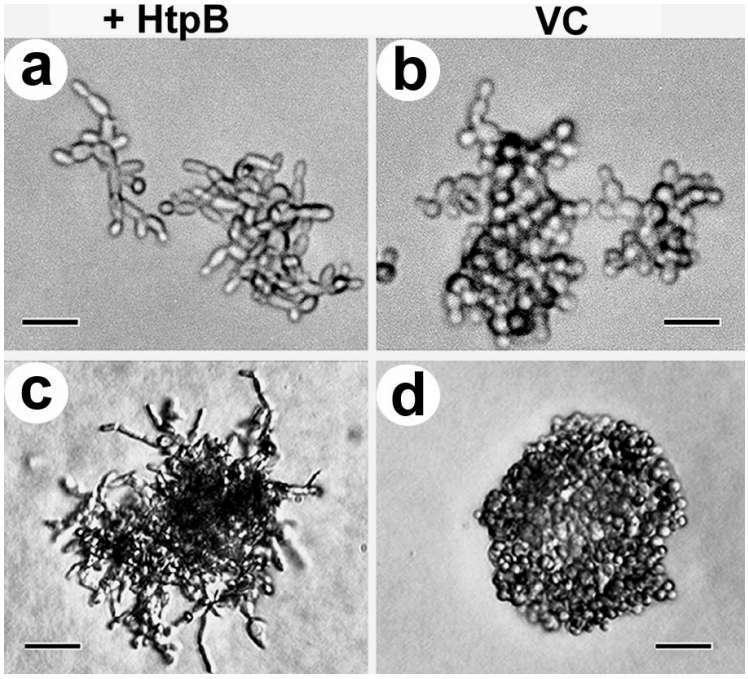

Figure 13. HtpB induces *S. cerevisiae* to form pseudohyphae that invade solid medium. Cells within microcolonies (**a**&**b**) and small colonies (**c**&**d**) of yeast strain W303-1b grown on solid medium containing galactose. Cells carry either the galactose-inducible construct pEMBLyex4::*htpB* for expression of HtpB (**a**&**c**, +HtpB), or the vector control pEMBLyex4 (**b**&**d**, VC). The filamentous colony shown in (**c**) had penetrated the agar. Size bars represent 9 μm (**a**&**b**), and 25 μm (**c**&**d**). This Figure was generated by Dr. Angela Riveroll. Adapted from reference (295) and used with permission from the Journal of Bacteriology.

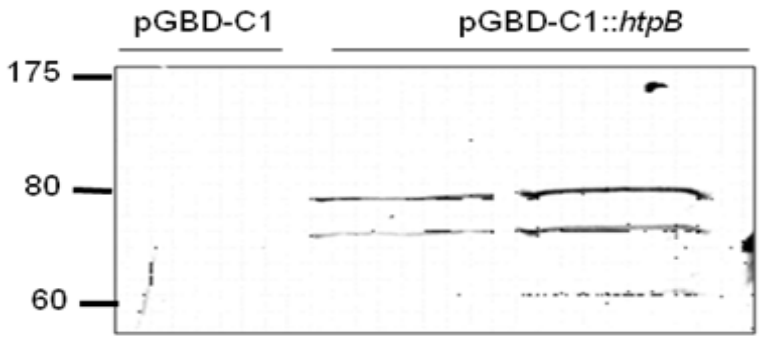

Figure 14. Expression of the Gal4BD-HtpB chimera detected by immunoblotting.

Y187 carrying the indicated vectors were grown in SD- glucose medium without tryptophan. Whole cell lysates from these yeast strains were separated by SDS-PAGE, transferred to a nitrocellulose membrane, and immunostained with monoclonal antibody specific for HtpB. The sizes (kDa) and position of protein standards are marked at the left side of the blot. This figure was generated by Gheyath Nasrallah.

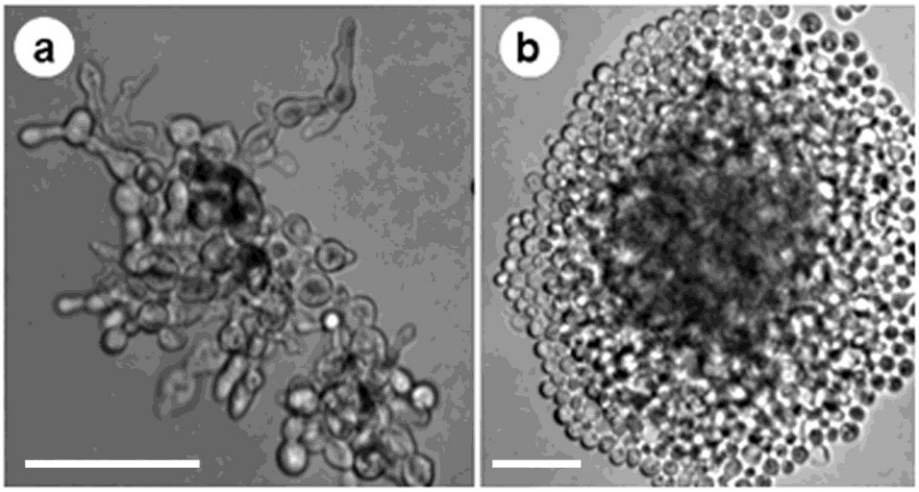

Figure 15. The Gal4DBD-HtpB chimera induces pseudohyphal growth on glucose-replete medium**.**

(a) and **(b)** *S. cerevisiae* strain W303-1b within microcolonies grown on non-inducing SD-glucose solid medium for 5 days. This strain carrying either pGBD-C1:: *htp*B for expression of HtpB **(a)**, or the empty vector pGBD-C1 **(b)** as a negative control**.** The filamentous colony shown in **(a)** had penetrated the agar. Size bars represent 20 μm. This figure was generated by Gheyath Nasrallah.

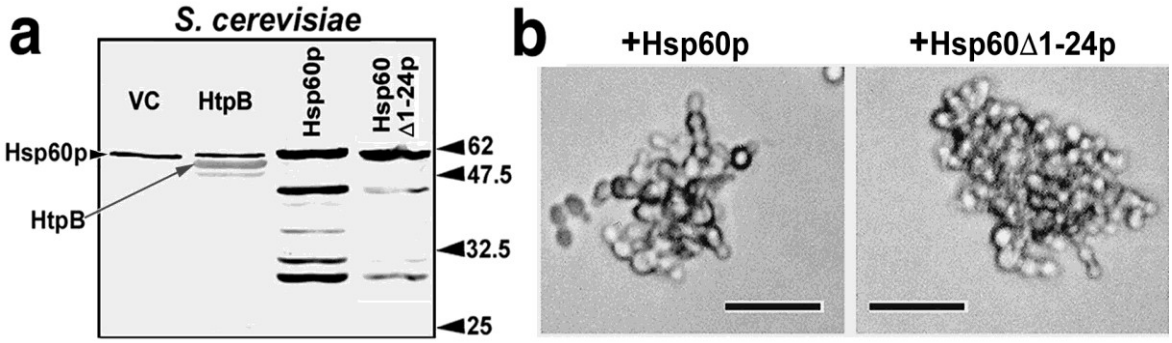

Figure 16. Overexpression of the *S. cerevisiae* mitochondrial chaperonin (Hsp60p) does not induce pseudohyphae.

Yeast strain W303-1b contained pPP389 (vector control, VC) or one of the galactose-inducible constructs pPP389::*htpB* (HtpB), pPP389::*HSP60* (Hsp60p), or pPP389::*hsp60*Δ1-72 (Hsp60Δ1-24p). (**a**) Immuno-blot of whole yeast cell lysates grown in medium containing galactose. The blot was probed with a mixture of non-cross reacting monoclonal antibodies, one specific for yeast Hsp60p and the other specific for *L. pneumophila* HtpB. Arrows and numbers indicate the position and mass of pre-stained protein markers in kilodaltons. (**b**) Yeast cells expressing the indicated version of Hsp60 did not elongate or form pseudohyphae (size bars represent 20 μm). This Figure was generated by Dr. Angela Riveroll. Adapted from reference (295) and used with permission from the Journal of Bacteriology.

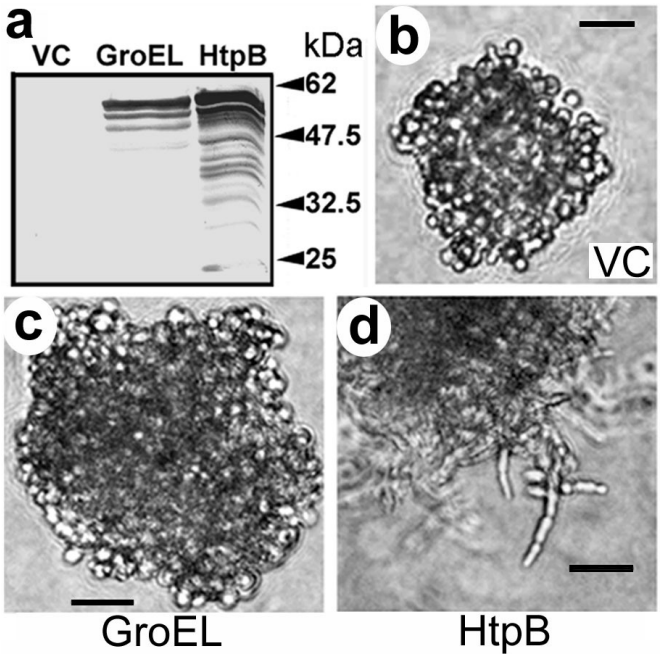

Figure 17. The *E. coli* chaperonin GroEL does not cause *S. cerevisiae* to form pseudohyphae.

(**a**) Immunoblot of whole cell lysates of yeast strain W303-1b grown in inducing medium containing galactose, separated by SDS-PAGE, transferred to a nitrocellulose membrane, and stained with an HtpB-specific polyclonal antibody (cross-reactive with GroEL). Arrows and numbers indicate the position and mass of pre-stained protein markers in kilodaltons (kDa). (**b** to **d**) Colonies of yeast strain W303-1b on solid medium containing galactose. Yeast cells contained pEMBLyex4 (vector control, VC), or one of the galactose-inducible constructs: pEMBLyex4::*groEL* (GroEL), or pEMBLyex4::*htpB* (HtpB). Size bars represent 28 μm in (**b**) and 21.5 μm in (**c**) and (**d**). This Figure was generated by Dr. Angela Riveroll. Adapted from reference (295) and used with permission from the Journal of Bacteriology.

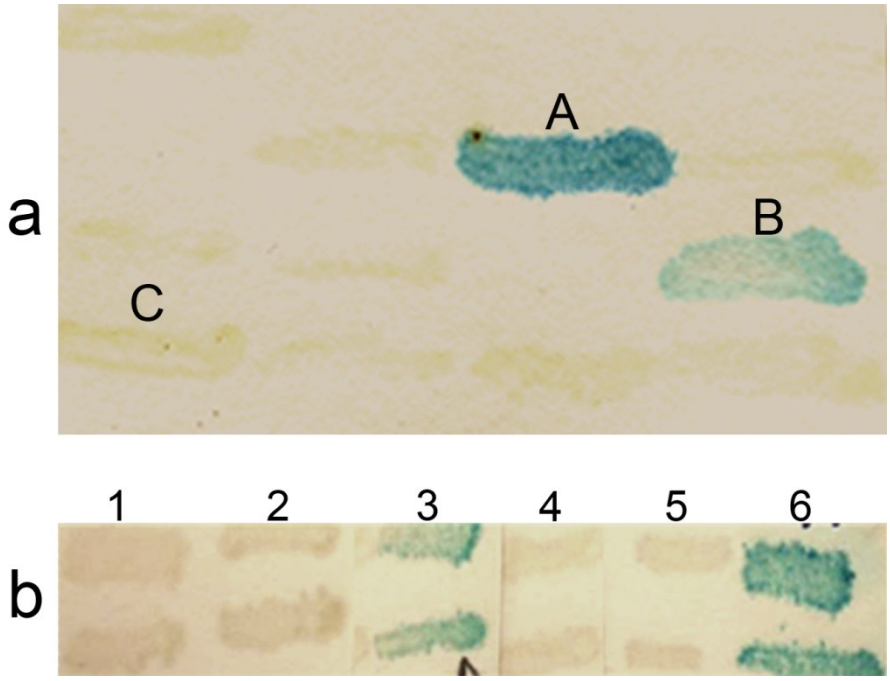

Figure 18. Yeast two-hybrid screening and β-galactosidase filter assay identified SAMDC as a putative HtpB interacting protein**.**

(a) A filter assay was used to detect clones that produce a blue color resulting from induction of β-galactosidase, mediated by the interaction of putative interacting proteins. Blue positive clone **(A)** carries pGBD-C1*::htpB* and pGAD-C1::*20A*, and clone (B) carries pGBD-C1*::htpB* and pGAD-C1::*20B* **(**positive library plasmids**)**. Patches of pale yellow [one indicated by (C)] represent clones carrying pGBD-C1::*htpB* and library plasmids encoding non-interacting proteins. **(b)** Confirmation of HtpB and SAMDC interaction in freshly transformed yeast cells. Duplicate patches of yeast cells carrying pGAD-C1:*20B* (columns 1-3) or pGAD-C1:*20A* (columns 4-6) in combination with pGBD-C1 (1 and 4), pSE1111 (2 and 5), or pGBD-C1::*htpB* (3 and 6), were tested by the β-galactosidase filter assay. Positive interactions show as blue patches. This figure was generated by Gheyath Nasrallah.

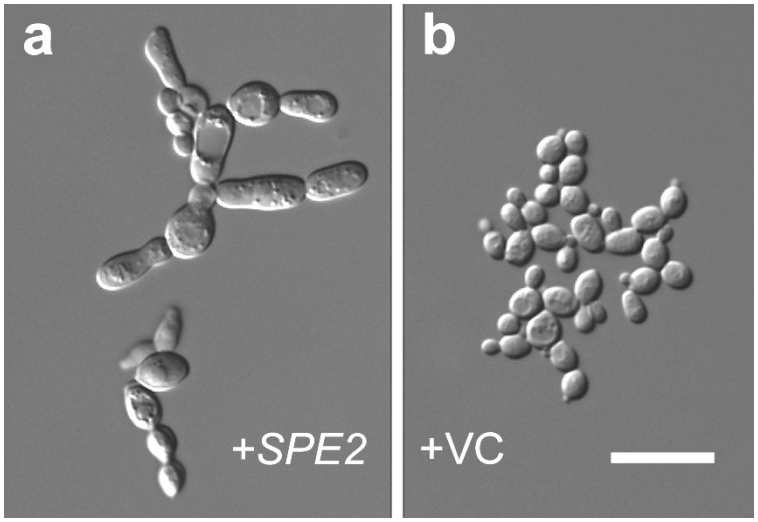

Figure 19. Overexpression of SAMDC induces pseudohyphal growth.

(**a and b**) Microcolonies of yeast strain W303-1b grown on SD medium containing galactose. Yeast cells carried the galactose-inducible construct pPP389*::SPE2* (**a**, +*SPE2*), or the vector controlpPP389 (**b**, +VC). The microcolony shown in (**a**) had penetrated the agar after incubation for 5 days at 30°C. Size bar represents 12 μm and applies to both panels. This figure was generated by Gheyath Nasrallah. Adapted from reference (295) and used with permission from the Journal of Bacteriology.

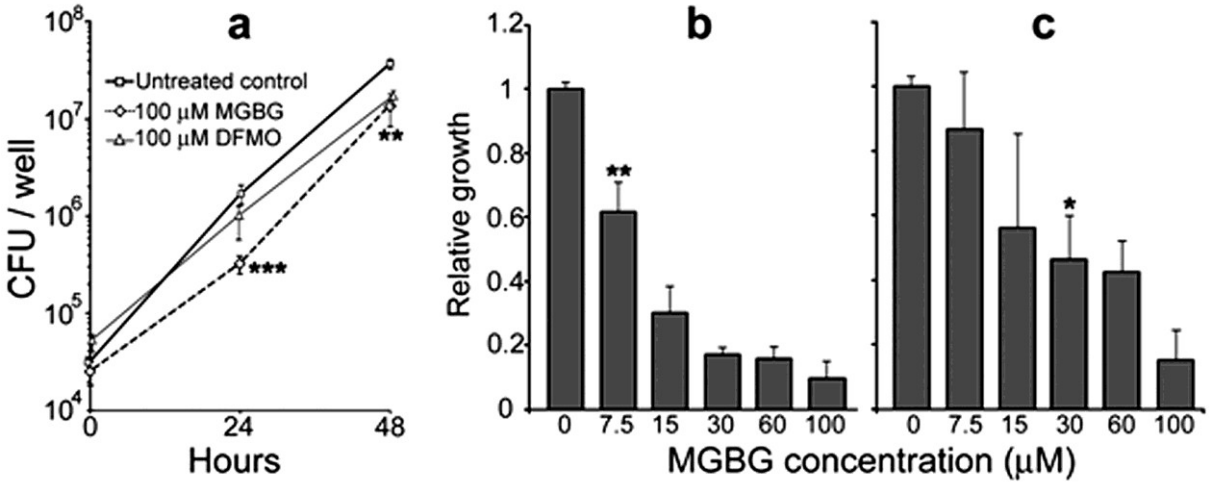

Figure 20. Pharmacological inhibition of polyamine biosynthetic enzymes decreases *L. pneumophila* replication in mammalian cells.

(**a**) Intracellular growth of *L. pneumophila* strain JR32 in L929 cells treated with MGBG or DFMO. (**b and c**) Dose-dependent inhibition by MGBG in L929 cells (**b**), or in U937-derived macrophages (**c**), at 24 h post-infection. Results are shown as mean ± one std. deviation of the treated/untreated ratio for 3 independent experiments (n = 3), each run in triplicate. Statistical significance was calculated against the corresponding untreated control by the two-way ANOVA test. * P<0.05, ** P<0.01, *** P<0.001. In (**b**) and (**c**) statistical significance is shown only above the concentration of inhibitor that first imparted a significant growth difference in relation to the untreated control. This figure was generated by Gheyath Nasrallah. Adapted from reference (295) and used with permission from the Journal of Bacteriology.

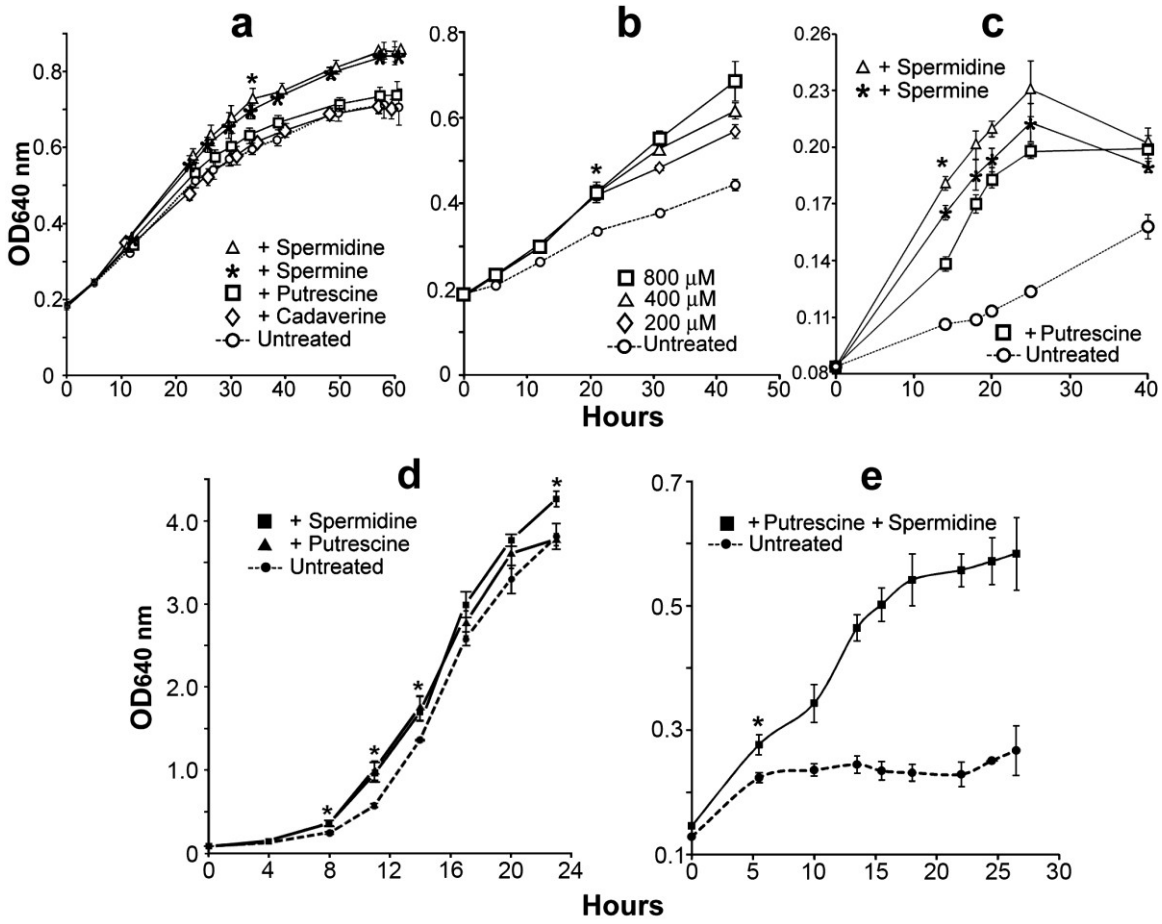

Figure 21. Exogenous polyamines enhance the growth of *L. pneumophila in vitro*. Panels **a** to **c** represent experiments performed in 96-well plates (200 µL/well) incubated without agitation, and panels **d** and **e** represent experiments performed in shaken 50-mL liquid cultures. Individual polyamines were added at 100 µM, except for panel B where polyamines were added at the concentrations indicated. (**a**) BYE broth was individually supplemented with four polyamines and the growth of strain JR32 was followed for 60 h. (**b**) A dose-response effect obtained with spermidine supplementation of BYE broth. (**c**) Growth in the absence or presence of polyamines in synthetic DM without choline. (**d**) Growth curves in BYE broth, or BYE supplemented with spermidine or putrescine. (**e**) Growth curves in DM or DM supplemented with putrescine and spermidine. Panels **a** to

c show mean ± one std. deviation (n=16 replicates) from one of three experiments conducted showing similar results. Panels **d** and **e** show mean ± one std. deviation of three independent cultures (n=3). Statistical significance was calculated at each time point against the corresponding untreated control by the Student *t*-test (* = $P<0.05$). For panels **a-c** the differences between treated and untreated cultures were statistically significant at and after the time point marked with the asterisk, except for the putrescine- and cadaverine-treated cultures in panel **a**. For panel **d**, only the time points marked with an asterisk showed significant growth differences between spermidine-treated samples and the untreated control. For panel **e** the differences between treated and untreated cultures were statistically significant at all-time points except for time zero. This figure was generated by Gheyath Nasrallah. Adapted from reference (295) and used with permission from the Journal of Bacteriology.

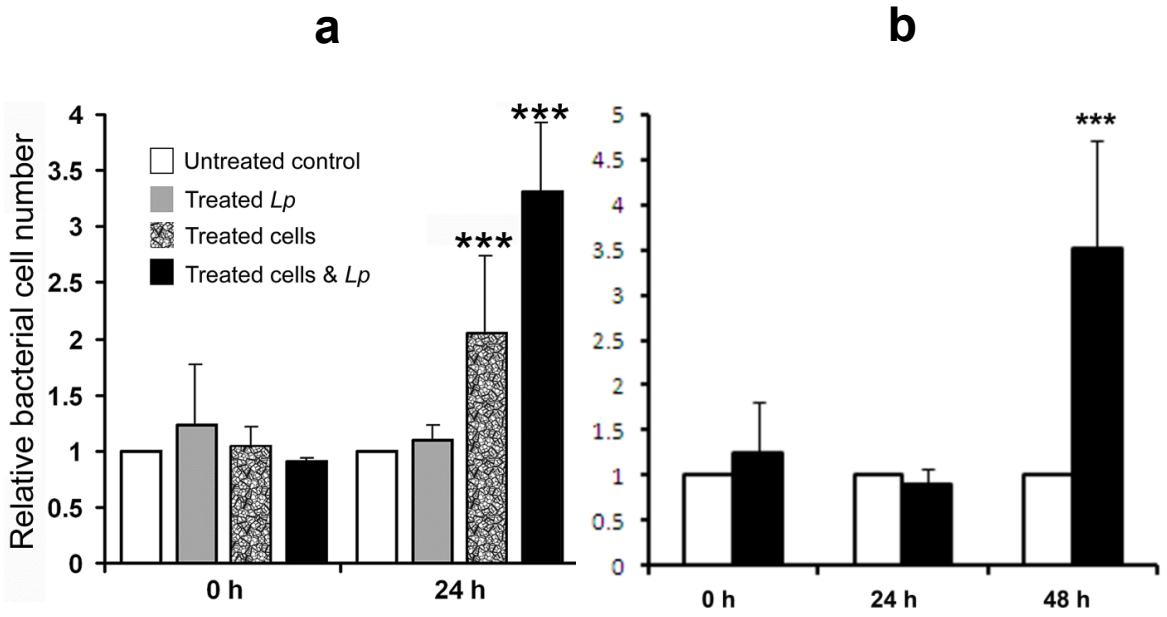

Figure 22. Treatment of *L. pneumophila* and (or) host cells with exogenous polyamines enhances bacterial intracellular growth.

L. pneumophila strain JR32 (*Lp*) grown overnight in BYE with or without polyamine supplements (spermidine and spermine).was used to infect L929 cells **(a)** or U937 macrophages **(b)** that were grown in a tissue culture medium in the presence or absence of spermidine and spermine at the time of infection. Results are presented as relative numbers of intracellular bacteria (calculated as CFU/mL of the treated test samples divided by the CFU/mL of the untreated control), and represent the mean + one std. deviation for 3 independent experiments (n = 3), each run in triplicate.**(a)** The statistical significance of differences in *L. pneumophila* replication, in relation to the untreated control, is indicated as *** = P<0.001. This figure was generated by Gheyath Nasrallah. Adapted from reference (295) and used with permission from the Journal of Bacteriology.

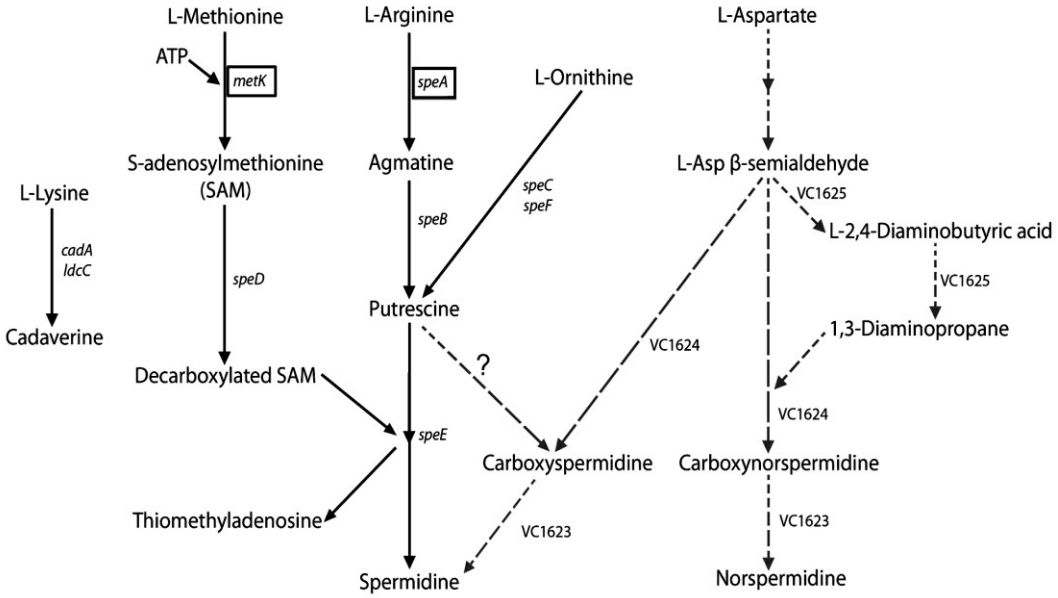

Figure 23. Integrated polyamine biosynthetic pathways in *E. coli* and *V. cholerae*. The *V. cholerae* pathway is marked by the broken arrows. Enzymatic nomenclature is given by the encoding gene names. For *V. cholerae*, genes encoding biosynthetic enzymes are indicated by letters beginning with VC. In alphabetical order: *cadA* (inducible lysine decarboxylase), *ldcC* (constitutive lysine decarboxylase), *metK* (methionine adenosyltransferase), *speA* (arginine decarboxylase), *speB* (agmatine ureohydrolase), *speC* (constitutive ornithine decarboxylase), *speD* (SAMDC), *speE* (spermidine synthase), *speF* (inducible ornithine decarboxylase), VC1623 (carboxynorspermidine decarboxylase), VC1624 (carboxynorspermidine dehydrogenase), and VC1625 (encoding a large fusion protein comprising the two enzymes di-aminobutyrate aminotransferase and di-aminobutyrate decarboxylase). The genes that have homologs in the *L. pneumophila* genome are indicated by boxes. This figure was generated by Gheyath Nasrallah. Adapted from reference (295) and used with permission from the Journal of Bacteriology.

CHAPTER 5: THE PUTATIVE POLYAMINE BINDING PROTEIN, POTD, IS REQUIRED FOR OPTIMAL INTRACELLULAR GROWTH OF *LEGIONELLA PNEUMOPHILA.*

Gheyath K. Nasrallah[1], Nicholas Tompkins[1], Kaitlyn R. Carson[1], and Rafael A. Garduño[1,2],*

[1] Department of Microbiology and Immunology, Dalhousie University, Halifax, Nova Scotia, Canada.

[2] Department of Medicine – Division of Infectious Diseases, Dalhousie University, Halifax, Nova Scotia, Canada.

*Corresponding author

A manuscript to be submitted to the Journal of Infection and Immunity will be adapted from this Chapter.

5.1. Abstract

Polyamines such as putrescine and spermidine are small polycationic compounds ubiquitous in prokaryotes and eukaryotes. These compounds are crucial for normal cell growth, DNA, RNA and protein synthesis, cell differentiation, and proliferation. In Chapter 4 of this thesis, we showed that exogenous polyamines enhance the intracellular growth of *L. pneumophila*, whereas pharmacological inhibition of host polyamine synthesis impairs such growth. Moreover, *in silico* analysis showed that *L. pneumophila* lacks ten of the twelve enzymes involved in bacterial polyamine synthesis, suggesting that its capacity to synthesize polyamines is compromised. Therefore, *L. pneumophila* might need to import polyamines directly from host cells. Here, we found that *L. pneumophila* possesses only one putative polyamine transporter operon that consists of four genes, *potABCD*, in contrast to *E. coli* which possesses at least four polyamine transporters in addition to that encoded by the *potABCD* operon. To test the function of the *L. pneumophila* PotABCD transporter, *potD* was deleted from strain JR32. Although deletion of *potD* did not affect *L. pneumophila* growth *in vitro*, it significantly reduced attachment to phagocytic cells (THP-1 and U937 macrophages, and *A. castellanii*), intracellular growth, and recruitment of vesicles to the *Legionella*-containing vacuole. Moreover, the Δ*potD* mutant was found to be 1000-fold more sensitive to Na^+ in relation to its parental strain, and unable to efficiently form filaments. Using GFP as a reporter of *potABCD* promoter (P_{potA}), we found that P_{potA} activity was turned on during exponential phase of growth *in vitro*. Collectively, these findings suggest that PotD plays a virulence-related role, and further confirms the importance of polyamines in *L. pneumophila* pathogenesis.

5.2. Introduction

L. pneumophila is a Gram negative opportunistic pathogen that causes Legionnaire's disease, an atypical nosocomial and community acquired pneumonia (120). Infection occurs when aerosols of contaminated water are inhaled by susceptible individuals (120). In nature, *L. pneumophila* replicates in protozoa and, in humans, it primarily replicates in mononuclear leukocytes (191). Once internalized by host cells, *L. pneumophila* prevents phagosome acidification and fusion with lysosomes, and establishes a permissive replicative vacuole called the *Legionella*-containing vacuole (LCV). The LCV acquires mitochondria and small vesicles derived from the ER and Golgi (376). The membranes of these vesicles make contact with and fuse along the surface of the LCV, where the exchange of membranes between the two compartments occurs (409). This process of fusion could also deliver nutrients to the LCV, but this has not yet been demonstrated. Within the LCV, *L. pneumophila* apparently senses the nutrient supply (361). When nutrients are adequate, the bacterium differentiates from a transmissive form (TF) into a replicative form (RF) and begins intracellular growth (361). The differentiation process is crucial to *L. pneumophila*, as mutations in a number of genes that regulate differentiation cause severe intracellular growth defects (286). The nutrients sensed within the LCV that trigger differentiation of the TF into the RF are largely unknown, but the presence of amino acids has been identified as one nutritional signal(58,361). For more information on the *L. pneumophila* life cycle and the differentiation processes of TF and RF, see Section 1.1.4 and 1.1.4.1 of Chapter 1.

In Chapter 4 of this thesis, we established that *L. pneumophila* requires polyamines for optimal intracellular growth (295). For instance, addition of exogenous

polyamines to L929 mouse fibroblasts and U937-derived human macrophages enhanced the intracellular growth of *L. pneumophila*, whereas pharmacological inhibition of polyamine synthesis in those cells significantly inhibited intracellular growth. In addition, bioinformatic analysis of the *L. pneumophila* genome indicated that *L. pneumophila* lacks ten of the twelve enzymes described in bacteria for biosynthesis of polyamines (see Fig. 23 in Chapter 4 of this thesis). These findings led us to hypothesize that *L. pneumophila* is incapable of synthesizing all the polyamines that are required for its optimal growth and that *L. pneumophila* acquires these polyamines directly from the host cell. Additionally, based on our results presented in Chapter 4 of this thesis, we have hypothesized that the multifunctional *L. pneumophila* chaperonin, HtpB, plays a role in assuring that the supply of host polyamines is plentiful to support the growth of *L. pneumophila*. This is achieved through the interaction of HtpB with SAMDC, a host cell enzyme that is critical for polyamine synthesis (295). Collectively, our experimental findings imply that *L. pneumophila* might depend upon polyamine transport to acquire polyamines from host cells.

The polyamines putrescine, spermidine, spermine, and cadaverine are part of a group of small polycationic compounds with a hydrocarbon backbone and multiple amino groups. Polyamines are present in all cells and they are similarly important in eukaryotes and prokaryotes, being crucial for DNA, RNA and protein synthesis, as well as for normal cell growth, cell differentiation, proliferation, and signalling (74,316,394,395). However, it remains unknown how biogenic polyamines exert their biochemical activities. The intracellular content of polyamines in eukaryotes and prokaryotes is strictly regulated and maintained by both endogenous synthesis (using

amino acids as precursors), and uptake from the surrounding environment (197,198). The endogenous polyamine synthesis pathway is conserved in all eukaryotes. Although prokaryotes have polyamine biosynthetic pathways similar to those of eukaryotes, they exploit additional enzymes and precursors for polyamine biosynthesis, as shown in Figure 23, in Chapter 4 of this thesis.

Putrescine and spermidine are the most prominent cellular polyamines in bacteria, and not all bacteria can synthesize them at the same capacity (252,425). Therefore, bacteria often rely on transport of exogenous polyamines to fulfil their cellular polyamine requirements. This notion is supported by the fact that *E. coli* mutants unable to transport exogenous polyamines (224), or mutants unable to endogenously synthesize polyamines (396) grow at a lower rate in relation to their parental strains. Additionally, the genome of *Mycoplasma genitalium*, which does not encode any of the known bacterial enzymes required for polyamine synthesis does require polyamines for growth (119). *M. genitalium* must rely solely on polyamine transport from the surrounding environment to maintain sufficient intracellular levels of polyamines(198). These observations demonstrate the importance of polyamine transport in bacterial growth and survival.

The most studied bacterial polyamine transporters are those of *E. coli*. These include (i) ABC transporters: PotFGHI, that selectively transports putrescine and PotABCD, that preferentially transports spermidine (with high capacity) and putrescine (with low capacity), (ii) antiporters: PotE, that exchanges putrescine for ornithine, and CadB, that exchanges lysine for cadaverine(197,198,375), and (iii) the newly described putrescine uniporter, PuuP (244,245). Among these, the PotABCD transporter is the most widespread among human bacterial pathogens (375). The PotABCD transporter is

encoded by four genes organized in one operon (the *pot* operon). PotA is a cytoplasmic ATPase with an ATP binding motif that couples ATP hydrolysis to translocation of polyamines. PotB and PotC are two cytoplasmic membrane permeases, each containing six transmembrane α-helical hydrophobic domains that form a polyamine specific channel in the cytoplasmic membrane. PotD is a periplasmic polyamine-binding protein that binds spermidine with high affinity, and putrescine with low affinity. In *E. coli*, mutations in any of the *potABCD* genes constitute loss of function mutations, indicating that each of the four genes is essential for polyamine transport (125).

Little is known about the importance of nutrient transport for the replication of *L. pneumophila* in the LCV. However, several recent reports suggest that amino acid transporters are important for bacterial differentiation and intracellular growth. The valine transporter, PhtJ, and the recently identified threonine transporter, PhtA, are required for normal *L. pneumophila* differentiation and replication within macrophages (58,133,361). The only predicted *L. pneumophila* polyamine transporter is encoded by the *potABCD* operon. Here, we investigate the importance of the *PotABCD* operon on the intracellular growth of *L. pneumophila.* To do this, we constructed a Δ*potD* mutant of strain JR32. We showed, using three different types of host cells that PotD is important for *L. pneumophila* attachment to host cells, intracellular growth, LCV trafficking within the host cell, and resistance of *L. pneumophila* to NaCl. In addition, we found that the *potD* promoter (P_{potA}) activity was turned on during exponential phase (EP) of growth *in vitro*. Our findings suggest that PotD might play an important virulence-related role, and further confirms the importance of polyamines in *L. pneumophila* pathogenesis.

5.3. Results

5.3.1. The *L. pneumophila* Genome Encodes Only One Putative Polyamine Transporter (PotABCD)

In a comparative bioinformatics analysis against the most widespread polyamine transport systems among bacteria, we found that while the *L. pneumophila* Philadelphia-1 strain genome lacked homologs of PotFGHI, PotE, CadB, and PuuP, it had a gene cluster with high homology to the *potABCD* operon of *E. coli.* The PotA ATPase of *L. pneumophila* showed ~51% amino acid sequence identity to the *E. coli* PotA, and also possesses the conserved ABC transporter and ATP binding domains. PotB, PotC, and PotD of *L. pneumophila* showed lower but still significant amino acid sequence identities, 43%, 47%, and 40% respectively, with their corresponding *E. coli* homologs. My *in silico* comparative analysis results cannot rule out the possibility that the genome of *L. pneumophila* encodes polyamine transporters bearing no sequence similarity to other known bacterial polyamine transporters identifiable by BLAST.

5.3.2.PotD is Predicted to Function As a Polyamine Binding Protein

Based on its amino acid sequence similarity to the *E. coli* PotD protein, which functions to bind spermidine and putrescine, we hypothesized that the *L. pneumophila* PotD could function as a polyamine binding protein. We first wanted to conduct a more detailed bioinformatic analysis that could provide insight into PotD function. An amino acid sequence alignment between *L. pneumophila* and *E. coli* PotD is shown in Fig. 24. Kashiwagi et al.(225) found, by site directed mutagenesis, that 13 amino acid residues of the *E. coli* PotD protein are involved in binding spermidine (29). Among these, 3 residues were the most important (indicated by * above the *E. coli* PotD sequence in Fig. 24), 5

residues had a moderate contribution (indicated by # in Fig. 24), and 5 other residues made only a weak contribution (indicated by + in Fig. 243), to spermidine binding (198,225). Out of these 13 amino acids identified in PotD of *E. coli*, the *L. pneumophila* PotD has all of the 3 amino acids residues characterized as the most important, 4 of the 5 residues characterized as moderately important, and 2 of the 5 amino acids characterized as the least important for binding spermidine (Fig. 24). This bioinformatic analysis suggests that *L. pneumophila* PotD will bind spermidine with high affinity.

The mechanism by which the *E. coli* PotD protein binds putrescine is not well understood(198). Therefore, it is hard to predict whether the *L. pneumophila* PotD is also capable of binding putrescine. It should be noted that these bioinformatic results do not rule out the possibility that PotD may have functions other than binding spermidine and putrescine.

5.3.3. PotABCD Promoter (P_{potA}) Is Turned on During Exponential Phase and Its Activity Is Independent of RpoS

The *in vitro L. pneumophila* life cycle alternates between the exponential phase (EP) form, which is equivalent to the *in vivo* replicative forms (RF), and the stationary phase (SP) form, which is equivalent to the *in vivo* transmissive forms (TF) (as explained in Chapter 1, Section 1.1.3). To gain insight into the involvement of PotABCD in *L. pneumophila*'s biphasic life cycle, we investigated PotABCD promoter (P_{potA}) activity along the *L. pneumophila* growth curve *in vitro* in BYE. For this purpose, we used a JR32 strain transformed with the GFP reporter plasmid pMMB-P_{potA}:*gfp*, in which GFP expression is solely driven by P_{potA}. Immunoblot results (Fig. 25A) showed that GFP expression coincided with the initiation of bacterial replication (i.e. when the bacterial

enters the EP). Since GFP is a stable protein with a half life of more than 24 h (55), it is expected to accumulate in the bacterial cells for as long as P_{potA} remains active, accounting for the more intense GFP bands seen at $O.D_{620}$ >0.8 (Fig. 25A).

The immunoblot results were confirmed by fluorometric analysis of strain JR32(pMMB-P_{potA}:*gfp*) along its growth curve (Fig. 25B). A significant increase in GFP fluorescence occurred during EP (Fig. 25B), confirming that the activity of P_{potA} coincides with bacterial replication. Based on these *in vitro* results, we can hypothesize that PotABCD would be active in the *L. pneumophila* RF *in vivo*. This view is compatible with the transcriptome analysis results of Bruggemann et al.(38), which show that *potB* expression in the RF is 2-fold higher than in the TF.

If P_{potA} is preferentially active in EP, we would expect it not to be controlled by the SP-specific sigma factor RpoS (σ^S/σ^{38}), as the latter is one of the major regulators of genes expressed in SP (15,286). The expression of GFP from pMMB-P_{potA}:*gfp* was analyzed by fluorometry in strain MB379 (Δ*rpoS* mutant) and in its parent strain Lp02. As seen in Figure 25D, there was no difference in the P_{potA} activity between the parental strain and the Δ*rpoS* mutant in SP or EP, suggesting that P_{potA} activity is regulated by a mechanism that does not depend on RpoS.

5.3.4. PotD is Dispensable for *L. pneumophila* Growth *in vitro*

Due to the potential role of PotD in polyamine transport (Section 5.3.2) and the high activity of its promoter in actively dividing *L. pneumophila* cells (Section 5.3.3), we wanted to study known polyamine-associated phenotypes *in vitro*, such as growth rate, biofilm formation and resistance to Na^+. Therefore, we deleted *potD* from *L.*

pneumophila strain JR32 (see Section 2.4.3) and determined the effect of this deletion on these phenotypes.

The Δ*potD* mutant and its parental strain JR32 showed similar growth rates in BYE medium (Fig. 26A) or in modified SD medium (without choline) (Fig. 26B). Addition of spermidine and putrescine to the modified SD medium markedly enhanced *L. pneumophila* growth, confirming our previous findings (Chapter 4) that polyamines are enhancers of *L. pneumophila* replication. However, this enhancing effect was independent of the presence of PotD (Fig. 26B). These results suggest that PotD is dispensable for *L. pneumophila* growth *in vitro,* and imply that an alternative polyamine transport mechanism, or an alternative polyamine binding protein capable of substituting for PotD, exists in *L. pneumophila.*

5.3.5. Deletion of *potD* Affects *L. pneumophila* Phenotypes Associated with Biofilm Formation

Polyamines have been implicated in the control of biofilm formation in several bacterial pathogens (221,252,280,375). In *V. cholerae*, deletion of one of the two putative *potD* homologues, *nspS* or *potD,* affects biofilm formation (221,280). In *L. pneumophila*, the abilities to form filaments and biofilms appear to be correlated (322). Therefore, we investigated whether deletion of *potD* could affect biofilm and filament formation by *L. pneumophila*. We found that deletion of *potD* reduced the ability of *L. pneumophila* to form filaments when grown on BCYE at 37^{o}C for 3-5 days (Fig. 27). However, the Δ*potD*(pMMB207C) mutant strain was as able as the parent strain JR32(pMMB207C) to adhere to the pegs of the Calgary biofilm device (Fig. 28), suggesting that deletion of *potD* did no affect the ability of *L. pneumophila* to form biofilms under the conditions

tested. Although Piao et al. (322) previously showed a correlation between filamentation and biofilm formation, our results suggest that these appear to be independent phenotypes. Additionally, our results suggest that PotD itself, or polyamines, are involved in the regulation of cell growth and (or) differentiation of *L. pneumophila*, as previously shown for *Proteus mirabilis* (389) and other microorganisms [reviewed in (74,375,395)].

5.3.6. Deletion of *potD* Decrease *L. pneumophila* Resistance to Na^+

Polyamines have been shown to have a direct effect on several ion channels and play a role in regulation of sodium homeostasis in mammals and plants [reviewed in(246)]. In *E. coli*, spermidine and putrescine alter the charge and pore size of the outer membrane porins OmpC and OmpF resulting in channel closure and subsequently decreasing outer membrane permeability to ions and small water-soluble molecules (82,84,206). Additionally, in *E. coli*, putrescine efflux has been implicated in sodium tolerance by allowing the influx and accumulation of K^+ and compatible osmolytes like proline and betaine (364). Therefore, due to its potential involvement in ion trafficking, we investigated whether deletion of *potD* has an effect on *L. pneumophila* tolerance to Na^+.

L. pneumophila strains JR32(pMMB207C), Δ*potD*(pMMB207C), and Δ*potD*(pMMB-P_{potA}:*potD*) were grown to EP or SP and spotted on BCYE plates in the containing or lacking 100 mM NaCl. The mutant Δ*potD*(pMMB207C) in SP or EP was found to be ~1000-fold more sensitive to NaCl than the parent strain JR32(pMMB207C) (Fig. 29A-C). Genetic complementation with pMMB-P_{potA}:*potD* (in which PotD

expression is solely driven by P_{potA}) partially restored the ability of the mutant strain Δ*potD*(pMMB-P_{potA}:*potD*) to grow on 100 mM NaCl, indicating that PotD enhances the resistance of *L. pneumophila* to sodium. To determine whether the Δ*potD* mutant is sensitive to sodium in particular, rather than to osmotic stress in general, we examined the sensitivity of the mutant strain Δ*potD*(pMMB207C) to KCl. The Δ*potD*(pMMB207C) mutant was able to grow on 100 mM KCl in a manner similar to the parent strain JR32(pMMB207C) (Fig. 29D), indicating that PotD is specifically important for tolerance to Na^+ rather than to osmotic stress in general.

5.3.7. PotD Promotes *L. pneumophila* Attachment to Phagocytic Cells and Intracellular Growth

Ware et al. (421) previously studied the implications of *potD* deletion on *Streptococcus pneumoniae* virulence. They showed that although deletion of *potD* has no effect on the growth of the *S. pneumoniae* Δ*potD* mutant *in vitro*, this mutant displayed a significant attenuation in virulence within murine models of systemic and pulmonary infection. Therefore, we wanted to investigate whether PotD participates in the interaction of *L. pneumophila* with host cells *in vivo*. First, we set out to test the role of PotD in attachment of *L. pneumophila* to host cells. The human derived macrophages THP-1 [an established model to study attachment of *L. pneumophila* (67)], were used.

The parental *L. pneumophila* strain JR32(pMMB207C) was three times more efficient than the mutant strain Δ*potD*(pMMB207C) at attaching to THP-1 (Fig. 30). The complemented strain Δ*potD*(pMMB:*potD*),which expresses *potD* under the control of the inducible promoter P_{tac}, partially recovered the ability to attach to THP-1 macrophages.

This suggests that, in spite of not playing a role in attachment to solid surface and biofilm formation (Fig. 28), PotD and (or) polyamines appears to play a role in the surface properties of *L. pneumophila* that enhance adherence to macrophages (Fig. 30).

Next, we investigated the role of PotD in the intracellular growth of *L. pneumophila* using three different host cell types (*A. castellanii*, U937-derived human macrophages, and L929 mouse fibroblasts). At time zero (which measures attachment before replication begins), the mutant strain Δ*potD*(pMMB207C) showed 2 to 3-fold lower CFU/well counts than the parental strain JR32(pMMB207C) in *A. castellanii*, and 5 to 6 fold lower counts than the parental strain in U937 macrophages (Fig. 31A &B), confirming the role of PotD in attachment to phagocytic cells. This attachment defect at zero time was not observed in non-phagocytic L929 cells (Fig. 31C). The mutant strain Δ*potD*(pMMB207C) showed a 6 to 7-fold decrease in CFU/well 24 h post infection in *A. castellanii*, U937, and L929 cells (Fig. 31A-C). However, no defect in intracellular growth of Δ*potD*(pMMB207C) was noticed 48 h post-infection. The fact that the growth defect observed for the mutant strain Δ*potD*(pMMB207C) in amoeba at 24 h (6 to 7-fold) is larger than the attachment defect (2 to 3-fold) (Fig. 31A), suggests that PotD has a transient role in early replication in amoeba (not entirely due to its reduced attachment to host cells). In addition, although there was no difference in the attachment to L929 cells between the mutant strain Δ*potD*(pMMB207C) and the parental strain JR32(pMMB207C) (Fig. 31C), there was a 6-fold difference in intracellular growth at 24 h, clearly indicating that, while PotD is not important for attachment toL929 cells, it plays a role in *L. pneumophila*'s early intracellular replication in these cells.

5.3.8. Deletion of *potD* Has No Effect on *L. pneumophila* Cytotoxicity to U937 Macrophages

L. pneumophila is cytotoxic to mouse macrophages (15,45). To test whether the pronounced attachment defect observed for the mutant strain Δ*potD*(pMMB207C) in U937 macrophages (Fig. 31B) was due to cytotoxicity towards these cells, I used the LDH release assay to measure cytotoxicity inU937 macrophages. Since *L. pneumophila* cytotoxicity is an early effect that occurs before establishment of the LCV and the initiation of intracellular replication (15,45), cytotoxicity was assayed 3 h post-infection. As shown in Figure 32, there was no difference in LDH release seen in U937 cells infected with the parent strain JR32(pMMB207C),the mutant strain Δ*potD*(pMMB207C), or the complemented strain Δ*potD*(pMMB:*potD*), suggesting that deletion of *potD* does not affect *L. pneumophila* cytotoxicity towards U937 cells, and that cytotoxicity does not contribute to the attachment defect of the mutant.

5.3.9. The *L. pneumophila* Δ*potD* Mutant Is Unable to Compete with Its Parental Strain in U937 Macrophages

We have shown that the Δ*potD* mutant strain displayed a growth defect only at 24 h post-infection.If the growth defect observed in U937 macrophages at the early time of infection (Fig. 31B) is due solely to the initial defect in attachment observed at time zero, we would expect the Δ*potD* mutant to effectively compete with the parent strain. In Figure 31B, when the parent and the Δ*potD* mutant strains were tested separately, cultures of the mutant and parent strains had different CFU/ml at 24 h but similar CFU/ml at 48 h post-infection. Therefore, the question was whether or not a competition

assay would allow us to determine if the Δ*potD* mutant could still recover in the 24-48 h period in the presence of the parent strain.

To differentiate between the competing strains, GFP was expressed in the parental strain JR32 (by introducing the plasmid pMMB207-Km14-GFPc) and the red fluorescent protein Ds-Red was expressed in the Δ*potD* mutant strain (by introducing the plasmid pSW001).The parental strain was named JR32-GFP and the Δ*potD* mutant strain Δ*potD*-RED (refer to Section 2.4.13 of Chapter 2). A 1:1 mixture of JR32-GFP and Δ*potD*-RED (used as inoculum in the competition assay) yielded nearly equal CFU numbers for each strain at time zero, [log competitive index (CI) for the input ≈ 0] (Fig. 33A, black bars). However at 24 and 48 h post-infection of U937 macrophages, JR32-GFP significantly outcompeted Δ*potD*-RED (log CI output ≈– 0.5). It is important to note that, in contrast to the intracellular growth assay performed separately with the parent strain and the Δ*potD* mutant strain (Fig. 31B), the growth defect of the mutant was still present at48 h in the competition assay with U937 cells (log CI ≈–0.5). Similar results (Fig. 33A, white bars) were obtained with strains Δ*potD*-GFP and JR32-RED in which the plasmids carrying the fluorescent proteins were switched to rule out any effects associated with the plasmids themselves or expression of their genes (refer to Section 2.4.13 of Chapter 2).

During the course of the competition assay, we *quantitated* the percentage of U937 cells infected by JR32-GFP or Δ*potD* -RED at 24 and 48 h post-infection. As shown in Figure 33B, the number of JR32-GFP infected cells (Fig. 33C, green bars) is about 3-fold higher than the number of Δ*potD*-RED infected cells (Fig. 33C, red bars) 24 or 48 h post infection. In addition, at 48 h post infection, I noticed that LCVs containing JR32-GFP (Fig. 33B, green cells) were much bigger than the LCVs containing Δ*potD*-

RED (Fig. 33B, red cells), confirming that Δ*potD*-RED had a low intracellular growth rate in the presence of JR32-GFP. Similar results were obtained with JR32-RED and Δ*potD*-GFP (Fig. 33D). Together, these findings confirm that (as shown in amoeba and L929 cells) PotD plays a role in the intracellular replication of *L. pneumophila* in U937 macrophages.

5.3.10. Inhibition of Spermidine Synthesis in L929 Cells Abolishes the Intracellular Growth of the Δ*potD* Mutant

In Chapter 4 of this thesis we showed that the inhibition of polyamine biosynthesis in L929 cells, using the pharmacological inhibitor MGBG, significantly reduces *L. pneumophila* intracellular growth (295). To determine if PotD plays a role in the uptake of exogenous polyamines provided by host cells to *L. pneumophila*, we set out to test the combined effects of MGBG treatment and the deletion of *potD* on the intracellular growth of *L. pneumophila.* As shown in Figure 34, deletion of *potD* or inhibition of polyamine synthesis by MGBG significantly reduced *L. pneumophila* growth within L929 cells. Neither administration of MGBG nor deletion of *potD* alone was able to completely block the intracellular growth of *L. pneumophila* in L929 cells. Only the combined effect of *potD* deletion and MGBG treatment completely inhibited *L. pneumophila* intracellular growth in L929 cells (Fig. 34). These results suggest that PotD is critical for the intracellular growth of *L. pneumophila* in polyamine-depleted L929 cells.

5.3.11. Deletion of *potD* Affects LCV Trafficking in U937 Cells

Aberrant trafficking of LCVs in macrophages confers early intracellular replication defects in *L. pneumophila*(376). To begin an investigation on the mechanism responsible for the growth defect of Δ*potD*(pMMB207C) in U937 macrophages (Fig. 31), we used electron and fluorescence microscopy to investigate whether PotD is required for normal LCV trafficking(Fig. 35A). We found that the number of LCVs formed by the parent strain JR32(pMMB207C) and the complemented strain Δ*potD*(pMMB:P_{potA}:*potD*) was significantly higher than the number of LCVs formed by the mutant strain Δ*potD*(pMMB207C) (Fig. 35B).These results suggest that the reduced attachment capacity of the Δ*potD* mutant led to a reduced net number of internalized bacteria and, consequently, fewer LCVs being formed in U937 macrophages by the Δ*potD* mutant.

LCV trafficking was first studied by determining phagosome-lysosome fusion, through the colocalization of *L. pneumophila* with the lysosomal marker LAMP-1. The mutant Δ*potD*-RED or its parent strain JR32-RED equally avoided colocalization with LAMP-1 (Fig. 35C), suggesting that the Δ*potD* mutant is not defective at inhibiting fusion with lysosomes. Next, the effect of PotD on LCV trafficking within U937 cells was analyzed by scoring the number of vesicles and mitochondria associated with LCVs, as well as the presence of ER around the LCV (Fig. 35A & B). Interestingly, the parent JR32(pMMB207C) and the complemented Δ*potD*(pMMB:P_{potA}:*potD*) strains showed a higher ability to recruit vesicles (~2.6 vesicles per LCV) than the Δ*potD*(pMMB207C) mutant strain (~1.25 vesicles per LCV), yet there was no difference in mitochondrial or rough ER recruitment (Fig. 35A & B). These results suggest that the mechanism underlying the intracellular growth defect of the Δ*potD* mutant might be related to a

reduced ability to recruit vesicles, which could be involved in nutrient delivery to the LCV.

5.4. Discussion

In Chapter 4 of this thesis, we proposed that: (i) due to its lack of polyamine biosynthetic enzymes, *L. pneumophila* depends on exogenous polyamines to fulfil its physiological needs, and (ii) polyamines are important in *L. pneumophila* pathogenesis as enhancers of intracellular growth. If *L. pneumophila* depends on exogenous polyamines, it should be able to transport polyamines from the extracellular environment into its cytoplasm. In this Chapter, we report that the *L. pneumophila* genome encodes only one putative polyamine transporter, the ABC transporter PotABCD. The role of this putative transporter in *L. pneumophila* physiology and pathogenesis was assessed by characterizing a Δ*potD* mutant. The results presented in this Chapter suggest that PotD, polyamines (putatively transported by the PotABCD transporter) and(or) processes associated with polyamine transport, are required for the optimal intracellular growth of *L. pneumophila*.

5.4.1. Effect of Polyamines and Polyamine Transport on *L.* pneumophila Growth

Shortly after its internalization in a membrane-bound phagosome, *L. pneumophila* departs from the endocytic pathway and, through alterations in organelle and vesicular trafficking, it gets established in a specialized vacuole called the *Legionella*-containing vacuole (LCV). This represents a virulence strategy that trades access to host cell cytoplasmic nutrients for protection from degradation by lysosomes (361). Little is

known about the importance of nutrient transport for the replication of *L. pneumophila* in the LCV. However, recently it has been shown that the macrophage amino acid transporter SLC1A5 promotes *L. pneumophila* replication in the LCV, presumably by increasing the amount of available amino acids in the LCV (431). Sauer et al. (361) suggested that a Δ*phtA L. pneumophila* mutant, lacking the threonine transporter, exhibits a severe defect in both intracellular growth and differentiation of transmissive forms (TFs) into replicative forms (RFs). However, the PhtA transporter defect can be bypassed by the addition of threonine to the infected cells, suggesting that amino acids added to the medium where infected cells are cultured somehow reach the lumen of the LCV, and that the threonine levels normally present in the LCV are low and insufficient to bypass the PhtA defect (361). PhtA may play a dual role: a nutritional one (simply mediating acquisition of a nutrient), and a signalling one (triggering differentiation).

Applying these principles to polyamines, we propose that the polyamine content of the LCV at an early time of infection is normally low. This view is supported by previous results (Chapter 4 of this thesis) showing that the inhibitory effect of MGBG was more obvious at the early stages of infection (24 h) and that addition of exogenous polyamines enhanced the intracellular growth of *L. pneumophila* in L929 cells but only at 24 h post-infection (Chapter 4, Fig. 22) (295). In the presence of the parental strain, the early delay in intracellular growth observed for the Δ*potD* mutant at 24 h was extended to 48 h, as shown in the competition assay (Fig. 33). In contrast, when tested alone (in the absence of the parent strain) the Δ*potD* mutant efficiently recovered from its early delay in intracellular growth at 24 h (Fig 31). One simple explanation for this difference would

be that during the competition assay the parent strain was able to take up and consume the available polyamines depriving the mutant of these nutrients.

A nutritional role of polyamines is supported by the *in vitro* growth pattern of *L. pneumophila* in synthetic defined (SD) medium supplemented with polyamines (Fig. 26B), and by our previous findings (Chapter 4, Fig. 22) showing that addition of exogenous polyamines to L929 cells enhances the intracellular growth of *L. pneumophila* (295). However, the strongest support comes from the experiment shown in Figure 34, in which MGBG-mediated inhibition of polyamine synthesis in L929 cells completely abolished the intracellular growth of the Δ*potD* mutant. We can speculate that, in a polyamine-limited environment, *L. pneumophila* would require an efficient polyamine transporter to support intracellular growth.

Many reports have been published recently correlating polyamines with changes in gene expression of bacterial pathogens [reviewed in (375)].. For example, the interaction of *Francsisella tularensis* or uropathogenic *E. coli* with polyamines triggers a change in gene expression that preconditions the pathogens to better invade their hosts (32,49,147). It has also been reported that the uptake of polyamines, mediated by PotABCD in *E. coli*, results in changes in gene expression including the down-regulation of the *potABCD* operon (9,198). Igarashi and Kashaiwagi (199) proposed a "polyamine modulon" theory to explain how polyamines enhance bacterial cell growth. In this model polyamines act as mRNA-binding compounds that stimulate synthesis of bacterial growth factors such as oligopeptide binding proteins (required for oligopeptide uptake), adenylate cyclase, RNA polymerase sigma subunits, and several other transcription factors. Accordingly, it is possible that polyamines could bind to RNA and induce the

expression of some key genes required for intracellular growth and virulence of *L. pneumophila*. Additionally, polyamines might provide a signal [as do amino acids (58,286,361)] that is important in *L. pneumophila* differentiation, not only during *L. pneumophila* growth *in vitro* (BYE) but also during intracellular growth. If polyamines, then, provide a signal for differentiation, the induction of P_{potA} activity during EP would correspond to the timing of transition of *L. pneumophila* from TF into RF.

As a putative polyamine binding protein, (Fig. 24), the most obvious function of PotD would be to bring polyamines into the cytoplasm of *L. pneumophila*. However, PotD could have other functions. Not all the observed functions of PotD appear to be linked to polyamine transport. Compared to its parental strain, the Δ*potD* mutant had a lower ability to attach to phagocytic host cells (Fig. 30) and modify vesicular trafficking (Fig. 35), two processes that appear to be not directly related to polyamine transport. Since PotD in *E. coli* has been shown to bind to DNA and to act as a transcription factor that regulates its own promoter (9), it is possible that, in *L. pneumophila,* PotD could also be involved in gene regulation.

PotD in Gram-negative bacteria is a periplasmic protein (197,198,375). Therefore, another contribution of PotD could be that its presence or absence in the periplasm of *L. pneumophila* affects the structural characteristics of the cell envelope. It could be speculated that the absence of PotD in the periplasm of the Δ*potD* mutant changes its cell surface properties, and results in a defect in attachment to phagocytic cells (amoeba and macrophages).

5.4.2. Does *L. pneumophila* Have Polyamine Transporters Other Than PotABCD?

Clearly, PotD is dispensable during growth *in vitro*. One interpretation for these results is that *L. pneumophila* possesses alternative polyamine transport systems. However, to fully explain these results, we propose that these alternative transport systems have lower affinity for polyamines than PotABCD, and are inactive in the early phase of host cell infections. A mechanism by which these alternate transport systems could be activated is through an increase of polyamine concentrations in the surrounding environment. Above a threshold level of polyamines (not present in the early LCV, but reached after the first 24 h of infection) the alternate transport systems would be functionally relevant. In BYE broth, the high levels of polyamines provided in the yeast extract would be above such a threshold, leading to absence of an *in vitro* growth defect of the Δ*potD* mutant. A similar phenotype would be seen in bacterial cells grown in SD medium supplemented with polyamines.

The existence of alternative polyamine transport systems has been reported in many other facultative intracellular pathogens. For instance, *Shigella boydii* and *Salmonella enterica* sv. Typhimurium have at least three polyamine transport systems (PotABCD, potFGHI, and PotE) (375). In *Mycoplasma genitalium* and *M. pneumoniae,* gene products with detectable similarity to known polyamine binding proteins (such as PotD and PotF) are lacking. Because *Mycoplasma* cannot synthesize polyamines, there must be alternate (unknown)transport systems that allow this pathogen to meet its requirement for polyamines(198).

Another explanation of the results that show that PotD is dispensable is that in *L. pneumophila* deletion of *potD* is not a loss-of-function mutation, and that in the absence

of PotD, the PotABC transporter still has enough residual activity to maintain intracellular growth. To confirm whether this is the case or not, I propose to repeat the intracellular growth assays in a *L. pneumophila* mutant harboring a deletion of the entire *potABCD* operon.

5.4.3. Effect of Polyamines and Polyamine Transport in the Tolerance of *L. pneumophila* to Na^+

L. pneumophila grown to SP is salt sensitive, a trait that is intimately linked to virulence, and avirulent mutants are usually sodium tolerant (158). To our knowledge, the Δ*potD* mutant is the first reported *L. pneumophila* sodium sensitive mutant that has a virulence-related defect. Sodium sensitivity of the Δ*potD* mutant was seen not only in SP, but also in EP (Fig. 29). This is surprising, because it is accepted that exponentially growing *L. pneumophila* is not sensitive to Na^+. It has been established that some ABC transporters can function as antiporters controlling the influx and efflux of small molecules(290). In bacteria, many ABC transporters are specialized in the efflux of antibiotics, ions and heavy metals (182,262,290,300). In *E. coli*, efflux of putrescine by PotE plays an important role in Na^+ tolerance (364). Therefore, it is possible that PotABCD in *L. pneumophila* could function as an antiporters (as PotE does) that takes in polyamines and takes out sodium ions. Polyamines have been shown to stabilize halophilic organisms and other fragile bacteria by increasing the stability of the cell membrane or cell wall (395,397). In plant and bacterial cells, polyamines or other compatible organic salts, such as those from amino acids and betaines, accumulate within the cell during exposure to high concentration of sodium to function as modulators of salt tolerance (osmolytes) (227,240,270,364,408). To this end, I believe that deletion of *potD*

leads to a reduction in polyamine influx into the bacterial cells, which results in reduced efflux (and a consequent accumulation of) intracellular Na^+, leading to growth inhibition.

When a pathogen infects a host, it must adapt rapidly to a new environment to avoid killing and to initiate cellular division. *L. pneumophila*, in particular, needs to activate cellular processes, such as DNA, RNA and protein synthesis, during its differentiation from a TF into an RF, and polyamines have been shown to be involved in these processes. Here, we show that deletion of *potD* in *L pneumophila* results in a number of virulence-related defects. We therefore propose that PotD has a novel role as a virulence factor.

5.5. Acknowledgements

I thank Dr. Jessica Boyd, Dr. Lois Murray, and Dr. Jason Leblanc for their advice and discussions in relation to the role of PotD in *L. pneumophila* pathogenesis. I thank Sahar Da'as for her help in formatting the figures of this manuscript, Hany Abdelhady for activation of U937 macrophages, and David Allan for preparation of L929 cells. I also acknowledge the following individuals for providing plasmids and (or) strains needed for this work: Dr. Hubert Hilbi, Dr. Howard Shuman, Dr. Michelle Swanson, Dr. Karen Brassinga, and Dr. Paul Hoffman. This work was funded by a Discovery Grant from the Natural Sciences and Engineering Research Council of Canada (NSERC) to RAG.

5.6. Figures, and Legends to Figures

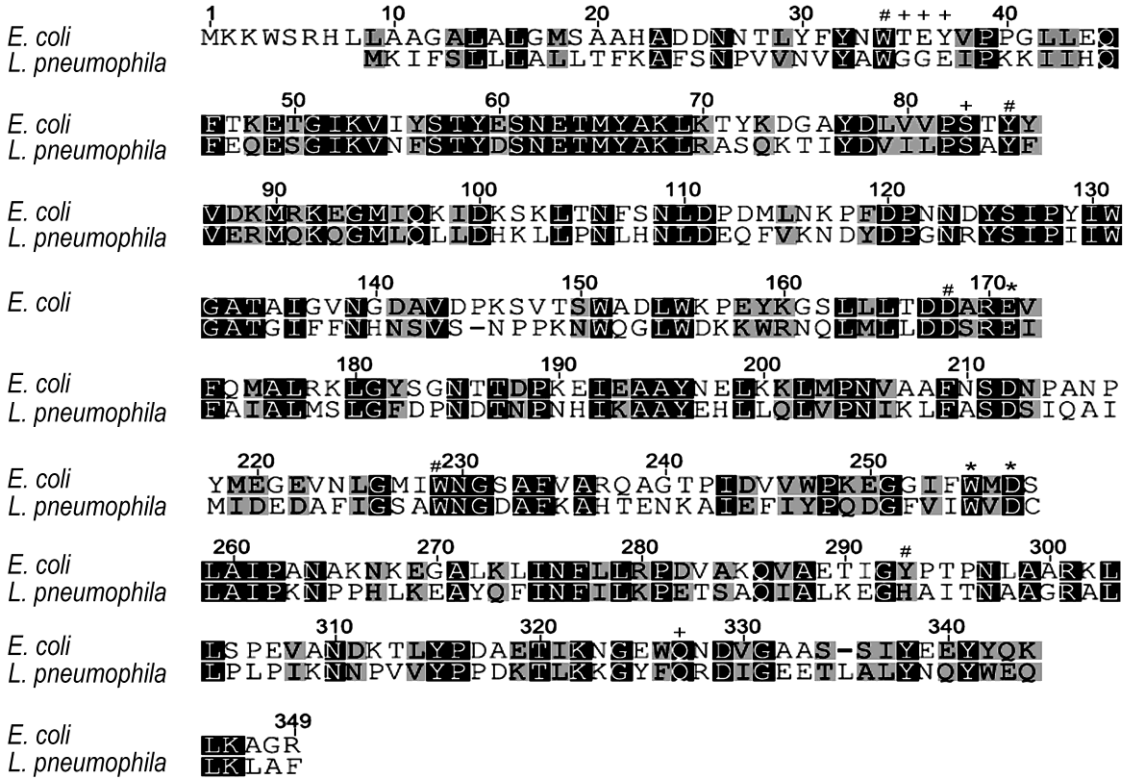

Figure 24. Alignment of the amino acid sequence of *E. coli* PotD and *L. pneumophila* putative PotD.

Identical amino acid residues are shown in black boxes and similar amino acids are shown in gray boxes. The amino acids involved in spermidine binding in the *E. coli* PotD are categorized as follows: (*) highly important, (#) important, and (+) modestly important.

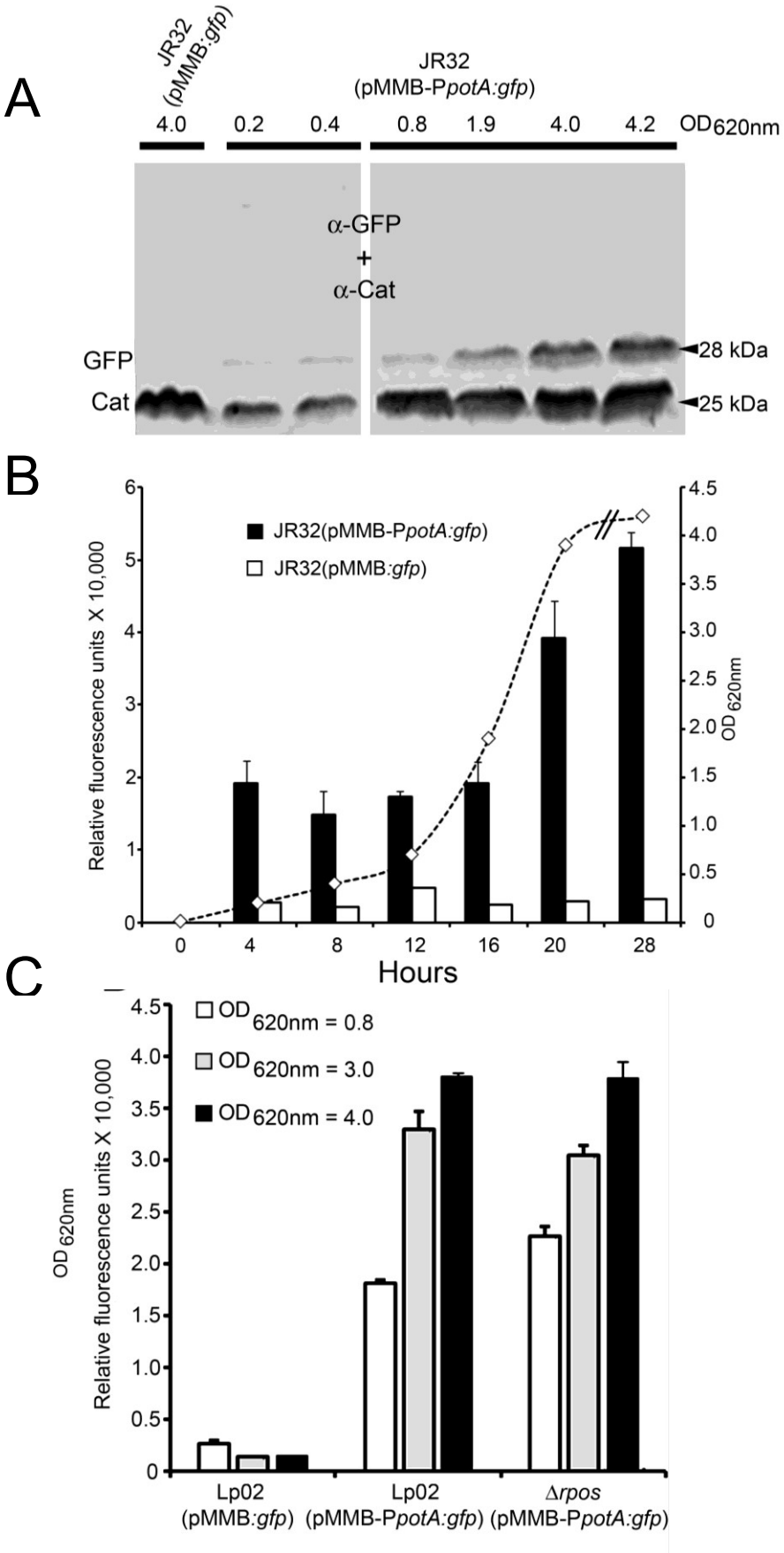
A
JR32 (pMMB:gfp)
JR32 (pMMB-PpotA:gfp)
4.0
0.2
0.4
0.8
1.9
4.0
4.2
OD620nm
α-GFP + α-Cat
GFP
Cat
28 kDa
25 kDa
B
JR32(pMMB-PpotA:gfp)
JR32(pMMB:gfp)
Relative fluorescence units X 10,000
OD 620nm
Hours
C
OD 620nm = 0.8
OD 620nm = 3.0
OD 620nm = 4.0
Relative fluorescence units X 10,000
OD 620nm
Lp02 (pMMB:gfp)
Lp02 (pMMB-PpotA:gfp)
Δrpos (pMMB-PpotA:gfp)

Figure 25. The *potABCD* promoter (P_{potA}) is activated during exponential phase (EP). **(A)** Composite immunoblot of whole cell lysates from strain JR32(pMMB-P_{potA}:*gfp*) or strain JR32(pMMB:*gfp*) harvested from BYE broth cultures at the indicated OD_{620}, separated by SDS-PAGE and transferred to a nitrocellulose membrane. Polyclonal antibodies specific for green fluorescent protein (GFP), and chloramphenicol acetyl transferase (Cat) were added together (α-GFP + α-Cat) for immunostaining. Cat was used as a loading control. The position and size of protein standards are indicated in kDa. the indicated OD_{620} values correspond to the growth curve shown in panel **B**. **(B)** Double axis graph showing the fluorometric analysis of GFP fluorescence in JR32(pMMB-P_{potA}:*gfp*) or JR32(pMMB:*gfp*) strains at different growth stages. The right y-axis indicates $OD_{620\ nm}$ values (mean of triplicate cultures) and was used to construct the growth curve for strain JR32(pMMB-P_{potA}:*gfp*). The left y-axis indicates relative fluorescence units normalized to an OD_{620} of 1.0 unit, and was used to construct the bar graph pairs for GFP fluorescence (P_{potA} activity) along the growth curve (mean of triplicate cultures). **(C)** Bar graph showing P_{potA} activity measured as relative fluorescence units normalized to an OD_{620} of 1.0 unit. The Lp02-derived strains used for this experiment are indicated on the x-axis. For each strain measurements were made at three growth stages (white, gray and black bars). An OD_{620} value of 0.8 corresponds to early exponential growth phase and the values of 3.0 and 4.0 correspond to late exponential phase and stationary phase, respectively. Results are shown as mean + one standard deviation of 3 independent cultures (n=3). This Figure was generated by Nicholas Tompkins and Gheyath Nasrallah.

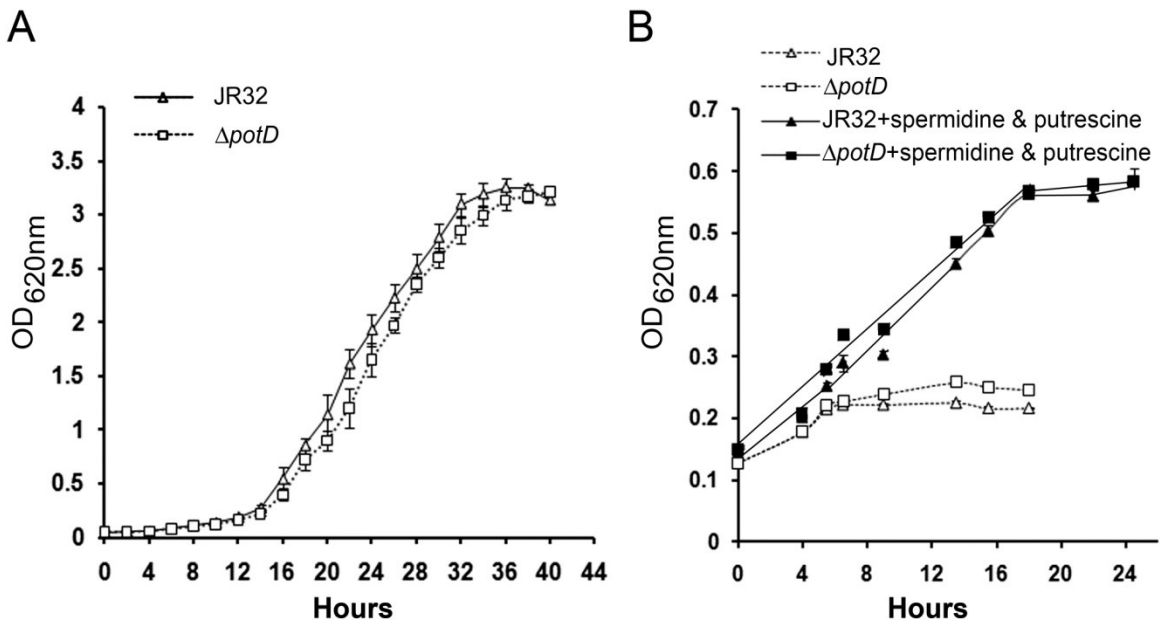

Figure 26. PotD is dispensable for *L. pneumophila* growth *in vitro***.**

(A) BYE broth or **(B)** SD medium with or without spermidine and putrescine was inoculated in triplicate with three independent cultures of parent JR32 or mutant Δ*potD* strains grown to late exponential phase. Growth was monitored by OD_{620} readings. All panels show data points as mean ± one std. deviation (n=3 replicates) from one experiment. The experiment in panel **B** was done by Gheyath Nasrallah and Nicholas Tompkins.

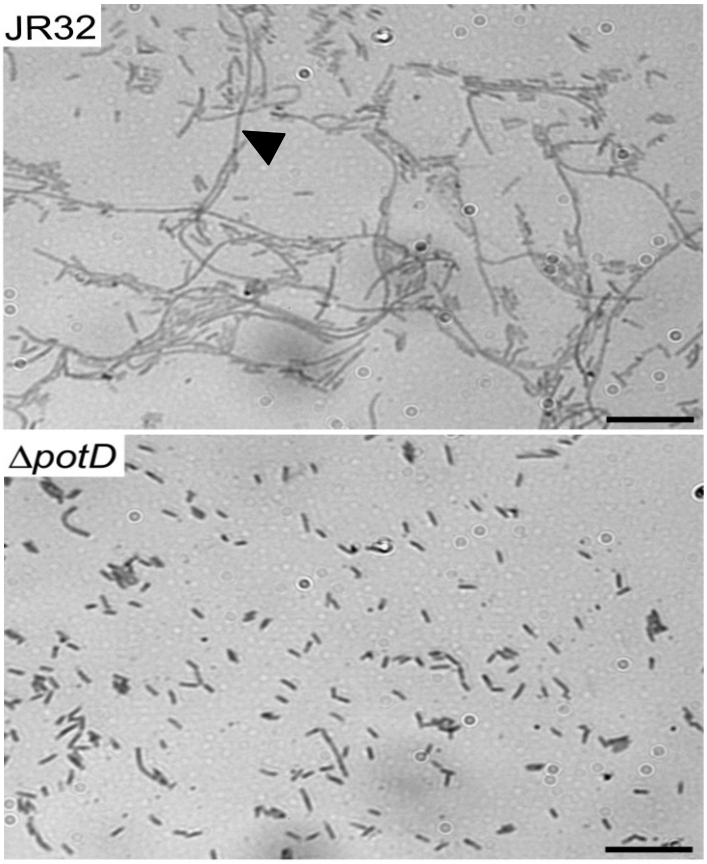

Figure 27. Deletion of *potD* reduces the ability of *L. pneumophila* to form filaments.

Light micrographs of smears prepared from the indicated *L. pneumophila* strains grown on BCYE agar for 4 days, and stained with crystal violet. The parental strain JR32 forms long filaments (one is indicated by the black arrowhead), while the Δ*potD* mutant strain predominantly grows as short rods. Size bars represent 10 μm. Similar results were obtained from three independent experiments. This figure was generated by Gheyath Nasrallah.

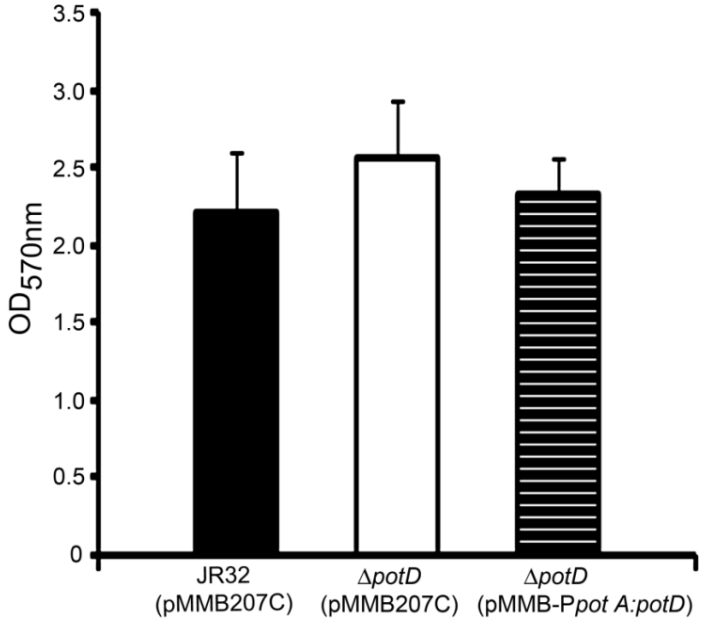

Figure 28. PotD does not contribute to biofilm formation by *L. pneumophila* under static conditions in rich medium.

Biofilm formation by *L. pneumophila* strains was evaluated in the Calgary Biofilm Device (CBD) using the crystal violet incorporation assay (Section 2.4.8 of Chapter 2). The amount of released crystal violet is proportional to the number of bacterial cells attached to the CBD pegs and was measured spectrophotometrically ($OD_{570\ nm}$). Results are shown for the strains indicated as mean + one standard deviation for one experiment donein 18 wells per strain (n=18). Similar results were obtained from two other independent experiments. This figure was generated by Gheyath Nasrallah.

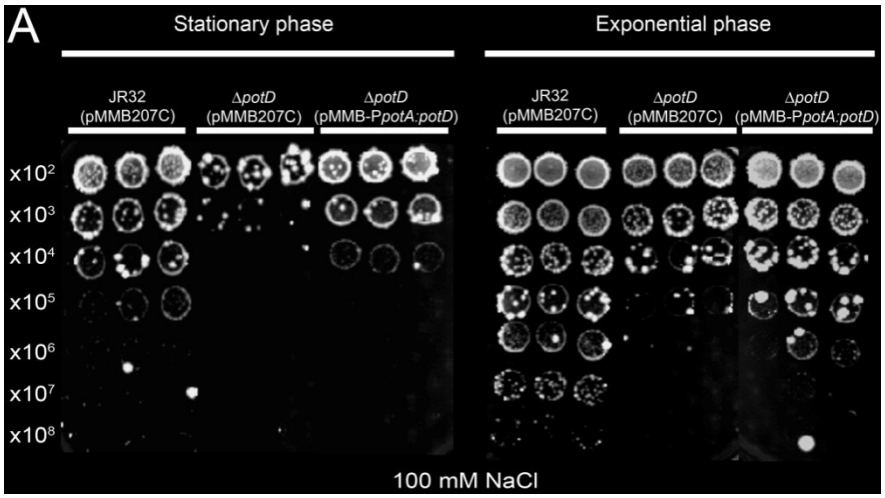
A
Stationary phase
Exponential phase
JR32 (pMMB207C)
ΔpotD (pMMB207C)
ΔpotD (pMMB-PpotA:potD)
x10²
x10³
x10⁴
x10⁵
x10⁶
x10⁷
x10⁸
100 mM NaCl

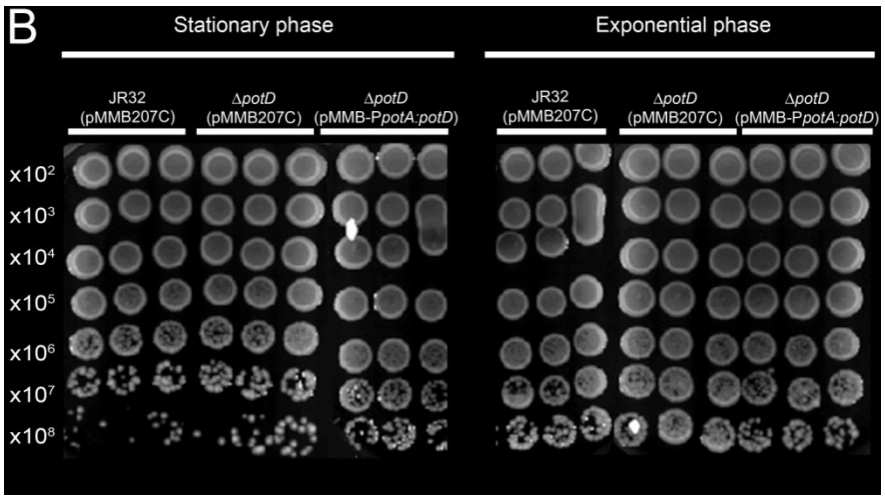
B
Stationary phase
Exponential phase
JR32 (pMMB207C)
ΔpotD (pMMB207C)
ΔpotD (pMMB-PpotA:potD)
x10²
x10³
x10⁴
x10⁵
x10⁶
x10⁷
x10⁸

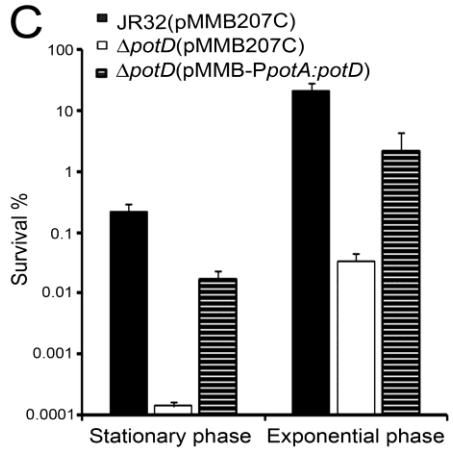
C
JR32(pMMB207C)
ΔpotD(pMMB207C)
ΔpotD(pMMB-PpotA:potD)
Survival %
100
10
1
0.1
0.01
0.001
0.0001
Stationary phase
Exponential phase

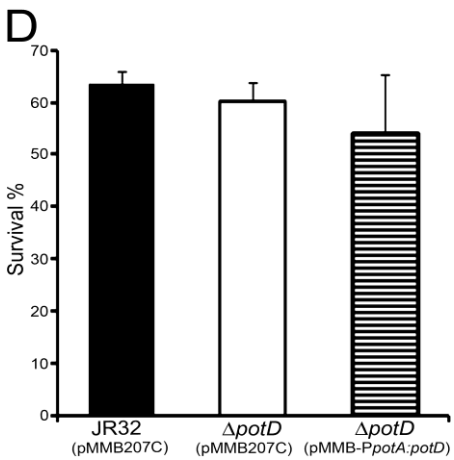
D
Survival %
70
60
50
40
30
20
10
0
JR32 (pMMB207C)
ΔpotD (pMMB207C)
ΔpotD (pMMB-PpotA:potD)

Figure 29. PotD enhances resistance of *L. pneumophila* to sodium chloride.

Serial 10-fold dilutions of stationary or exponential phase *L. pneumophila* parent JR32(pMMB207C), mutant Δ*potD*(pMMB207C) and mutant complemented Δ*potD*(pMMB:*potD*) strains spotted onto a BCYE agar plate containing **(A)** or lacking 100 mM NaCl **(B)**. **(C)** Bar graph showing a quantitative analysis of sodium tolerance**.** Results are presented as percent survival calculated as CFU/ml in the presence of 100 mM NaCl **(A)** divided by CFU/ml in the absence of NaCl **(B)**. **(D)** Bar graph showing a quantitative analysis of tolerance to KCl (spot plates not shown). Results are presented as percent survival which were calculated as described in (**C).** Bars in **(C)** and **(D)** represent mean + one standard deviation of one experiment done in triplicate. Similar results were obtained from two other independent experiments. This figure was generated by Gheyath Nasrallah.

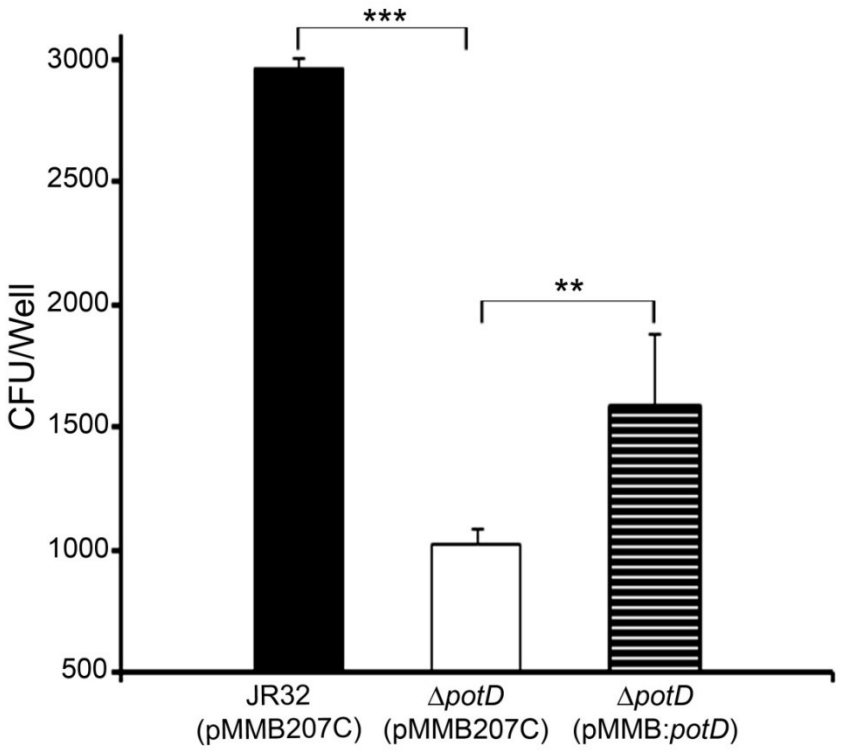

Figure 30. PotD promotes attachment of *L. pneumophila* to macrophages.

THP-1 macrophages were infected for 90 min with IPTG-treated *L. pneumophila* strains, grown to late exponential phase, bearing the plasmids indicated in parentheses, at a bacteria to cell ratio of 20:1, and attached bacteria were counted by dilution-plating after extensive washing (see Section 2.4.9). Results are shown as CFU per well and represent the mean + one standard deviation for 3 independent experiments (n = 3), each done in duplicate. The statistical significance of differences between bars is indicated as ** P<0.01, *** P<0.001. This figure was generated by Gheyath Nasrallah.

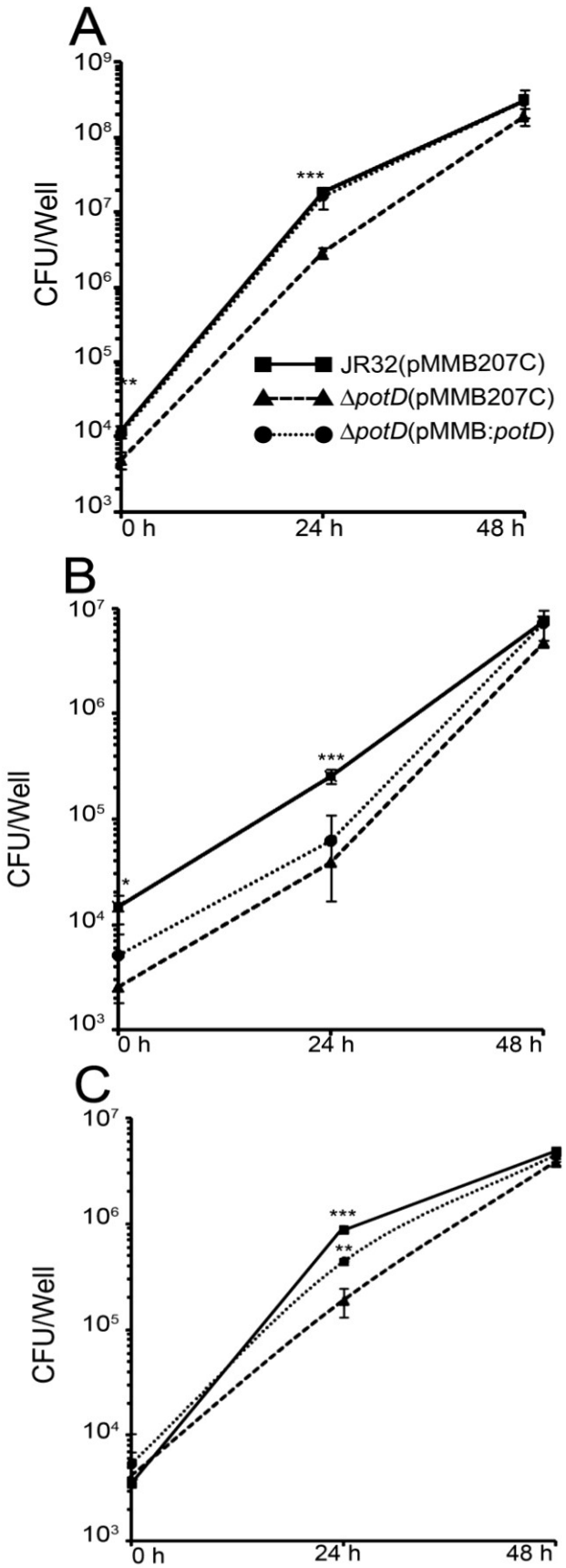
A
B
C
CFU/Well
10^9
10^8
10^7
10^6
10^5
10^4
10^3
0 h
24 h
48 h
***
**
*
JR32(pMMB207C)
Δ*potD*(pMMB207C)
Δ*potD*(pMMB:*potD*)

Figure 31. The *L. pneumophila* Δ*potD* mutant shows impaired intracellular growth. *A. castellanii* **(A),** U937 macrophages **(B)**, and L929 cells **(C)** were infected with the indicated IPTG- treated *L. pneumophila* strains grown to late exponential phase. The number of intracellular bacteria/well at the time points indicated were determined by dilution-plating (see Section 2.4.10) *L. pneumophila* intracellular numbers are shown as CFU/well. Results represent the mean + one standard deviation for 3 independent experiments (n = 3), each done in duplicate. The statistical significance of differences in CFU values is indicated as: * P<0.05, ** P<0.01, *** P<0.001. This figure was generated by Gheyath Nasrallah.

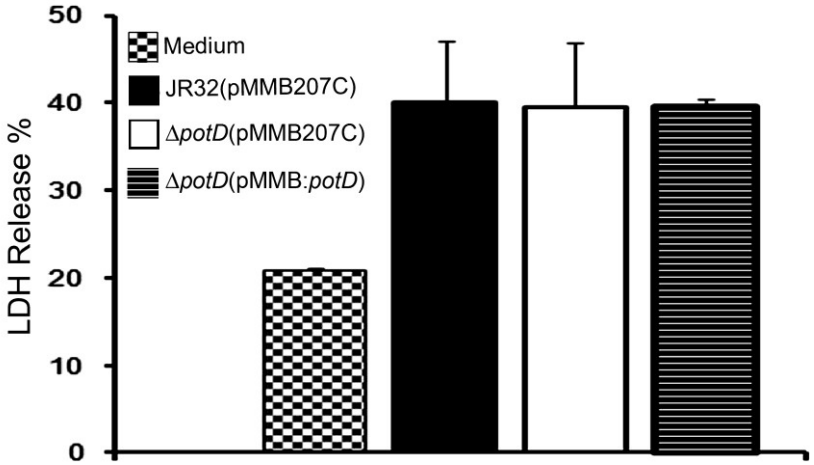

Figure 32. PotD does not contribute to *L. pneumophila* cytotoxicity towards U937-derived human macrophages.

U937 macrophages grown in 48-well plates were infected for 3 h with the indicated *L. pneumophila* strains. Contact-dependent cytotoxicity was quantified as percentage of lactate dehydrogenase (LDH) release in to the supernatant of the infected cell culture. Supernatants from the uninfected cells (medium control) were used to set the background release of LDH, and a positive control (supernatants of cells treated with lysis solution) was used to set the 100 % release of LDH. Results are shown as mean LDH Release + one standard deviation from one experiment, done in 8 wells per strain (n=8 replicate). Similar results were obtained from two other independent experiments. This figure was generated by Gheyath Nasrallah.

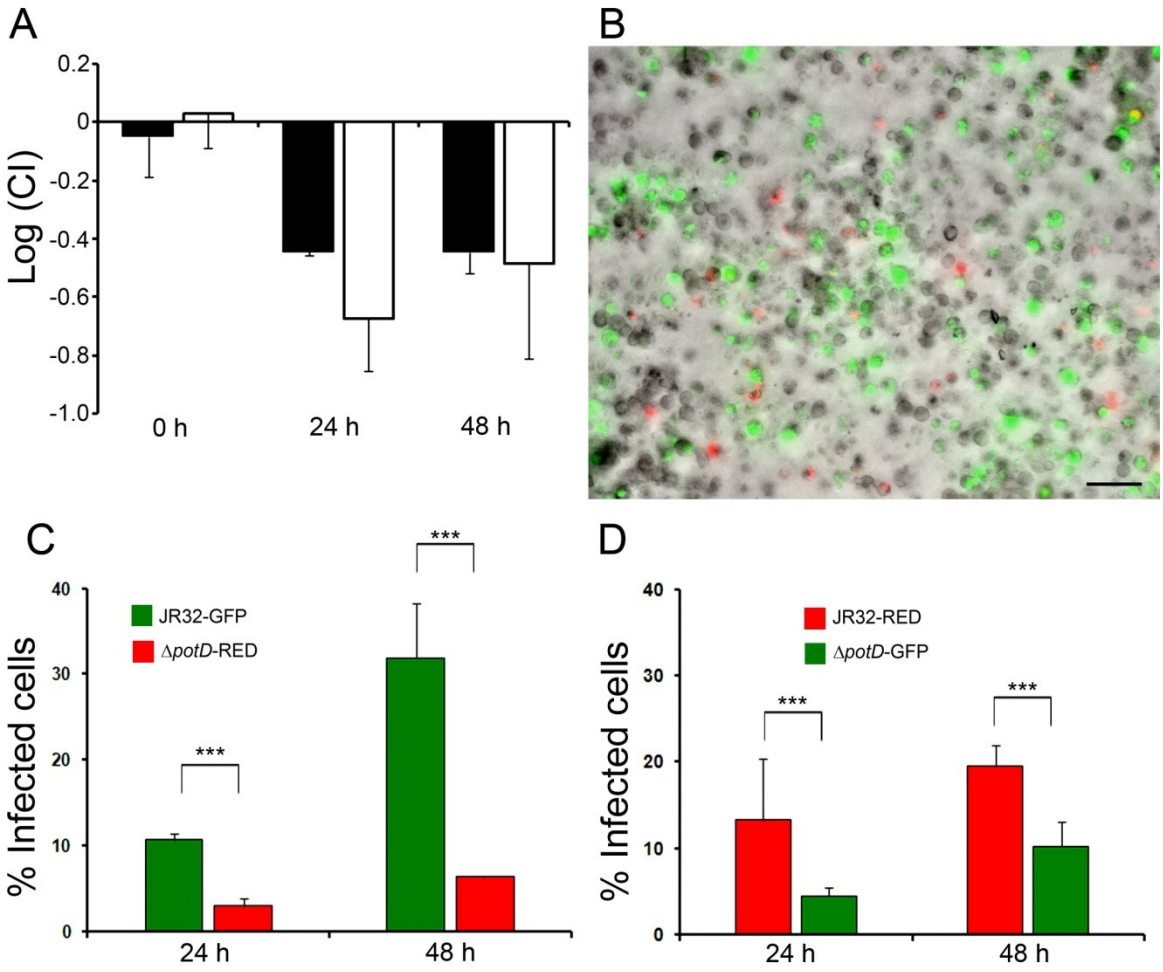

Figure 33. The *L. pneumophila* Δ*potD* mutant is unable to compete with the JR32 parent strain during intracellular growth.

(A) U937 macrophages were infected with a 1:1 mixture of JR32-GFP and Δ*potD*-RED strains (black bars) or a 1:1 mixture of JR32-RED and Δ*potD*-GFP strains (white bars), and the number of CFU/well was calculated at different times by dilution-plating. The competitive index (CI) of the mutant in relation to the parental strain was calculated at the time points indicated as described in Section 2.4.13. The negative CI values indicate poor competition by the Δ*potD* mutant. **(B)** Light micrograph captured 48 h after infection of U937 macrophages with a 1:1 mixture of JR32-GFP and Δ*potD*-RED strains. Colors of infected cells are as follows; green: cells infected only with JR32-GFP, red:

cells infected only with Δ*potD*-RED, yellow: cells infected with both JR32-GFP and Δ*potD*-RED, gray: uninfected cells. Size bar represents 50 μm. **(C)** Quantitative fluorescence microscopy results of U937 macrophages infected with a 1:1 mixture of JR32-GFP and Δ*potD*-RED (panel **C**) or a 1:1 mixture of JR32-RED and Δ*potD*-GFP (panel **D**). Green bars represent the percentage of U937 macrophages infected with bacteria expressing GFP. Red bars: represent the percentage of U937 macrophages infected with bacteria expressing Ds-Red. Results represent the mean + one standard deviation for 3 independent experiments (n = 3), each done in quadruplicate. The statistical significance of differences is indicated as *** $P<0.001$. This figure was generated by Gheyath Nasrallah.

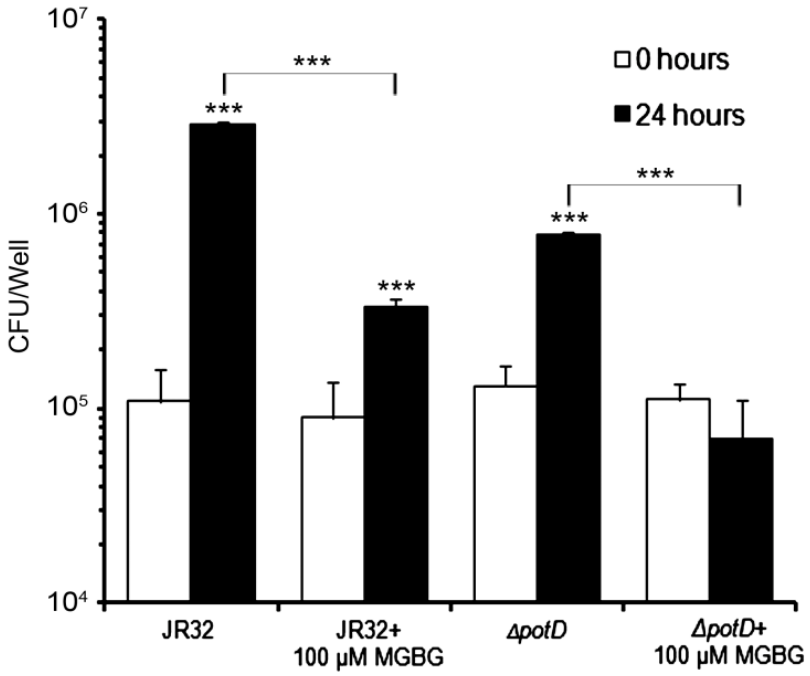

Figure 34. Pharmacological inhibition of SAMDC activity in L929 cells abolishes the intracellular growth of Δ*potD* mutant.

L929 cells treated or not treated with 100 µM MGBG were infected with the parent strain JR32 or the mutant strain Δ*potD*. Intracellular growth was measured by dilution-plating *Legionella* and is expressed as CFU/well at two time points (0 and 24 h). Results are shown as mean CFU+ one standard deviation for 3 independent experiments, each run in quadruplicate ($n = 3$). Asterisks above black bars (CFU/well at 24 h) indicate significance in relation to the 0 h CFU/well value (corresponding white bars). Asterisks above square brackets indicate significance of the differences between MGBG-treated and untreated cells at 24 h. This figure was generated by Gheyath Nasrallah.

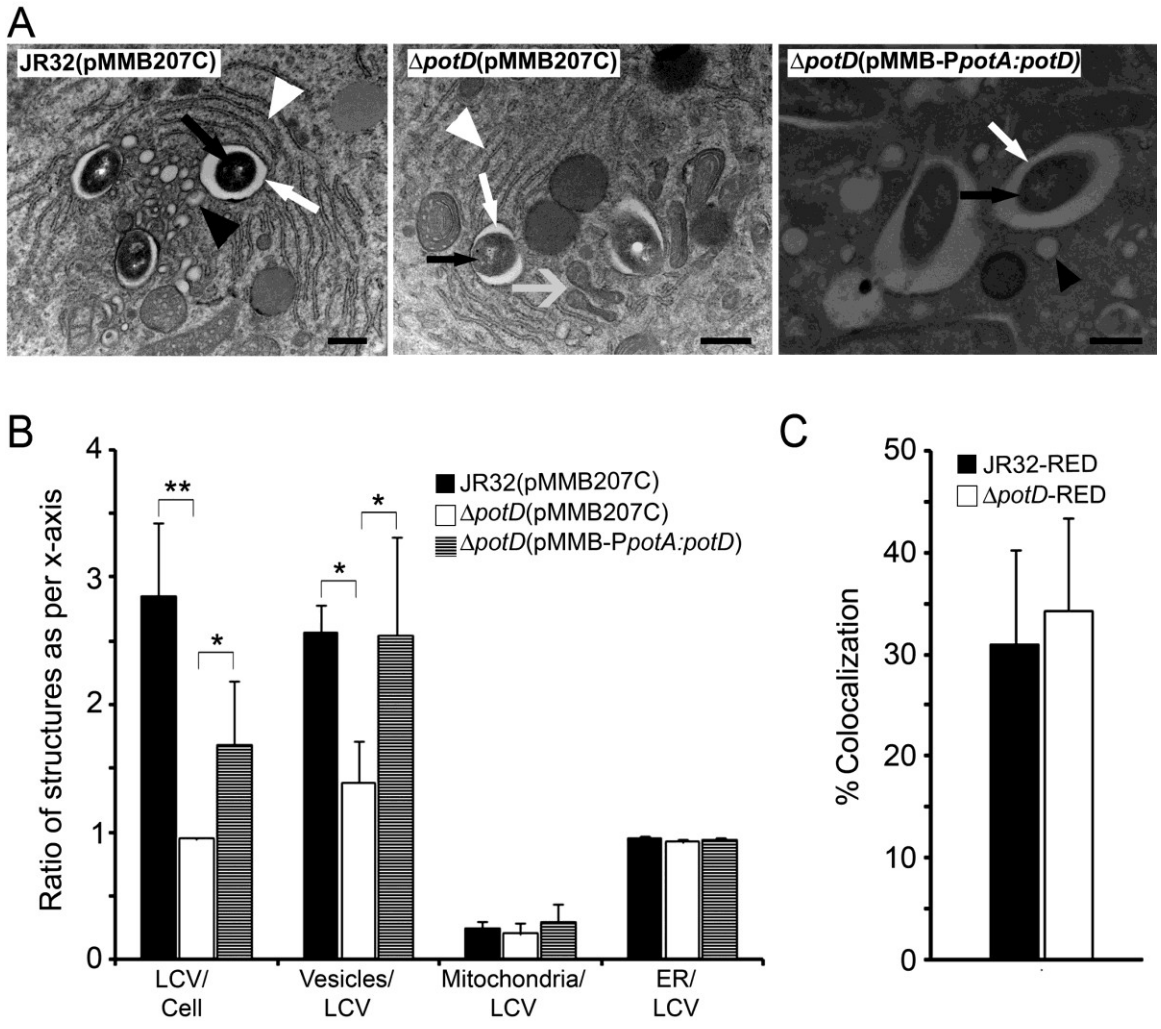

Figure 35. Deletion of *potD* reduces recruitment of vesicles by LCVs.

(A) Transmission electron micrographs of U937 macrophages infected for 8 h with *L. pneumophila* parent JR32(pMMB207C), mutant Δ*potD*(pMMB207C), or complemented Δ*potD*(pMMB-P$_{potA}$:*potD*) strains. Black arrows indicate sectioned bacteria, white arrows indicate LCVs, black arrowheads indicate ER-derived vesicles, white arrow heads indicate ER, and the gray large arrow indicates mitochondria. Size bars represent 500 nm. **(B)** Quantitative electron microscopy analysis of macrophages infected as described in panel **A**. Infected U937 macrophages were examined to determine the number of LCVs

per cell, and each LCV was examined to determine the number of associated mitochondria and vesicles, and the presence or absence of ER. Sections obtained from two different experiments were examined for each condition. The statistical significance of differences was determined on data obtained from ~100 macrophages. * $P<0.05$, ** $P<0.01$. **(C)** Quantitative immunofluorescence microscopy analysis of phagosome-lysosome colocalization in U937 macrophages infected for 8 hours with *L. pneumophila*parent J32-RED, or mutant Δ*potD*-RED strain, and immunostained for the lysosomal marker LAMP-1 (green). Results are shown as % localization of red bacteria with green lysosomes, and were obtained from ~100 randomly selected infected U937 cells per condition. This figure was generated by Gheyath Nasrallah.

CHAPTER 6: DISCUSSION

As previously explained (Chapter 1, Section 1.3.5), the multiple functions observed for HtpB and the fact that some of these functions are related to virulence, proved an involvement of HtpB in *L. pneumophila* pathogenesis *in vivo*, and opened an experimental need to identify host protein targets for HtpB. In fact, in chapter 4, we showed that HtpB interacts with SAMDC and proposed that through this interaction HtpB could function as a cytoplasmic effector that helps *L. pneumophila* to achieve optimal intracellular growth, particularly in the early stages of cell infection. This finding adds to the previously reported virulence-related functions of HtpB, i.e. as an invasion factor (139) and as a factor that recruits mitochondria to the LCV (65). In Chapter 3, I demonstrated that the *htpAB* operon is essential in *L. pneumophila*, strongly suggesting that HtpB must fulfill a protein folding function that cannot be compensated for by GroEL. Therefore, if HtpB functions as a protein folding chaperonin in the cytoplasm of *L. pneumophila*, but displays virulence-related functions when is expressed on the bacterial cell surface or when it reaches the cytoplasm of infected cells, HtpB could be regarded as a moonlighting protein. In the next few sections of this general Discussion, I will discuss the functional diversity of bacterial chaperonins and will introduce the concept of moonlighting proteins, which will help me discuss the multifunctional nature of HtpB in the context of its location in the bacterial and the host cell (compartmentalization).

6.1. Functional Diversity of Group I Chaperonin

In spite of the high amino acid sequence similarity that exists between bacterial chaperonins, we and others (65) showed that HtpB is capable of performing unique roles that are not shared by the *E. coli* protein GroEL. These roles (summarized in Table 5) are not necessarily related to protein folding. The fact that we could not delete the *htpAB* operon from the LpgroE+ genome and that the cloned *htpAB* operon was unable to complement a *groEL* temperature-sensitive mutation in *E. coli* (177) indicates that the differences in the amino acid sequences that exist between these chaperonins provide them with specific functions within their respective host. It is now evident that, in addition to their essential function in protein folding, group I chaperonins perform other functions. For instance, in many rhizobiae and nodulating bacteria such as *Sinorhizobium meliloti,* group I chaperonins have been found to perform functions related *to* root-nodulation and nitrogen-fixation (264). In photosynthetic bacteria, such as *Cyanobacteria,* chaperonins perform functions related to photosynthesis (11). Moreover, chaperonins from bacterial pathogens can function as cell-signalling molecules stimulating human monocytes, leukocytes, fibroblasts and epithelial cells to release pro-inflammatory cytokines (269,446).

It is believed that group I chaperonins have evolved through the accumulation of mutations that led to changes in amino acid sequence. Support for this view comes from the unique functions of bacterial chaperonins that have been attributed to the effect of a few amino acid changes. Yoshida et al. (440) showed that the GroEL from endosymbiotic *Enterobacter aerogenes* acts as an insect toxin. This toxic GroEL differs from the non-toxic GroEL from *E. coli* by eleven amino acids, four of which are critical for insect

toxicity. In fact, the *E. coli* GroEL also becomes an insect toxin when these four critical residues are engineered to resemble the *E. aerogenes* GroEL. Additionally, it has been shown that the GroEL of *M. leprae* contains three amino acids (Thr-375, Lys-409 and Ser-502), not found in *E. coli* GroEL, which form a threonine catalytic group responsible for protease activity (326). Similarly, it can be hypothesized that the DNA sequence of *htpB,* encoding amino acids that are not necessary for the essential function of HtpB, would be allowed to evolve under less selective constraints, leading to the acquisition of novel functions. These new function(s) of HtpB might have allowed *L. pneumophila* to adapt to the intracellular environment of its hosts.

Based on a bioinformatic analysis of 669 bacterial genome sequences, Lund (264) found that 30 % of the studied bacterial genomes contained two to seven chaperonin genes. To this end, the author suggested that functional diversity of group I chaperonins depends on the presence of multiple chaperonin genes within a particular bacterial genome. In this view, the essential protein folding needs of a bacterial cell are met by a single chaperonin whose gene would be restricted for change by mutation(s), whereas the duplicated chaperonin gene(s) would be free to mutate and acquire functional specializations that are not necessarily related to protein folding. The most spectacular example of multiple chaperonin genes, in terms of number, is *Bradyrhizobium japonicum which has* seven copies of *cpn60* (264). A good convincing example for a high degree of specialization in the functions of multiple chaperonin genes is found in *M. tuberculosis*. The genome of *M. tuberculosis* has two genes encoding the chaperonins Cpn60.1 and Cpn60.2. Despite Cpn60.1 and Cpn60.2 sharing 61 % sequence identity, there are major differences in the cellular actions of these chaperonins (53). *cpn60.1* can be deleted from

the genome whereas *cpn60.2* is essential (195). The inability to delete *cpn60.2*, suggests that its gene product is the chaperonin responsible for the essential protein-folding function, whereas Cpn60.1 has acquired protein folding-independent functions such as inducing the formation of multinucleated giant cells (as it happens during formation tuberculous granulomas), and binding to monocyte cell surface receptors to trigger immune responses (53). In fact, a *M. tuberculosis* mutant lacking *cpn60.1* is viable but fails to induce an inflammatory response in animal models of infection (195,264,301).

There are other cases in which functional diversity rests on a single chaperonin. One of these cases, as shown in this study, is the chaperonin of *L. pneumophila*, HtpB. In other pathogenic bacteria with a single chaperonin, it has been reported that the surface- and membrane-associated chaperonin performs diverse functions related to bacterial virulence and host response to bacterial infection. Similar to HtpB, the extracytoplasmically localized chaperonins of *Salmonella enterica* sv. Typhimurium (94), *Haemophilus ducreyi* (124), *Helicobacter pylori* (47,437), *Borrelia burgdorferi* (367), and *Clostridium difficile* (167) have been implicated in adhesion and(or) cell invasion. Additionally, it has been shown that some surface-exposed bacterial chaperonins have the capacity to interact with cell surface receptors of a variety of mammalian cell types, to initiate signalling events that result in strong cytokine production and other immunological responses (269,446), thus these chaperonins are considered as immunodominant antigens (230,441). In these cases of bacteria with a single chaperonin, it seems that the diversity of chaperonin functions depends on cellular location, as we have determined for HtpB. To this end, chaperonins have been recently added to the list of "moonlighting" proteins (209). The term moonlighting is defined by the Webster's

Dictionary as “working at another job in addition to one’s regular job”, and was introduced in the biochemical field to describe those proteins that perform different functions in different environments or at different cellular locations (209). According to this definition, HtpB would be a chaperonin that moonlights as a virulence effector that interacts with host cell surface receptors, reaches the cytoplasm of infected cells and modulates the levels of polyamines by interacting with SAMDC. The known or hypothetical functions of HtpB, according to its location, are summarized in Table 5, and discussed in the following Section.

6.2. Moonlighting Functions of HtpB According to Its Location

Table 5. The confirmed and hypothesized function(s) of HtpB based on its cellular location.

HtpB cellular location	Hypothetical* or confirmed function(s)[#]
Bacterial cytoplasm	- *protein folding (based on essentiality)*(65) - induction of bacterial filamentation phenotype (4)
Bacterial cytoplasmic membrane	- *stabilization of the bacterial cytoplasmic membrane by acting as lipochaperonin* (413)
Bacterial periplasm	- Unknown
Bacterial surface	- attachment and invasion of HeLa cells (139) - induction of cytokine production by macrophages (340)
LCV^{+} lumen	- *The compartment from where HtpB reaches the cytoplasmic face of the LCV and the cytoplasm of infected cells* (295)
Phagosome containing HtpB-coated microbeads	- transiently delays fusion of the microbeads with the lysosomes (65) - recruitment of mitochondria to the microbeads (65), *via interaction with the mitochondrial Hsp10* (Chapter 4) - alteration of actin cytoskeleton of infected cells (65)
LCV membrane	- *functions similar to those seen with the HtpB-coated bead*
Yeast cytoplasm	- interaction with SAMDC (295) (Chapter 4). - *the interaction with SAMDC increases the level of intracellular polyamines* (Chapter 4). - induction of yeast pseudohyphal growth (63,295,341).
Host cell cytoplasm	- alteration of actin cytoskeleton - Interaction with the mitochondrial Hsp10 (Chapter 4) - Interaction with the host SAMDC, *which leads to an increase in the level of intracellular polyamines* (295) that are important for optimal intracellular growth (295) (Chapter 4)

* *Italic font* indicates hypothetical functions. [#] Regular font indicates confirmed functions. +LCV: *Legionella*-containing vacuole

Because no structural or biochemical studies have yet been performed on HtpB to determine its capability to form 14-mer barrels (see Section 1.3.1 in Chapter 1), or fold proteins, the exact function of the cytoplasmic HtpB is still unknown. However, because HtpB is essential, and has 85% amino acid sequence similarity to GroEL, and is the sole chaperonin encoded in the *L. pneumophila* genome, one would expect that cytoplasmic HtpB in *L. pneumophila* functions in protein folding, just as do other GroEL family proteins. In addition to the hypothesized function of cytoplasmic HtpB in protein folding, David Allan (4) identified HtpB as the first *L. pneumophila* cytoplasmic protein directly involved in filamentation. He showed that overexpression of HtpB in *L. pneumophila* or in *E. coli* induces filamentation (4). The formation of long filaments by *L. pneumophila* (a form of bacterial differentiation) is well documented, and filamentation has been previously linked to the ability of *L. pneumophila* to survive in harsh environments and in biofilms (322). The mechanism by which HtpB induces bacterial filamentation needs to be explored. According to these findings, we conclude that the cytoplasmic HtpB in *L. pneumophila* is essential for protein folding and plays a role in filamentation.

About 40 % of the total cytoplasmic HtpB is found associated with the cytoplasmic membrane of *L. pneumophila* (137) but its function in this location is unknown. However, Török et al. (413) showed that membrane-bound *E. coli* GroEL interacts with phospholipids and can function as a lipochaperonin, whereby GroEL association with phospholipids can stabilize membranes under heat shock conditions. Similarly, as the major cytoplasmic membrane protein (126,137), we propose that HtpB could also fulfil a lipochaperonin function.

Surface-exposed HtpB enhances bacterial attachment to, and invasion of HeLa cells (139). HtpB is capable of interacting with cell surface receptors on macrophages, as HtpB-coated microbeads were shown to activate both the Protein kinase C signalling pathway and IL-1 production in human macrophages (340). Therefore, surface exposed HtpB is capable of interacting with host cell surface receptors to trigger internalization or immunological responses (136).

After internalization of *L. pneumophila* by host cells, HtpB continues to be abundantly produced and released into the LCV, and may thus have post-invasion functions (137). The function of HtpB in the LCV lumen is not yet defined, but it is possible that HtpB reaches the cytoplasm of host cells from this compartment (either free in the cytosol, or bound to the LCV membrane). In a recent study (65), we used two functional models (protein-coated beads and expression of recombinant HtpB in CHO cells) to investigate the competence of HtpB in mimicking early intracellular trafficking events of *L. pneumophila* in the LCV. We found that microbeads coated with purified HtpB (but not uncoated microbeads or microbeads coated with the *E. coli* GroEL) were sufficient to: (i) transiently delay fusion of beads with lysosomes, (ii) attract mitochondria, and (iii) modify the organization of actin microfilaments in human U937 macrophages and CHO cells. These three post-internalization events typify the early trafficking of the LCV (65).The mechanism by which HtpB attracts mitochondria in the context of coated microbeads is not yet understood, but immunogold electron microscopy has provided insights. Chong (62) showed, using immunogold electron microscopy, that HtpB is localized to the cytoplasmic face of the LCV of infected macrophages. She suggested that HtpB may have the ability to interact with host components that might

impact LCV trafficking. Indeed, in this study, using Y2H, we showed that HtpB can interact with the host mitochondrial co-chaperonin Hsp10. The HtpB-Hsp10 interactions could be relevant to the recruitment of mitochondria to the LCV. Hsp10 has been detected on the surface of mitochondria (354), therefore, it is possible that the HtpB that localizes to the LCV attracts mitochondria by interaction with the Hsp10 that resides on the mitochondrial surface. Further investigations are needed to confirm this hypothesis.

One of the prominent findings of this study was the delivery of HtpB from the LCV into the cytoplasm of CHO cells and human macrophages, which suggests that HtpB may have the ability to interact with host components that impact *L. pneumophila* intracellular establishment. The yeast model was used in this study to uncover potential functions of HtpB in the cytoplasm of host cells. We found that expression of HtpB in *S. cerevisiae* induces pseudohyphal growth (PHG). To explore the mechanism by which HtpB induces PHG, we performed a yeast two-hybrid (Y2H) screen. The Y2H screen showed that HtpB interacts with SAMDC, an essential yeast enzyme, encoded by *SPE2* that is required for polyamine biosynthesis in all eukaryotic cells. The fact that overexpression of SAMDC also induced PHG in *S. cerevisiae*, clearly linked polyamines with HtpB. This was particularly meaningful since a strong correlation exists between elevated polyamine levels and filamentation in a number of fungal species (152,168,201,277,358)**.** In addition, the-HtpB-SAMDC interaction and the link to polyamines could be relevant to the observation that HtpB modifies the organization of actin microfilaments of infected host cells (65), because many reports indicate that polyamines influence cytoskeleton organization (92,148,149,153,333,334). Therefore, I predicted that yeast cells expressing HtpB would have elevated levels of spermidine and spermine. Analytical determination

[using high performance liquid chromatography (HPLC)] of the levels of polyamines in these yeast cells could validate this prediction. To explain the mechanism by which HtpB induces PHG in yeast, we proposed the following model (illustrated in Fig. 36). SAMDC is a rate-limiting enzyme key in the biosynthesis of polyamines, which is tightly regulated in eukaryotic cells (320). Like other rate-limiting enzymes, SAMDC has a short half-life, its basal activity is low, and it is rapidly induced by different stimuli (316,318,320). Furthermore, SAMDC is synthesized as an inactive proenzyme that in response to different stimuli undergoes an intramolecular cleavage reaction to form the active enzyme (226,319,320). Thus, it is possible that one or more of the processes that affect the activity of SAMDC could be modulated upon interaction with HtpB, leading to increase activity of SAMDC, which in turn results in an increase in the amount of intracellular polyamines (required for triggering PHG).

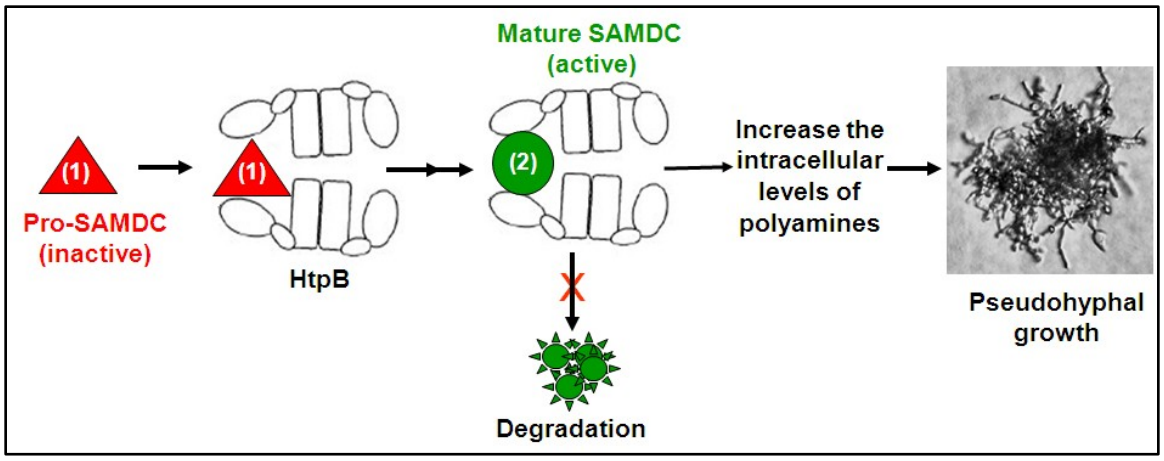

Figure 36. Model illustrating the potential consequences of the interaction of HtpB with SAMDC. We propose that HtpB induces pseudohyphal growth through enhancing SAMDC activity. SAMDC is synthesized as an inactive proenzyme **(1)** that undergoes intramolecular cleavage to form the active enzyme **(2)**. The interaction of SAMDC with HtpB could have a number of consequences. Because of its protein folding activity, HtpB could simply enhance the proper folding of SAMDC proenzyme which in turn could accelerate its rate of cleavage into active SAMDC. Alternatively, the interaction of active SAMDC with HtpB could extend its half-life by preventing its degradation. Finally, HtpB could increase the enzymatic activity of active SAMDC. This model assumes that the HtpB-bound SAMDC is still capable of interacting with its substrate. Any of these potential scenarios could lead to an increase in the level of intracellular polyamines that are important for induction of pseudohyphal growth in *S. cerevisiae.* This figure was generated by Gheyath Nasrallah.

Based on the findings of the yeast model, we also proposed that polyamines are important for the intracellular growth of *L. pneumophila*. Indeed, it turned out that inhibition of polyamine synthesis in host cells significantly reduced *L. pneumophila* replication in host cells, whereas addition of exogenous polyamines enhanced *L. pneumophila* replication (Fig. 21 and Section 4.3.9). Because *L. pneumophila* lacks most known enzymes required for polyamine biosynthesis, one would expect that *L. pneumophila* depends upon transport of exogenous polyamines from the host cell cytoplasm into the LCV to meet its needs. This led us to the second most relevant finding from my work, that the polyamine binding protein PotD might play a role not only in spermidine transport, but also as a factor required for optimal intracellular growth of *L. pneumophila*. The main conclusion that we drew from this study is that polyamines enhance *L. pneumophila* growth *in vitro* and *in vivo*. To our knowledge, this is the first report in the field of *L. pneumophila* biology showing that polyamines are enhancers of the intra- and extracellular growth of *L. pneumophila*.

Although the role of polyamines in bacterial growth and differentiation is very well documented in the literature, the exact molecular mechanisms by which these molecules act as enhancers for bacterial growth is poorly understood. Similarly, we were not able to determine the mechanism by which polyamines enhance *L. pneumophila* growth. However, we proposed a mechanistic model (Fig. 37) based on the PotABCD (P_{PotA}) promoter activity and the phenotype associated with the Δ*potD* mutant. In *vitro,* we found that P_{PotA} promoter activity is increased in RFs (Fig 25), and that PotD is important for *L. pneumophila* filamentation (Fig. 27). However, deletion of *potD* did not affect *L. pneumophila* growth in polyamine rich medium, whereas, *in vivo*, the Δ*potD*

mutant was unable to grow in host cells to the same level of the parent strain (particularly during the first 24 hours of infection) (Fig. 31). In addition, the Δ*potD* mutant was unable to efficiently mediate recruitment of vesicles to the LCV. Based on these findings, we propose that in a polyamine limited environment, such as the LCV, PotD is required for efficient polyamine transport from the LCV lumen into the bacterial cells. These polyamines are important for bacterial differentiation [from transmissive form (TF) into replicative form (RF)], and for recruitment of vesicles to the LCV. The recruitment of vesicles to the LCV could be very meaningful because these vesicles could deliver nutrients to the LCV, which in turn could enhance bacterial growth. Collectively, our findings have contributed to a better understanding of the biology of *L. pneumophila* by suggesting that HtpB and PotD might collaborate to ensure a supply of polyamines required for the optimal intracellular growth of *L. pneumophila.*

6.3. An Integrated Functional Model of HtpB and Polyamines in the Host Cell

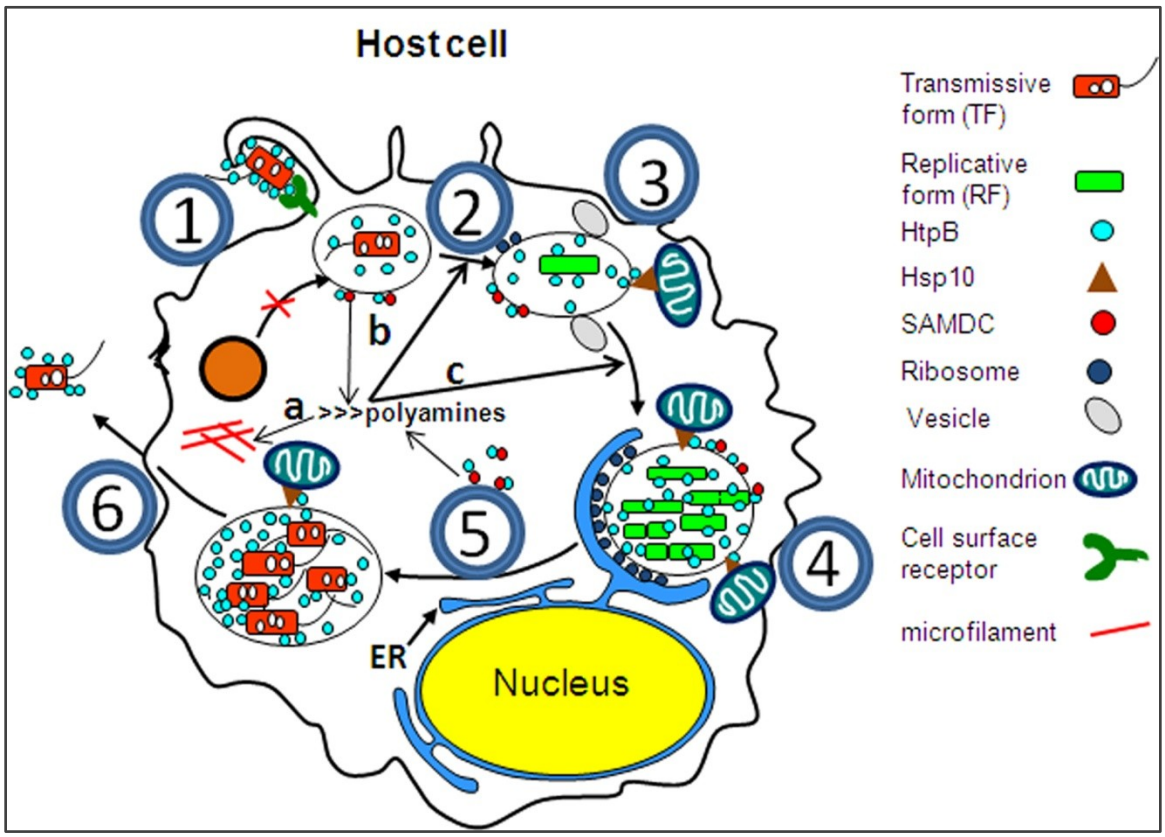

Figure 37. An integrated functional model of HtpB and polyamines in the host cell.

1. The surface-exposed HtpB mediates internalization of TF, through the interaction with host cell surface receptors. **2.** HtpB delays fusion of the LCV with lysosomes and is released into the LCV from which it reaches the cytoplasm of the host cell (either free in the cytosol, or bound to the LCV membrane). HtpB in the cytoplasm of the host cell interacts with host SAMDC, leading to an increase in the intracellular pool of polyamines, which might trigger a reorganization of microfilaments **(a)**. **3.** HtpB, as a protein bound to the cytoplasmic face of LCV, attracts mitochondria, possibly through an interaction with Hsp10. The spermidine binding protein PotD (or the polyamine transporter PotABCD) facilitates the recruitment of vesicles hypothesized to carry nutrients to the LCV. The presence of nutrients, including polyamines, triggers *L.*

pneumophila differentiation from TF into RF **(b)**. **4.** The RF replicates. During replication, *L. pneumophila* secretes HtpB, which accumulates in the LCV. Consequently the amount of HtpB bound to the cytoplasmic face of LCV and in the host cell cytoplasm increases, which in turn leads to a further increase in the intracellular pool of polyamines. Polyamines are then used for the optimal intracellular replication of *L. pneumophila* **(c). 5.** When nutrients become limited, RFs differentiate into TFs. **6.** TFs are released from the lysed host cell to start new infection cycle. This figure was generated by Gheyath Nasrallah.

6.4. Future Directions

6.4.1. Does the Dot/Icm System Mediate HtpB Release into the Cytoplasm of Infected cells?

Immunolocalization studies done in our laboratory showed that in *E. coli,* GroEL and recombinant HtpB are located in the cytoplasm (137). In contrast, both HtpB and recombinant GroEL can be found on the bacterial cell surface (4,137). Based on these observations, it is proposed that *L. pneumophila* must have a mechanism that is not present in *E. coli*, which permits the translocation of HtpB to extracytoplasmic locations including the bacterial cell surface (4). Experimental approaches including osmotic shock, protease-sensitivity, immunoblotting, and immunogold electron microscopy have indicated that about 1% of the total cell-associated HtpB is present in the periplasm of *L. pneumophila* (David Allan unpublished results). These unpublished results also suggested that surface localization of HtpB requires a functional Dot/Icm system since a mutation in *dot/icm* (Δ*dotA* or Δ*dotB*) led to accumulation of HtpB in the periplasm and the absence of HtpB from the cell surface of *L. pneumophila* (4,63). Additionally, it was reported that *dotA* and *dotB* mutants were unable to attract mitochondria to the LCV in CHO cells (65). In Chapter 4, using the CyaA reporter assay (a widely used assay to study translocation of Dot/Icm substrates from the LCV lumen into the cytoplasm of infected cells), we showed that a portion of the abundantly released HtpB in the LCV lumen reaches the cytoplasm of infected CHO cells and U937 macrophages. However, the mechanism by which HtpB reaches the cytoplasm of infected cells remains uncertain. It is tempting to speculate that HtpB is released into the cytoplasm of infected cells by the Dot/Icm system. This hypothesis can be tested by comparing the level of cAMP in mammalian cells infected with a *L. pneumophila dot/icm* mutant expressing the HtpB-

CyaA fusion protein, with that in cells infected with the parental strain expressing the same fusion protein. If the cAMP level in the cells infected with the parental strain is higher than that in cells infected with the *dot/icm* mutant, then it can be concluded that HtpB translocation requires a functional Dot/Icm system.

6.4.2. Is SAMDC a Target of HtpB in Mammalian Cells?

It was surprising that in spite of screening ~5 x 10^6 yeast clones of the HeLa cDNA library, SAMDC was not identified as prey for HtpB during the Y2H screen. In theory, our Y2H screen should be sufficient to cover 250X the estimated 2 x 10^4 protein-encoding mRNAs present in the human genome. Therefore, it can be concluded that, despite the many advantages of the Y2H system, it also has limitations [reviewed in (115,116)]. The failure in identifying SAMDC as prey for HtpB could be due to one or several of the following reasons: (i) the fusion proteins in the Y2H system must be targeted to the nucleus to activate the Gal4 transcription factor in order to activate the expression of reporter genes. The complex of mammalian SAMDC fused to Gal4AD and HtpB fused to Gal4BD may not be able to enter the nucleus to activate the reporter genes. (ii) SAMDC is expressed as proenzyme and undergoes post-translational modification to become an active enzyme. The SAMDC-HtpB interaction may thus depend upon posttranslational modifications of the human SAMDC that do not occur in yeast. (iii) The mammalian SAMDC fused to Gal4AD is unable to interact with HtpB fused to Gal4BD. (iv) SAMDC cDNA is not represented in the MATCHMAKER HeLa cDNA library. To overcome this last obstacle, we could have cloned the cDNA of the mammalian SAMDC into the Gal4AD Y2H vector and test it against our Gal4BD-HtpB bait for interaction.

Alternatively, instead of Y2H, we could have used biochemical methods such as co-immunoprecipitation (co-IP) to determine if mammalian SAMDC interacts with HtpB. In co-IP, crude cell lysates from L929 cells, U937-macrophages, or amoebae can be mixed with a purified HtpB. Subsequently, the proteins that interact with HtpB can be precipitated using latex beads coated with α-HtpB antibody. The presence of SAMDC in the precipitate could be confirmed by Western blotting using α-SAMDC antibody (commercially available).

We have hypothesized that HtpB may function to ensure a supply of polyamines in host cells via interaction with SAMDC (Chapter 4). This hypothesis could have been confirmed by measuring (using HPLC) the intracellular levels of polyamines in CHO-*htpB* cells induced to express HtpB (in the presence of doxycyclin), in relation to uninduced CHO-*htpB* cells (in the absence of doxycyclin). Higher levels of intracellular polyamines in CHO-*htpB* cells compared to parental CHO cells could provide indirect evidence that SAMDC is the mammalian target of HtpB, and further suggest that the reorganization of host cell actin filaments induced by HtpB might be mediated by high levels of intracellular polyamines.

6.4.3. Are HtpB-Directed Phenotypes Induced by Specific Amino Acid Domains of HtpB?

Despite the high degree of amino acid similarity between HtpB and *E. coli* GroEL (85%) (178), HtpB is capable of inducing phenotypes in *L. pneumophila* that GroEL cannot. We now know that HtpB, but not the *E. coli* GroEL, induces: PHG in yeast (Chapter 4), filamentation in Gram negative bacteria (4), and actin reorganization and mitochondrial recruitment in mammalian cells (65). This implies that the 15 % of the

amino acids that are different between GroEL and HtpB (or some portion of them) are responsible for these phenotypical differences. The observations that HtpB, but not GroEL, has the ability to induce PHG, and that the activity of SAMDC is important in induction of PHG, suggest that SAMDC is unable to interact with GroEL. Further experiments such as Y2H (using GroEL as a bait and SAMDC as a prey), or co-IP (using purified GroEL and yeast whole cell lysates) could be done to test this hypothesis. If SAMDC does not interact with GroEL, it can be concluded that specific amino acid residues within functional domains present in HtpB but not in GroEL are required for interaction with SAMDC, and thus these residues might be key factors required for induction of PHG. To identify the HtpB domains that contain key amino acids important for functional differences with GroEL, I suggest to do a series of domain swaps with GroEL, to generate protein chimeras. The phenotypes of the resulting chimeric proteins could be assessed by testing their ability to interact with *S. cerevisiae* (SAMDC), and (or) by testing their ability to induce some of the other identified HtpB-mediated phenotypes. Once the HtpB protein domain(s) important for particular HtpB-mediated phenotypes are identified, the corresponding region of *htpB* could be specifically mutagenized, and tested for functional competence as explained above.

6.4.4. Does PotD Function As a Polyamine Binding Protein?

The bioinformatic results presented in Chapter 5 suggest that *L. pneumophila* PotD binds spermidine and could potentially have the same affinity to putrescine as has the *E. coli* PotD. This finding could be confirmed by growing the Δ*potD* mutant and its parent strain in SD medium in the presence or absence of polyamines, followed by

measuring (using HPLC) the intracellular levels of polyamines of both strains. If PotABCD functions as a polyamine transporter, the intracellular levels of polyamines of the Δ*potD* mutant should be lower when compared to those found in the parent.

6.5. Conclusions

The work represented in this thesis reveals functions of HtpB that are potentially important for adaptation of *L. pneumophila* to intracellular environments. We showed that the chaperonin of *L. pneumophila* is essential for *Legionella* survival, likely because of its essential function in protein folding. A particularly significant finding presented in this thesis is the delivery of HtpB from the LCV into the cytoplasm of human macrophages, which suggests that HtpB may have the ability to interact with host components that have impact upon LCV trafficking and *L. pneumophila* intracellular establishment. Using the yeast two-hybrid assay, we showed that HtpB interacts with the mitochondrial Hsp10, which could be relevant to mitochondrial attraction and LCV trafficking. Using the same method, this study showed that HtpB interacts with a key enzyme required for polyamine synthesis in eukaryotic cells (SAMDC). This interaction might be of fundamental importance to *L. pneumophila* pathogenesis, because inhibition of SAMDC activity (and presumably polyamine synthesis) inhibits *L. pneumophila* growth, whereas addition of exogenous polyamines favours intracellular growth. *L. pneumophila* might be faced with nutrient limitations (including lack of polyamines) at early stages of macrophage and protozoan infection. Although it seems that PotABCD is not the only polyamine transporter that *L. pneumophila* utilizes, it still appears to be important for *L. pneumophila* as disruption of PotABCD function by deletion of *potD*

reduces the intracellular growth of *L. pneumophila* in a variety of host cells. The major findings in this study can be summarized as the characterization of two *L. pneumophila* proteins (HtpB and PotD) that might contribute to satisfy the requirement of polyamines for the optimal intracellular growth of *L. pneumophila*. Finally, this study constitutes a good example of how the yeast functional model has enabled us to uncover unique functions of HtpB and a novel aspect of chaperonin biology.

REFERENCE LIST

1. **Abu Kwaik, Y.** 1996. The phagosome containing *Legionella pneumophila* within the protozoan Hartmannella vermiformis is surrounded by the rough endoplasmic reticulum. Appl.Environ.Microbiol. **62**:2022-2028.

2. **Akira, S. and K. Takeda**. 2004. Toll-like receptor signalling. Nat.Rev.Immunol. **4**:499-511.

3. **Alam, K., F. L. Arlow, C. K. Ma, and T. T. Schubert**. 1994. Decrease in ornithine decarboxylase activity after eradication of Helicobacter pylori. Am.J.Gastroenterol. **89**:888-893.

4. **Allan, D. S.** 2002. Secretion of Hsp60 chaperonin (GroEL) homologs by *Legionella pneumophila*. MSc Thesis. Dalhousie University, Nova Scotia, Canada.

5. **Allard, K. A., J. Dao, P. Sanjeevaiah, K. McCoy-Simandle, C. H. Chatfield, D. S. Crumrine, D. Castignetti, and N. P. Cianciotto**. 2009. Purification of Legiobactin and importance of this siderophore in lung infection by *Legionella pneumophila*. Infect.Immun. **77**:2887-2895.

6. **Alleron, L., N. Merlet, C. Lacombe, and J. Frere**. 2008. Long-term survival of *Legionella pneumophila* in the viable but nonculturable state after monochloramine treatment. Curr.Microbiol. **57**:497-502.

7. **Alli, O. A., L. Y. Gao, L. L. Pedersen, S. Zink, M. Radulic, M. Doric, and K. Y. Abu**. 2000. Temporal pore formation-mediated egress from macrophages and alveolar epithelial cells by *Legionella pneumophila*. Infect.Immun. **68**:6431-6440.

8. **Altschul, S. F., T. L. Madden, A. A. Schaffer, J. Zhang, Z. Zhang, W. Miller, and D. J. Lipman**. 1997. Gapped BLAST and PSI-BLAST: a new generation of protein database search programs. Nucleic Acids Res. **25**:3389-3402.

9. **Antognoni, F., D. S. Del, A. Kuraishi, E. Kawabe, T. Fukuchi-Shimogori, K. Kashiwagi, and K. Igarashi**. 1999. Transcriptional inhibition of the operon for the spermidine uptake system by the substrate-binding protein PotD. J.Biol.Chem. **274**:1942-1948.

10. **Arsene, F., T. Tomoyasu, and B. Bukau**. 2000. The heat shock response of Escherichia coli. Int.J.Food Microbiol. **55**:3-9.

11. **Asadulghani, Y. Suzuki, and H. Nakamoto**. 2003. Light plays a key role in the modulation of heat shock response in the cyanobacterium *Synechocystis sp* PCC 6803. Biochem.Biophys.Res.Commun. **306**:872-879.

12. **Auvinen, M., A. Laine, A. Paasinen-Sohns, A. Kangas, L. Kangas, O. Saksela, L. C. Andersson, and E. Holtta**. 1997. Human ornithine decarboxylase-overproducing NIH3T3 cells induce rapidly growing, highly vascularized tumors in nude mice. Cancer Res. **57**:3016-3025.

13. **Auvinen, M., A. Paasinen, L. C. Andersson, and E. Holtta**. 1992. Ornithine decarboxylase activity is critical for cell transformation. Nature **360**:355-358.

14. **Auvinen, M., A. Paasinen-Sohns, H. Hirai, L. C. Andersson, and E. Holtta**. 1995. Ornithine decarboxylase- and ras-induced cell transformations: reversal by protein tyrosine kinase inhibitors and role of pp130CAS. Mol.Cell Biol. **15**:6513-6525.

15. **Bachman, M. A. and M. S. Swanson**. 2001. RpoS co-operates with other factors to induce *Legionella pneumophila* virulence in the stationary phase. Mol.Microbiol. **40**:1201-1214.

16. **Bachman, M. A. and M. S. Swanson**. 2004. The LetE protein enhances expression of multiple LetA/LetS-dependent transmission traits by *Legionella pneumophila*. Infect.Immun. **72**:3284-3293.

17. **Balasundaram, D., J. D. Dinman, C. W. Tabor, and H. Tabor**. 1994. *SPE1* and *SPE2*: two essential genes in the biosynthesis of polyamines that modulate +1 ribosomal frameshifting in *Saccharomyces cerevisiae*. J.Bacteriol. **176**:7126-7128.

18. **Balasundaram, D., C. W. Tabor, and H. Tabor**. 1991. Spermidine or spermine is essential for the aerobic growth of *Saccharomyces cerevisiae*. Proc.Natl.Acad.Sci.U.S.A **88**:5872-5876.

19. **Balasundaram, D., C. W. Tabor, and H. Tabor**. 1993. Oxygen toxicity in a polyamine-depleted spe2 delta mutant of *Saccharomyces cerevisiae*. Proc.Natl.Acad.Sci.U.S.A **90**:4693-4697.

20. **Bancroft, D., L. D. Williams, A. Rich, and M. Egli**. 1994. The low-temperature crystal structure of the pure-spermine form of Z-DNA reveals binding of a spermine molecule in the minor groove. Biochemistry **33**:1073-1086.

21. **Bandyopadhyay, P., H. Xiao, H. A. Coleman, A. Price-Whelan, and H. M. Steinman**. 2004. Icm/dot-independent entry of *Legionella pneumophila* into amoeba and macrophage hosts. Infect.Immun. **72**:4541-4551.

22. **Barlowe, C.** 2002. COPII-dependent transport from the endoplasmic reticulum. Curr.Opin.Cell Biol. **14**:417-422.

23. **Basu, H. S., M. C. Sturkenboom, J. G. Delcros, P. P. Csokan, J. Szollosi, B. G. Feuerstein, and L. J. Marton**. 1992. Effect of polyamine depletion on chromatin structure in U-87 MG human brain tumour cells. Biochem.J. **282 (Pt 3)**:723-727.

24. **Berger, K. H. and R. R. Isberg**. 1993. Two distinct defects in intracellular growth complemented by a single genetic locus in *Legionella pneumophila*. Mol.Microbiol. **7**:7-19.

25. **Bergonzelli, G. E., D. Granato, R. D. Pridmore, L. F. Marvin-Guy, D. Donnicola, and I. E. Corthesy-Theulaz**. 2006. GroEL of *Lactobacillus johnsonii* La1 (NCC 533) is cell surface associated: potential role in interactions with the host and the gastric pathogen Helicobacter pylori. Infect.Immun. **74**:425-434.

26. **Berk, S. G., G. Faulkner, E. Garduno, M. C. Joy, M. A. Ortiz-Jimenez, and R. A. Garduno**. 2008. Packaging of live *Legionella pneumophila* into pellets expelled by *Tetrahymena spp*. does not require bacterial replication and depends on a Dot/Icm-mediated survival mechanism. Appl.Environ.Microbiol. **74**:2187-2199.

27. **Berk, S. G., R. S. Ting, G. W. Turner, and R. J. Ashburn**. 1998. Production of respirable vesicles containing live *Legionella pneumophila* cells by two *Acanthamoeba spp*. Appl.Environ.Microbiol. **64**:279-286.

28. **Beuzon, C. R. and D. W. Holden**. 2001. Use of mixed infections with *Salmonella* strains to study virulence genes and their interactions in vivo. Microbes.Infect. **3**:1345-1352.

29. **Bitar, D. M., M. Molmeret, and Y. A. Kwaik**. 2005. Structure-function analysis of the C-terminus of *IcmT* of *Legionella pneumophila* in pore formation-mediated egress from macrophages. FEMS Microbiol.Lett. **242**:177-184.

30. **Blander, S. J. and M. A. Horwitz**. 1993. Major cytoplasmic membrane protein of *Legionella pneumophila*, a genus common antigen and member of the hsp 60 family of heat shock proteins, induces protective immunity in a guinea pig model of Legionnaires' disease. J.Clin.Invest **91**:717-723.

31. **Bochkareva, E. S., N. M. Lissin, and A. S. Girshovich**. 1988. Transient association of newly synthesized unfolded proteins with the heat-shock GroEL protein. Nature **336**:254-257.

32. **Bower, J. M., H. B. Gordon-Raagas, and M. A. Mulvey**. 2009. Conditioning of uropathogenic *Escherichia coli* for enhanced colonization of host. Infect.Immun. **77**:2104-2112.

33. **Braig, K., Z. Otwinowski, R. Hegde, D. C. Boisvert, A. Joachimiak, A. L. Horwich, and P. B. Sigler**. 1994. The crystal structure of the bacterial chaperonin GroEL at 2.8 A. Nature **371**:578-586.

34. **Braig, K., Z. Otwinowski, R. Hegde, D. C. Boisvert, A. Joachimiak, A. L. Horwich, and P. B. Sigler**. 1994. The crystal structure of the bacterial chaperonin GroEL at 2.8 A. Nature **371**:578-586.

35. **Brassinga, A. K., A.C Mathew, C.J Hoemaker, M.G Morash, J.J Leblanc, and P.S Hoffman**. 2006. Novel use of *Helicobacter pylori* nitroreductase(*rdxA*) as a counterselectable marker in allelic vector exchange to create *Legionella pneumophila* Philadelphia-1 mutants. I*n Legionella*: state of the art 30 years after its recognition. edited by N. P. Cianciotto, Y. Abukwaik, P. H. Edelstein, B. S. Fields, D. F. Geary, T. G. Harrison, C. A. Joseph, R. M. Ratcliff, J. E. Stout, and M. S. Swanson (ed.), p.339-342. ASM Press, Washington, DC, *In*.

36. **Brenner, D. J., A. G. Steigerwalt, and J. E. McDade**. 1979. Classification of the Legionnaires' disease bacterium: *Legionella pneumophila*, genus novum, species nova, of the family Legionellaceae, familia nova. Ann.Intern.Med. **90**:656-658.

37. **Brieland, J., M. McClain, L. Heath, C. Chrisp, G. Huffnagle, M. LeGendre, M. Hurley, J. Fantone, and C. Engleberg**. 1996. Coinoculation with Hartmannella vermiformis enhances replicative *Legionella pneumophila* lung infection in a murine model of Legionnaires' disease. Infect.Immun. **64**:2449-2456.

38. **Bruggemann, H., A. Hagman, M. Jules, O. Sismeiro, M. A. Dillies, C. Gouyette, F. Kunst, M. Steinert, K. Heuner, J. Y. Coppee, and C. Buchrieser**. 2006. Virulence strategies for infecting phagocytes deduced from the in vivo transcriptional program of *Legionella pneumophila*. Cell Microbiol. **8**:1228-1240.

39. **Buchmeier, N. A. and F. Heffron**. 1990. Induction of *Salmonella* stress proteins upon infection of macrophages. Science **248**:730-732.

40. **Bulut, Y., E. Faure, L. Thomas, H. Karahashi, K. S. Michelsen, O. Equils, S. G. Morrison, R. P. Morrison, and M. Arditi**. 2002. Chlamydial heat shock protein 60 activates macrophages and endothelial cells through Toll-like receptor 4 and MD2 in a MyD88-dependent pathway. J.Immunol. **168**:1435-1440.

41. **Bulut, Y., K. S. Michelsen, L. Hayrapetian, Y. Naiki, R. Spallek, M. Singh, and M. Arditi**. 2005. *Mycobacterium tuberculosis* heat shock proteins use diverse Toll-like receptor pathways to activate pro-inflammatory signals. J.Biol.Chem. **280**:20961-20967.

42. **Burstein, D., T. Zusman, E. Degtyar, R. Viner, G. Segal, and T. Pupko**. 2009. Genome-scale identification of *Legionella pneumophila* effectors using a machine learning approach. PLoS.Pathog. **5**:e1000508.

43. **Byrd, T. F. and M. A. Horwitz**. 1989. Interferon gamma-activated human monocytes downregulate transferrin receptors and inhibit the intracellular multiplication of *Legionella pneumophila* by limiting the availability of iron. J.Clin.Invest **83**:1457-1465.

44. **Byrd, T. F. and M. A. Horwitz**. 2000. Aberrantly low transferrin receptor expression on human monocytes is associated with nonpermissiveness for *Legionella pneumophila* growth. J.Infect.Dis. **181**:1394-1400.

45. **Byrne, B. and M. S. Swanson**. 1998. Expression of *Legionella pneumophila* virulence traits in response to growth conditions. Infect.Immun. **66**:3029-3034.

46. **Campodonico, E. M., L. Chesnel, and C. R. Roy**. 2005. A yeast genetic system for the identification and characterization of substrate proteins transferred into host cells by the *Legionella pneumophila* Dot/Icm system. Mol.Microbiol. **56**:918-933.

47. **Cao, P., M. S. McClain, M. H. Forsyth, and T. L. Cover**. 1998. Extracellular release of antigenic proteins by *Helicobacter pylori*. Infect.Immun. **66**:2984-2986.

48. **Capela, D., F. Barloy-Hubler, J. Gouzy, G. Bothe, F. Ampe, J. Batut, P. Boistard, A. Becker, M. Boutry, E. Cadieu, S. Dreano, S. Gloux, T. Godrie, A. Goffeau, D. Kahn, E. Kiss, V. Lelaure, D. Masuy, T. Pohl, D. Portetelle, A. Puhler, B. Purnelle, U. Ramsperger, C. Renard, P. Thebault, M. Vandenbol, S. Weidner, and F. Galibert**. 2001. Analysis of the chromosome sequence of the legume symbiont *Sinorhizobium meliloti* strain 1021. Proc.Natl.Acad.Sci.U.S.A **98**:9877-9882.

49. **Carlson, P. E., Jr., J. Horzempa, D. M. O'Dee, C. M. Robinson, P. Neophytou, A. Labrinidis, and G. J. Nau**. 2009. Global transcriptional response to spermine, a component of the intramacrophage environment, reveals regulation of *Francisella* gene expression through insertion sequence elements. J.Bacteriol. **191**:6855-6864.

50. **Carreiro, M. M., D. C. Laux, and D. R. Nelson**. 1990. Characterization of the heat shock response and identification of heat shock protein antigens of *Borrelia burgdorferi*. Infect.Immun. **58**:2186-2191.

51. **Cavanagh, A. T., A. D. Klocko, X. Liu, and K. M. Wassarman**. 2008. Promoter specificity for 6S RNA regulation of transcription is determined by core promoter sequences and competition for region 4.2 of sigma70. Mol.Microbiol. **67**:1242-1256.

52. **Cazalet, C., C. Rusniok, H. Bruggemann, N. Zidane, A. Magnier, L. Ma, M. Tichit, S. Jarraud, C. Bouchier, F. Vandenesch, F. Kunst, J. Etienne, P. Glaser, and C. Buchrieser**. 2004. Evidence in the *Legionella pneumophila* genome for exploitation of host cell functions and high genome plasticity. Nat.Genet. **36**:1165-1173.

53. **Cehovin, A., A. R. Coates, Y. Hu, Y. Riffo-Vasquez, P. Tormay, C. Botanch, F. Altare, and B. Henderson**. 2010. Comparison of the moonlighting actions of the two highly homologous chaperonin 60 proteins of *Mycobacterium tuberculosis*. Infect.Immun. **78**:3196-3206.

54. **Ceri, H., M. E. Olson, C. Stremick, R. R. Read, D. Morck, and A. Buret**. 1999. The Calgary Biofilm Device: new technology for rapid determination of antibiotic susceptibilities of bacterial biofilms. J.Clin.Microbiol. **37**:1771-1776.

55. **Chalfie, M., Y. Tu, G. Euskirchen, W. W. Ward, and D. C. Prasher**. 1994. Green fluorescent protein as a marker for gene expression. Science **263**:802-805.

56. **Chattopadhyay, M. K., C. W. Tabor, and H. Tabor**. 2009. Polyamines are not required for aerobic growth of *Escherichia coli*: preparation of a strain with deletions in all of the genes for polyamine biosynthesis. J.Bacteriol. **191**:5549-5552.

57. **Chaturvedi, R., Y. Cheng, M. Asim, F. I. Bussiere, H. Xu, A. P. Gobert, A. Hacker, R. A. Casero, Jr., and K. T. Wilson**. 2004. Induction of polyamine oxidase 1 by Helicobacter pylori causes macrophage apoptosis by hydrogen peroxide release and mitochondrial membrane depolarization. J.Biol.Chem. **279**:40161-40173.

58. **Chen, D. E., S. Podell, J. D. Sauer, M. S. Swanson, and M. H. Saier, Jr.** 2008. The phagosomal nutrient transporter (Pht) family. Microbiology **154**:42-53.

59. **Chen, J., K. S. de Felipe, M. Clarke, H. Lu, O. R. Anderson, G. Segal, and H. A. Shuman**. 2004. *Legionella* effectors that promote nonlytic release from protozoa. Science **303**:1358-1361.

60. **Cheng, Y., R. Chaturvedi, M. Asim, F. I. Bussiere, A. Scholz, H. Xu, R. A. Casero, Jr., and K. T. Wilson**. 2005. *Helicobacter pylori*-induced macrophage apoptosis requires activation of ornithine decarboxylase by c-Myc. J.Biol.Chem. **280**:22492-22496.

61. **Chien, M., I. Morozova, S. Shi, H. Sheng, J. Chen, S. M. Gomez, G. Asamani, K. Hill, J. Nuara, M. Feder, J. Rineer, J. J. Greenberg, V. Steshenko, S. H. Park, B. Zhao, E. Teplitskaya, J. R. Edwards, S. Pampou, A. Georghiou, I. C. Chou, W. Iannuccilli, M. E. Ulz, D. H. Kim, A. Geringer-Sameth, C. Goldsberry, P. Morozov, S. G. Fischer, G. Segal, X. Qu, A. Rzhetsky, P. Zhang, E. Cayanis, P. J. De Jong, J. Ju, S. Kalachikov, H. A. Shuman, and J. J. Russo**. 2004. The genomic sequence of the accidental pathogen *Legionella pneumophila*. Science **305**:1966-1968.

62. **Chong, A.** 2007. Characterization of the Virulence-Related Roles of the *Legionella pneumophila* Chaperonin, HtpB, in Mammalian Cells. Ph.D Thesis. Dalhousie University, Nova Scotia, Canada.

63. **Chong, A., A. L. Reviroll, D. S. Allan, E. Garduno, and R. A. Garduno**. 2006. The Hsp60 chaperonin of *Legionella pneumophila*: an intriguing player in infection of host cells. *In*: *Legionella:* state of the Art 30 years after its recognition. N. P. Cianciotto, Y. Abu Kwaik, P. H. Edelstein, B. S. Fields, D. F. Geary, T. G. Harrison, C. A. Joseph, R. M. Ratcliff, J. E. Stout, M. S. Swanson (ed.), ASM Press, Washington. pp. 255-260.

65. **Chong, A., C. A. Lima, D. S. Allan, G. K. Nasrallah, and R. A. Garduno**. 2009. The purified and recombinant *Legionella pneumophila* chaperonin alters mitochondrial trafficking and microfilament organization. Infect.Immun. **77**:4724-4739.

66. **Cianciotto, N. P., J. M. Bangsborg, B. I. Eisenstein, and N. C. Engleberg**. 1990. Identification of mip-like genes in the genus *Legionella*. Infect.Immun. **58**:2912-2918.

67. **Cirillo, J. D., S. Falkow, and L. S. Tompkins**. 1994. Growth of *Legionella pneumophila* in *Acanthamoeba castellanii* enhances invasion. Infect.Immun. **62**:3254-3261.

68. **Cirillo, S. L., L. E. Bermudez, S. H. El-Etr, G. E. Duhamel, and J. D. Cirillo**. 2001. *Legionella pneumophila* entry gene *rtxA* is involved in virulence. Infect.Immun. **69**:508-517.

69. **Cirillo, S. L., J. Lum, and J. D. Cirillo**. 2000. Identification of novel loci involved in entry by *Legionella pneumophila*. Microbiology **146 (Pt 6)**:1345-1359.

70. **Clemens, D. L., B. Y. Lee, and M. A. Horwitz**. 2000. Deviant expression of Rab5 on phagosomes containing the intracellular pathogens *Mycobacterium tuberculosis* and *Legionella pneumophila* is associated with altered phagosomal fate. Infect.Immun. **68**:2671-2684.

71. **Clontech, L. I.** 1999. MATCHMAKER GAL4 two-hybrid system 3 & libraries user manual. 38.

72. **Coers, J., J. C. Kagan, M. Matthews, H. Nagai, D. M. Zuckman, and C. R. Roy**. 2000. Identification of Icm protein complexes that play distinct roles in the biogenesis of an organelle permissive for *Legionella pneumophila* intracellular growth. Mol.Microbiol. **38**:719-736.

73. **Coers, J., C. Monahan, and C. R. Roy**. 1999. Modulation of phagosome biogenesis by *Legionella pneumophila* creates an organelle permissive for intracellular growth. Nat.Cell Biol. **1**:451-453.

74. **Cohen, S.** 1998. A Guide to the Polyamines, (ed.). Oxford University Press, New York.

75. **Corti, A., C. Dave, H. G. Williams-Ashman, E. Mihich, and A. Schenone**. 1974. Specific inhibition of the enzymic decarboxylation of S-adenosylmethionine by methylglyoxal bis(guanylhydrazone) and related substances. Biochem.J. **139**:351-357.

76. **Coulombe, B. and Z. F. Burton**. 1999. DNA bending and wrapping around RNA polymerase: a "revolutionary" model describing transcriptional mechanisms. Microbiol. Mol.Biol.Rev. **63**:457-478.

77. **Cursons, R. T., T. J. Brown, and E. A. Keys**. 1980. Effect of disinfectants on pathogenic free-living amoebae: in axenic conditions. Appl.Environ.Microbiol. **40**:62-66.

78. **D'Auria, G., N. Jimenez-Hernandez, F. Peris-Bondia, A. Moya, and A. Latorre**. 2010. *Legionella pneumophila* pangenome reveals strain-specific virulence factors. BMC.Genomics **11**:181.

79. **Dalebroux, Z. D., R. L. Edwards, and M. S. Swanson**. 2009. SpoT governs *Legionella pneumophila* differentiation in host macrophages. Mol.Microbiol. **71**:640-658.

80. **Dalebroux, Z. D., S. L. Svensson, E. C. Gaynor, and M. S. Swanson**. 2010. ppGpp conjures bacterial virulence. Microbiol.Mol.Biol.Rev. **74**:171-199.

81. **de Felipe, K. S., S. Pampou, O. S. Jovanovic, C. D. Pericone, S. F. Ye, S. Kalachikov, and H. A. Shuman**. 2005. Evidence for acquisition of *Legionella* type IV secretion substrates via interdomain horizontal gene transfer. J.Bacteriol. **187**:7716-7726.

82. **Dela Vega, A. L. and A. H. Delcour**. 1996. Polyamines decrease Escherichia coli outer membrane permeability. J.Bacteriol. **178**:3715-3721.

83. **delaVega, A. L. and A. H. Delcour**. 1995. Cadaverine induces closing of E. coli porins. EMBO J. **14**:6058-6065.

84. **delaVega, A. L. and A. H. Delcour**. 1995. Cadaverine induces closing of E. coli porins. EMBO J. **14**:6058-6065.

85. **Deng, H., V. A. Bloomfield, J. M. Benevides, and G. J. Thomas, Jr.** 2000. Structural basis of polyamine-DNA recognition: spermidine and spermine interactions with genomic B-DNAs of different GC content probed by Raman spectroscopy. Nucleic Acids Res. **28**:3379-3385.

86. **Dennis, J. J. and G. J. Zylstra**. 1998. Improved antibiotic-resistance cassettes through restriction site elimination using Pfu DNA polymerase PCR. Biotechniques **25**:772-4, 776.

87. **Donaldson, J. G., A. Honda, and R. Weigert**. 2005. Multiple activities for Arf1 at the Golgi complex. Biochim.Biophys.Acta **1744**:364-373.

88. **Donaldson, J. G. and C. L. Jackson**. 2000. Regulators and effectors of the ARF GTPases. Curr.Opin.Cell Biol. **12**:475-482.

89. **Dubin, D. T. and S. M. ROSENTHAL**. 1960. The acetylation of polyamines in *Escherichia coli*. J.Biol.Chem. **235**:776-782.

90. **Durand, J. M. and G. R. Bjork**. 2003. Putrescine or a combination of methionine and arginine restores virulence gene expression in a tRNA modification-deficient mutant of *Shigella flexneri*: a possible role in adaptation of virulence. Mol.Microbiol. **47**:519-527.

91. **Durfee, T., K. Becherer, P. L. Chen, S. H. Yeh, Y. Yang, A. E. Kilburn, W. H. Lee, and S. J. Elledge**. 1993. The retinoblastoma protein associates with the protein phosphatase type 1 catalytic subunit. Genes Dev. **7**:555-569.

92. **Elias, B. C., S. Bhattacharya, R. M. Ray, and L. R. Johnson**. 2010. Polyamine-dependent activation of Rac1 is stimulated by focal adhesion-mediated Tiam1 activation. Cell Adh.Migr. **4**:419-430.

93. **England, J., D. Lucent, and V. Pande**. 2008. Rattling the cage: computational models of chaperonin-mediated protein folding. Curr.Opin.Struct.Biol. **18**:163-169.

94. **Ensgraber, M. and M. Loos**. 1992. A 66-kilodalton heat shock protein of Salmonella typhimurium is responsible for binding of the bacterium to intestinal mucus. Infect.Immun. **60**:3072-3078.

95. **Erhart, E. and C. P. Hollenberg**. 1983. The presence of a defective *LEU2* gene on 2 mu DNA recombinant plasmids of *Saccharomyces cerevisiae* is responsible for curing and high copy number. J.Bacteriol. **156**:625-635.

96. **Ewann, F. and P. S. Hoffman**. 2006. Cysteine metabolism in *Legionella pneumophila*: characterization of an L-cystine-utilizing mutant. Appl. Environ. Microbiol. **72**:3993-4000.

97. **Ewann, F. and P. S. Hoffman**. 2006. antisense strategy. *In Legionella*-State of the art 30 years after its Recognition. N. P. Cianciotto, Y. AbuKwaik, P. H. Edelstein, B. S. Fields, D. F. Geary, T. G. Harrison, C. A. Joseph, R. M. Ratcliff, J. E. Stout, and M. S. Swanson (ed.), ASM Press, Washington, DC. p. 336-338

98. **Eylert, E., V. Herrmann, M. Jules, N. Gillmaier, M. Lautner, C. Buchrieser, W. Eisenreich, and K. Heuner**. 2010. Isotopologue profiling of Legionella pneumophila: role of serine and glucose as carbon substrates. J.Biol.Chem. **285**:22232-22243.

99. **Fares, M. A., E. Barrio, B. Sabater-Munoz, and A. Moya**. 2002. The evolution of the heat-shock protein GroEL from Buchnera, the primary endosymbiont of aphids, is governed by positive selection. Mol.Biol.Evol. **19**:1162-1170.

100. **Fares, M. A., A. Moya, and E. Barrio**. 2005. Adaptive evolution in GroEL from distantly related endosymbiotic bacteria of insects. J.Evol.Biol. **18**:651-660.

101. **Faucher, S. P., G. Friedlander, J. Livny, H. Margalit, and H. A. Shuman**. 2010. *Legionella pneumophila* 6S RNA optimizes intracellular multiplication. Proc.Natl.Acad.Sci.U.S.A **107**:7533-7538.

102. **Faulkner, G. and R. A. Garduno**. 2002. Ultrastructural analysis of differentiation in *Legionella pneumophila*. J.Bacteriol. **184**:7025-7041.

103. **Fayet, O., T. Ziegelhoffer, and C. Georgopoulos**. 1989. The *groES* and *groEL* heat shock gene products of *Escherichia coli* are essential for bacterial growth at all temperatures. J.Bacteriol. **171**:1379-1385.

104. **Feeley, J. C., R. J. Gibson, G. W. Gorman, N. C. Langford, J. K. Rasheed, D. C. Mackel, and W. B. Baine**. 1979. Charcoal-yeast extract agar: primary isolation medium for *Legionella pneumophila*. J.Clin.Microbiol. **10**:437-441.

105. **Felschow, D. M., J. MacDiarmid, T. Bardos, R. Wu, P. M. Woster, and C. W. Porter**. 1995. Photoaffinity labeling of a cell surface polyamine binding protein. J.Biol.Chem. **270**:28705-28711.

106. **Felschow, D. M., Z. Mi, J. Stanek, J. Frei, and C. W. Porter**. 1997. Selective labelling of cell-surface polyamine-binding proteins on leukaemic and solid-tumour cell types using a new polyamine photoprobe. Biochem.J. **328 (Pt 3)**:889-895.

107. **Fernandez, R. C., S. M. Logan, S. H. Lee, and P. S. Hoffman**. 1996. Elevated levels of *Legionella pneumophila* stress protein Hsp60 early in infection of human monocytes and L929 cells correlate with virulence. Infect.Immun. **64**:1968-1976.

108. **Fernandez-Moreira, E., J. H. Helbig, and M. S. Swanson**. 2006. Membrane vesicles shed by *Legionella pneumophila* inhibit fusion of phagosomes with lysosomes. Infect.Immun. **74**:3285-3295.

109. **Fettes, P. S., V. Forsbach-Birk, D. Lynch, and R. Marre**. 2001. Overexpresssion of a *Legionella pneumophila* homologue of the *E. coli* regulator *csrA* affects cell size, flagellation, and pigmentation. Int.J.Med.Microbiol. **291**:353-360.

110. **Feuerstein, B. G., N. Pattabiraman, and L. J. Marton**. 1990. Molecular mechanics of the interactions of spermine with DNA: DNA bending as a result of ligand binding. Nucleic Acids Res. **18**:1271-1282.

111. **Feuerstein, B. G., L. D. Williams, H. S. Basu, and L. J. Marton**. 1991. Implications and concepts of polyamine-nucleic acid interactions. J.Cell Biochem. **46**:37-47.

112. **Ficker, E., M. Taglialatela, B. A. Wible, C. M. Henley, and A. M. Brown**. 1994. Spermine and spermidine as gating molecules for inward rectifier K+ channels. Science **266**:1068-1072.

113. **Fields, B. S.** 1996. The molecular ecology of legionellae. Trends Microbiol. **4**:286-290.

114. **Fields, B. S., R. F. Benson, and R. E. Besser**. 2002. *Legionella* and Legionnaires' disease: 25 years of investigation. Clin.Microbiol.Rev. **15**:506-526.

115. **Fields, S.** 2005. High-throughput two-hybrid analysis. The promise and the peril. FEBS J. **272**:5391-5399.

116. **Fields, S.** 2009. Interactive learning: lessons from two hybrids over two decades. Proteomics. **9**:5209-5213.

117. **Fliermans, C. B., W. B. Cherry, L. H. Orrison, S. J. Smith, D. L. Tison, and D. H. Pope**. 1981. Ecological distribution of *Legionella pneumophila*. Appl.Environ.Microbiol. **41**:9-16.

118. **Forsbach-Birk, V., T. McNealy, C. Shi, D. Lynch, and R. Marre**. 2004. Reduced expression of the global regulator protein CsrA in *Legionella pneumophila* affects virulence-associated regulators and growth in *Acanthamoeba castellanii*. Int.J.Med.Microbiol. **294**:15-25.

119. **Fraser, C. M., J. D. Gocayne, O. White, M. D. Adams, R. A. Clayton, R. D. Fleischmann, C. J. Bult, A. R. Kerlavage, G. Sutton, J. M. Kelley, R. D. Fritchman, J. F. Weidman, K. V. Small, M. Sandusky, J. Fuhrmann, D. Nguyen, T. R. Utterback, D. M. Saudek, C. A. Phillips, J. M. Merrick, J. F. Tomb, B. A. Dougherty, K. F. Bott, P. C. Hu, T. S. Lucier, S. N. Peterson, H. O. Smith, C. A. Hutchison, III, and J. C. Venter**. 1995. The minimal gene complement of *Mycoplasma genitalium*. Science **270**:397-403.

120. **Fraser, D. W., T. R. Tsai, W. Orenstein, W. E. Parkin, H. J. Beecham, R. G. Sharrar, J. Harris, G. F. Mallison, S. M. Martin, J. E. McDade, C. C. Shepard, and P. S. Brachman**. 1977. Legionnaires' disease: description of an epidemic of pneumonia. N.Engl.J.Med. **297**:1189-1197.

121. **Fredlund, J. O. and S. M. Oredsson**. 1996. Impairment of DNA replication within one cell cycle after seeding of cells in the presence of a polyamine-biosynthesis inhibitor. Eur.J.Biochem. **237**:539-544.

122. **Fredlund, J. O. and S. M. Oredsson**. 1996. Normal G1/S transition and prolonged S phase within one cell cycle after seeding cells in the presence of an ornithine decarboxylase inhibitor. Cell Prolif. **29**:457-466.

123. **Friedland, J. S., R. Shattock, D. G. Remick, and G. E. Griffin**. 1993. Mycobacterial 65-kD heat shock protein induces release of proinflammatory cytokines from human monocytic cells. Clin.Exp.Immunol. **91**:58-62.

124. **Frisk, A., C. A. Ison, and T. Lagergard**. 1998. GroEL heat shock protein of *Haemophilus ducreyi*: association with cell surface and capacity to bind to eukaryotic cells. Infect.Immun. **66**:1252-1257.

125. **Furuchi, T., K. Kashiwagi, H. Kobayashi, and K. Igarashi**. 1991. Characteristics of the gene for a spermidine and putrescine transport system that maps at 15 min on the *Escherichia coli* chromosome. J.Biol.Chem. **266**:20928-20933.

126. **Gabay, J. E. and M. A. Horwitz**. 1985. Isolation and characterization of the cytoplasmic and outer membranes of the Legionnaires' disease bacterium (*Legionella pneumophila*). J.Exp.Med. **161**:409-422.

127. **Gabay, J. E. and M. A. Horwitz**. 1985. Isolation and characterization of the cytoplasmic and outer membranes of the Legionnaires' disease bacterium (*Legionella pneumophila*). J.Exp.Med. **161**:409-422.

128. **Gal-Mor, O. and G. Segal**. 2003. Identification of CpxR as a positive regulator of icm and dot virulence genes of *Legionella pneumophila*. J.Bacteriol. **185**:4908-4919.

129. **Galdiero, M., G. C. de l'Ero, and A. Marcatili**. 1997. Cytokine and adhesion molecule expression in human monocytes and endothelial cells stimulated with bacterial heat shock proteins. Infect.Immun. **65**:699-707.

130. **Galka, F., S. N. Wai, H. Kusch, S. Engelmann, M. Hecker, B. Schmeck, S. Hippenstiel, B. E. Uhlin, and M. Steinert**. 2008. Proteomic characterization of the whole secretome of *Legionella pneumophila* and functional analysis of outer membrane vesicles. Infect.Immun. **76**:1825-1836.

131. **Gancedo, J. M.** 2001. Control of pseudohyphae formation in *Saccharomyces cerevisiae*. FEMS Microbiol.Rev. **25**:107-123.

132. **Gao, L. Y. and K. Y. Abu**. 1999. Activation of caspase 3 during *Legionella pneumophila*-induced apoptosis. Infect.Immun. **67**:4886-4894.

133. **Gao, L. Y., O. S. Harb, and Y. A. Kwaik**. 1998. Identification of macrophage-specific infectivity loci (*mil*) of *Legionella pneumophila* that are not required for infectivity of protozoa. Infect.Immun. **66**:883-892.

134. **Gao, L. Y. and Y. A. Kwaik**. 2000. The mechanism of killing and exiting the protozoan host Acanthamoeba polyphaga by *Legionella pneumophila*. Environ.Microbiol. **2**:79-90.

135. **Garcia-del, P. F., J. W. Foster, M. E. Maguire, and B. B. Finlay**. 1992. Characterization of the micro-environment of *Salmonella typhimurium*-containing vacuoles within MDCK epithelial cells. Mol.Microbiol. **6**:3289-3297.

136. **Garduno, R. A., A. Chong, G. K. Nasrallah, and D. S. Allan**. 2011. The *Legionella pneumophila* Chaperonin - An Unusual Multifunctional Protein in Unusual Locations. Front Microbiol. **2**:122.

137. **Garduno, R. A., G. Faulkner, M. A. Trevors, N. Vats, and P. S. Hoffman**. 1998. Immunolocalization of Hsp60 in *Legionella pneumophila*. J.Bacteriol. **180**:505-513.

138. **Garduno, R. A., E. Garduno, M. Hiltz, and P. S. Hoffman**. 2002. Intracellular growth of *Legionella pneumophila* gives rise to a differentiated form dissimilar to stationary-phase forms. Infect.Immun. **70**:6273-6283.

139. **Garduno, R. A., E. Garduno, and P. S. Hoffman**. 1998. Surface-associated hsp60 chaperonin of *Legionella pneumophila* mediates invasion in a HeLa cell model. Infect.Immun. **66**:4602-4610.

140. **Garufi, A., S. Visconti, L. Camoni, and P. Aducci**. 2007. Polyamines as physiological regulators of 14-3-3 interaction with the plant plasma membrane H+-ATPase. Plant Cell Physiol **48**:434-440.

141. **George, J. R., L. Pine, M. W. Reeves, and W. K. Harrell**. 1980. Amino acid requirements of *Legionella pneumophila*. J.Clin.Microbiol. **11**:286-291.

142. **George, R., S. M. Kelly, N. C. Price, A. Erbse, M. Fisher, and P. A. Lund**. 2004. Three GroEL homologues from *Rhizobium leguminosarum* have distinct in vitro properties. Biochem.Biophys.Res.Commun. **324**:822-828.

143. **Georgopoulos, C. P. and H. Eisen**. 1974. Bacterial mutants which block phage assembly. J.Supramol.Struct. **2**:349-359.

144. **Gietz, D., J. A. St, R. A. Woods, and R. H. Schiestl**. 1992. Improved method for high efficiency transformation of intact yeast cells. Nucleic Acids Res. **20**:1425.

145. **Glockner, G., C. Albert-Weissenberger, E. Weinmann, S. Jacobi, E. Schunder, M. Steinert, J. Hacker, and K. Heuner**. 2008. Identification and characterization of a new conjugation/type IVA secretion system (trb/tra) of *Legionella pneumophila* Corby localized on two mobile genomic islands. Int.J.Med.Microbiol. **298**:411-428.

146. **Gould, P. S., H. R. Burgar, and P. A. Lund**. 2007. Homologous cpn60 genes in Rhizobium leguminosarum are not functionally equivalent. Cell Stress.Chaperones. **12**:123-131.

147. **Goytia, M. and W. M. Shafer**. 2010. Polyamines can increase resistance of *Neisseria gonorrhoeae* to mediators of the innate human host defense. Infect.Immun. **78**:3187-3195.

148. **Grant, N. J. and C. Oriol-Audit**. 1985. Influence of the polyamine spermine on the organization of cortical filaments in isolated cortices of Xenopus laevis eggs. Eur.J.Cell Biol. **36**:239-246.

149. **Grant, N. J., C. Oriol-Audit, and M. J. Dickens**. 1983. Supramolecular forms of actin induced by polyamines; an electron microscopic study. Eur.J.Cell Biol. **30**:67-73.

150. **Greub, G. and D. Raoult**. 2004. Microorganisms resistant to free-living amoebae. Clin.Microbiol.Rev. **17**:413-433.

151. **Grove, J., J. R. Fozard, and P. S. Mamont**. 1981. Assay of alpha-difluoromethylornithine in body fluids and tissues by automatic amino-acid analysis. J.Chromatogr. **223**:409-416.

152. **Guevara-Olvera, L., B. Xoconostle-Cazares, and J. Ruiz-Herrera**. 1997. Cloning and disruption of the ornithine decarboxylase gene of *Ustilago maydis*: evidence for a role of polyamines in its dimorphic transition. Microbiology **143 (Pt 7)**:2237-2245.

153. **Guo, H., R. M. Ray, and L. R. Johnson**. 2003. RhoA stimulates IEC-6 cell proliferation by increasing polyamine-dependent Cdk2 activity. Am.J.Physiol Gastrointest.Liver Physiol **285**:G704-G713.

154. **Gupta, R. S.** 1995. Evolution of the chaperonin families (Hsp60, Hsp10 and Tcp-1) of proteins and the origin of eukaryotic cells. Mol.Microbiol. **15**:1-11.

155. **Guthrie, C. and G. R. Fink**. 1991. Guide to Yeast Genetics and Molecular Biology. Methods Enzymol. Vol. **194**.

156. **Ha, H. C., N. S. Sirisoma, P. Kuppusamy, J. L. Zweier, P. M. Woster, and R. A. Casero, Jr.** 1998. The natural polyamine spermine functions directly as a free radical scavenger. Proc.Natl.Acad.Sci.U.S.A **95**:11140-11145.

157. **Hagele, S., J. Hacker, and B. C. Brand**. 1998. *Legionella pneumophila* kills human phagocytes but not protozoan host cells by inducing apoptotic cell death. FEMS Microbiol.Lett. **169**:51-58.

158. **Hales, L. M. and H. A. Shuman**. 1999. The *Legionella pneumophila rpoS* gene is required for growth within *Acanthamoeba castellanii*. J.Bacteriol. **181**:4879-4889.

159. **Hammer, B. K. and M. S. Swanson**. 1999. Co-ordination of *legionella pneumophila* virulence with entry into stationary phase by ppGpp. Mol.Microbiol. **33**:721-731.

160. **Hammer, B. K., E. S. Tateda, and M. S. Swanson**. 2002. A two-component regulator induces the transmission phenotype of stationary-phase *Legionella pneumophila*. Mol.Microbiol. **44**:107-118.

161. **Hammerschlag, M. R.** 2002. The intracellular life of chlamydiae. Semin.Pediatr.Infect.Dis. **13**:239-248.

162. **Harb, O. S. and K. Y. Abu**. 2000. Characterization of a macrophage-specific infectivity locus (milA) of *Legionella pneumophila*. Infect.Immun. **68**:368-376.

163. **Hasan, R., M. K. Alam, and R. Ali**. 1995. Polyamine induced Z-conformation of native calf thymus DNA. FEBS Lett. **368**:27-30.

164. **Helbig, J. H., B. Konig, H. Knospe, B. Bubert, C. Yu, C. P. Luck, A. Riboldi-Tunnicliffe, R. Hilgenfeld, E. Jacobs, J. Hacker, and G. Fischer**. 2003. The PPIase active site of *Legionella pneumophila* Mip protein is involved in the infection of eukaryotic host cells. Biol.Chem. **384**:125-137.

165. **Helsel, L. O., W. F. Bibb, C. A. Butler, P. S. Hoffman, and R. M. Mckinney**. 1988. Recognition of A Genus-Wide Antigen of *Legionella* by A Monoclonal-Antibody. Current Microbiology **16**:201-208.

166. **Hemmingsen, S. M., C. Woolford, S. M. van der Vies, K. Tilly, D. T. Dennis, C. P. Georgopoulos, R. W. Hendrix, and R. J. Ellis**. 1988. Homologous plant and bacterial proteins chaperone oligomeric protein assembly. Nature **333**:330-334.

167. **Hennequin, C., F. Porcheray, A. Waligora-Dupriet, A. Collignon, M. Barc, P. Bourlioux, and T. Karjalainen**. 2001. GroEL (Hsp60) of *Clostridium difficile* is involved in cell adherence. Microbiology **147**:87-96.

168. **Herrero, A. B., M. C. Lopez, S. Garcia, A. Schmidt, F. Spaltmann, J. Ruiz-Herrera, and A. Dominguez**. 1999. Control of filament formation in *Candida albicans* by polyamine levels. Infect.Immun. **67**:4870-4878.

169. **Herrmann, V., A. Eidner, K. Rydzewski, I. Bladel, M. Jules, C. Buchrieser, W. Eisenreich, and K. Heuner**. 2011. GamA is a eukaryotic-like glucoamylase responsible for glycogen- and starch-degrading activity of *Legionella pneumophila*. Int.J.Med.Microbiol. **301**:133-139.

170. **Heuner, K., C. Dietrich, C. Skriwan, M. Steinert, and J. Hacker**. 2002. Influence of the alternative sigma(28) factor on virulence and flagellum expression of *Legionella pneumophila*. Infect.Immun. **70**:1604-1608.

171. **Hickey, E. K. and N. P. Cianciotto**. 1994. Cloning and sequencing of the *Legionella pneumophila fur* gene. Gene **143**:117-121.

172. **Hickey, E. K. and N. P. Cianciotto**. 1997. An iron- and *fur*-repressed *Legionella pneumophila* gene that promotes intracellular infection and encodes a protein with similarity to the *Escherichia coli* aerobactin synthetases. Infect.Immun. **65**:133-143.

173. **Higashi, K., K. Kashiwagi, S. Taniguchi, Y. Terui, K. Yamamoto, A. Ishihama, and K. Igarashi**. 2006. Enhancement of +1 frameshift by polyamines during translation of polypeptide release factor 2 in Escherichia coli. J.Biol.Chem. **281**:9527-9537.

174. **Hilbi, H., G. Segal, and H. A. Shuman**. 2001. Icm/dot-dependent upregulation of phagocytosis by *Legionella pneumophila*. Mol.Microbiol. **42**:603-617.

175. **Hirsch, P. R. and J. E. Beringer**. 1984. A physical map of pPH1JI and pJB4JI. Plasmid **12**:139-141.

176. **Hisert, K. B., M. MacCoss, M. U. Shiloh, K. H. Darwin, S. Singh, R. A. Jones, S. Ehrt, Z. Zhang, B. L. Gaffney, S. Gandotra, D. W. Holden, D. Murray, and C. Nathan**. 2005. A glutamate-alanine-leucine (EAL) domain protein of *Salmonella* controls bacterial survival in mice, antioxidant defence and killing of macrophages: role of cyclic diGMP. Mol.Microbiol. **56**:1234-1245.

177. **Hoffman, P. S., C. A. Butler, and F. D. Quinn**. 1989. Cloning and temperature-dependent expression in *Escherichia coli* of a *Legionella pneumophila* gene coding for a genus-common 60-kilodalton antigen. Infect.Immun. **57**:1731-1739.

178. **Hoffman, P. S., L. Houston, and C. A. Butler**. 1990. *Legionella pneumophila htpAB* heat shock operon: nucleotide sequence and expression of the 60-kilodalton antigen in *L. pneumophila*-infected HeLa cells. Infect.Immun. **58**:3380-3387.

179. **Hoffman, P. S., L. Pine, and S. Bell**. 1983. Production of superoxide and hydrogen peroxide in medium used to culture *Legionella pneumophila:* catalytic decomposition by charcoal. Appl.Environ.Microbiol. **45**:784-791.

180. **Hoffman, P. S., M. Ripley, and R. Weeratna**. 1992. Cloning and nucleotide sequence of a gene (ompS) encoding the major outer membrane protein of *Legionella pneumophila*. J.Bacteriol. **174**:914-920.

181. **Hoffman, P. S., J. H. Seyer, and C. A. Butler**. 1992. Molecular characterization of the 28- and 31-kilodalton subunits of the *Legionella pneumophila* major outer membrane protein. J.Bacteriol. **174**:908-913.

182. **Holmes, D. E., R. A. O'Neil, M. A. Chavan, L. A. N'Guessan, H. A. Vrionis, L. A. Perpetua, M. J. Larrahondo, R. DiDonato, A. Liu, and D. R. Lovley**. 2009. Transcriptome of *Geobacter uraniireducens* growing in uranium-contaminated subsurface sediments. ISME.J. **3**:216-230.

183. **Holtta, E. and T. Hovi**. 1985. Polyamine depletion results in impairment of polyribosome formation and protein synthesis before onset of DNA synthesis in mitogen-activated human lymphocytes. Eur.J.Biochem. **152**:229-237.

184. **Holtta, E., A. Paasinen-Sohns, M. Povelainen, K. Jarvinen, K. Ravanko, and A. Kangas**. 1998. Cell transformation by ornithine decarboxylase is associated with phosphorylation of the transactivation domain of c-Jun. Biochem.Soc.Trans. **26**:621-627.

185. **Holtta, E., L. Sistonen, and K. Alitalo**. 1988. The mechanisms of ornithine decarboxylase deregulation in c-Ha-ras oncogene-transformed NIH 3T3 cells. J.Biol.Chem. **263**:4500-4507.

186. **Horne, S. M., T. J. Kottom, L. K. Nolan, and K. D. Young**. 1997. Decreased intracellular survival of an *fkpA* mutant of *Salmonella typhimurium* Copenhagen. Infect.Immun. **65**:806-810.

187. **Horwitz, M. A.** 1983. Formation of a novel phagosome by the Legionnaires' disease bacterium *(Legionella pneumophila)* in human monocytes. J.Exp.Med. **158**:1319-1331.

188. **Horwitz, M. A.** 1983. The Legionnaires' disease bacterium *(Legionella pneumophila*) inhibits phagosome-lysosome fusion in human monocytes. J.Exp.Med. **158**:2108-2126.

189. **Horwitz, M. A.** 1984. Phagocytosis of the Legionnaires' disease bacterium (*Legionella pneumophila*) occurs by a novel mechanism: engulfment within a pseudopod coil. Cell **36**:27-33.

190. **Horwitz, M. A.** 1987. Characterization of avirulent mutant *Legionella pneumophila* that survive but do not multiply within human monocytes. J.Exp.Med. **166**:1310-1328.

191. **Horwitz, M. A. and S. C. Silverstein**. 1980. Legionnaires' disease bacterium (*Legionella pneumophila*) multiples intracellularly in human monocytes. J.Clin.Invest **66**:441-450.

192. **Horwitz, M. A. and S. C. Silverstein**. 1981. Interaction of the legionnaires' disease bacterium (*Legionella pneumophila)* with human phagocytes. II. Antibody promotes binding of L. pneumophila to monocytes but does not inhibit intracellular multiplication. J.Exp.Med. **153**:398-406.

193. **Hougaard, D. M., K. Fujiwara, and L. I. Larsson**. 1987. Immunocytochemical localization of polyamines in normal and neoplastic cells. Comparisons to the formaldehyde-fluorescamine and o-phthalaldehyde methods. Histochem.J. **19**:643-650.

194. **Houry, W. A.** 2001. Mechanism of substrate recognition by the chaperonin GroEL. Biochem.Cell Biol. **79**:569-577.

195. **Hu, Y., B. Henderson, P. A. Lund, P. Tormay, M. T. Ahmed, S. S. Gurcha, G. S. Besra, and A. R. Coates**. 2008. A *Mycobacterium tuberculosis* mutant lacking the *groEL* homologue *cpn60.1* is viable but fails to induce an inflammatory response in animal models of infection. Infect.Immun. **76**:1535-1546.

196. **Hubber, A. and C. R. Roy**. 2010. Modulation of host cell function by *Legionella pneumophila* type IV effectors. Annu.Rev.Cell Dev.Biol. **26**:261-283.

197. **Igarashi, K., K. Ito, and K. Kashiwagi**. 2001. Polyamine uptake systems in *Escherichia coli*. Res.Microbiol. **152**:271-278.

198. **Igarashi, K. and K. Kashiwagi**. 1999. Polyamine transport in bacteria and yeast. Biochem.J. **344 Pt 3**:633-642.

199. **Igarashi, K. and K. Kashiwagi**. 2006. Polyamine Modulon in *Escherichia coli:* genes involved in the stimulation of cell growth by polyamines. J.Biochem. **139**:11-16.

200. **Igarashi, K., K. Sugawara, I. Izumi, C. Nagayama, and S. Hirose**. 1974. Effect of polyamines of polyphenylalanine synthesis by Escherichia coli and rat-liver ribosomes. Eur.J.Biochem. **48**:495-502.

201. **Inderlied, C. B., R. L. Cihlar, and P. S. Sypherd**. 1980. Regulation of ornithine decarboxylase during morphogenesis of *Mucor racemosus*. J.Bacteriol. **141**:699-706.

202. **Ingmundson, A., A. Delprato, D. G. Lambright, and C. R. Roy**. 2007. *Legionella pneumophila* proteins that regulate Rab1 membrane cycling. Nature **450**:365-369.

203. **Ingmundson, A. and C. R. Roy**. 2008. Analyzing association of the endoplasmic reticulum with the *legionella pneumophila*-containing vacuoles by fluorescence microscopy. Methods Mol.Biol. **445**:379-387.

204. **Isomaa, V. V., A. E. Pajunen, C. W. Bardin, and O. A. Janne**. 1983. Ornithine decarboxylase in mouse kidney. Purification, characterization, and radioimmunological determination of the enzyme protein. J.Biol.Chem. **258**:6735-6740.

205. **Ito, K. and K. Igarashi**. 1986. The increase by spermidine of fidelity of protamine synthesis in a wheat-germ cell-free system. Eur.J.Biochem. **156**:505-510.

206. **Iyer, R. and A. H. Delcour**. 1997. Complex inhibition of OmpF and OmpC bacterial porins by polyamines. J.Biol.Chem. **272**:18595-18601.

207. **James, P., J. Halladay, and E. A. Craig**. 1996. Genomic libraries and a host strain designed for highly efficient two-hybrid selection in yeast. Genetics **144**:1425-1436.

208. **Janne, O. A., A. Crozat, J. Palvimo, and L. M. Eisenberg**. 1991. Androgen-regulation of ornithine decarboxylase and S-adenosylmethionine decarboxylase genes. J.Steroid Biochem.Mol.Biol. **40**:307-315.

209. **Jeffery, C. J.** 2009. Moonlighting proteins--an update. Mol.Biosyst. **5**:345-350.

210. **Jenal, U.** 2004. Cyclic di-guanosine-monophosphate comes of age: a novel secondary messenger involved in modulating cell surface structures in bacteria? Curr.Opin.Microbiol. **7**:185-191.

211. **Johnson, T. D.** 1996. Modulation of channel function by polyamines. Trends Pharmacol.Sci. **17**:22-27.

212. **Johnston, S. A. and J. E. Hopper**. 1982. Isolation of the yeast regulatory gene GAL4 and analysis of its dosage effects on the galactose/melibiose regulon. Proc.Natl.Acad.Sci.U.S.A **79**:6971-6975.

213. **Jonas, K., A. N. Edwards, R. Simm, T. Romeo, U. Romling, and O. Melefors**. 2008. The RNA binding protein CsrA controls cyclic di-GMP metabolism by directly regulating the expression of GGDEF proteins. Mol.Microbiol. **70**:236-257.

214. **Joshi, A. D., S. Sturgill-Koszycki, and M. S. Swanson**. 2001. Evidence that Dot-dependent and -independent factors isolate the *Legionella pneumophila* phagosome from the endocytic network in mouse macrophages. Cell Microbiol. **3**:99-114.

215. **Jung, I. L. and I. G. Kim**. 2003. Polyamines and glutamate decarboxylase-based acid resistance in Escherichia coli. J.Biol.Chem. **278**:22846-22852.

216. **Jung, I. L. and I. G. Kim**. 2003. Polyamines reduce paraquat-induced soxS and its regulon expression in Escherichia coli. Cell Biol.Toxicol. **19**:29-41.

217. **Kagan, J. C. and C. R. Roy**. 2002. *Legionella phagosomes* intercept vesicular traffic from endoplasmic reticulum exit sites. Nat.Cell Biol. **4**:945-954.

218. **Kagan, J. C., M. P. Stein, M. Pypaert, and C. R. Roy**. 2004. *Legionella* subvert the functions of Rab1 and Sec22b to create a replicative organelle. J.Exp.Med. **199**:1201-1211.

219. **Kamio, Y., H. Poso, Y. Terawaki, and L. Paulin**. 1986. Cadaverine covalently linked to a peptidoglycan is an essential constituent of the peptidoglycan necessary for the normal growth in Selenomonas ruminantium. J.Biol.Chem. **261**:6585-6589.

220. **Kaneda, K., T. Masuzawa, K. Yasugami, T. Suzuki, Y. Suzuki, and Y. Yanagihara**. 1997. Glycosphingolipid-binding protein of Borrelia burgdorferi sensu lato. Infect.Immun. **65**:3180-3185.

221. **Karatan, E., T. R. Duncan, and P. I. Watnick**. 2005. NspS, a predicted polyamine sensor, mediates activation of *Vibrio cholerae* biofilm formation by norspermidine. J.Bacteriol. **187**:7434-7443.

222. **Karlin, S. and L. Brocchieri**. 2000. Heat shock protein 60 sequence comparisons: duplications, lateral transfer, and mitochondrial evolution. Proc.Natl.Acad.Sci.U.S.A **97**:11348-11353.

223. **Karunakaran, K. P., Y. Noguchi, T. D. Read, A. Cherkasov, J. Kwee, C. Shen, C. C. Nelson, and R. C. Brunham**. 2003. Molecular analysis of the multiple GroEL proteins of Chlamydiae. J.Bacteriol. **185**:1958-1966.

224. **Kashiwagi, K., H. Endo, H. Kobayashi, K. Takio, and K. Igarashi**. 1995. Spermidine-preferential uptake system in *Escherichia coli.* ATP hydrolysis by PotA protein and its association with membrane. J.Biol.Chem. **270**:25377-25382.

225. **Kashiwagi, K., R. Pistocchi, S. Shibuya, S. Sugiyama, K. Morikawa, and K. Igarashi**. 1996. Spermidine-preferential uptake system in *Escherichia coli*. Identification of amino acids involved in polyamine binding in PotD protein. J.Biol.Chem. **271**:12205-12208.

226. **Kashiwagi, K., S. K. Taneja, T. Y. Liu, C. W. Tabor, and H. Tabor**. 1990. Spermidine biosynthesis in *Saccharomyces cerevisiae*. Biosynthesis and processing of a proenzyme form of S-adenosylmethionine decarboxylase. J.Biol.Chem. **265**:22321-22328.

227. **Kasinathan, V. and A. Wingler**. 2004. Effect of reduced arginine decarboxylase activity on salt tolerance and on polyamine formation during salt stress in *Arabidopsis thaliana*. Physiol Plant **121**:101-107.

228. **Katz, S. M.** 1978. The morphology of the Legionnaires' disease organism. Am.J.Pathol. **90**:701-722.

229. **Katz, S. M., I. Brodsky, and S. B. Kahn**. 1979. Legionnaires' disease: ultrastructural appearance of the agent in a lung biopsy specimen. Arch.Pathol.Lab Med. **103**:261-264.

230. **Kaufmann, S. H.** 1990. Heat shock proteins and the immune response. Immunol.Today **11**:129-136.

231. **Kaufmann, S. H., B. Schoel, J. D. van Embden, T. Koga, A. Wand-Wurttenberger, M. E. Munk, and U. Steinhoff**. 1991. Heat-shock protein 60: implications for pathogenesis of and protection against bacterial infections. Immunol.Rev. **121**:67-90.

232. **Keating, T. A., C. G. Marshall, and C. T. Walsh**. 2000. Vibriobactin biosynthesis in *Vibrio cholerae*: VibH is an amide synthase homologous to nonribosomal peptide synthetase condensation domains. Biochemistry **39**:15513-15521.

233. **Kerner, M. J., D. J. Naylor, Y. Ishihama, T. Maier, H. C. Chang, A. P. Stines, C. Georgopoulos, D. Frishman, M. Hayer-Hartl, M. Mann, and F. U. Hartl**. 2005. Proteome-wide analysis of chaperonin-dependent protein folding in *Escherichia coli*. Cell **122**:209-220.

234. **Kirby, J. E., J. P. Vogel, H. L. Andrews, and R. R. Isberg**. 1998. Evidence for pore-forming ability by *Legionella pneumophila*. Mol.Microbiol. **27**:323-336.

235. **Kojima, S., K. C. Ko, Y. Takatsuka, N. Abe, J. Kaneko, Y. Itoh, and Y. Kamio**. 2010. Cadaverine covalently linked to peptidoglycan is required for interaction between the peptidoglycan and the periplasm-exposed S-layer-homologous domain of major outer membrane protein Mep45 in *Selenomonas ruminantium*. J.Bacteriol. **192**:5953-5961.

236. **Kol, A., T. Bourcier, A. H. Lichtman, and P. Libby**. 1999. Chlamydial and human heat shock protein 60s activate human vascular endothelium, smooth muscle cells, and macrophages. J.Clin.Invest **103**:571-577.

237. **Kol, A., A. H. Lichtman, R. W. Finberg, P. Libby, and E. A. Kurt-Jones**. 2000. Cutting edge: heat shock protein (HSP) 60 activates the innate immune response: CD14 is an essential receptor for HSP60 activation of mononuclear cells. J.Immunol. **164**:13-17.

238. **Kong, T. H., A. R. Coates, P. D. Butcher, C. J. Hickman, and T. M. Shinnick**. 1993. Mycobacterium tuberculosis expresses two chaperonin-60 homologs. Proc.Natl.Acad.Sci.U.S.A **90**:2608-2612.

239. **Koski, P. and M. Vaara**. 1991. Polyamines as constituents of the outer membranes of Escherichia coli and Salmonella typhimurium. J.Bacteriol. **173**:3695-3699.

240. **Krishnamurthy, R. and K. A. Bhagwat**. 1989. Polyamines as modulators of salt tolerance in rice cultivars. Plant Physiol **91**:500-504.

241. **Kuchin, S., V. K. Vyas, and M. Carlson**. 2002. Snf1 protein kinase and the repressors Nrg1 and Nrg2 regulate *FLO11*, haploid invasive growth, and diploid pseudohyphal differentiation. Mol.Cell Biol. **22**:3994-4000.

242. **Kuchin, S., V. K. Vyas, and M. Carlson**. 2003. Role of the yeast Snf1 protein kinase in invasive growth. Biochem.Soc.Trans. **31**:175-177.

243. **Kumagai, Y., O. Takeuchi, and S. Akira**. 2008. Pathogen recognition by innate receptors. J.Infect.Chemother. **14**:86-92.

244. **Kurihara, S., S. Oda, K. Kato, H. G. Kim, T. Koyanagi, H. Kumagai, and H. Suzuki**. 2005. A novel putrescine utilization pathway involves gamma-glutamylated intermediates of *Escherichia coli* K-12. J.Biol.Chem. **280**:4602-4608.

245. **Kurihara, S., Y. Tsuboi, S. Oda, H. G. Kim, H. Kumagai, and H. Suzuki**. 2009. The putrescine Importer PuuP of *Escherichia coli* K-12. J.Bacteriol. **191**:2776-2782.

246. **Kusano, T., T. Berberich, C. Tateda, and Y. Takahashi**. 2008. Polyamines: essential factors for growth and survival. Planta **228**:367-381.

247. **Kwon, D. H. and C. D. Lu**. 2006. Polyamines induce resistance to cationic peptide, aminoglycoside, and quinolone antibiotics in Pseudomonas aeruginosa PAO1. Antimicrob.Agents Chemother. **50**:1615-1622.

248. **Laitinen, J., K. Stenius, T. O. Eloranta, and E. Holtta**. 1998. Polyamines may regulate S-phase progression but not the dynamic changes of chromatin during the cell cycle. J.Cell Biochem. **68**:200-212.

249. **Lasbury, M. E., S. Merali, P. J. Durant, D. Tschang, C. A. Ray, and C. H. Lee**. 2007. Polyamine-mediated apoptosis of alveolar macrophages during *Pneumocystis pneumonia*. J.Biol.Chem. **282**:11009-11020.

250. **Lathigra, R. B., P. D. Butcher, T. R. Garbe, and D. B. Young**. 1991. Heat shock proteins as virulence factors of pathogens. Curr.Top.Microbiol.Immunol. **167**:125-143.

251. **Leblanc, J. J., R. J. Davidson, and P. S. Hoffman**. 2006. Compensatory functions of two alkyl hydroperoxide reductases in the oxidative defense system of *Legionella pneumophila*. J.Bacteriol. **188**:6235-6244.

252. **Lee, J., V. Sperandio, D. E. Frantz, J. Longgood, A. Camilli, M. A. Phillips, and A. J. Michael**. 2009. An alternative polyamine biosynthetic pathway is widespread in bacteria and essential for biofilm formation in *Vibrio cholerae*. J.Biol.Chem. **284**:9899-9907.

253. **Lema, M. W. and A. Brown**. 1995. *Legionella pneumophila* has two 60-kilodalton heat-shock proteins. Curr.Microbiol. **31**:332-335.

254. **Lema, M. W., A. Brown, C. A. Butler, and P. S. Hoffman**. 1988. Heat-shock response in *Legionella pneumophila*. Can.J.Microbiol. **34**:1148-1153.

255. **Lewis, J. S., T. J. Thomas, A. Shirahata, and T. Thomas**. 2000. Self-assembly of an oligodeoxyribonucleotide harboring the estrogen response element in the presence of polyamines: ionic, structural, and DNA sequence specificity effects. Biomacromolecules. **1**:339-349.

256. **Li, J., K. M. Doyle, and T. Tatlisumak**. 2007. Polyamines in the brain: distribution, biological interactions, and their potential therapeutic role in brain ischaemia. Curr.Med.Chem. **14**:1807-1813.

257. **Liles, M. R., P. H. Edelstein, and N. P. Cianciotto**. 1999. The prepilin peptidase is required for protein secretion by and the virulence of the intracellular pathogen *Legionella pneumophila*. Mol.Microbiol. **31**:959-970.

258. **Liles, M. R., T. A. Scheel, and N. P. Cianciotto**. 2000. Discovery of a nonclassical siderophore, legiobactin, produced by strains of *Legionella pneumophila*. J.Bacteriol. **182**:749-757.

259. **Liles, M. R., V. K. Viswanathan, and N. P. Cianciotto**. 1998. Identification and temperature regulation of *Legionella pneumophila* genes involved in type IV pilus biogenesis and type II protein secretion. Infect.Immun. **66**:1776-1782.

260. **Liu, Y. and Z. Q. Luo**. 2007. *The Legionella pneumophila* effector SidJ is required for efficient recruitment of endoplasmic reticulum proteins to the bacterial phagosome. Infect.Immun. **75**:592-603.

261. **Lu, H. and M. Clarke**. 2005. Dynamic properties of *Legionella*-containing phagosomes in Dictyostelium amoebae. Cell Microbiol. **7**:995-1007.

262. **Lubelski, J., W. N. Konings, and A. J. Driessen**. 2007. Distribution and physiology of ABC-type transporters contributing to multidrug resistance in bacteria. Microbiol.Mol.Biol.Rev. **71**:463-476.

263. **Lund, P. A.** 2001. Microbial molecular chaperones. Adv.Microb.Physiol **44**:93-140.

264. **Lund, P. A.** 2009. Multiple chaperonins in bacteria--why so many? FEMS Microbiol.Rev. **33**:785-800.

265. **Luo, Z. Q. and R. R. Isberg**. 2004. Multiple substrates of the *Legionella pneumophila* Dot/Icm system identified by interbacterial protein transfer. Proc.Natl.Acad.Sci.U.S.A **101**:841-846.

266. **Macellaro, A., E. Tujulin, K. Hjalmarsson, and L. Norlander**. 1998. Identification of a 71-kilodalton surface-associated Hsp70 homologue in Coxiella burnetii. Infect.Immun. **66**:5882-5888.

267. **Machner, M. P. and R. R. Isberg**. 2006. Targeting of host Rab GTPase function by the intravacuolar pathogen *Legionella pneumophila*. Dev.Cell **11**:47-56.

268. **Machner, M. P. and R. R. Isberg**. 2007. A bifunctional bacterial protein links GDI displacement to Rab1 activation. Science **318**:974-977.

269. **Maguire, M., A. R. Coates, and B. Henderson**. 2002. Chaperonin 60 unfolds its secrets of cellular communication. Cell Stress.Chaperones. **7**:317-329.

270. **Maiale, S., D. H. Sanchez, A. Guirado, A. Vidal, and O. A. Ruiz**. 2004. Spermine accumulation under salt stress. J.Plant Physiol **161**:35-42.

271. **Mamont, P. S., M. C. Duchesne, J. Grove, and P. Bey**. 1978. Anti-proliferative properties of DL-alpha-difluoromethyl ornithine in cultured cells. A consequence of the irreversible inhibition of ornithine decarboxylase. Biochem.Biophys.Res.Commun. **81**:58-66.

272. **Mampel, J., T. Spirig, S. S. Weber, J. A. Haagensen, S. Molin, and H. Hilbi**. 2006. Planktonic replication is essential for biofilm formation by *Legionella pneumophila* in a complex medium under static and dynamic flow conditions. Appl.Environ.Microbiol. **72**:2885-2895.

273. **Mariggio, M. A., A. Vinella, N. Pasquetto, E. Curci, A. Cassano, and R. Fumarulo**. 2004. In vitro effects of polyamines on polymorphonuclear cell apoptosis and implications in the pathogenesis of periodontal disease. Immunopharmacol.Immunotoxicol. **26**:93-101.

274. **Marra, A., S. J. Blander, M. A. Horwitz, and H. A. Shuman**. 1992. Identification of a *Legionella pneumophila* locus required for intracellular multiplication in human macrophages. Proc.Natl.Acad.Sci.U.S.A **89**:9607-9611.

275. **Marrie, T. J., C. E. de, V. L. Yu, and J. Stout**. 2003. Legionnaires' disease - Results of a multicentre Canadian study. Can.J.Infect.Dis. **14**:154-158.

276. **Marrie, T. J., D. Raoult, S. B. La, R. J. Birtles, and C. E. de**. 2001. *Legionella*-like and other amoebal pathogens as agents of community-acquired pneumonia. Emerg.Infect.Dis. **7**:1026-1029.

277. **Martinez, J. P., J. L. Lopez-Ribot, M. L. Gil, R. Sentandreu, and J. Ruiz-Herrera**. 1990. Inhibition of the dimorphic transition of *Candida albicans* by the ornithine decarboxylase inhibitor 1,4-diaminobutanone: alterations in the glycoprotein composition of the cell wall. J.Gen.Microbiol. **136**:1937-1943.

278. **Marty, C., G. Mori, L. Sabini, and V. Rivarola**. 2000. Effects of alpha-difluoromethylornithine on the cyclin A expression in Hep-2 cells. Biocell **24**:49-52.

279. **McDade, J. E., C. C. Shepard, D. W. Fraser, T. R. Tsai, M. A. Redus, and W. R. Dowdle**. 1977. Legionnaires' disease: isolation of a bacterium and demonstration of its role in other respiratory disease. N.Engl.J.Med. **297**:1197-1203.

280. **McGinnis, M. W., Z. M. Parker, N. E. Walter, A. C. Rutkovsky, C. Cartaya-Marin, and E. Karatan**. 2009. Spermidine regulates *Vibrio cholerae* biofilm formation via transport and signaling pathways. FEMS Microbiol.Lett. **299**:166-174.

281. **McNealy, T. L., V. Forsbach-Birk, C. Shi, and R. Marre**. 2005. The Hfq homolog in *Legionella pneumophila* demonstrates regulation by LetA and RpoS and interacts with the global regulator CsrA. J.Bacteriol. **187**:1527-1532.

282. **Minnick, M. F., L. S. Smitherman, and D. S. Samuels**. 2003. Mitogenic effect of Bartonella bacilliformis on human vascular endothelial cells and involvement of GroEL. Infect.Immun. **71**:6933-6942.

283. **Molmeret, M., S. D. Zink, L. Han, A. Abu-Zant, R. Asari, D. M. Bitar, and K. Y. Abu**. 2004. Activation of caspase-3 by the Dot/Icm virulence system is essential for arrested biogenesis of the *Legionella*-containing phagosome. Cell Microbiol. **6**:33-48.

284. **Molofsky, A. B., L. M. Shetron-Rama, and M. S. Swanson**. 2005. Components of the *Legionella pneumophila* flagellar regulon contribute to multiple virulence traits, including lysosome avoidance and macrophage death. Infect.Immun. **73**:5720-5734.

285. **Molofsky, A. B. and M. S. Swanson**. 2003. *Legionella* pneumophila CsrA is a pivotal repressor of transmission traits and activator of replication. Mol.Microbiol. **50**:445-461.

286. **Molofsky, A. B. and M. S. Swanson**. 2004. Differentiate to thrive: lessons from the *Legionella pneumophila* life cycle. Mol.Microbiol. **53**:29-40.

287. **Morash, M. G., A. K. Brassinga, M. Warthan, P. Gourabathini, R. A. Garduno, S. D. Goodman, and P. S. Hoffman**. 2009. Reciprocal expression of integration host factor and HU in the developmental cycle and infectivity of *Legionella pneumophila*. Appl.Environ.Microbiol. **75**:1826-1837.

288. **Morioka, M., H. Muraoka, K. Yamamoto, and H. Ishikawa**. 1994. An endosymbiont chaperonin is a novel type of histidine protein kinase. J.Biochem. **116**:1075-1081.

289. **Morita, M., M. Kanemori, H. Yanagi, and T. Yura**. 1999. Heat-induced synthesis of sigma32 in Escherichia coli: structural and functional dissection of rpoH mRNA secondary structure. J.Bacteriol. **181**:401-410.

290. **Moussatova, A., C. Kandt, M. L. O'Mara, and D. P. Tieleman**. 2008. ATP-binding cassette transporters in *Escherichia coli*. Biochim.Biophys.Acta **1778**:1757-1771.

291. **Murata, T., A. Delprato, A. Ingmundson, D. K. Toomre, D. G. Lambright, and C. R. Roy**. 2006. The *Legionella pneumophila* effector protein DrrA is a Rab1 guanine nucleotide-exchange factor. Nat.Cell Biol. **8**:971-977.

292. **Murga, R., T. S. Forster, E. Brown, J. M. Pruckler, B. S. Fields, and R. M. Donlan**. 2001. Role of biofilms in the survival of *Legionella pneumophila* in a model potable-water system. Microbiology **147**:3121-3126.

293. **Nagai, H., E. D. Cambronne, J. C. Kagan, J. C. Amor, R. A. Kahn, and C. R. Roy**. 2005. A C-terminal translocation signal required for Dot/Icm-dependent delivery of the *Legionella* RalF protein to host cells. Proc.Natl.Acad.Sci.U.S.A **102**:826-831.

294. **Nagai, H., J. C. Kagan, X. Zhu, R. A. Kahn, and C. R. Roy**. 2002. A bacterial guanine nucleotide exchange factor activates ARF on *Legionella* phagosomes. Science **295**:679-682.

295. **Nasrallah, G. K., A. L. Riveroll, A. Chong, L. E. Murray, P. J. Lewis, and R. A. Garduno**. 8 July 2011. *Legionella pneumophila* requires polyamines for optimal intracellular growth. J.Bacteriol. doi:10.1128/JB.01506-10

296. **Newton, H. J., D. K. Ang, I. R. van Driel, and E. L. Hartland**. 2010. Molecular pathogenesis of infections caused by *Legionella pneumophila*. Clin.Microbiol.Rev. **23**:274-298.

297. **Newton, H. J., F. M. Sansom, V. Bennett-Wood, and E. L. Hartland**. 2006. Identification of *Legionella pneumophila*-specific genes by genomic subtractive hybridization with *Legionella micdadei* and identification of *lpnE*, a gene required for efficient host cell entry. Infect.Immun. **74**:1683-1691.

298. **Newton, H. J., F. M. Sansom, J. Dao, C. Cazalet, H. Bruggemann, C. Albert-Weissenberger, C. Buchrieser, N. P. Cianciotto, and E. L. Hartland**. 2008. Significant role for *ladC* in initiation of *Legionella pneumophila i*nfection. Infect.Immun. **76**:3075-3085.

299. **Newton, H. J., F. M. Sansom, J. Dao, A. D. McAlister, J. Sloan, N. P. Cianciotto, and E. L. Hartland**. 2007. Sel1 repeat protein LpnE is a *Legionella pneumophila* virulence determinant that influences vacuolar trafficking. Infect.Immun. **75**:5575-5585.

300. **Nies, D. H.** 1995. The cobalt, zinc, and cadmium efflux system CzcABC from Alcaligenes eutrophus functions as a cation-proton antiporter in *Escherichia coli*. J.Bacteriol. **177**:2707-2712.

301. **Ojha, A., M. Anand, A. Bhatt, L. Kremer, W. R. Jacobs, Jr., and G. F. Hatfull**. 2005. GroEL1: a dedicated chaperone involved in mycolic acid biosynthesis during biofilm formation in mycobacteria. Cell **123**:861-873.

302. **Oliver, D., T. Baukrowitz, and B. Fakler**. 2000. Polyamines as gating molecules of inward-rectifier K+ channels. Eur.J.Biochem. **267**:5824-5829.

303. **Oliver, D., N. Klocker, J. Schuck, T. Baukrowitz, J. P. Ruppersberg, and B. Fakler**. 2000. Gating of Ca2+-activated K+ channels controls fast inhibitory synaptic transmission at auditory outer hair cells. Neuron **26**:595-601.

304. **Orrison, L. H., W. B. Cherry, C. B. Fliermans, S. B. Dees, L. K. McDougal, and D. J. Dodd**. 1981. Characteristics of environmental isolates of *Legionella pneumophila*. Appl.Environ.Microbiol. **42**:109-115.

305. **Oves-Costales, D., N. Kadi, M. J. Fogg, L. Song, K. S. Wilson, and G. L. Challis**. 2007. Enzymatic logic of anthrax stealth siderophore biosynthesis: AsbA catalyzes ATP-dependent condensation of citric acid and spermidine. J.Am.Chem.Soc. **129**:8416-8417.

306. **Paasinen-Sohns, A. and E. Holtta**. 1997. Cells transformed by ODC, c-Ha-ras and v-src exhibit MAP kinase/Erk-independent constitutive phosphorylation of Sos, Raf and c-Jun activation domain, and reduced PDGF receptor expression. Oncogene **15**:1953-1966.

307. **Pajunen, A., A. Crozat, O. A. Janne, R. Ihalainen, P. H. Laitinen, B. Stanley, R. Madhubala, and A. E. Pegg**. 1988. Structure and regulation of mammalian S-adenosylmethionine decarboxylase. J.Biol.Chem. **263**:17040-17049.

308. **Pan, Y. H., C. C. Liao, C. C. Kuo, K. J. Duan, P. H. Liang, H. S. Yuan, S. T. Hu, and K. F. Chak**. 2006. The critical roles of polyamines in regulating ColE7 production and restricting ColE7 uptake of the colicin-producing *Escherichia coli*. J.Biol.Chem. **281**:13083-13091.

309. **Pantzar, M., S. Teneberg, and T. Lagergard**. 2006. Binding of *Haemophilus ducreyi* to carbohydrate receptors is mediated by the 58.5-kDa GroEL heat shock protein. Microbes.Infect. **8**:2452-2458.

310. **Park, M. H.** 2006. The post-translational synthesis of a polyamine-derived amino acid, hypusine, in the eukaryotic translation initiation factor 5A (eIF5A). J.Biochem. **139**:161-169.

311. **Pasculle, A. W., J. C. Feeley, R. J. Gibson, L. G. Cordes, R. L. Myerowitz, C. M. Patton, G. W. Gorman, C. L. Carmack, J. W. Ezzell, and J. N. Dowling**. 1980. *Pittsburgh pneumonia* agent: direct isolation from human lung tissue. J.Infect.Dis. **141**:727-732.

312. **Patel, C. N., B. W. Wortham, J. L. Lines, J. D. Fetherston, R. D. Perry, and M. A. Oliveira**. 2006. Polyamines are essential for the formation of plague biofilm. J.Bacteriol. **188**:2355-2363.

313. **Payne, N. R. and M. A. Horwitz**. 1987. Phagocytosis of *Legionella pneumophila* is mediated by human monocyte complement receptors. J.Exp.Med. **166**:1377-1389.

314. **Pearson, W. R.** 1995. Comparison of methods for searching protein sequence databases. Protein Sci. **4**:1145-1160.

315. **Pegg, A. E.** 1979. Investigation of the turnover of rat liver S-adenosylmethionine decarboxylase using a specific antibody. J.Biol.Chem. **254**:3249-3253.

316. **Pegg, A. E.** 1986. Recent advances in the biochemistry of polyamines in eukaryotes. Biochem.J. **234**:249-262.

317. **Pegg, A. E.** 2006. Regulation of ornithine decarboxylase. J.Biol.Chem. **281**:14529-14532.

318. **Pegg, A. E.** 2009. S-Adenosylmethionine decarboxylase. Essays Biochem. **46**:25-45.

319. **Pegg, A. E., T. Kameji, A. Shirahata, B. Stanley, R. Madhubala, and A. Pajunen**. 1988. Regulation of mammalian S-adenosylmethionine decarboxylase. Adv.Enzyme Regul. **27**:43-55.

320. **Pegg, A. E., H. Xiong, D. J. Feith, and L. M. Shantz**. 1998. S-adenosylmethionine decarboxylase: structure, function and regulation by polyamines. Biochem.Soc.Trans. **26**:580-586.

321. **Persson, L., L. Stjernborg, I. Holm, and O. Heby**. 1989. Polyamine-mediated control of mammalian S-adenosyl-L-methionine decarboxylase expression: effects on the content and translational efficiency of the mRNA. Biochem.Biophys.Res.Commun. **160**:1196-1202.

322. **Piao, Z., C. C. Sze, O. Barysheva, K. Iida, and S. Yoshida**. 2006. Temperature-regulated formation of mycelial mat-like biofilms by *Legionella pneumophila*. Appl.Environ.Microbiol. **72**:1613-1622.

323. **Pine, L., M. J. Franzus, and G. B. Malcolm**. 1986. Guanine is a growth factor for *Legionella* species. J.Clin.Microbiol. **23**:163-169.

324. **Plikaytis, B. B., G. M. Carlone, C. P. Pau, and H. W. Wilkinson**. 1987. Purified 60-kilodalton *Legionella* protein antigen with *Legionella*-specific and nonspecific epitopes. J.Clin.Microbiol. **25**:2080-2084.

325. **Pope, C. D., W. O'Connell, and N. P. Cianciotto**. 1996. *Legionella pneumophila* mutants that are defective for iron acquisition and assimilation and intracellular infection. Infect.Immun. **64**:629-636.

326. **Portaro, F. C., M. A. Hayashi, L. J. De Arauz, M. S. Palma, M. T. Assakura, C. L. Silva, and A. C. de Camargo**. 2002. The *Mycobacterium leprae hsp65* displays proteolytic activity. Mutagenesis studies indicate that the *M. leprae hsp65* proteolytic activity is catalytically related to the HslVU protease. Biochemistry **41**:7400-7406.

327. **Poulin, R., L. Lu, B. Ackermann, P. Bey, and A. E. Pegg**. 1992. Mechanism of the irreversible inactivation of mouse ornithine decarboxylase by alpha-difluoromethylornithine. Characterization of sequences at the inhibitor and coenzyme binding sites. J.Biol.Chem. **267**:150-158.

328. **Poulin, R., G. Pelletier, and A. E. Pegg**. 1995. Induction of apoptosis by excessive polyamine accumulation in ornithine decarboxylase-overproducing L1210 cells. Biochem.J. **311 (Pt 3)**:723-727.

329. **Ragaz, C., H. Pietsch, S. Urwyler, A. Tiaden, S. S. Weber, and H. Hilbi**. 2008. The *Legionella pneumophila* phosphatidylinositol-4 phosphate-binding type IV substrate SidC recruits endoplasmic reticulum vesicles to a replication-permissive vacuole. Cell Microbiol. **10**:2416-2433.

330. **Ranford, J. C., A. R. Coates, and B. Henderson**. 2000. Chaperonins are cell-signalling proteins: the unfolding biology of molecular chaperones. Expert.Rev.Mol.Med. **2**:1-17.

331. **Rao, S. P., K. Ogata, S. L. Morris, and A. Catanzaro**. 1994. Identification of a 68 kd surface antigen of Mycobacterium avium that binds to human macrophages. J.Lab Clin.Med. **123**:526-535.

332. **Ravanko, K., K. Jarvinen, A. Paasinen-Sohns, and E. Holtta**. 2000. Loss of p27Kip1 from cyclin E/cyclin-dependent kinase (CDK) 2 but not from cyclin D1/CDK4 complexes in cells transformed by polyamine biosynthetic enzymes. Cancer Res. **60**:5244-5253.

333. **Ray, R. M. and L. R. Johnson**. 2006. Polyamines and cytoskeletal regulation during intestinal epithelial restitution. Biomed Life Sc **3**:349-362.

334. **Ray, R. M., S. A. McCormack, C. Covington, M. J. Viar, Y. Zheng, and L. R. Johnson**. 2003. The requirement for polyamines for intestinal epithelial cell migration is mediated through Rac1. J.Biol.Chem. **278**:13039-13046.

335. **Ray, R. M., S. A. McCormack, and L. R. Johnson**. 2001. Polyamine depletion arrests growth of IEC-6 and Caco-2 cells by different mechanisms. Am.J.Physiol Gastrointest.Liver Physiol **281**:G37-G43.

336. **Ray, R. M., M. J. Viar, Q. Yuan, and L. R. Johnson**. 2000. Polyamine depletion delays apoptosis of rat intestinal epithelial cells. Am.J.Physiol Cell Physiol **278**:C480-C489.

337. **Ray, R. M., B. J. Zimmerman, S. A. McCormack, T. B. Patel, and L. R. Johnson**. 1999. Polyamine depletion arrests cell cycle and induces inhibitors p21(Waf1/Cip1), p27(Kip1), and p53 in IEC-6 cells. Am.J.Physiol **276**:C684-C691.

338. **Reimer, A. R., S. Au, S. Schindle, and K. A. Bernard**. 2010. *Legionella pneumophila* monoclonal antibody subgroups and DNA sequence types isolated in Canada between 1981 and 2009: Laboratory Component of National Surveillance. Eur.J.Clin.Microbiol.Infect.Dis. **29**:191-205.

339. **Retzlaff, C., Y. Yamamoto, P. S. Hoffman, H. Friedman, and T. W. Klein**. 1994. Bacterial heat shock proteins directly induce cytokine mRNA and interleukin-1 secretion in macrophage cultures. Infect.Immun. **62**:5689-5693.

340. **Retzlaff, C., Y. Yamamoto, S. Okubo, P. S. Hoffman, H. Friedman, and T. W. Klein**. 1996. *Legionella pneumophila* heat-shock protein-induced increase of interleukin-1 beta mRNA involves protein kinase C signalling in macrophages. Immunology **89**:281-288.

341. **Riveroll, A.** 2005. The *Legionella pneumophila* chaperonin- An investigation of virulence-related roles in a yeast model. Ph.D thesis. Dalhousie University, NS, Canada.

342. **Robey, M. and N. P. Cianciotto**. 2002. *Legionella pneumophila feoAB* promotes ferrous iron uptake and intracellular infection. Infect.Immun. **70**:5659-5669.

343. **Robinson, C. G. and C. R. Roy**. 2006. Attachment and fusion of endoplasmic reticulum with vacuoles containing *Legionella pneumophila*. Cell Microbiol. **8**:793-805.

344. **Rodgers, F. G.** 1979. Ultrastructure of *Legionella pneumophila*. J.Clin.Pathol. **32**:1195-1202.

345. **Rodriguez-Quinones, F., M. Maguire, E. J. Wallington, P. S. Gould, V. Yerko, J. A. Downie, and P. A. Lund**. 2005. Two of the three groEL homologues in *Rhizobium leguminosarum* are dispensable for normal growth. Arch.Microbiol. **183**:253-265.

346. **Rogers, J., A. B. Dowsett, P. J. Dennis, J. V. Lee, and C. W. Keevil**. 1994. Influence of Plumbing Materials on Biofilm Formation and Growth of *Legionella pneumophila* in Potable Water Systems. Appl.Environ.Microbiol. **60**:1842-1851.

347. **Rogers, J., A. B. Dowsett, and C. W. Keevil**. 1995. A paint incorporating silver to control mixed biofilms containing *Legionella pneumophila*. J.Ind.Microbiol. **15**:377-383.

348. **Rogers, J. and C. W. Keevil**. 1992. Immunogold and fluorescein immunolabelling of *Legionella pneumophila* within an aquatic biofilm visualized by using episcopic differential interference contrast microscopy. Appl.Environ.Microbiol. **58**:2326-2330.

349. **Romling, U. and D. Amikam**. 2006. Cyclic di-GMP as a second messenger. Curr.Opin.Microbiol. **9**:218-228.

350. **Rossier, O. and N. P. Cianciotto**. 2001. Type II protein secretion is a subset of the PilD-dependent processes that facilitate intracellular infection by *Legionella pneumophila*. Infect.Immun. **69**:2092-2098.

351. **Rossier, O., S. R. Starkenburg, and N. P. Cianciotto**. 2004. *Legionella pneumophila* type II protein secretion promotes virulence in the A/J mouse model of Legionnaires' disease pneumonia. Infect.Immun. **72**:310-321.

352. **Rowbotham, T. J.** 1986. Current views on the relationships between amoebae, *legionellae* and man. Isr.J.Med.Sci. **22**:678-689.

353. **Roy, C. R., K. H. Berger, and R. R. Isberg**. 1998. *Legionella pneumophila* DotA protein is required for early phagosome trafficking decisions that occur within minutes of bacterial uptake. Mol.Microbiol. **28**:663-674.

354. **Sadacharan, S. K., A. C. Cavanagh, and R. S. Gupta**. 2001. Immunoelectron microscopy provides evidence for the presence of mitochondrial heat shock 10-kDa protein (chaperonin 10) in red blood cells and a variety of secretory granules. Histochem.Cell Biol. **116**:507-517.

355. **Sadosky, A. B., L. A. Wiater, and H. A. Shuman**. 1993. Identification of *Legionella pneumophila* genes required for growth within and killing of human macrophages. Infect.Immun. **61**:5361-5373.

356. **Sahr, T., H. Bruggemann, M. Jules, M. Lomma, C. Albert-Weissenberger, C. Cazalet, and C. Buchrieser**. 2009. Two small ncRNAs jointly govern virulence and transmission in *Legionella pneumophila*. Mol.Microbiol. **72**:741-762.

357. **Sambrook, J. and D. W. Russell**. 2001. Molecular cloning: a laboratory manual, 3rd ed. Cold Spring Harbor Laboratory Press, Cold Spring Harbor, N.Y.

358. **San-Blas, G., F. San-Blas, F. Sorais, B. Moreno, and J. Ruiz-Herrera**. 1996. Polyamines in growth and dimorphism of *Paracoccidioides brasiliensis*. Arch.Microbiol. **166**:411-413.

359. **Sandegren, L. and D. I. Andersson**. 2009. Bacterial gene amplification: implications for the evolution of antibiotic resistance. Nat.Rev.Microbiol. **7**:578-588.

360. **Sasu, S., D. LaVerda, N. Qureshi, D. T. Golenbock, and D. Beasley**. 2001. Chlamydia pneumoniae and chlamydial heat shock protein 60 stimulate proliferation of human vascular smooth muscle cells via toll-like receptor 4 and p44/p42 mitogen-activated protein kinase activation. Circ.Res. **89**:244-250.

361. **Sauer, J. D., M. A. Bachman, and M. S. Swanson**. 2005. The phagosomal transporter A couples threonine acquisition to differentiation and replication of *Legionella pneumophila* in macrophages. Proc.Natl.Acad.Sci.U.S.A **102**:9924-9929.

362. **Sauer, J. D., J. G. Shannon, D. Howe, S. F. Hayes, M. S. Swanson, and R. A. Heinzen**. 2005. Specificity of *Legionella pneumophila* and *Coxiella burnetii* vacuoles and versatility of *Legionella pneumophila* revealed by coinfection. Infect.Immun. **73**:4494-4504.

363. **Sauve, D. M., H. J. Anderson, J. M. Ray, W. M. James, and M. Roberge**. 1999. Phosphorylation-induced rearrangement of the histone H3 NH2-terminal domain during mitotic chromosome condensation. J.Cell Biol. **145**:225-235.

364. **Schiller, D., D. Kruse, H. Kneifel, R. Kramer, and A. Burkovski**. 2000. Polyamine transport and role of *potE* in response to osmotic stress in *Escherichia coli*. J.Bacteriol. **182**:6247-6249.

365. **Schipper, R. G., L. C. Penning, and A. A. Verhofstad**. 2000. Involvement of polyamines in apoptosis. Facts and controversies: effectors or protectors? Semin.Cancer Biol. **10**:55-68.

366. **Schroeder, G. N., N. K. Petty, A. Mousnier, C. R. Harding, A. J. Vogrin, B. Wee, N. K. Fry, T. G. Harrison, H. J. Newton, N. R. Thomson, S. A. Beatson, G. Dougan, E. L. Hartland, and G. Frankel**. 2010. *Legionella pneumophila* strain 130b possesses a unique combination of type IV secretion systems and novel Dot/Icm secretion system effector proteins. J.Bacteriol. **192**:6001-6016.

367. **Scopio, A., P. Johnson, A. Laquerre, and D. R. Nelson**. 1994. Subcellular localization and chaperone activities of *Borrelia burgdorferi* Hsp60 and Hsp70. J.Bacteriol. **176**:6449-6456.

368. **Seely, J. E., H. Poso, and A. E. Pegg**. 1982. Measurement of the number of ornithine decarboxylase molecules in rat and mouse tissues under various physiological conditions by binding of radiolabelled alpha-difluoromethylornithine. Biochem.J. **206**:311-318.

369. **Segal, G. and E. Z. Ron**. 1996. Heat shock activation of the groESL operon of Agrobacterium tumefaciens and the regulatory roles of the inverted repeat. J.Bacteriol. **178**:3634-3640.

370. **Segal, G., J. J. Russo, and H. A. Shuman**. 1999. Relationships between a new type IV secretion system and the icm/dot virulence system of *Legionella pneumophila*. Mol.Microbiol. **34**:799-809.

371. **Seiler, N., J. G. Delcros, and J. P. Moulinoux**. 1996. Polyamine transport in mammalian cells. An update. Int.J.Biochem.Cell Biol. **28**:843-861.

372. **Sexton, J. A. and J. P. Vogel**. 2002. Type IVB secretion by intracellular pathogens. Traffic. **3**:178-185.

373. **Shah, P., B. Nanduri, E. Swiatlo, Y. Ma, and K. Pendarvis**. 2010. Polyamine biosynthesis and transport mechanisms are crucial for fitness and pathogenesis of *Streptococcus pneumoniae*. Microbiology.

374. **Shah, P., D. G. Romero, and E. Swiatlo**. 2008. Role of polyamine transport in *Streptococcus pneumoniae* response to physiological stress and murine septicemia. Microb.Pathog. **45**:167-172.

375. **Shah, P. and E. Swiatlo**. 2008. A multifaceted role for polyamines in bacterial pathogens. Mol.Microbiol. **68**:4-16.

376. **Shin, S. and C. R. Roy**. 2008. Host cell processes that influence the intracellular survival of *Legionella pneumophila*. Cell Microbiol. **10**:1209-1220.

377. **Shirahata, A. and A. E. Pegg**. 1985. Regulation of S-adenosylmethionine decarboxylase activity in rat liver and prostate. J.Biol.Chem. **260**:9583-9588.

378. **Shirahata, A. and A. E. Pegg**. 1986. Increased content of mRNA for a precursor of S-adenosylmethionine decarboxylase in rat prostate after treatment with 2-difluoromethylornithine. J.Biol.Chem. **261**:13833-13837.

379. **Shohdy, N., J. A. Efe, S. D. Emr, and H. A. Shuman**. 2005. Pathogen effector protein screening in yeast identifies *Legionella* factors that interfere with membrane trafficking. Proc.Natl.Acad.Sci.U.S.A **102**:4866-4871.

380. **Sigler, P. B., Z. Xu, H. S. Rye, S. G. Burston, W. A. Fenton, and A. L. Horwich**. 1998. Structure and function in GroEL-mediated protein folding. Annu.Rev.Biochem. **67**:581-608.

381. **Sistonen, L., E. Holtta, H. Lehvaslaiho, L. Lehtola, and K. Alitalo**. 1989. Activation of the neu tyrosine kinase induces the fos/jun transcription factor complex, the glucose transporter and ornithine decarboxylase. J.Cell Biol. **109**:1911-1919.

382. **Sistonen, L., E. Holtta, T. P. Makela, J. Keski-Oja, and K. Alitalo**. 1989. The cellular response to induction of the p21 c-Ha-ras oncoprotein includes stimulation of jun gene expression. EMBO J. **8**:815-822.

383. **Sompolinsky, D., J. B. Hertz, N. Hoiby, K. Jensen, B. Mansa, V. B. Pedersen, and Z. Samra**. 1980. An antigen common to a wide range of bacteria. 2. A biochemical study of a "common antigen" from Pseudomonas aeruginosa. Acta Pathol.Microbiol.Scand.B **88**:253-260.

384. **Sompolinsky, D., J. B. Hertz, N. Hoiby, K. Jensen, B. Mansa, and Z. Samra**. 1980. An antigen common to a wide range of bacteria. I. The isolation of a 'common antigen' from Pseudomonas aeruginosa. Acta Pathol.Microbiol.Scand.B **88**:143-149.

385. **Spirig, T., A. Tiaden, P. Kiefer, C. Buchrieser, J. A. Vorholt, and H. Hilbi**. 2008. The *Legionella* autoinducer synthase LqsA produces an alpha-hydroxyketone signaling molecule. J.Biol.Chem. **283**:18113-18123.

386. **Steinert, M., L. Emody, R. Amann, and J. Hacker**. 1997. Resuscitation of viable but nonculturable *Legionella pneumophila* Philadelphia JR32 by *Acanthamoeba castellanii*. Appl.Environ.Microbiol. **63**:2047-2053.

387. **Steinert, M., U. Hentschel, and J. Hacker**. 2002. *Legionella pneumophila*: an aquatic microbe goes astray. FEMS Microbiol.Rev. **26**:149-162.

388. **Stone, B. J. and K. Y. Abu**. 1998. Expression of multiple pili by *Legionella pneumophila*: identification and characterization of a type IV pilin gene and its role in adherence to mammalian and protozoan cells. Infect.Immun. **66**:1768-1775.

389. **Sturgill, G. and P. N. Rather**. 2004. Evidence that putrescine acts as an extracellular signal required for swarming in *Proteus mirabilis*. Mol.Microbiol. **51**:437-446.

390. **Sturgill-Koszycki, S. and M. S. Swanson**. 2000. *Legionella pneumophila* replication vacuoles mature into acidic, endocytic organelles. J.Exp.Med. **192**:1261-1272.

391. **Svensson, F., H. Mett, and L. Persson**. 1997. CGP 48664, a potent and specific S-adenosylmethionine decarboxylase inhibitor: effects on regulation and stability of the enzyme. Biochem.J. **322 (Pt 1)**:297-302.

392. **Swanson, M. S. and B. K. Hammer**. 2000. *Legionella pneumophila* pathogesesis: a fateful journey from amoebae to macrophages. Annu.Rev.Microbiol. **54**:567-613.

393. **Swanson, M. S. and R. R. Isberg**. 1995. Association of *Legionella pneumophila* with the macrophage endoplasmic reticulum. Infect.Immun. **63**:3609-3620.

394. **Tabor, C. W. and H. Tabor**. 1984. Polyamines. Annu.Rev.Biochem. **53**:749-790.

395. **Tabor, C. W. and H. Tabor**. 1985. Polyamines in microorganisms. Microbiol.Rev. **49**:81-99.

396. **Tabor, H., E. W. Hafner, and C. W. Tabor**. 1980. Construction of an *Escherichia coli* strain unable to synthesize putrescine, spermidine, or cadaverine: characterization of two genes controlling lysine decarboxylase. J.Bacteriol. **144**:952-956.

397. **Tabor, H. and C. W. Tabor**. 1972. Biosynthesis and metabolism of 1,4-diaminobutane, spermidine, spermine, and related amines. Adv.Enzymol.Relat Areas Mol.Biol. **36**:203-268.

398. **Takemoto, T., Y. Nagamatsu, and T. Oka**. 1983. The study of spermidine-stimulated polypeptide synthesis in cell-free translation of mRNA from lactating mouse mammary gland. Biochim.Biophys.Acta **740**:73-79.

399. **Taylor, J. S. and J. Raes**. 2004. Duplication and divergence: the evolution of new genes and old ideas. Annu.Rev.Genet. **38**:615-643.

400. **Techtmann, S. M. and F. T. Robb**. 2010. Archaeal-like chaperonins in bacteria. Proc.Natl.Acad.Sci.U.S.A **107**:20269-20274.

401. **Temmerman, R., H. Vervaeren, B. Noseda, N. Boon, and W. Verstraete**. 2006. Necrotrophic growth of *Legionella pneumophila*. Appl.Environ.Microbiol. **72**:4323-4328.

402. **Tesh, M. J. and R. D. Miller**. 1981. Amino acid requirements for *Legionella pneumophila* growth. J.Clin.Microbiol. **13**:865-869.

403. **Tesh, M. J., S. A. Morse, and R. D. Miller**. 1983. Intermediary metabolism in *Legionella pneumophila*: utilization of amino acids and other compounds as energy sources. J.Bacteriol. **154**:1104-1109.

404. **Thomas, T. J. and V. A. Bloomfield**. 1984. Ionic and structural effects on the thermal helix-coil transition of DNA complexed with natural and synthetic polyamines. Biopolymers **23**:1295-1306.

405. **Thomas, V., T. Bouchez, V. Nicolas, S. Robert, J. F. Loret, and Y. Levi**. 2004. Amoebae in domestic water systems: resistance to disinfection treatments and implication in *Legionella* persistence. J.Appl.Microbiol. **97**:950-963.

406. **Tiaden, A., T. Spirig, T. Sahr, M. A. Walti, K. Boucke, C. Buchrieser, and H. Hilbi**. 2010. The autoinducer synthase LqsA and putative sensor kinase LqsS regulate phagocyte interactions, extracellular filaments and a genomic island of *Legionella pneumophila*. Environ.Microbiol. **12**:1243-1259.

407. **Tiaden, A., T. Spirig, S. S. Weber, H. Bruggemann, R. Bosshard, C. Buchrieser, and H. Hilbi**. 2007. The *Legionella pneumophila* response regulator LqsR promotes host cell interactions as an element of the virulence regulatory network controlled by RpoS and LetA. Cell Microbiol. **9**:2903-2920.

408. **Tiburcio, A. F., M. A. Masdeu, F. M. Dumortier, and A. W. Galston**. 1986. Polyamine metabolism and osmotic stress. I. Relation to protoplast viability. Plant Physiol **82**:369-374.

409. **Tilney, L. G., O. S. Harb, P. S. Connelly, C. G. Robinson, and C. R. Roy**. 2001. How the parasitic bacterium *Legionella pneumophila* modifies its phagosome and transforms it into rough ER: implications for conversion of plasma membrane to the ER membrane. J.Cell Sci. **114**:4637-4650.

410. **Tobias, K. E. and C. Kahana**. 1995. Exposure to ornithine results in excessive accumulation of putrescine and apoptotic cell death in ornithine decarboxylase overproducing mouse myeloma cells. Cell Growth Differ. **6**:1279-1285.

411. **Toledo-Arana, A., F. Repoila, and P. Cossart**. 2007. Small noncoding RNAs controlling pathogenesis. Curr.Opin.Microbiol. **10**:182-188.

412. **Tome, M. E., S. M. Fiser, and E. W. Gerner**. 1994. Consequences of aberrant ornithine decarboxylase regulation in rat hepatoma cells. J.Cell Physiol **158**:237-244.

413. **Torok, Z., I. Horvath, P. Goloubinoff, E. Kovacs, A. Glatz, G. Balogh, and L. Vigh**. 1997. Evidence for a lipochaperonin: association of active protein-folding GroESL oligomers with lipids can stabilize membranes under heat shock conditions. Proc.Natl.Acad.Sci.U.S.A **94**:2192-2197.

414. **Towbin, H., T. Staehelin, and J. Gordon**. 1979. Electrophoretic transfer of proteins from polyacrylamide gels to nitrocellulose sheets: procedure and some applications. Proc.Natl.Acad.Sci.U.S.A **24**:145-149.

415. **Vabulas, R. M., P. Ahmad-Nejad, C. C. Da, T. Miethke, C. J. Kirschning, H. Hacker, and H. Wagner**. 2001. Endocytosed HSP60s use toll-like receptor 2 (TLR2) and TLR4 to activate the toll/interleukin-1 receptor signaling pathway in innate immune cells. J.Biol.Chem. **276**:31332-31339.

416. **VanBogelen, R. A., M. A. Acton, and F. C. Neidhardt**. 1987. Induction of the heat shock regulon does not produce thermotolerance in *Escherichia coli*. Genes Dev. **1**:525-531.

417. **VanRheenen, S. M., Z. Q. Luo, T. O'Connor, and R. R. Isberg**. 2006. Members of a *Legionella pneumophila* family of proteins with ExoU (phospholipase A) active sites are translocated to target cells. Infect.Immun. **74**:3597-3606.

418. **Vinogradov, E. and M. B. Perry**. 2000. Structural analysis of the core region of lipopolysaccharides from Proteus mirabilis serotypes O6, O48 and O57. Eur.J.Biochem. **267**:2439-2446.

419. **Viswanathan, V. K., Cianciotto, and N.P**. 2001. Electroporation of *Legionella* species, p. 203-211. *In* N. Eynard, and J. Teissie (ed.), *In*: Electro-transformation of Bacteria. Springer Verlag Publications, Heidelberg, Germany..

420. **Vogel, J. P., H. L. Andrews, S. K. Wong, and R. R. Isberg**. 1998. Conjugative transfer by the virulence system of *Legionella pneumophila*. Science **279**:873-876.

421. **Ware, D., Y. Jiang, W. Lin, and E. Swiatlo**. 2006. Involvement of *potD* in *Streptococcus pneumoniae* polyamine transport and pathogenesis. Infect.Immun. **74**:352-361.

422. **Warrell, R. P., Jr. and J. H. Burchenal**. 1983. Methylglyoxal-bis(guanylhydrazone) (Methyl-GAG): current status and future prospects. J.Clin.Oncol. **1**:52-65.

423. **Watarai, M., I. Derre, J. Kirby, J. D. Growney, W. F. Dietrich, and R. R. Isberg**. 2001. *Legionella pneumophila* is internalized by a macropinocytotic uptake pathway controlled by the Dot/Icm system and the mouse Lgn1 locus. J.Exp.Med. **194**:1081-1096.

424. **Watarai, M., S. Kim, J. Erdenebaatar, S. Makino, M. Horiuchi, T. Shirahata, S. Sakaguchi, and S. Katamine**. 2003. Cellular prion protein promotes *Brucella* infection into macrophages. J.Exp.Med. **198**:5-17.

425. **Watson, N., D. S. Dunyak, E. L. Rosey, J. L. Slonczewski, and E. R. Olson**. 1992. Identification of elements involved in transcriptional regulation of the *Escherichia coli* cad operon by external pH. J.Bacteriol. **174**:530-540.

426. **Weber, S. S., C. Ragaz, K. Reus, Y. Nyfeler, and H. Hilbi**. 2006. *Legionella pneumophila* exploits PI(4)P to anchor secreted effector proteins to the replicative vacuole. PLoS.Pathog. **2**:e46.

427. **Weeratna, R., D. A. Stamler, P. H. Edelstein, M. Ripley, T. Marrie, D. Hoskin, and P. S. Hoffman**. 1994. Human and guinea pig immune responses to *Legionella pneumophila* protein antigens OmpS and Hsp60. Infect.Immun. **62**:3454-3462.

428. **Whitfield, N. N., B. G. Byrne, and M. S. Swanson**. 2010. Mouse macrophages are permissive to motile *Legionella* species that fail to trigger pyroptosis. Infect.Immun. **78**:423-432.

429. **Wiater, L. A., K. Dunn, F. R. Maxfield, and H. A. Shuman**. 1998. Early events in phagosome establishment are required for intracellular survival of *Legionella pneumophila*. Infect.Immun. **66**:4450-4460.

430. **Wieland, H., F. Goetz, and B. Neumeister**. 2004. Phagosomal acidification is not a prerequisite for intracellular multiplication of *Legionella pneumophila* in human monocytes. J.Infect.Dis. **189**:1610-1614.

431. **Wieland, H., S. Ullrich, F. Lang, and B. Neumeister**. 2005. Intracellular multiplication of *Legionella pneumophila* depends on host cell amino acid transporter SLC1A5. Mol.Microbiol. **55**:1528-1537.

432. **Williams, K.** 1997. Interactions of polyamines with ion channels. Biochem.J. **325 (Pt 2)**:289-297.

433. **Williams, K.** 1997. Modulation and block of ion channels: a new biology of polyamines. Cell Signal. **9**:1-13.

434. **Williams-Ashman, H. G. and A. Schenone**. 1972. Methyl glyoxal bis(guanylhydrazone) as a potent inhibitor of mammalian and yeast S-adenosylmethionine decarboxylases. Biochem.Biophys.Res.Commun. **46**:288-295.

435. **Wintermeyer, E., B. Ludwig, M. Steinert, B. Schmidt, G. Fischer, and J. Hacker**. 1995. Influence of site specifically altered Mip proteins on intracellular survival of *Legionella pneumophila* in eukaryotic cells. Infect.Immun. **63**:4576-4583.

436. **Xie, X., M. E. Tome, and E. W. Gerner**. 1997. Loss of intracellular putrescine pool-size regulation induces apoptosis. Exp.Cell Res. **230**:386-392.

437. **Yamaguchi, H., T. Osaki, N. Kurihara, H. Taguchi, and S. Kamiya**. 1998. [The role of heat shock protein 60 (HSP60) of *Helicobacter pylori* in adhesion of *H. pylori* to human gastric epithelial cell]. Kansenshogaku Zasshi **72**:487-492.

438. **Yang, G., R. F. Benson, R. Ratcliff, E. W. Brown, A. G. Steigerwalt, L. W. Thacker, M. Daneshvar, R. E. Morey, A. Saito, and B. S. Fields**. 2011. *Legionella nagasakiensis* sp. nov., isolated from water samples in Japan and Australia and from a patient with pneumonia in the United States. Int.J.Syst.Evol.Microbiol.

439. **Yoshida, M., D. Meksuriyen, K. Kashiwagi, G. Kawai, and K. Igarashi**. 1999. Polyamine stimulation of the synthesis of oligopeptide-binding protein (OppA). Involvement of a structural change of the Shine-Dalgarno sequence and the initiation codon aug in oppa mRNA. J.Biol.Chem. **274**:22723-22728.

440. **Yoshida, N., K. Oeda, E. Watanabe, T. Mikami, Y. Fukita, K. Nishimura, K. Komai, and K. Matsuda**. 2001. Protein function. Chaperonin turned insect toxin. Nature **411**:44.

441. **Young, R. A. and T. J. Elliott**. 1989. Stress proteins, infection, and immune surveillance. Cell **59**:5-8.

442. **Yu, V. L., J. F. Plouffe, M. C. Pastoris, J. E. Stout, M. Schousboe, A. Widmer, J. Summersgill, T. File, C. M. Heath, D. L. Paterson, and A. Chereshsky**. 2002. Distribution of *Legionella* species and serogroups isolated by culture in patients with sporadic community-acquired legionellosis: an international collaborative survey. J.Infect.Dis. **186**:127-128.

443. **Yura, T., H. Nagai, and H. Mori**. 1993. Regulation of the heat-shock response in bacteria. Annu.Rev.Microbiol. **47**:321-350.

444. **Zeilstra-Ryalls, J., O. Fayet, and C. Georgopoulos**. 1991. The universally conserved GroE (Hsp60) chaperonins. Annu.Rev.Microbiol. **45**:301-325.

445. **Zerial, M. and H. McBride**. 2001. Rab proteins as membrane organizers. Nat.Rev.Mol.Cell Biol. **2**:107-117.

446. **Zhang, L., S. L. Pelech, D. Mayrand, D. Grenier, J. Heino, and V. J. Uitto**. 2001. Bacterial heat shock protein-60 increases epithelial cell proliferation through the ERK1/2 MAP kinases. Exp.Cell Res. **266**:11-20.

447. **Zhang.J**. 2003. Evolution by gene duplication: an update. Trends in Ecology & Evolution **18**:292-298.

448. **Zhu, W., S. Banga, Y. Tan, C. Zheng, R. Stephenson, J. Gately, and Z. Q. Luo**. 2011. Comprehensive identification of protein substrates of the Dot/Icm type IV transporter of *Legionella pneumophila*. PLoS.One. **6**:e17638.

449. **Zink, S. D., L. Pedersen, N. P. Cianciotto, and Y. Abu-Kwaik**. 2002. The Dot/Icm type IV secretion system of *Legionella pneumophila* is essential for the induction of apoptosis in human macrophages. Infect.Immun. **70**:1657-1663.

450. **Zusman, T., G. Aloni, E. Halperin, H. Kotzer, E. Degtyar, M. Feldman, and G. Segal**. 2007. The response regulator PmrA is a major regulator of the icm/dot type IV secretion system in *Legionella pneumophila* and *Coxiella burnetii*. Mol.Microbiol. **63**:1508-1523.

APPENDIX: COPYRIGHT PERMISSION

Nasrallah, G. K., A. L. Riveroll, A. Chong, L. E. Murray, P. J. Lewis, and R. A. Garduno. 8 July 2011. *Legionella pneumophila* requires polyamines for optimal intracellular growth. J. Bacteriol. doi:10.1128/JB.01506-10.

Dear Gheyath Nasrallah,

Thank you for your permission inquiry. Please cite the JB Accepts content according to ASM style: http://jb.asm.org/misc/journal-ita_org.dtl#02

Specifically, section (iv): Referencing ASM Accepts (publish-ahead-of-print) manuscripts. Citations of ASM Accepts manuscripts should look like the following example:

- Wang, G. G., M. P. Pasillas, and M. P. Kamps. 15 May 2006. Persistent transactivation by Meis1 replaces Hox function in myeloid leukemogenesis models: evidence for co-occupancy of Meis1-Pbx and Hox-Pbx complexes on promoters of leukemia-associated genes. Mol. Cell. Biol. doi:10.1128/MCB.00586-06.

Please see the attached documentation confirming that permission has been granted.

Let us know how we may be of further assistance.

Thank you.
ASM Journals department
journals@asmusa.org

PERMISSION GRANTED
CONTINGENT ON AUTHOR PERMISSION (which you must obtain)
AND APPROPRIATE CREDIT
American Society for Microbiology